

## INFORMATION TO USERS

This manuscript has been reproduced from the microfilm master. UMI films the text directly from the original or copy submitted. Thus, some thesis and dissertation copies are in typewriter face, while others may be from any type of computer printer.

**The quality of this reproduction is dependent upon the quality of the copy submitted.** Broken or indistinct print, colored or poor quality illustrations and photographs, print bleedthrough, substandard margins, and improper alignment can adversely affect reproduction.

In the unlikely event that the author did not send UMI a complete manuscript and there are missing pages, these will be noted. Also, if unauthorized copyright material had to be removed, a note will indicate the deletion.

Oversize materials (e.g., maps, drawings, charts) are reproduced by sectioning the original, beginning at the upper left-hand corner and continuing from left to right in equal sections with small overlaps. Each original is also photographed in one exposure and is included in reduced form at the back of the book.

Photographs included in the original manuscript have been reproduced xerographically in this copy. Higher quality 6" x 9" black and white photographic prints are available for any photographs or illustrations appearing in this copy for an additional charge. Contact UMI directly to order.

# UMI

A Bell & Howell Information Company  
300 North Zeeb Road, Ann Arbor MI 48106-1346 USA  
313/761-4700 800/521-0600



**University of Alberta**

**Development and Testing of Porous VYCOR Membrane Reactors for the Oxidative  
Dehydrodimerization of Propylene**

by

**Robert Andrew Jenkins**



A thesis submitted to the Faculty of Graduate Studies and Research in partial fulfillment  
of the requirements for the degree of Doctor of Philosophy

in  
Chemical Engineering

Department of Chemical and Materials Engineering

Edmonton, Alberta

Fall 1997



National Library  
of Canada

Acquisitions and  
Bibliographic Services

395 Wellington Street  
Ottawa ON K1A 0N4  
Canada

Bibliothèque nationale  
du Canada

Acquisitions et  
services bibliographiques

395, rue Wellington  
Ottawa ON K1A 0N4  
Canada

*Your file Votre référence*

*Our file Notre référence*

The author has granted a non-exclusive licence allowing the National Library of Canada to reproduce, loan, distribute or sell copies of this thesis in microform, paper or electronic formats.

The author retains ownership of the copyright in this thesis. Neither the thesis nor substantial extracts from it may be printed or otherwise reproduced without the author's permission.

L'auteur a accordé une licence non exclusive permettant à la Bibliothèque nationale du Canada de reproduire, prêter, distribuer ou vendre des copies de cette thèse sous la forme de microfiche/film, de reproduction sur papier ou sur format électronique.

L'auteur conserve la propriété du droit d'auteur qui protège cette thèse. Ni la thèse ni des extraits substantiels de celle-ci ne doivent être imprimés ou autrement reproduits sans son autorisation.

0-612-22997-1



**University of Alberta**

**Library Release Form**

**Name of Author:** Robert Andrew Jenkins

**Title of Thesis:** Development and Testing of Porous VYCOR Membrane Reactors  
for the Oxidative Dehydrodimerization of Propylene

**Degree:** Doctor of Philosophy

**Year this Degree Granted:** 1997

Permission is hereby granted to the University of Alberta Library to reproduce single copies of this thesis and to lend or sell such copies for private, scholarly, or scientific research purposes only.

The author reserves all other publication and other rights in association with the copyright in the thesis, and except as hereinbefore provided, neither the thesis nor any substantial portion thereof may be printed or otherwise reproduced in any material form whatever without the author's prior written permission



---


3702 - 45 St.  
Red Deer, Alberta  
T4N 1J4

September 30, 1997

**University of Alberta**

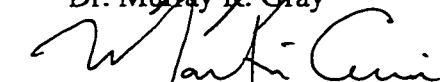
**Faculty of Graduate Studies and Research**


The undersigned certify that they have read, and recommend to the Faculty of Graduate Studies and Research for acceptance, a thesis entitled "Development and Testing of Porous VYCOR Membrane Reactors for the Oxidative Dehydrodimerization of Propylene" submitted by Robert Andrew Jenkins in partial fulfillment of the requirements for the degree of Doctor of Philosophy in Chemical Engineering.

  
\_\_\_\_\_  
Dr. David T. Lynch

  
\_\_\_\_\_  
Dr. Karl T. Chuang

  
\_\_\_\_\_  
Dr. Murray R. Gray

  
\_\_\_\_\_  
Dr. Martin Cowie

  
\_\_\_\_\_  
Dr. Kevin J. Smith

Date: SEPTEMBER 30, 1997

## Abstract

This thesis describes the development, design and construction of a unique porous VYCOR membrane reactor and its application to the oxidative dehydrodimerization (ODHD) of propylene.

A novel method of treating porous VYCOR glass membranes to substantially decrease the tendency of the membrane to promote reactions between propylene and oxygen has been developed. The method involves sequential treatment of the membrane in aqueous NaOH and high temperature steam and results in the removal of most of the acid characteristics of the membrane pores. A shell and tube type membrane reactor has been constructed from the treated membrane. The tube section of the reactor is constructed of both treated VYCOR and quartz tubing. Traditional glass working techniques cannot be applied in this case, so a new method to bond treated VYCOR to quartz has been developed called the "shrink wrap" method.

The membrane reactor has some residual activity which promotes oxidation of propylene under operating conditions. The extent of these reactions is governed primarily by the permeability of the membrane, particularly to propylene. The membrane permeability is controlled by Knudsen diffusion.

The effectiveness of the membrane reactor in Inert Membrane Packed Bed Reactor (IMPBR) mode is compared to a standard tubular reactor for ODHD of propylene using  $\text{Bi}_2\text{O}_3$  as a catalyst. The membrane reactor is designed to maintain the oxygen

concentration in the catalyst bed at a low but constant level over the entire length of the reactor. A study of the kinetic behaviour of the catalyst indicates that the low oxygen concentration will increase the selectivity of the catalytic reactions to the desired product, 1,5-hexadiene. Experimental results verify that a 10-20% (relative) increase in selectivity is possible using the membrane reactor in IMPBR mode.

The effectiveness of the membrane reactor technology used in Catalytic Membrane Reactor (CMR) mode for ODHD of propylene has been compared to the tubular reactor using  $\text{In}_2\text{O}_3$  as a catalyst. CMR mode proves to be less effective than the tubular reactor.

## **Acknowledgement**

I would like to acknowledge and thank my supervisor, Dr. David T. Lynch, and others in the Department of Chemical and Materials Engineering for their guidance, support and patience as I plotted a tortuous and somewhat tortured path through graduate school. Thank you for letting me find my own way.

I would also like to acknowledge the skill, craftsmanship and ingenuity of Mr. Peter Lea and Mr. Murray Connors of the Technical Services Glass Blowing Shop. Without their interest and efforts my work would not have been possible.

The financial support provided by NSERC, the Department of Chemical and Materials Engineering, Petro-Canada, the University of Alberta, the Teagle Foundation and Dr. Lynch were greatly appreciated.

To those who have traveled with me through graduate school, Kevin Dorma, Sean Sanders, Dave Spagnolo and Alan Ayasse, I thank you for the friendship, moral support and understanding of what we have all gone through.

I would like thank my parents and family for their love, support and encouragement and for continuing to believe in me even when I had stopped doing so.

Most of all, I would like to thank my wife Pamela for her unwavering love and encouragement. Without her support I would not have succeeded and I owe her a world of gratitude and love.

## Table of Contents

Chapter 1 - Introduction.....	1
1.1 Light Hydrocarbon/Oxygen Reactions .....	1
1.2 Oxidative Dehydrodimerization of Propylene .....	7
1.3 Membrane Reactors .....	11
1.3.1 Membrane Types .....	12
1.3.2 Membrane Reactor Uses .....	16
1.4 Goals of the Research .....	19
1.5 Structure of the Thesis .....	20
Chapter 2 - Review of the Literature .....	22
2.1 Oxidative Dehydrodimerization of Propylene .....	22
2.1.1 Catalysts.....	24
2.1.2 Reaction Mechanism.....	31
2.1.3 Kinetic Models.....	36
2.2 Inorganic Membrane Reactors.....	40
2.2.1 Dense Membranes.....	40
2.2.2 Porous Membranes.....	46
Chapter 3 - Experimental Equipment and Methods.....	52
3.1 Experimental Equipment .....	52
3.1.1 Reactor System (excluding membrane reactor).....	52
3.1.2 Feed Gas Supply .....	52
3.1.3 Feed Gas Metering and Control.....	52
3.1.4 Electrical Resistance Tube Furnace .....	58
3.1.5 Instrumentation and Data Collection .....	59
3.1.6 Remaining Hardware .....	59
3.1.7 Gas Chromatograph and Analytical Method for Gaseous Streams.....	60
3.2 Experimental Procedures (Reaction) .....	72
3.2.1 Packed Bed, Tubular Reactor Test Protocol:.....	73
3.2.2 Membrane Reactor Test Protocol: .....	74
3.3 Experimental Procedures/Equipment (Study of Catalysts).....	76
3.3.1 X-Ray Diffraction (XRD):.....	76
3.3.2 Surface Area and Pore Size Distribution: .....	77
3.3.3 Thermogravimetric Analysis (TGA): .....	77
3.3.4 Energy Dispersive X-Ray Analysis (EDX) .....	77
3.4 Experimental Procedures (Treatment of Reactor Composition Data) .....	77

## Table of Contents (cont'd)

Chapter 4 - Design and Construction of a Porous VYCOR Membrane Reactor.....	80
4.1 Key Characteristics of a Porous Membrane.....	80
4.1.1 Permeability and Selectivity .....	81
4.1.2 Inertness of the Membrane.....	85
4.1.3 Strength and Stability of the Membrane .....	86
4.2 Key Characteristics for an ODHD of Propylene Membrane Reactor.....	87
4.3 Selection of a Membrane Material.....	88
4.3.1 Screening of Potential Candidate Materials.....	88
4.3.2 Treatment of Porous VYCOR.....	93
4.4 Construction of a Porous VYCOR Membrane Reactor .....	98
 Chapter 5 - Aspects of Safety .....	 106
 Chapter 6 - Testing of Blank Membrane Reactors .....	 111
6.1 Membrane Permeability.....	112
6.2 Membrane Catalytic Activity.....	121
6.2.1 Test Conditions .....	121
6.2.2 Evaluation of Activity Caused by the Shell.....	123
6.2.3 Results of the Reaction Tests.....	125
6.2.3.1 Conversion of Propylene.....	126
6.2.3.2 Selectivity to Carbon Oxides .....	133
6.2.3.3 Selectivity of Other Product Species .....	143
6.3 Other Aspects of Reactor Operation.....	144
6.4 Changes in Membrane Permeability.....	146
6.5 Limits to Propylene Diffusion .....	148
6.6 Modeling of the Results.....	152
 Chapter 7 - Reaction Tests with Bismuth (III) Oxide as a Catalyst.....	 154
7.1 Catalyst and Reaction Parameter Evaluation.....	154
7.1.1 Description of the Catalyst.....	154
7.1.2 Description of the Tests .....	155
7.1.3 Propylene Kinetic Tests .....	156
7.1.3.1 Description of the Tests .....	156
7.1.3.2 Activation Energy Evaluation.....	157
7.1.3.3 Kinetic Model Order (Power Law).....	163
7.1.4 1,5-Hexadiene Tests.....	166
7.1.4.1 Description of the Tests .....	166
7.1.4.2 Evaluation of Potential Mass Transfer Limitations .....	168
7.1.4.3 Heterogeneous and Homogeneous Reactions.....	169
7.1.4.4 Evaluation of Reaction Kinetics .....	173

Table of Contents (cont'd)

7.2	External Mass Transfer Limitations Evaluation .....	179	
7.3	Evaluation of the Stability of the Catalyst .....	180	
7.4	Membrane Reactor and Tubular Reactor Results .....	182	
7.4.1	Description of the Experimental Regime.....	182	
7.4.2	Issues Surrounding IMPBR Data.....	183	
7.4.3	Comparison of IMPBR and Tubular Reactor Operation .....	188	
7.5	Supporting Bi <sub>2</sub> O <sub>3</sub> in the Pores of the VYCOR Membrane Reactor.....	197	
7.5.1	Preparation of the Membrane with Supported Catalyst.....	198	
7.5.2	Testing of Supported Bismuth .....	201	
Chapter 8 - Investigation of Catalytic Membrane Reactor Mode of Operation using Indium (III) Oxide .....			207
8.1	Finding an Appropriate Catalyst.....	208	
8.1.1	Tin (IV) Oxide .....	208	
8.1.2	Thallic Oxide .....	208	
8.1.3	Indium (III) Oxide.....	211	
8.2	Comparison of CMR Mode to a Tubular Reactor using an In <sub>2</sub> O <sub>3</sub> Catalyst .....	214	
8.2.1	Description of Operating Conditions .....	214	
8.2.2	Discussion of Reaction Test Results.....	218	
Chapter 9 - Conclusions and Recommendations .....			224
9.1	Conclusions.....	224	
9.1.1	Equipment.....	224	
9.1.2	Catalysts.....	226	
9.1.3	Evaluation of Membrane Reactor Technology .....	227	
9.2	Recommendations.....	228	
9.2.1	Membrane Reactor Development .....	228	
9.2.2	Study of Bi <sub>2</sub> O <sub>3</sub> as a Catalyst .....	229	
9.2.3	Membrane Reactor Operation.....	229	
References.....			230
Appendix A - Working with Porous VYCOR Glass .....			241
Appendix B - Blank Membrane Reactor Reaction Data.....			248
Appendix C - Reaction Data for Tests Involving Bi <sub>2</sub> O <sub>3</sub> .....			278
Appendix D - Reaction Data for Indium (III) Oxide Tests.....			318
Appendix E - Fortran Code for Data Collection Program (OPTO 22).....			330



## List of Tables

Table 2.1 - Single Metal Oxide Catalysts for ODHD of Propylene .....	25
Table 3.1 - Analysis of Propylene Feed Gas.....	54
Table 3.2 - Typical Operating Ranges for Feed Gases .....	55
Table 3.3 - Flow Meter Calibration Equations .....	57
Table 3.4 - Elution Times for Components in Reactor Effluent.....	69
Table 3.5 - Composition of Primary Calibration Gas .....	70
Table 3.6 - GC Calibration Correlations.....	72
Table 4.1 - Standard Reaction Conditions .....	89
Table 4.2 - Membrane Material Bulk Reaction Test Results.....	89
Table 4.3 - Results of Standard Reaction Test from Corning Treatments.....	96
Table 4.4 - Pore Size and Surface Area of Treated and Untreated VYCOR.....	97
Table 5.1 - Limits of Flammability of Propylene at Atmospheric Pressure and Room Temperature.....	107
Table 6.1 - Constants for Equation 6.1 .....	113
Table 6.2 - Selectivity Trends for Ethylene, Acrolein and 1,5-Hexadiene in the Blank Membrane Reactor.....	144
Table 6.3 - Physical properties of Propylene-Helium System.....	150
Table 6.4 - Mass Velocities and Reynolds Numbers of Propylene-Helium System .....	150
Table 6.5 - Partial Pressure Difference Across the Thin Film for the Propylene-Helium System.....	151
Table 7.1 - Operating Parameters for Propylene Kinetic Tests over Bi <sub>2</sub> O <sub>3</sub> .....	156
Table 7.2 - Measured Activation Energies for Formation of 1,5-Hexadiene and CO <sub>2</sub> from Propylene over Bi <sub>2</sub> O <sub>3</sub> .....	158
Table 7.3 - Measured Power Law Exponents for Formation of 1,5-Hexadiene and CO <sub>2</sub> from Propylene and Oxygen over Bi <sub>2</sub> O <sub>3</sub> .....	163
Table 7.4 - Operating Parameters for 1,5-Hexadiene Reaction Tests over Bi <sub>2</sub> O <sub>3</sub> .....	167
Table 7.5 - Comparison of Catalyst and non-Catalyst Tests for 0.188 mol% 1,5-Hexadiene and 6 mol% Oxygen in the Feed.....	171
Table 7.6 - Measured Activation Energies for Formation of CO <sub>2</sub> and Benzene from 1,5-Hexadiene over Bi <sub>2</sub> O <sub>3</sub> .....	174
Table 7.7 - Measured Power Law Exponents for Formation of CO <sub>2</sub> and Benzene from 1,5-Hexadiene and Oxygen over Bi <sub>2</sub> O <sub>3</sub> .....	178
Table 7.8 - Operating Parameters for Membrane and Tubular Reactor Tests using Bi <sub>2</sub> O <sub>3</sub> Catalyst.....	183
Table 7.9 - Bismuth Loaded "Catalytic Membrane Reactor" Initial Reaction Test .....	201
Table 8.1 - Operating Parameters for Membrane and Tubular Reactor Tests using In <sub>2</sub> O <sub>3</sub> Catalyst .....	215
Table 8.2 - Size Distribution of Crushed VYCOR used for In <sub>2</sub> O <sub>3</sub> Support.....	215

## List of Figures

Figure 1.1 - Homogeneous, Non-Tortuous Membrane.....	14
Figure 1.2 - Asymmetric Non-Tortuous Membrane.....	14
Figure 1.3 - Asymmetric Composite Membrane.....	15
Figure 1.4 - Flow Reactor with Continuous Differential Feed of One Component.....	18
Figure 2.1 - Formation of Surface $\pi$ Complex.....	33
Figure 2.2 - Formation of Surface Allylic Radicals.....	33
Figure 2.3 - Surface Re-oxidation.....	34
Figure 3.1 - Schematic Drawing of Experimental Equipment.....	53
Figure 3.2 - Ten Port Valve in ON and OFF Positions.....	63
Figure 3.3a - Typical TCD Chromatogram of ODHD of Propylene Reactor Effluent.....	68
Figure 3.3b - Typical FID Chromatogram of ODHD of Propylene Reactor Effluent.....	68
Figure 3.4 - Saturator for GC Calibrations.....	71
Figure 4.1 - Transport Through Porous Membranes.....	82
Figure 4.2 - Effect of Pore Size on Diffusion Mode in Pores.....	83
Figure 4.3 - Adhesive Bonded Membrane Reactor Prototype.....	101
Figure 4.4 - Shrink Wrap Construction Process.....	102
Figure 4.5 - Dimensions of Membrane Reactor Tube Assembly.....	103
Figure 4.6 - Membrane Reactor Details.....	105
Figure 5.1 - Flammability Limits for Propylene-Air-Nitrogen System at 1 atm and 26°C.....	108
Figure 5.2 - Flammability Limits for Propylene-Helium-Oxygen System at 1 atm, 26°C and 530°C.....	109
Figure 6.1a - Relative Contributions of Knudsen and Surface Flow for Oxygen and Helium in VYCOR.....	114
Figure 6.1b - Estimates of Relative Contributions of Knudsen and Surface Flow for Propylene in VYCOR.....	115
Figure 6.2 - Effect of Steam Treatment on Membrane Permeability to Oxygen.....	116
Figure 6.3 - Oxygen Permeation Rates through a Fully Treated Membrane (Variation with Temperature).....	117
Figure 6.4 - Oxygen and Helium Permeation Rates through a Fully Treated Membrane at 23°C.....	118
Figure 6.5 - Propylene Conversion in the Blank Membrane Reactor (250 sccm Total Flow, 20% Propylene) as a Function of Temperature and Oxygen Feed Concentration.....	127
Figure 6.6 - Propylene Conversion in the Blank Membrane Reactor (125 sccm Total Flow, 10% Propylene) as a Function of Temperature and Oxygen Feed Concentration.....	128
Figure 6.7 - Propylene Conversion in the Blank Membrane Reactor (250 sccm Total Flow, 4% Oxygen) as a Function of Temperature and Propylene Feed Concentration.....	131
Figure 6.8 - Propylene Conversion in the Blank Membrane Reactor (125 sccm Total Flow, 3% Oxygen) as a Function of Temperature and Propylene Feed Concentration.....	131

## List of Figures (cont'd)

Figure 6.9 - Relative Propylene Conversion in the Blank Membrane Reactor (20% Propylene, 4% Oxygen) as a Function of Temperature and Total Feed Flow Rate .....	132
Figure 6.10 - Absolute Propylene Conversion in the Blank Membrane Reactor (20% Propylene, 4% Oxygen) as a Function of Temperature and Total Feed Flow Rate .....	132
Figure 6.11a - Propylene Selectivity to CO and CO <sub>2</sub> in the Blank Membrane Reactor (250 sccm Total Flow, 20% Propylene) as a Function of Temperature and Oxygen Feed Composition .....	135
Figure 6.11b - Propylene Selectivity to CO <sub>x</sub> in the Blank Membrane Reactor (250 sccm Total Flow, 20% Propylene) as a Function of Temperature and Oxygen Feed Composition.....	135
Figure 6.12 - Propylene Yield to CO and CO <sub>2</sub> in the Blank Membrane Reactor (250 sccm Total Flow, 20% Propylene) as a Function of Temperature and Oxygen Feed Composition.....	136
Figure 6.13a - Propylene Selectivity to CO and CO <sub>2</sub> in the Blank Membrane Reactor (125 sccm Total Flow, 4% Oxygen) as a Function of Temperature and Propylene Feed Composition.....	137
Figure 6.13b - Propylene Selectivity to CO <sub>x</sub> in the Blank Membrane Reactor (125 sccm Total Flow, 4% Oxygen) as a Function of Temperature and Propylene Feed Composition .....	138
Figure 6.14 - Propylene Yield to CO and CO <sub>2</sub> in the Blank Membrane Reactor (125 sccm Total Flow, 4% Oxygen) as a Function of Temperature and Propylene Feed Composition .....	139
Figure 6.15a - Propylene Selectivity to CO and CO <sub>2</sub> in the Blank Membrane Reactor (15% Propylene, 6% Oxygen) as a Function of Temperature and Total Feed Flow Rate .....	140
Figure 6.15b - Propylene Selectivity to CO <sub>x</sub> in the Blank Membrane Reactor (15% Propylene, 6% Oxygen) as a Function of Temperature and Total Feed Flow Rate .....	140
Figure 6.16 - Propylene Yield to CO and CO <sub>2</sub> in the Blank Membrane Reactor (15% Propylene, 6% Oxygen) as a Function of Temperature and Total Feed Flow Rate .....	141
Figure 7.1 - Arrhenius Plot for 1,5-Hexadiene Formation from Propylene over Bi <sub>2</sub> O <sub>3</sub> .....	159
Figure 7.2 - Arrhenius Plot for CO <sub>2</sub> Formation from Propylene over Bi <sub>2</sub> O <sub>3</sub> .....	160
Figure 7.3 - Conversion and Selectivity with respect to Temperature with 0.196 mol% 1,5-Hexadiene, 2 mol% Oxygen in Feed .....	169
Figure 7.4 - Conversion and Selectivity with respect to 1,5-Hexadiene Feed Concentration with 2 mol% Oxygen in Feed at 540°C.....	170
Figure 7.5 - Conversion and Selectivity with respect to O <sub>2</sub> Feed Concentration with ~0.2 mol% 1,5-Hexadiene in Feed at 540°C .....	170
Figure 7.6 - Arrhenius Plot for CO <sub>2</sub> Formation from 1,5-Hexadiene over Bi <sub>2</sub> O <sub>3</sub> .....	175

### List of Figures (cont'd)

Figure 7.7 - Arrhenius Plot for Benzene Formation from 1,5-Hexadiene over Bi <sub>2</sub> O <sub>3</sub> .....	176
Figure 7.8 - Variation in Conversion of Propylene and Oxygen over Bi <sub>2</sub> O <sub>3</sub> with Feed Flow Rate (W/F = 0.01024, 10 mol% Propylene and 3 mol% Oxygen in Feed) .....	180
Figure 7.9 - Propylene Conversion and Product Selectivities During Catalyst Stability Test (W/F = 0.01024, T=540°C, 10 mol% Propylene and 3 mol% Oxygen in Feed) .....	181
Figure 7.10 - Effect of Membrane Temperature Correction on 1,5-Hexadiene Selectivity .....	187
Figure 7.11 - Fraction of Propylene Conversion due to Membrane Reactions during Membrane Reactor with Catalyst Tests.....	187
Figure 7.12 - Catalyst Bed Temperature Profiles (250 sccm Total Flow, 15 mol% Propylene and 3 mol% Oxygen in Feed, 490°C Nominal Furnace Temperature).....	190
Figure 7.13 - Product Selectivity for Membrane and Tubular Reactor Configurations as a Function of Temperature (250 sccm Total Flow, 20 mol% Propylene and 6 mol% Oxygen in Feed).....	192
Figure 7.14 - Product Selectivity for Membrane and Tubular Reactor Configurations as a Function of Oxygen Feed Concentration (250 sccm Total Flow, 20 mol% Propylene in Feed, Mid-bed Temperature is 520°C) .....	193
Figure 7.15 - Product Selectivity for Membrane and Tubular Reactor Configurations as a Function of Propylene Feed Concentration (187.5 sccm Total Flow, 3 mol% in Oxygen Feed, Mid-bed Temperature is 520°C).....	194
Figure 7.16 - Product Selectivity for Membrane and Tubular Reactor Configurations as a Function of Total Feed Flow Rate (15 mol% Propylene and 4 mol% in Oxygen Feed, Mid-bed Temperature is 540°C).....	195
Figure 7.17 - X-ray Diffraction Pattern for High Temperature Bismuth on VYCOR.....	203
Figure 7.18 - Comparison of Standard XRD Pattern for Bismuth Silicate (Bi <sub>2</sub> SiO <sub>5</sub> ) with Experimental Bismuth-VYCOR Pattern .....	205
Figure 8.1 - EDX analysis for Indium on Scanning Electron Micrograph of Membrane Cross Section.....	216
Figure 8.2 - Changes in Propylene Conversion over the 1 wt% In <sub>2</sub> O <sub>3</sub> on Crushed VYCOR Catalyst at 480°C (7 Day Period) .....	217
Figure 8.3 - Comparison of Propylene Conversion Between Operating Modes (250 sccm Total Flow, 20 mol% Propylene and 6 mol% Oxygen in Feed).....	220

### List of Figures (cont'd)

Figure 8.4 - Comparison of Key Product Selectivities Between Operating Modes (125 sccm Total Flow, 20 mol% Propylene and 6 mol% Oxygen in Feed).....	221
Figure 8.5 - Comparison of Propylene Conversion to Acrolein Between Operating Modes (20 mol% Propylene and 6 mol% Oxygen in Feed).....	222

## List of Symbols

A	Arrhenius constant
$a_m$	Specific surface area for mass transfer
a, b	Constants for GC calibration equations (Table 3.6)
$C_i$	Concentration of component i
$D_K$	Knudsen diffusion coefficient
$D_{ij}$	Binary diffusion coefficient for component i into component j
d	pore diameter
E	Activation energy
$e^*/k$	Energy coefficient for equation 6.1
F	Molar feed rate to reactor
G	Superficial mass velocity
$\Delta G$	Gibbs free energy of reaction
$\Delta H$	enthalpy of reaction
$\Delta H_c$	enthalpy of combustion
$\Delta H_{ads}$	enthalpy of adsorption
$j_D$	Chilton-Colburn factor
K	permeability coefficient for equation 6.1
$K_i$	Adsorption equilibrium coefficient for component i
k, k', k''	Reaction rate constants
$k_g$	Mass transfer coefficient
$L_{25}, L_T$	Lower explosive limit at room temperature, at any other temperature
M	Molar mass
$n_1, n_2$	Kinetic power law exponents
P	Pressure or partial pressure
$\Delta P$	Differential pressure or differential partial pressure
$p_{fa}$	Film pressure factor
Q	Permeability
R	Gas constant
Re	Reynolds number
$Re''$	Particle Reynolds number
r	Reaction rate
$r^2$	Correlation coefficient
$S_i$	Selectivity of reaction to component i
Sc	Schmidt number
Sh	Sherwood number
$St_D$	Stanton number for diffusion
T	Temperature
t	time
$U_{25}, U_T$	Upper explosive limit at room temperature, at any other temperature
$\bar{u}$	Maxwellian velocity
W	Mass of catalyst
x	fractional conversion

## List of Symbols (cont'd)

$y_i$  Gas-phase mole fraction of component  $i$   
 $z$  distance

### Greek Symbols

$\alpha, \beta$  Constants for equation 6.1  
 $X_i$  Electronegativity of metal ions in metal oxides  
 $\delta$  Change of moles upon reaction  
 $\lambda$  Mean free path  
 $\mu$  Viscosity  
 $\theta_i$  Fractional surface coverage of component  $i$   
 $2\theta$  XRD diffraction angle

# Chapter 1

## Introduction

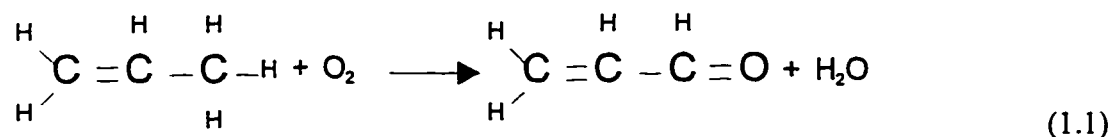
This thesis work seeks to combine a novel reactor technology, membrane reactors, and a class of ever more important, but often difficult to carry out reactions, light hydrocarbon/oxygen reactions. This introductory chapter is intended to provide some background information on both of these topics. The background should help the reader to understand why it is advantageous to investigate these two ideas together and to understand where in the overall research picture this work resides. The chapter also includes sections which explain the goals of the research and outline the structure of the thesis.

### 1.1 Light Hydrocarbon/Oxygen Reactions

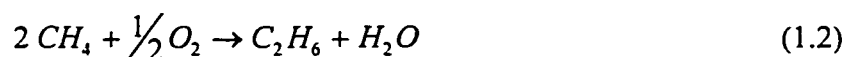
There are basically four types of reactions involving light hydrocarbons and oxygen. The first type is partial oxidation of the hydrocarbon. Partial oxidations are selective addition of one or more oxygen atoms to the hydrocarbon structure. Aldehydes, ketones, acids, ethers and alcohols are all examples of materials that can be made by direct partial oxidation of light hydrocarbon molecules. In most cases the direct partial oxidation of the hydrocarbon is the most direct route (one reaction step) for the formation of the oxygenated species. However, in many cases it is difficult to carry out the desired reaction selectively and with high yield of the desired product. This class of reactions is very often carried out with higher than stoichiometric ratio of hydrocarbon to oxygen, a hydrocarbon rich atmosphere, to increase selectivity to the desired product. One of the distinguishing features of this class of reactions is that the carbon backbone of the hydrocarbon molecule is not significantly altered, if it is altered at all, by the reaction.



For example the oxidation of propylene to acrolein does not alter the basic structure of the carbon backbone at all.



The second type of hydrocarbon/oxygen reaction is oxidative dehydrogenation (ODH) or oxidative dehydrodimerization (ODHD). Typically the dehydrogenation reactions are used to produce olefins from paraffins or diolefins from olefins. However, dehydrogenation of other types of hydrocarbon molecules is possible as is dehydrogenation of partially oxidized hydrocarbons. In all these cases water is the primary co-product rather than hydrogen. Examples of oxidative dehydrogenation reactions which are garnering research efforts at this time are ethylene production from ethane and butadiene production from 1-butene. Dimerization reactions are similar to the dehydrogenation reactions except that they combine two identical hydrocarbons by removing one hydrogen from each to allow the new carbon-carbon bond to form. Perhaps the most thoroughly investigated example of light hydrocarbon oxidative dimerization is the oxidative coupling of methane (OCM) to produce ethane.



The study of this reaction began in earnest in 1982 with the publication of work done at Union Carbide (Keller and Bhasin (1982)), and research output has been prolific in the intervening 15 years. This reaction could represent an important route for upgrading of the world's abundant, but often remote, supply of natural gas. To date it has not reached a level of technical success that allows for commercialization of the process. However, what this reaction does clearly show are the reasons for using oxygen in any of the dehydrogenation or dimerization reactions. The primary reason for using oxygen in these reactions is to remove hydrogen as water rather than as hydrogen gas. Producing water rather than hydrogen results in the reaction being exothermic, rather than endothermic as

in the non-oxidative route. Since the heat of reaction terms dominate over the entropy terms, the free energy change upon reaction is large and negative. Thus, for the oxidative reactions the thermodynamic equilibrium limit that is often encountered for endothermic dehydrogenation reactions is avoided.

To illustrate the previous point consider the production of ethylene from ethane. Non-oxidative dehydrogenation is the standard process for production of ethylene from ethane. This process has to be operated at 825°C to allow 75% one-pass conversion of ethane and is endothermic. The oxidative dehydrogenation reaction, by contrast, is exothermic with no significant thermodynamic limit, and, given the proper catalyst, can operate between 500-700°C.

The third type of hydrocarbon/oxygen interaction is oxidative reforming of hydrocarbons. This type of reaction applies most often to methane but can apply to any hydrocarbon. It is an alternative to the standard steam reforming method for producing synthesis gas. Since the reaction involves the production of carbon monoxide and hydrogen, a destruction of the basic backbone and structure of the reactant hydrocarbons occurs for hydrocarbons containing two or more carbons. It is this feature that distinguishes reforming from the partial oxidation and dehydrogenation reactions previously mentioned. Reforming results in a greater degree of oxidation of the carbon atoms than either of the previous two types of reactions.

All three of the previously listed reaction types have three very important features in common: (1) the reactions are typically carried out in hydrocarbon rich atmospheres, (2) they involve incomplete oxidation (to varying degrees) of the feed hydrocarbon, and (3) they are intended to produce usable products. By a combination of reaction conditions and catalyst all three of these types of reactions produce products that can be considered "thermodynamic intermediates". The thermodynamically most favourable reaction between a hydrocarbon and oxygen is complete combustion producing only carbon dioxide and water. Thus, any products of incomplete oxidation could be considered

intermediates. Often the most prevalent undesired reaction that occurs in parallel with these 3 reaction types is complete combustion.

The fourth reaction type is combustion. Under this category, incomplete combustion (production of carbon monoxide instead of carbon dioxide) can be considered. The goal of this reaction is either to produce the maximum amount of thermal energy possible from the hydrocarbon or to eliminate any residual hydrocarbon from a stream by producing the most innocuous products possible. In either case carbon dioxide and water are the desired products. Since complete oxidation is desired, the reaction usually operates in an oxygen rich regime. As noted above, this reaction is often an undesired side reaction, even in oxygen lean environments, when any of the first three types of reactions are desired. Often it may be one of the desired products which is more susceptible to combustion than the feed hydrocarbon component that undergoes complete oxidation. It is these complete oxidation reactions which reduce the selectivity to a desired product in a hydrocarbon/oxygen reaction process. The partial oxidation and dehydrogenation/dehydrodimerization reactions are very prone to this problem as the desired product is often more susceptible to complete combustion than are the feed materials.

Given that a number of the partial oxidation reactions and dehydrogenation reactions can be carried out via non-oxidative routes (routes not involving molecular oxygen), why would the oxidative routes be used? One very important reason, as previously noted, is that thermodynamic restrictions encountered in non-oxidative routes can be avoided. As an illustration consider the reaction that is used as a model light hydrocarbon/oxygen reaction for this thesis work, oxidative dehydrodimerization (ODHD) of propylene, and compare it with the non-oxidative route. The oxidative route is used to produce C<sub>6</sub> hydrocarbons, most predominantly the linear diolefin, 1,5-hexadiene. Other potential hydrocarbon products can be formed because 1,5-hexadiene can be further oxidized to benzene or because propylene can react with oxygen to form acrolein. Typically the oxidative route is carried out at approximately 800 K, so this temperature will be used as

the point for comparison of the two routes. Without oxygen, the normal dehydrogenation/dimerization reaction is as follows.



$$\Delta H_{298} = 21.6 \text{ kJ/mol propylene}$$

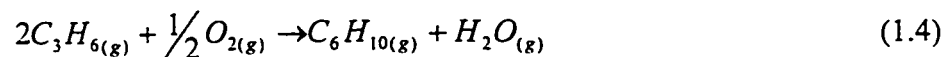
$$\Delta H_{800} = 27.2 \text{ kJ/mol propylene}$$

$$\Delta G_{298} = 26.8 \text{ kJ/mol propylene}$$

$$\Delta G_{800} = 32.4 \text{ kJ/mol propylene}$$

The Gibbs free energy change of reaction is positive and increasing with temperature indicating that equilibrium will severely limit the extent of reaction. At 800 K the maximum possible conversion of a propylene feed to 1,5-hexadiene is approximately 7.5% and the reaction is endothermic.

In contrast, the oxidative route, ODHD of propylene, is as follows.



$$\Delta H_{298} = -99.3 \text{ kJ/mol propylene}$$

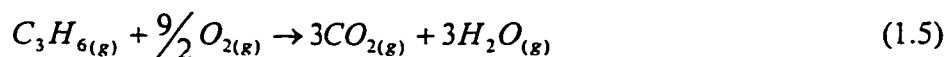
$$\Delta H_{800} = -96.0 \text{ kJ/mol propylene}$$

$$\Delta G_{298} = -87.5 \text{ kJ/mol propylene}$$

$$\Delta G_{800} = -69.4 \text{ kJ/mol propylene}$$

The Gibbs free energy change of reaction in this case is significantly negative, meaning that there is effectively no equilibrium limit at any reasonable reaction temperature. In addition the reaction is exothermic so energy need not be supplied from an external source.

The oxidative process is not without drawbacks. The primary drawback is the thermodynamic favourability of non-selective oxidation. The complete combustion of propylene has a much more negative Gibbs energy change of reaction than ODHD of propylene.



$$\Delta H_{298} = -1927.4 \text{ kJ/mol propylene}$$

$$\Delta H_{800} = -1925.2 \text{ kJ/mol propylene}$$

$$\Delta G_{298} = -1932.4 \text{ kJ/mol propylene}$$

$$\Delta G_{800} = -1943.8 \text{ kJ/mol propylene}$$

Thus if propylene and oxygen react at an elevated temperature, 800 K, then thermodynamic considerations dictate that complete combustion products would be expected to be predominant in the effluent. It must be noted that the non-oxidative route also suffers from selectivity problems because thermodynamics dictates that branched C<sub>6</sub> olefins and non-C<sub>6</sub> products are mostly likely to form.

The second drawback is less serious. Water is produced in all oxidative dehydrogenation processes instead of the hydrogen produced in simple dehydrogenation reactions. It is basically the selective oxidation of hydrogen, and hydrogen only, that makes these types of reactions successful. Oxidation of carbon atoms reduces the selectivity to the desired hydrocarbon product. Oxidation of hydrogen removes hydrogen as a product (overcoming the equilibrium limitation) and provides the energy that converts the endothermic dehydrogenation reaction into an exothermic oxidative dehydrogenation reaction. The drawback is that water is a valueless byproduct whereas hydrogen can be potentially valuable. The loss of hydrogen as a co-product must be considered when evaluating the potential economic feasibility of such a process.

Given that the primary drawback is that thermodynamic considerations dictate that combustion products are the most favoured products of light hydrocarbon/oxygen interactions at elevated temperatures, the key to success, then, is to preferentially kinetically promote the desired reactions over the combustion reactions. As engineers and experimentalists we potentially have control over four parameters that affect the rates of reaction: (1) concentration or partial pressure of the reactants, (2) reaction temperature, (3) activation energy for each of the reactions, and possibly (4) the overall order of the reaction. The first two parameters can be controlled for any reaction situation. The last two parameters require that the reactions be promoted by a catalyst. An appropriate catalyst will promote the desired reaction by reducing the activation energy of the desired reaction relative to the undesired reaction and/or by increasing the potential for the desired reaction to occur by providing “active sites” on which the reaction will selectively proceed. Having selected an appropriate catalyst, the reaction temperature can be selected to take advantage of differences in the activation energies of the competing reactions on the catalyst, and the feed concentrations can be specified to take advantage of the differences in reaction orders of the competing reactions. For example, a lower temperature and higher hydrocarbon concentration may favour a partial oxidation reaction over the complete oxidation reaction. Thus, maximizing selectivity and/or yield from the hydrocarbon/oxygen reactions requires integrating catalyst selection, reactor design and process design.

## **1.2 Oxidative Dehydrodimerization of Propylene**

As indicated in the previous section the key experimental reaction for this thesis work is the oxidative dehydrodimerization of propylene. At first glance this reaction does not seem like a natural choice as a model reaction for the study of hydrocarbon/oxygen interaction in membrane reactors. Numerous other reactions have received much more experimental attention in the literature and a number, particularly partial oxidation reactions such as production of acrolein from propylene and maleic anhydride from

butane, are used in large scale commercial processes. Thus, some explanation of the particular features of this reaction and the reasons for choosing it are in order.

The usual test of the ability of a membrane reactor to “add value” to a particular reaction is either to facilitate an increase in conversion (often overcoming an equilibrium limitation) or to increase the selectivity to the desired product or, ideally, both. In the case of hydrocarbon/oxygen interactions the goal is usually to increase selectivity. This increase in selectivity comes about primarily by reducing the opportunity for the undesired reactions to occur. Using a membrane reactor allows either one of the reactants to be kept, for the most part, separated from the other reactants and products, or for one of the products to be separated from the rest of the effluent stream. In either case the key is to prevent interaction between certain species to as large an extent as possible.

Generally in hydrocarbon/oxygen reactions, when the hydrocarbon has less stable carbon bonds and more of these types of bonds it is more susceptible to deep oxidation (disruption of the carbon backbone and oxidation of the carbon). Methane, for example, is a very stable molecule as it has only the four symmetric C:H bonds. Stability against oxidation generally decreases as the molecule becomes larger and as more unsaturated bonds appear in the molecule. Cyclic compounds and molecules with conjugated bonds deviate from this trend to some degree. If keeping oxygen and a hydrocarbon separated will help prevent deep oxidation, then the beneficial effect of keeping oxygen and a hydrocarbon apart will be most pronounced with less “stable” hydrocarbon molecules. This line of thinking leads to the conclusion that a longer hydrocarbon, and perhaps an olefin, would be an appropriate model compound for use in this type of study. Propylene is an example of such a compound.

The other advantage that larger molecules provide is that a lower temperature is required to “activate” the compound. The active species that will readily react is usually an ion or radical form of the feed species. Being able to operate at a lower temperature has two important practical advantages. The first advantage is that the reactions are much more likely to occur mainly or exclusively on the catalyst surface rather than homogeneously.

Confining the reaction to the surface makes understanding and potential analysis of the kinetics and possible reaction steps easier. Thus, a lower temperature helps simplify some of the theoretical aspects of the research. The second advantage is more practical. A lower temperature causes fewer material constraints on the membrane. A membrane will always be stronger and less catalytically active at lower temperatures and hence potential problems with the mechanical aspects of the design and the potential adverse catalytic effects of the membrane will be lessened.

Given that a larger molecule will be the model hydrocarbon, the other key question is what type of hydrocarbon/oxygen reaction to investigate: partial oxidation, dehydrogenation or dimerization. For many partial oxidation reactions involving  $C_3$  and heavier hydrocarbons there exist commercially viable catalytic processes that give very high yield at lower temperatures. The production of acrolein from propylene is an example. Existing processes provide >93% conversion with 80-90% selectivity to acrolein. There is not a great deal of room for improvement and hence investigation of partial oxidation reactions of  $C_3+$  hydrocarbons using a membrane reactor is perhaps not the best course of action for demonstrating the effectiveness of membrane reactor technology.

Dehydrogenation and dehydrodimerization reactions are very similar in nature. The key difference is that the latter involves coupling of two molecules and therefore is a more difficult reaction to carry out. It usually involves radical species (free or surface) and requires that the species exist long enough for two of them to collide (free radicals) or interact (surface radicals). The longer the life of the radical species the more likely they are to undergo additional oxidation reactions. Thus, a dimerization reaction will be a greater challenge than a simpler dehydrogenation and will hopefully show greater differences between a membrane reactor and a conventional reactor.

For both experimental and theoretical reasons, then, the oxidative dehydrodimerization of propylene appears to be an appropriate model reaction for studying the potential advantages of membrane reactor technology in light hydrocarbon/oxygen reactions. It



must be noted that other oxidative reactions, namely oxidative coupling of methane and oxidative dehydrogenation of ethane, propane and butane, have been investigated using membrane reactors. There are substantial economic reasons for investigating these processes. OCM has been viewed by many as an important potential step for upgrading the world's gas reserves and the oxidative dehydrogenation of the light alkanes provides a potentially lucrative alternative to the existing pyrolysis processes for the production of olefins. On the contrary, it may not appear that there is any sound economic/commercial reason for wanting to oxidatively produce 1,5-hexadiene - there is no large world demand for the chemical. However, selective hydrogenation of this linear diolefin will produce 1-hexene for which there is a large and growing market. The smaller linear alpha olefins ( $C_4$ - $C_8$ ), including 1-hexene, are used as comonomers in the production of polyethylene.

In areas, such as Alberta, where the polyethylene industry is large and growing, but the sources of higher  $\alpha$ -olefins are limited, a selective process to produce such chemicals from readily available feedstocks would be of considerable interest. There exist polymer supported hydrogenation catalysts for which claims of the ability to selectively hydrogenate di-olefins to olefins under mild conditions have been made. Thus, it seems that the production of 1,5-hexadiene (diolefin) would be the most difficult step in producing 1-hexene from propylene.

Existing commercial processes for producing 1-hexene from lower hydrocarbons suffer from poor selectivity. Institut Francais du Petrole's (IFP) Dimersol process produces primarily non-linear olefins and the linear olefin product distribution (what little there is) matches the thermodynamic equilibrium distribution meaning that there is little 1-hexene production (Andrews and Bonnifay (1977)). The oligimerization of ethylene (a process based on a Ziegler aluminum based catalyst or a proprietary nickel complex catalyst (Shell)) (Modler et al. (1997)) produces  $\alpha$ -olefins, but the primary product is 1-butene with smaller quantities of 1-hexene and 1-octene being produced. A geometric distribution of the products is encountered in some processes whereas a more uniform product distribution, at least up to  $C_{12}$  or  $C_{14}$ , is encountered in other processes (Modler et al. (1997)). Most of these process operate at pressures in excess of 30 MPa and

temperatures between 150-300°C. A Fischer-Tropsch synthesis route is employed by Sasol that produces 1-hexene along with other  $\alpha$ -olefins and linear paraffinic material (Fenton (1996)). The selectivity is not high because a Schultz-Flory distribution of products is encountered, but in Sasol's case, the throughput is very large so a significant amount of 1-hexene is produced. Most of the products of this process are in the gasoline and wax fractions. Thus the lower pressure, higher selectivity oxidative route may provide a feasible alternative to existing processes.

### 1.3 Membrane Reactors

The concept for a membrane reactor is very simple. The idea is that the ability of a membrane to permeate one or more species can be exploited to give "enhanced" reactor performance. That is, better performance than is possible with a standard reactor design. The "enhanced" reactor performance can be defined in a number of ways. It can mean a greater selectivity to a desired product, greater conversion of a reactant, or both, leading to higher yield of a product. Enhanced performance can also mean greater stability at normal operating conditions. It could mean the elimination of hot spots in the reactor, safer operation, or possibly that the separation of products can occur simultaneously with reaction, eliminating the need for other processing steps.

Membrane reactor technology could be termed an emerging technology. It has been long known (since Thomas Graham discovered, in 1866, that palladium could selectively adsorb large amounts of hydrogen (Graham (1866))) that membranes exist and could be an important part of chemical processing industries. However it was not until the 1940's that membrane technology was exploited on the industrial scale. Beginning in the 1940's membranes were used for separation of uranium isotopes by gas phase separation of  $U^{235}F_6$  from  $U^{238}F_6$  (Gillot (1991)). The enriched uranium product was necessary for the atomic weapons industry which flourished in that period and later for the nuclear energy industry. The membranes were used based on the ability of the membrane to cause different rates of gas diffusion through the membrane for different molecules. It was not until the late 1960's and early 1970's that papers began to appear in the open literature

regarding the use of membranes in reaction engineering. The amount of work in this area has been increasing steadily with time and with advances in a variety of membrane construction/preparation technologies. Today membranes are routinely used for gas separation and liquid filtering operations. However, after 25-30 years of research effort, the use of membranes in reaction technology has not yet progressed beyond the laboratory stage. It has shown great promise in a number of areas, but to date technological challenges still prevent application of this technology on a larger scale. In this sense, then, the technology must be considered as emerging.

### 1.3.1 Membrane Types

A membrane can be defined as a semipermeable barrier between two phases which prevents intimate contact of the two phases. The barrier must be permselective. That is, it must restrict the movement of molecules in a very specific way. Most commonly this permselectivity is obtained by size exclusion (molecular sieving) or by differences in diffusion coefficients among species. However differences in electrical charge, differences in solubility, or differences in adsorption or reactivity on internal surfaces can also give rise to permselectivity. The barrier (membrane) can be solid, liquid or gas but for the purposes of this thesis all discussions will assume that the membrane is a solid.

Solid membranes can be classified by two criteria: structure of the solid and material of construction. The structure of the solid is either dense or porous. A dense membrane has no pores at all. The permeability of such a membrane must arise from solid state diffusion of atomic species or ionic conduction of ionic species. The key characteristics of dense membranes are that they usually have very high selectivity (often only being permeable to a single species), but have very low permeability. There are three common types of dense membranes. The first type is the dense metal membrane which is most often produced as a thin metal foil or a film supported on another substrate. Common examples are palladium or palladium alloy membranes which are permeable only to hydrogen (Shu et al. (1991)), and silver or silver alloy membranes which are only permeable to oxygen (Anshits et al. (1989)). The second type of dense membrane is a

solid oxide electrolyte membrane. These membranes are usually only permeable to a single ionic species. Most often the species is  $O^{2-}$  which allows the membrane to permeate oxygen. PbO and a variety of rare earth oxides are also examples of solid oxide electrolyte membranes (Nozaki et al. (1992)). The third type of dense membrane is a liquid immobilized membrane in which liquid is trapped or immobilized in the pores of a substrate so that the pores are completely filled (Baker (1995)). The liquid then serves as the semipermeable medium.

A porous membrane, naturally, has pores. The pores are typically designated as macropores (pore diameter,  $d_p$ , greater than 50 nm), mesopores ( $d_p = 2-50$  nm) or micropores ( $d_p < 2$  nm) (Sing et al. (1985)). Porous membranes can have pore diameters that range in size from hundreds of microns down to a few nanometres and it is the pore size that dictates the appropriate applications for each membrane. It is the pores that give rise to permeability in porous membranes. The permselectivity is obtained by either molecular sieving (for very small pore size), differences in diffusion coefficients, or by size exclusion/filtering (for separation of molecular species from larger particles, viruses for example, in materials with larger pores). The key characteristics that differentiate porous membranes from dense membranes are that porous membranes have much higher permeability but very often lower selectivity. The permeability of a very small-pore porous membrane to hydrogen is typically 2 orders of magnitude greater than a dense membrane of similar thickness. The permeability of a porous membrane increases dramatically with increasing pore size. By its nature, however, a porous membrane can never be 100% selective for one gaseous species, and selectivity generally decreases as permeability increases.

There are a four basic types of porous membranes. The first type is perhaps the simplest and consists of relatively non-tortuous, uniform pores and is shown in Figure 1.1. This degree of homogeneity is possible in a single material using a technique such as anodic oxidation of aluminum for manufacturing an anodic oxide film membrane. The work by Furneaux et al. (1987) is an example. The second type of porous membrane is also made of a single material and has a relatively narrow pore size distribution. It differs from the

first type, primarily, because the pore structure is very tortuous or spongy. This type of membrane is most commonly made by mixing two materials to make a solid with two "phases", then removing one phase to leave a pore structure within the remaining solid. Two examples of this approach to construction are porous glass membranes which are formed by leaching out one phase and carbon sieve or silica membranes which can be made by controlled pyrolysis of a polymeric precursor containing the carbon or silica. It is possible to construct membranes with very small pores using these methods. The third basic type of membrane is an asymmetric membrane constructed of a single material. In this case asymmetric means that the properties of the pores change across the thickness of the membrane. The same anodic oxidation technique used to make the first type of membrane listed above is employed. Processing parameters are altered to form the pores in the different layers. A schematic representation of this type of membrane is shown in Figure 1.2.

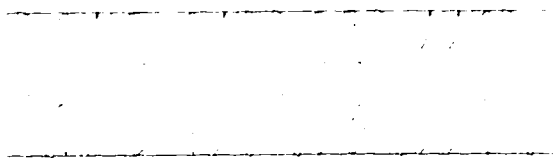


Figure 1.1 Homogeneous, Non-Tortuous Membrane

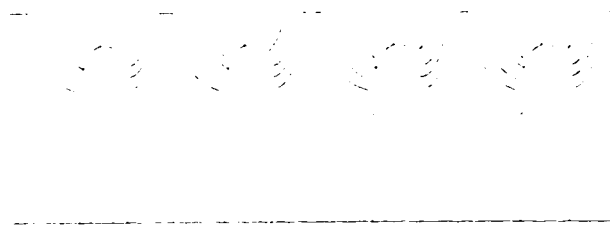


Figure 1.2 Asymmetric Non-Tortuous Membrane

The fourth type of porous membrane is the asymmetric composite membrane as shown schematically in Figure 1.3. These membranes have layers of different sized particles, although often each layer is made from the same substance. Most often it is ceramic membranes that are made in this manner. The largest particles form the support layer. This layer is often more than a millimetre thick and has pores that are usually 1-10  $\mu\text{m}$  in diameter. The intermediate layer is 10-100  $\mu\text{m}$  thick and has pores with a diameter of 50-

500 nm. It is the top layer that controls the permeability and selectivity of the membrane even though it typically contains less than 1% of the total pore volume of the membrane. This layer can be less than 1  $\mu\text{m}$  thick, but typically has a thickness between 1-10  $\mu\text{m}$ . The pore diameter of this top (separation) layer is typically 2-50 nm. These types of membranes are made by successive deposition of smaller and smaller particles on the coarse support material. Both sol-gel and slip casting methods have proven successful for the construction of crack/pin-hole free membranes, particularly when made of alumina.

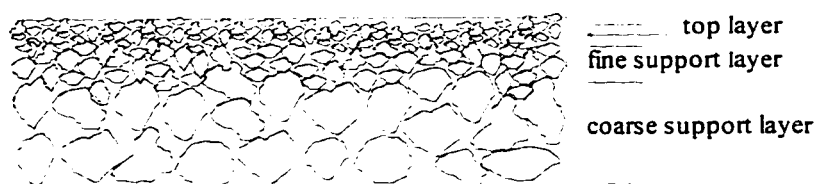


Figure 1.3 Asymmetric Composite Membrane

Solid membranes can be very broadly classified into two categories based on the material of construction: organic and inorganic. Organic membranes are polymeric in nature and inorganic membranes are made of metal, glass or ceramic (metal oxide).

Organic membranes represent the bulk of all commercially available membranes at this time and have had a reasonably long history of commercial use. In the early 1930's nitro-cellulose membranes became available for microfiltration applications, primarily water treatment (Baker (1995)). This application was one of the few uses of membrane technology until the 1960's. The discovery of a method for the production of asymmetric organic membranes made it possible to use organic membranes for more microfiltration applications, for ultrafiltration, for reverse osmosis and for electro dialysis (Baker (1995)). All of these applications involve the separation of material from a liquid phase. In the 1980's use of polymeric membranes for large scale industrial gas separation became common (Baker (1995)). Finally, in the 1990's these types of membranes are being used for pervaporation applications such as alcohol dehydration (Baker (1995)).

The characteristic that all these applications have in common is that they are carried out at, or near to, ambient temperature. Since the organic membranes are made of polymers such as polypropylene, cellulose acetate, nitro-cellulose and polyamides, they have mechanical and structural problems when subjected to elevated temperatures. It is for this very reason that organic membranes (at least as they exist today) will have few applications as membrane reactors. One exception to this rule may be for biotechnology applications or reactions catalyzed by enzymes (which are also destroyed by high temperatures). It is certain, however, that organic membranes cannot be used to carry out high temperature gas-phase reactions in the presence of oxygen. As a result, organic membranes have been excluded from consideration in this research work and will not be discussed further in this thesis.

In contrast to organic membranes, most inorganic membranes do not have thermal degradation problems until very high temperatures are reached. In this sense, they are the only type of membrane that could be suitable for the high temperature oxygen/hydrocarbon reactions to be investigated in this thesis. The characteristics which determine exactly what type of membrane best suits a particular membrane reactor application are discussed in Chapter 4 of this thesis.

### 1.3.2 Membrane Reactor Uses

The key characteristic that a membrane brings to a reactor system is the ability to selectively add or remove one or more species in a reaction mixture. Thus membrane reactor uses can be classified as either removal of a species from a reaction or addition of a species to a reaction.

There are two reasons why it is desirable to remove a species from a mixture of reactants and products. The first reason is that the species is the desired product and that it is somewhat unstable, that is, prone to further reaction/degradation. Thus that species should be removed from the reactor as quickly as possible to prevent degradation. The

second reason to remove a species is to help shift an equilibrium limited reaction further toward the desired products.

Whether or not membrane reactor technology is appropriate for a specific example of either of these two cases, removal of an unstable product or shifting of equilibrium, depends on whether the desired species can be preferentially separated from the rest of the reaction mixture. Flux of a species across a membrane is governed by the product of concentration driving force and diffusion coefficient. The type of diffusion that predominates dictates the functional form of the overall flux expression with respect to temperature and pressure. Except for dense metal membranes which are 100% selective for either hydrogen (palladium membranes) or oxygen (silver membranes) and some dense oxide ionic conductors, all other inorganic membranes allow the permeation of more than one species. The difference in diffusion coefficients, given that all species are at the same temperature and total pressure conditions, depends on molar mass and in some cases on the affinity of the species to the surface of the membrane pores. That is, smaller molecules diffuse more quickly and hence will be preferentially separated from other species. Generally speaking, smaller molecules are usually less prone to reaction than larger ones and so are not likely to be an "unstable" product. As a result membrane reactors are not used for separation of unstable products.

Membrane reactors, however, have been considered and tested in numerous instances for situations described in the second case, shifting of an equilibrium reaction constraint. In every instance the reactions considered are either dehydrogenation reactions or decomposition reactions in which one of the products is hydrogen. In all cases it is hydrogen that is selectively removed across the membrane (Shu et al. (1991).

Addition of a species to a reaction mixture across a membrane is theoretically the same as a flow reactor with an infinite number of feed points located axially along the reactor. This scenario is pictured in Figure 1.4



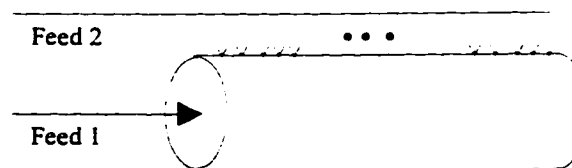


Figure 1.4 Flow Reactor with Continuous Differential Feed of One Component

In this instance only one species is added and thus the addition really is not “selective”. It is the capacity of the membrane to distribute the material evenly along the axial length that is being exploited rather than the permselectivity of the membrane. There are three key reasons why this approach may be preferable to other approaches. The first reason is to increase the selectivity to a desired product by controlling the concentration of a reactant species that, while necessary for promoting the desired reaction, also plays a role in unwanted side reactions. The second reason is to keep two species apart that could cause safety concerns when combined in certain concentration ranges. Avoiding operation within explosive limits is an example of this case. The third reason for using a distributed feed is that in some instances a more uniform rate of reaction throughout the reactor can be maintained. In so doing, more uniform temperature profiles can be maintained in the reactor, avoiding hot spots in the case of exothermic reactions. Examples of this use of a membrane reactor typically involve selective oxygenation or hydrogenation reactions where the concentration of oxygen or hydrogen in the reaction mixture needs to be kept at a low level to increase the selectivity to a desired product.

As a generic example of a selective oxidation reaction, consider the reaction of a component, A, with oxygen to produce a desired product, B, and an undesired product, C. If the rates of the two competing equations can be described by power law expressions (equations 1.6 and 1.7) in the region of interest, then the relative instantaneous, or point, selectivity to the desired product compared with the undesired product is given by equation 1.8.

$$r_B = k_1 C_A^m C_{O_2}^n \quad (1.6)$$

$$r_C = k_2 C_A^p C_{O_2}^q \quad (1.7)$$

$$\text{relative pt.select.} = \frac{r_B}{r_C} = \frac{k_1}{k_2} C_A^{m-p} C_{O_2}^{n-q} \quad (1.8)$$

If the desired reaction is assumed to be of greater order in A and lesser order in B than the undesired reaction ( $m > p$ ,  $n < q$ ), then at any particular point in a reactor the relative point selectivity can become very large (very high selectivity to the desired product) if the oxygen concentration is kept very low. Very high selectivity can be achieved in a normal tubular reactor, but the low oxygen feed rate necessary to keep the overall oxygen concentration low would severely limit the extent of reaction of A and yield of B. By contrast, in a membrane reactor the oxygen concentration can be maintained at a low level, but the oxygen is continuously fed so that it is not depleted and the extent of reaction of A can be much greater with high yields of B.

#### 1.4 Goals of the Research

The purpose of this study is to undertake the design and operation of a novel catalytic reactor, namely a membrane reactor, for use in investigating hydrocarbon/oxygen reactions, with the gas-phase oxidative dehydrodimerization of propylene selected as the model reaction. Since the focus is on the reactor design and operation, there is no catalyst development as such. Instead, catalysts that have proven to be relatively active and selective for the reaction are used so that some of the potential operating advantages of the novel reactor can be investigated. In particular bismuth oxide is used as a catalyst. Previous work in the literature indicates that ODHD of propylene is first order with respect to propylene and approximately zeroth order with respect to oxygen. Limited information on  $\text{CO}_2$  production (the undesired reaction) on the bismuth oxide catalyst indicates that the reaction kinetics are positive order with respect to both propylene and oxygen. Thus, following the example outlined at the end of Section 1.3.2, it is expected that the membrane reactors will help overcome some of the limitations and drawbacks associated with standard reactor designs.

Thus, the specific objectives of the project are as follows.

1. Development of a single, on line method for the analysis of all the components in the reactor effluent stream.
2. Design and construction of functional membrane reactors that are capable of withstanding the temperatures and pressures of the reaction and will be relatively inert with respect to conversion of the reactants and products.
3. Development of reactor operating configurations, including the method of placement of catalyst in the reactor, to exploit the potential of the membrane reactor.
4. Test the reactor configurations with respect to a variety of operating parameters in an attempt to better understand how the reactors work and to attempt to find "optimal" operating conditions where conversion, selectivity or yield is maximized.
5. Comparison of membrane reactor results to those of conventional flow reactors when applicable.

### **1.5 Structure of the Thesis**

This thesis has three major sections. The first section is introductory and background material and consists of the introduction (Chapter 1) and the literature review (Chapter 2). The literature review focuses on the two major topics in the thesis: ODHD of propylene and inorganic membrane reactors. The second section describes the design and development of the experimental equipment. Chapter 3 is devoted to the experimental equipment (excluding the membrane reactor), the analysis equipment and method, and the experimental protocols used for reaction testing. Chapter 4 is devoted to the design and construction process for the membrane reactor itself. Chapter 5 is a short chapter containing a discussion of one of the key safety aspects of this project.

The third major section is used to describe and discuss reaction tests. There are three chapters in this section. Chapter 6 is dedicated to reaction testing of the membrane reactor without any catalyst - blank testing. Chapter 7 is a very extensive chapter which discusses ODHD of propylene with a bismuth oxide catalyst. Aspects of the ODHD

reaction over this catalyst are discussed as well as performance of a tubular flow reactor and the membrane reactor in carrying out the reaction with the bismuth catalyst. Chapter 8 is a much shorter chapter describing reaction testing using indium oxide as the catalyst. This testing was carried out to demonstrate some aspects of membrane reactor operation that could not be adequately demonstrated with the bismuth oxide catalyst. The thesis is concluded with a brief chapter covering the key conclusions and recommendations drawn from this research effort.

## Chapter 2

### Review of the Literature

This literature review is divided into two distinct sections addressing the two key aspects of the research project: oxidative dehydrodimerization of propylene and inorganic membrane reactors. In addition to serving as a survey of the relevant literature in each of these areas this chapter also serves to highlight and discuss some topics that provide important technical and scientific background information, but that are not explored further in the research. This type of discussion is most prevalent in the information surrounding ODHD of propylene.

#### 2.1 Oxidative Dehydrodimerization of Propylene

There have been two relatively comprehensive reviews of the literature in the field published in the last twenty years. The first review by Mamedov (1981), originally published in Russian, covers work to that date and puts a greater emphasis on work being carried out by the author and his co-workers in the Soviet Union. The second review is one chapter in a larger review of oxidative coupling of hydrocarbons by Sokolovskii and Mamedov (1992). This review covers some extra key material published after the first review and provides a more balanced and complete approach to the subject.

The first appearance of the study of the oxidative dehydrodimerization of propylene in the literature occurred in the American patent literature. These patents were filed in the late 1960's and were granted in the early 1970's. The patents were assigned to Allied Chemical Corp. (Greene et al. (1970)), Dow Chemical (Friedli (1970, 1973)), Gulf Research and Development Company (Bozik et al. (1973a, 1973b)), Atlantic Richfield

Company (Lipsig (1971), D'Alessandro and Mitchell (1974)) and Standard Oil Company of Ohio (Jones (1974)).

Academic papers began to appear shortly after the initial patent applications detailing catalyst testing and development efforts. Catalyst development and study of the kinetics of the reaction were the main thrust of work on this reaction through to the mid-1970's. From that point until the early to mid-1980's efforts were applied to determining and modeling the reaction kinetics and reaction mechanism over the most favourable catalysts. However, by 1987 there was almost no new work on the topic being published. In fact since that time only 4 papers have appeared. This decade long void is due to the fact that the reaction had run its course of study. Catalysts had been thoroughly investigated to see if commercial advantage seemed feasible - it did not. The academic aspects of the reaction (kinetics, mechanism, surface aspects of the catalyst) have been covered in some depth and other more potentially commercially viable challenges confronted researchers in these areas.

The previous statements beg the question: "Why study this reaction further?" The answer is two fold. There are some academic aspects of the reaction that are either not well elucidated or are ignored in the open literature. In addition there are some reactor engineering approaches to the problems that have not been tried that may make the reaction more feasible, even though it seems that catalysis has taken the problem as far as it will go.

The following sections outline the key aspects of the existing literature on ODHD of propylene. They also include some discussion on how or why the existing information is incomplete and/or insufficient. From the presented information, key aspects of the ODHD reaction that are important to the present research are described.

### 2.1.1 Catalysts

Both homogeneous and heterogeneous catalysts exist for dimerization of propylene. The homogeneous catalysts are organometallic, liquid phase or gel-immobilized catalysts, the most successful of which are nickel-based materials. The review by Pillai et al. (1986) covers this material in great depth. This type of catalyst, however, is not an oxidative dimerization catalyst. These catalysts do not employ oxygen in the reaction and generally do not produce hydrogen. What they do produce is mostly branched six carbon olefins. The selectivity to linear olefins is low and the selectivity to 1-hexene is extremely low. Although this type of process does not meet the goals set out for this research, it does have practical uses. IFP's Dimersol process (and other similar processes) are used for dimerization and oligimerization of mixed olefin streams to make high octane blending streams for gasoline (Andrews and Bonnifay (1977)).

Successful ODHD of propylene is carried out as a gas phase, heterogeneously catalyzed reaction. With only rare exception the catalysts are metal oxides or mixed metal oxides. These rare cases have involved the use of a molten mixture of tin and bismuth metal as the catalyst (Jones, 1974), reaction over solid sodium bismuthate (Lipsig, 1971) and reaction over a supported silver catalyst (Vermel' et al., 1973). Although patents were filed for two of these three processes, there is no further evidence of development on any of these three options.

The results of the screening of a large number of single metal oxides as potential catalysts for ODHD of propylene are presented in the early patent literature and a handful of key academic papers. Table 2.1 outlines the single metal oxides that have been tested, test temperature, selectivity to the various products and the source of the information. The materials are grouped into three categories based on the relative acid characteristic of the surface of the material. In Table 2.1 the classification of the degree of acidity of the metal oxide is based on metal ion electronegativity,  $X_i$ , as per Seiyama et al. (1972a). Acidic oxides have values of  $X_i > 10$  and basic oxides are those with  $X_i < 6.5$ . Amphoteric oxides are electronegativity values between acidic and basic values.

Table 2.1 - Single Metal Oxide Catalysts for ODHD of Propylene

Oxide	Temperature	Selectivity to CO <sub>x</sub>	Selectivity to acrolein	Selectivity to C <sub>6</sub> products	Reference
<b>ACIDIC</b>					
MoO <sub>3</sub>	500°C	76.4	25.1	0	Seiyama et al. (1972a)
Sb <sub>2</sub> O <sub>4</sub>	500°C	63.3	16.3	0	Seiyama et al. (1972a)
V <sub>2</sub> O <sub>5</sub>	500°C	81.8	14.2	0	Seiyama et al. (1972a)
TiO <sub>2</sub>	500°C	85.8	12.0	0.3	Seiyama et al. (1972a)
Fe <sub>2</sub> O <sub>3</sub>	500°C	86.9	12.2	trace	Seiyama et al. (1972a)
SiO <sub>2</sub>	500°C	46.7	8.6	trace	Seiyama et al. (1972a)
WO <sub>3</sub>	500°C	90.0	6.3	0.9	Seiyama et al. (1972a)
Al <sub>2</sub> O <sub>3</sub>	500°C	38.5	42.1	0	Seiyama et al. (1972a)
<b>AMPHOTERIC</b>					
ZnO	500°C	49.2	0.5	48.2	Seiyama et al. (1972a)
Bi <sub>2</sub> O <sub>3</sub>	500°C	89.4	0	9.6	Seiyama et al. (1972a)
	575°C	28	0	72	Bozik et al. (1973b)
In <sub>2</sub> O <sub>3</sub> *	500°C	93.4	0.8	4.1	Seiyama et al. (1972a)
	500°C	34	0	63	Trimm & Doerr (1970)
SnO <sub>2</sub> *	500°C	91.5	3.2	2.5	Seiyama et al. (1972a)
Ga <sub>2</sub> O <sub>3</sub>	500°C	83.9	0.9	2.0	Seiyama et al. (1972a)
PbO	493°C	24	0	76	Greene et al. (1970)
CdO	500°C	98.5	0.8	0.1	Seiyama et al. (1972a)
	650°C	30	0	70	Greene et al. (1970)
Th <sub>2</sub> O <sub>3</sub>	520°C	22	0	78	Trimm & Doerr (1970)
	500°C	41	0	59	Greene et al. (1970)
<b>BASIC</b>					
CuO *	500°C	92.5	3.8	0	Seiyama et al. (1972a)
Co <sub>3</sub> O <sub>4</sub> *	500°C	96.2	2.2	0	Seiyama et al. (1972a)
NiO *	500°C	75.7	2.3	0	Seiyama et al. (1972a)
MnO <sub>2</sub>	500°C	97.5	0.7	0	Seiyama et al. (1972a)
Cr <sub>2</sub> O <sub>3</sub>	500°C	69.3	2.1	4.0	Seiyama et al. (1972a)
GeO <sub>2</sub>	500°C	99.9	0	0	Seiyama et al. (1972a)
CaO	500°C	86.5	0	0	Seiyama et al. (1972a)
MgO	500°C	94.0	trace	0	Seiyama et al. (1972a)
CeO <sub>2</sub>	500°C	94.0	trace	0	Seiyama et al. (1972a)

\* = very active

C<sub>6</sub> products include both 1,5-hexadiene and benzene

If the sum of the selectivities does not equal 100 (as in Seiyama et al. (1972a) in some instances) it is indicated that other products, "ethylene, acetaldehyde and so on", were formed.



The work by Seiyama et al. (1972a) was done under a set of standard conditions (feed stream composition of 9% propylene, 18% oxygen, balance inert; reaction run to give 25% conversion of propylene) which were certainly not optimal for high selectivity for non-combustion products. That is why the results in some of the other references look so good in comparison. However, what the Seiyama work gives is a consistent reference point and it is still very clear what some of the key characteristics of a good catalyst should be. Examination of Table 2.1 indicates that the amphoteric oxides provide the highest selectivity towards dimerization products. Carbon oxides, as a result of deep oxidation are also produced, but some combinations of catalyst and operating conditions can give selectivity to C<sub>6</sub> hydrocarbons approaching 100%. Basic catalysts primarily produce deep oxidation products (CO<sub>2</sub> and H<sub>2</sub>O). Acid catalysts tend to form acrolein as the primary hydrocarbon product. Other oxygenates including acetaldehyde are formed in smaller amounts. In addition the acid catalysts tend to promote cracking of propylene to produce methane, ethylene and ethane and the resultant formation of carbonaceous deposits (coke) on the catalyst. Some explanation of how surface acidity affects the interaction of reactants and products with the surface, and thus determines product composition, is given in the discussion of the reaction mechanism.

Discussions of the important characteristics of a catalyst for the ODHD of propylene appear in Mamedov (1979, 1981, 1984), Sokolovskii and Mamedov (1992) and Seiyama et al. (1972a). These authors focus on three key properties. The first property, as noted above, is the acid/base nature of the surface. Increased acidity will increase the strength with which the olefin will be attracted to the acid centre on the catalysts. A very strong attraction will mean that the resulting surface species will have limited mobility and this in turn will decrease the likelihood of recombination to form dimers. Thus a strongly acid surface is not desired, but a surface which has some basic characteristics would be better. That is a surface that is weakly acidic, amphoteric or weakly basic is best. Hand in hand with the strength of an acid centre is the nucleophilic nature of the adjacent oxygen ions. These ions must be nucleophilic enough to remove a proton from the adsorbed olefin, but not so nucleophilic that the proton cannot be subsequently easily removed as the site is re-oxidized. A slightly basic characteristic is required, but it

cannot be too strong. Again, amphoteric oxides provide the correct balance of characteristics. Sokolovskii and Bulgakov (1977) refer to oxides having "optimum nucleophilicity" as being the best for promoting dimerization.

The second characteristic is a n-type rather than p-type semiconductive nature. The electron donating nature of propylene and the ease with which electrons can move within an n-type semiconductor mean that this type of oxide has a greater affinity for propylene than oxygen and thus the propylene to oxygen ratio at the surface will be higher. This higher ratio should decrease the selectivity to complete combustion. One notable exception is  $\text{Bi}_2\text{O}_3$  which is a p-type semiconductor. White and Hightower (1981) have investigated the electrical properties of bismuth oxide as they relate to the ODHD of propylene. They concluded that  $\text{Bi}_2\text{O}_3$  takes on some n-type characteristics under reaction conditions.

The third characteristic is relatively high strength of oxygen bonding to the surface of the catalyst. It must be noted that there is a somewhat blurry line between oxygen atoms which are part of the metal oxide lattice and oxygen atoms or  $\text{O}_2$  which are chemisorbed on the surface of the catalyst. Weakly held oxygen is easily converted into  $\text{CO}_2$  and hence decreases selectivity to the desired product. The mixed Bi-Sn oxide catalysts have a stronger oxygen bond than  $\text{Bi}_2\text{O}_3$  and hence have a higher selectivity to hydrocarbon products (Mamedov and Pankrat'ev (1982)). On the surface of these active, selective catalysts under steady-state reaction conditions all of the "loosely" bonded surface oxygen has been removed and it is only the strongly chemisorbed/lattice oxygen that participates in the reaction. Gamid-Zade et al. (1979) determined for  $\text{Bi}_2\text{Sn}_2\text{O}_7$  that under normal reaction conditions the extent of surface reduction is approximately 70-80% and the remaining oxygen has a bond strength (uniform) of  $\sim 377$  kJ/mol. A fully oxidized surface is characterized by the presence of surface oxygen with a bond energy of  $\sim 209$  kJ/mol.

A fourth property that is sometimes alluded to but rarely noted as extremely important is the specific surface area of the catalyst. This property concerns the bulk structure of the

catalyst rather than detailed electronic or catalytic properties of the atoms on the catalyst surface. As such it has tended to be ignored or downplayed in studies of catalysts. However it can play an important role in the effectiveness of the reaction and hence must be considered. Effective ODHD of propylene catalysts generally have very low specific surface areas ( $< 1 \text{ m}^2/\text{g}$ ). Propylene, and in particular, surface activated propylene radicals are substances that are very susceptible to chemical attack. High surface area materials have very extensive and fine pore structures that can trap propylene for extended periods (this is really an internal mass transfer problem) and greatly increase the likelihood of conversion to coke or oxidation products. The analogy also applies to the products of the dimerization reaction, particularly 1,5-hexadiene. It is a "less stable" compound than propylene and is more readily converted to undesired products. In addition it is a larger molecule than propylene and will suffer from even greater diffusion problems in very small pores than will propylene.

The preceding discussion is based primarily on single oxide catalysts. However, the important characteristics of the catalysts can be applied equally well to catalysts with more than one component. Tailoring of the properties of successful single oxide catalysts by addition of other components was the route that investigators took in trying to find more successful catalysts. Mixing of two oxides was the most popular and fruitful method for investigating more complex catalysts. In all cases the materials are either unsupported catalysts or are supported on very low surface area carriers.

Early work on mixed oxide catalysts is disclosed in a patent by Friedli (1970) where a supported manganese/sodium oxide catalyst is used. Investigation of bismuth-phosphorous catalysts and a variety of catalysts using bismuth oxide combined with another oxide are first described by Seiyama et al. (1970). A full disclosure of these results is given by Seiyama et al. (1972b). This paper serves as the first and perhaps most wide ranging study of mixed metal oxide catalysts for ODHD of propylene. They studied bismuth oxide in a variety of mixtures and tin (IV) oxide in a variety of mixtures as follows:

a)  $\text{Bi}_2\text{O}_3 - \text{MO}_x$

where  $\text{MO}_x = \text{MoO}_4, \text{TiO}_2, \text{NiO}, \text{Sb}_2\text{O}_4, \text{SiO}_2, \text{Fe}_2\text{O}_3, \text{Al}_2\text{O}_3, \text{CdO}$

b)  $\text{SnO}_2 - \text{MO}_x$

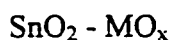
where  $\text{MO}_x = \text{Li}_2\text{O}, \text{Na}_2\text{O}, \text{K}_2\text{O}, \text{MgO}, \text{CaO}, \text{BaO}, \text{P}_2\text{O}_5, \text{As}_2\text{O}_5, \text{Sb}_2\text{O}_4, \text{MoO}_3, \text{WO}_3$

The most promising of the group was the Bi-Ti catalyst.

Disclosures in the American patent literature by Bozik et al. (1973a, 1973b) continued the investigation of Bi-Ti catalysts as well as some mixed oxides of bismuth and either iron, zirconium or tin (Bozik et al. (1973a)). They found that the bismuth-titanium catalysts performed marginally better than the other mixed oxide catalysts. However, even though the Bi-Ti catalysts performed well, they presented no significant advantages over  $\text{Bi}_2\text{O}_3$  alone.

In 1974 Vaabel' et al. (1974b) carried out further testing of Bi-P catalysts to determine if the ratio of metals affected catalyst performance. A patent (Vaabel' (1974a)) was granted based on this work. In the same year, Seiyama et al. (1974) tested the  $\text{Bi}_2\text{O}_3\text{-SnO}_2$  catalyst with  $\text{Bi/Sn} = 1$ . This catalyst was to become the most popular mixed oxide catalyst for ODHD of propylene and the one by which other catalysts could be judged. Solymosi and Bozsó (1977) confirmed the effectiveness of this catalyst and determined that a new and active component,  $\text{Bi}_2\text{Sn}_2\text{O}_7$ , was responsible for the activity of the catalyst.

Mamedov et al. (1978) tested a series of mixed oxides containing tin (IV) oxide to determine the effect of surface acidity on the ODHD reaction. The study was very similar in nature to the study of Seiyama et al. (1974), although for the most part a different set of second oxides were used. In this case the systems were



where  $\text{MO}_x = \text{TiO}_2, \text{Bi}_2\text{O}_3, \text{In}_2\text{O}_3, \text{Cr}_2\text{O}_3, \text{PbO}, \text{CdO}, \text{ZnO}, \text{V}_2\text{O}_5, \text{Sb}_2\text{O}_4, \text{MoO}_3$

This research group came to the same conclusion that Seiyama et al. (1974) and Solymosi and Bozsó (1977) had, namely that the bismuth-tin oxide was the best mixed oxide catalyst. Subsequently this group carried out an extensive study of the catalyst and its characteristics and published numerous papers in both English and Russian. It must be noted that several of the papers appeared in very similar form in both languages.

However, the key papers involve the study of:

- a) experimental kinetics (Mamedov et al. (1979), Gamid-Zade et al. (1979))
- b) kinetic model (Mamedov et al. (1978a))
- c) reduction and re-oxidation of the surface of the catalyst (Mamedov et al. (1981))
- d) bond energy of the surface oxygen (Mamedov and Pankrat'ev (1982))
- e) reaction mechanism (Mamedov (1984))

Work on catalyst development for ODHD of propylene has slowed dramatically in the last 15 years. All work has been focused on development of mixed oxide catalysts and since 1984 only five papers have been published on the topic. Di Cosimo et al. (1986b) investigated the use of a  $\text{Bi}_2\text{O}_3\text{-La}_2\text{O}_3$  catalyst that served as both catalyst and dense oxide conductor membrane. This work will be discussed in greater depth later in this chapter when the topic of membrane reactors is covered. The researchers patented this work (Di Cosimo et al. (1986a)). Azgui et al. (1995) duplicated the work of Di Cosimo et al. (1986b) and found slightly different results. Wang et al. (1988, 1989) investigated bismuth-cerium catalysts and found that a Bi/Ce=1 atomic ratio gave the best catalyst, but that it was still outperformed by the Bi-Sn catalyst with which it was compared. Ramarosan et al. (1992) studied mixed bismuth-zinc oxide catalysts. They determined that for these catalysts the highly selective, active species is  $\text{Bi}_{48}\text{ZnO}_{73}$ . Under optimum

conditions (very high propylene:oxygen in the feed) the catalyst gives 64% selectivity to 1,5-hexadiene.

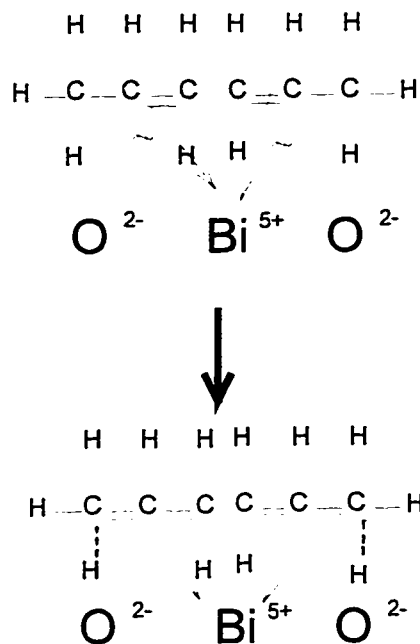
Although the use of mixed oxide catalysts have produced catalytic materials that perform better than the best single oxide catalyst, bismuth oxide, the improvements have not been dramatic. The enhancements come mainly from adjusting the bond strength of the oxygen bonds under reaction conditions and from altering the acid/base characteristics of the surface to an "optimum" level. It seems apparent, at least to this author, that gains in catalyst productivity or selectivity may not arise from a new catalyst, but rather from alternate utilization of existing catalysts. This line of thinking leads to the use of membrane reactors for carrying out the reaction. At the outset of this project, one of the goals involved supporting catalysts in the pores of a porous membrane. Since it was not clear that a mixed oxide material could be formed and then supported in the pores of a membrane, the decision, early in the project was made to avoid the use of mixed metal oxide catalysts.

### 2.1.2 Reaction Mechanism

In the simplest form the reaction that occurs to form dimers of propylene is a reduction-oxidation (redox) mechanism that takes place on the surface of the catalyst. It is the lattice oxygen (or tightly bound surface oxygen) that is directly involved in the hydrocarbon activation and subsequent formation of water. Gaseous oxygen then re-oxidizes the reduced catalyst surface. Since it is the lattice oxygen of the metal oxide which interacts with the hydrocarbon, numerous researchers have investigated using metal oxide as both catalyst and oxidant. That is, the reaction occurs in the absence of gaseous oxygen and then the catalyst is regenerated in either a separate step or a separate vessel in the presence of gaseous oxygen but the absence of hydrocarbon. Swift et al. (1971) using  $\text{Bi}_2\text{O}_3$ , Solymosi and Bozsó (1977) with a Bi-Sn catalyst, and Kaliberdo et al. (1979) with  $\text{TiO}_2$ ,  $\text{SnO}_2$  and  $\text{Bi}_2\text{O}_3$  are all example of researchers having taken this approach. From an understanding of the reaction mechanism it is clear why this approach can be successful in some cases.

Researchers have proposed reaction mechanisms for a variety of catalysts. Trimm and Doerr (1971, 1972) for  $Tl_2O_3$  and  $In_2O_3$ , Solymosi and Bozsó (1977) for  $SnO_2$ , Seiyama et al. (1974) and Mamedov (1984) for  $Bi_2O_3-SnO_2$  catalysts, and White and Hightower (1983) for  $Bi_2O_3$  have all proposed mechanisms. Although there are small differences in the mechanisms, all the authors agree on the basic steps. The generally agreed upon mechanism, as illustrated using bismuth oxide, is as follows:

1. Adsorption of propylene on a metal cation on the catalyst surface. Depending upon the catalysts and the available oxidation states of the metal, the two necessary propylene molecules may adsorb on the same metal site or on adjacent sites, and if they adsorb on the same site the adsorption may be sequential or simultaneous. Since this is not the rate determining step, it is difficult to discriminate between possible mechanisms in some cases. For indium (III) oxide, thallic oxide and bismuth oxide, the available oxidation states are  $M^{n+}$  and  $M^{(n+2)+}$  so both propylene molecules must adsorb on the same metal site (presumably relatively simultaneously). The metal centre (cation acting as a Lewis acid site) attracts electrons from the propylene  $\pi$ -bond and the nucleophilic  $O^{2-}$  adjacent to the metal ion attracts a hydrogen of the carbon in the  $\alpha$  position to the double bond. This step is shown in Figure 2.1.

Figure 2.1 Formation of Surface  $\pi$  Complex

2. As the nucleophilic oxygen attracts the proton from the adsorbed propylene molecule, the C-H bond is cleaved and the result is a surface hydroxyl group and an adsorbed carbanion. The breaking of the C-H to form the adsorbed carbanion is generally agreed to be the rate determining step in the reaction as demonstrated by Driscoll and Lunsford (1983). The carbanion very quickly transfers an electron to the metal cation (actually in the pictured scheme both propylene molecules must transfer an electron at the "same" time since the only stable oxidation states for bismuth are  $\text{Bi}^{3+}$  and  $\text{Bi}^{5+}$ ) to become an adsorbed allylic radical. This step is shown in Figure 2.2.

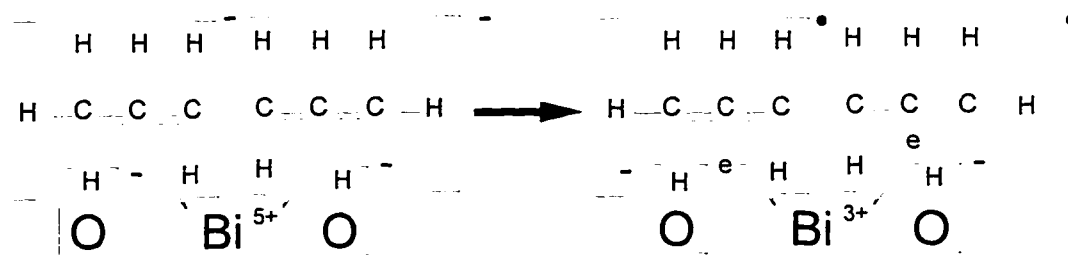


Figure 2.2 Formation of Surface Allylic Radicals



3. The combination of the allylic radicals (head to head) to form 1,5-hexadiene can theoretically happen in a number of ways. The simplest way to is combine on the catalyst surface and then desorb as 1,5-hexadiene. It has also been suggested that the radicals can desorb and recombine in the gas phase to form the diallyl. There is some evidence that this homogeneous radical reaction can occur over  $\text{Bi}_2\text{O}_3$  (Martir and Lunsford (1981)). The degree to which it will occur is dictated by operating conditions and the presence or absence of free gas volume. A closely packed reactor (especially with quartz chips as inert packing) almost completely eliminates the free radicals from the gas phase. It is also possible that the free radicals undergo propagation reactions producing, in particular, allylperoxide radicals from which partial oxidation products result. The production of free radicals becomes more pronounced at temperatures greater than  $550\text{ }^\circ\text{C}$  as the bond between the surface and the adsorbed radicals weakens.
4. Two surface hydroxyls will react to form water, which is rapidly desorbed, and a lattice vacancy. Gaseous oxygen will adsorb and be transformed to fill the vacancy as follows.

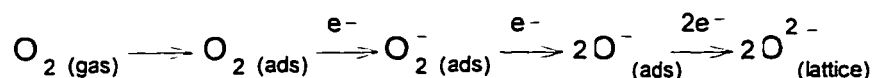


Figure 2.3 Surface Re-oxidation

In so doing, the two electrons are drawn out of the 3+ bismuth oxidation state to restore the 5+ oxidation state. The re-oxidation of the catalyst is a very rapid step.

Although the preceding example of the reaction mechanism involves both propylene molecules adsorbing and reacting on one metal cation site, it is possible with different catalysts that the adsorption of the two molecules may occur on different sites. It is also possible that an adsorbed radical will interact with a gas phase propylene molecule to produce diallyl (Mamedov et al. (1978a)).

It must be noted that this general mechanism is not very different from the proposed mechanisms for partial oxidation of propylene to acrolein and ammoxidation of propylene to acrylonitrile. The catalysts for these reactions are also mixed metal oxides often containing bismuth. The primary difference is that the partial oxidation reactions occur on the more acidic metal centres of the partial oxidation catalysts. In the partial oxidation case, the acid sites are considered to be Lewis acids (electron acceptors). The stronger Lewis acid centres will cause the electron rich  $\pi$ -bonded propylene to lose two electrons to form a positive ion (instead of the anion to radical mechanism of dimerization). The positively charged propylene undergoes the same nucleophilic attraction to a neighbouring  $O^{2-}$  that the proton of the  $\alpha$ -carbon did in the dimerization case and in this case an oxygenated product (primarily acrolein) is formed. The importance of the acid-base nature of the surface is plain.

It has been postulated, particularly by Trimm and Doerr (1972), that benzene, as the other primary dimerization product, is formed from 1,5-hexadiene in a very similar fashion to the original production of the dimer from propylene. The diene would adsorb on a fresh active centre in a bidentate fashion with each of the terminal double bonds donating an electron to the metal. A cyclic  $C_6$  molecule, 1,3-cyclohexadiene, would be formed. It is also possible to form 1,3,5-hexatriene at this stage which is quickly, thermally converted into the cyclic diene (Lewis and Steiner (1964)). Finally the cyclic diene will interact with a new active site, where two more hydrogen atoms are removed and benzene is formed. No large quantities of 1,3-cyclohexadiene are ever reported in ODHD of propylene tests. Benzene is a much more stable product.

There is much less written in the literature on the mechanism for the formation of carbon oxides, mostly carbon dioxide, over ODHD of propylene catalysts. Mamedov et al. (1979) suggest that carbon dioxide is produced from propylene on a second type of active centre that involves loosely bound atomic oxygen and/or gaseous oxygen. It is suggested that the propylene is converted to carbon dioxide very rapidly through intermediate compounds of the carbonate-carboxylate type. However, other work from this research group, Gamid-Zade et al. (1979), indicates that the selectivity to  $CO_2$  varies little as the

surface is reduced. If the surface is being reduced one would expect that the weakly bonded oxygen is disappearing and hence the selectivity to CO<sub>2</sub> should drop dramatically.

In their work on bismuth oxide and mixed bismuth oxides Kaliberdo et al. (1979) note that some of the product CO<sub>2</sub> must be the result of conversion of the dimer product. White and Hightower (1983) experimented with carbon-13 labeled propylene and unlabelled 1,5-hexadiene using oxygen-free pulse experiments over Bi<sub>2</sub>O<sub>3</sub>. They determined that the hexadiene:propylene combustion ratio was 2.22:1. Although this makes it clear that hexadiene is likely the source of a portion of the carbon dioxide in the product (>80% in this case), it does not really suggest a mechanism or predict how the reaction would occur in the presence of oxygen. They are able to come to no other conclusion except that CO<sub>2</sub> is formed as a result of “series-parallel reaction pathways involving propylene and all other hydrocarbon products”.

### 2.1.3 Kinetic Models

A variety of kinetic models for the ODHD of propylene have been proposed by investigators for a number of catalysts. Swift et al. (1971) and Trimm and Doerr (1972) have used power law expressions. Several Langmuir-Henshelwood type schemes have also been proposed. Seiyama et al. (1974) proposed a mechanism for a Bi-Sn catalyst that assumed the surface dimerization reaction to be rate limiting and only considered adsorption of propylene on the surface. The expression takes the form of equation 2.1.

$$r = k \left[ \frac{KP}{1 + KP} \right]^2 \quad (2.1)$$

where P is the partial pressure of propylene

Trimm and Doerr (1972) suggest a dual site mechanism for indium oxide in which two propylene molecules adsorb simultaneously on one site and dissociative oxygen

adsorption occurs on a different site. The reaction is inhibited by both diallyl and acrolein (another product on  $\text{In}_2\text{O}_3$ ). This expression takes the form:

$$r = k \left[ \frac{K_p C_p}{1 + K_p C_p + K_H C_H + K_A C_A} \right]^2 \left[ \frac{K_o C_o}{(1 + \sqrt{K_o C_o})^2} \right] \quad (2.2)$$

where the subscripts P, H, A and O represent propylene, 1,5-hexadiene, acrolein and oxygen respectively

Although this is the expression Trimm and Doerr present, it must be noted that the Langmuir-Henshelwood expression for reaction between two adsorbed propylene molecules and one dissociatively adsorbed oxygen atom dictates that the oxygen term (fractional surface coverage by oxygen,  $\theta_o$ ) should be as follows.

$$\theta_o = \left[ \frac{\sqrt{K_o C_o}}{(1 + \sqrt{K_o C_o})} \right] \quad (2.3)$$

No explanation for this apparent discrepancy is provided.

Mamedov et al. (1978b) suggest a mechanism for a Bi-Sn catalyst whereby oxygen and propylene adsorb competitively on the same site and the rate limiting reaction occurs between adsorbed propylene and gaseous propylene. This scheme takes the form:

$$r = k \left[ \frac{(K_p C_p)^2}{1 + K_p C_p + \sqrt{K_o C_o}} \right] \quad (2.4)$$

Mamedov later extended this work (Mamedov et al. (1979)) to consider that the reaction occurs primarily on a highly reduced surface so that the adsorption/reaction of oxygen and the surface is very rapid and that the propylene is adsorbing onto a sort of composite site which is made up of the surface metal site and an adsorbed or lattice oxygen (M-O).

The authors do not consider the kinetic model to be of the Langmuir-Henshelwood type.

The model is:

$$r = k'k'' \left[ \frac{C_p^2}{k' C_p + k'' C_o} \right] \quad (2.5)$$

White and Hightower (1983) developed a L-H model to best fit their data for ODHD of propylene using  $\text{Bi}_2\text{O}_3$  as a catalyst. The model that best fit the data is a triple site competitive adsorption model in which oxygen is associatively adsorbed.

$$r = k \left[ \frac{(K_p C_p)^2 K_o C_o}{(1 + K_p C_p + K_o C_o)^3} \right] \quad (2.6)$$

The authors clearly recognized that this model has a number of shortcomings, the primary one being the associative adsorption of oxygen. They found, however, that none of the models that considered dissociative adsorption of oxygen fit their data as well as the model based on molecular adsorption of  $\text{O}_2$ . It must be noted that they used the rate of oxygen consumption as the rate they modeled. Since oxygen reacts in at least two reactions (dimerization and propylene combustion) and likely many more (oxidation of hydrocarbon products), it seems unwise to try to model its consumption this way. This model seems to assume a single reaction and this is likely why the model does not seem logical.

White and Hightower also fit their data to a Mars-van Krevelan model and found significant scatter in the data. On this basis they tended not to favour this model. It should be noted however that the selection of exponents for propylene and oxygen are never explained and that, as before, the rate modeled was the rate of oxygen consumption.

It is widely accepted that the ODHD of propylene proceeds through an adsorbed allylic complex and that the rate determining step is a surface reaction involving the allylic complex (formation or conversion). Spectroscopic evidence has proven that the  $\pi$ -allyl complex is formed on the surface. Further work by Driscoll and Lunsford (1983) also showed that allyl radicals were formed on the surface of a  $\text{Bi}_2\text{O}_3$  catalyst. Within this framework any or all of the above models may be valid. Their validity depends on how one considers the allylic reaction step(s) to have occurred and on how one interprets the interaction between oxygen and the surface. In the end, all of these models can be appropriately reduced to generally explain the experimental data which typically shows a positive order of reaction with respect to propylene and a slightly positive to slightly negative order for oxygen. However, the reader must be cautioned that some of the hydrocarbon products, notably 1,5-hexadiene, are very susceptible to oxidation. At higher levels of conversion it may be that the oxidation of 1,5-hexadiene is significant and that that reaction partially hides the true kinetics of the dimerization reaction. It is difficult or impossible to discern from the information presented in the literature the concentration of 1,5-hexadiene in the reactor during these kinetic tests.

The development of kinetic models for the complete combustion of propylene in these systems has been much less rigorous. One of the key problems is that many forms of hydrocarbon (propylene, products and surface intermediates) and oxygen (gaseous, adsorbed and lattice) can participate in the combustion reaction. This problem often makes it very difficult to know how to model  $\text{CO}_2$  formation. Should one try to model it as purely combustion of propylene (the simplest approach) or should a more elaborate reaction network be utilized? Since the reaction has not found industrial favour and there has not been the need to precisely understand exactly how combustion is occurring, the simplest methods have in the past been selected. The kinetic model, if one is presented in the literature, is generally given as a power law expression or a very simple Langmuir-Henshelwood type expression (Mamedov et al. (1978a)). These models, although simple and in this author's opinion incomplete, have helped to elucidate some of the important points about combustion during the ODHD of propylene. It is recognized that factors such as high surface area or diffusion limitations promote complete combustion and

hence are deleterious to diallyl selectivity. It is also clear that increasing the concentration of oxygen more readily promotes combustion rather than dimerization.

## **2.2 Inorganic Membrane Reactors**

There have been 4 comprehensive reviews of this topic in the literature in the last 8 years: Armor (1989), Hsieh (1991), Saracco and Specchia (1994) and Zaman and Chakma (1994). These reviews cover methods of construction and characterization of membranes as well as reactor applications for both dense and porous membranes. In addition Hsieh (1991) and Zaman and Chakma (1994) cover modeling of membrane reactor systems. A recent monograph, by Bhave (1991), has excellent chapters on synthesis and characterization of inorganic membranes and a chapter on inorganic membrane reactors.

The review of the literature contained in this thesis will be less comprehensive and will focus on inorganic membrane reactor applications with particular emphasis on porous membranes. Some of the literature cited covers topics such as construction and characterization of membranes and modeling of membrane reactors will be cited, but the reader is referred to any of the above mentioned review sources as a starting point for finding additional information.

### **2.2.1 Dense Membranes**

As noted in Chapter 1 dense membranes allow the permeation of only one species. In practice only two components are usually permeated through dense, inorganic membranes: hydrogen or oxygen.

Applications involving hydrogen, either selective hydrogenation or dehydrogenation (including decomposition reactions that produce hydrogen), are carried out, with rare exception, using palladium or palladium alloy membranes. The use of palladium alloys is favoured because repeated adsorption and desorption of hydrogen from palladium makes the metal very brittle. This topic has very important industrial ramifications and is

presented here for sake of complete coverage of the area of inorganic membrane reactors. However, it does not have any direct bearing on the research undertaken in this thesis. As such only a limited number of examples will be presented along with a brief discussion of the state of the art and some of the challenges that will need to be overcome for this type of application to have commercial success. For a much more detailed review of the topic readers are referred to the papers by Shu et al. (1991) and Saracco and Specchia (1994), both of which cover the subject in considerable depth.

Popular and practical applications of palladium based reactors are the hydrogenation of unsaturated aliphatic and cyclic hydrocarbons. For example Gryaznov and Slin'ko (1981) investigated hydrogenation of acetylene to ethylene, Gryaznov et al. (1973) studied hydrogenation of benzene to cyclohexane, Ermilova et al. (1985) and Gryaznov and Slin'ko (1981) have studied hydrogenation of 1,3-cyclooctadiene to cyclooctene and Nagamoto and Inoue (1986) investigated 1,3-butadiene hydrogenation to butene. There are several other examples but the important features of all are as follows. The reactions generally occur at low to moderate temperatures ( $<350^{\circ}\text{C}$ ), there is no back permeation of any of the species since the membrane is permeable only to hydrogen, and the membrane serves as both selective barrier and as catalyst. This technology could also potentially be used to selectively convert 1,5-hexadiene to 1-hexene.

Dehydrogenation reactions or decomposition reactions in which hydrogen is a product have also garnered much attention. Itoh (1987) studied cyclohexane dehydrogenation to benzene while Gobina and Hughes (1994) and Gobina et al. (1995) have studied ethane dehydrogenation to ethylene and Sheintuch and Dessau (1996) have investigated propane and isobutane dehydrogenation. Uemiya et al. (1991a) investigated steam reforming of methane (hydrogen product) and Uemiya et al. (1991b) looked at the water-gas shift reaction, another hydrogen producing, equilibrium-limited reaction. All of these examples use a separate catalyst packed inside the tube of the reactor. The reactors all have a shell and tube configuration where hydrogen permeates out from the tube side to the shell side of the reactor and is carried away by a purge stream flowing in the shell. With the exception of Itoh (1987) and Sheintuch and Dessau (1996) all the reactors have



a very thin layer of palladium or palladium alloy supported on a porous substrate tube. In this way the reactor combines the strength of the porous substrate with the increased permeability of a very thin metal layer ( $<20 \mu\text{m}$ ). All of these examples were able to increase conversion to some degree over the equilibrium limit at the operating temperature.

An ingenious method of helping increase the rate of permeation across a palladium membrane in a dehydrogenation reaction is to consume the hydrogen as it permeates through the membrane. To this end the dehydrogenation reaction can be coupled with either a hydrogenation reaction or an oxidation reaction (to produce water) on the other side of the membrane. Not only is the hydrogen consumed, but heat is often provided to drive the endothermic dehydrogenation reaction. A series of papers by Itoh and co-workers (Itoh and Govind (1989), Itoh (1990), Zhao et al. (1990)) demonstrated theoretically and experimentally that this approach would work for dehydrogenation of 1-butene to butadiene coupled with hydrogen oxidation by air. Gobina et al. (1995) demonstrate the same principle (both theoretically and experimentally) for the ethane dehydrogenation to ethylene. Gobina et al. (1995) do point out, however, that the enhancement of hydrogen flux, and hence increase in conversion of the dehydrogenation reaction, is lower than predicted. The reason is that oxygen forms a palladium oxide layer on the membrane which inhibits the hydrogen flux rate by preventing recombination of permeated hydrogen atoms. In later work involving dehydrogenation of butane in their membrane reactor Gobina and Hughes (1996) found that the palladium oxidation problem could be eliminated by pre-reducing the membrane in hydrogen at high temperature.

Palladium based dense membrane reactors are perhaps the most studied and developed branch of the inorganic membrane reactor field. Work in the area has been on-going for approximately 30 years and is showing great promise. At present the primary barrier to achieving commercial success in this field is the low flux rates in such reactors. Very thin metal films are required to give sufficient hydrogen flux, but the thinner the film the greater the problems of construction and long term stability of the membrane, particularly

for dehydrogenation reactions. For this reason researchers have turned away from using metal foils and are developing membranes where the metal film is deposited on a porous substrate. Shu et al. (1991) cite a number of construction methods that have produced palladium films of thickness  $<0.1 \mu\text{m}$ , but the stability of such films is not known.

The rare exception, in the field of dense inorganic membranes, to the use of palladium membranes for selective hydrogen flux is the use of very thin silica membranes. Gavalas et al. (1989) describe the production of thin films of silica in porous VYCOR membranes by reaction of  $\text{SiH}_4$  and  $\text{O}_2$  in the pores. The two reactants travel towards each other from opposite sides of the membrane and react in a reaction plane. The reaction ceases when the pores are completely blocked by the thin film formed by reaction. This type of membrane has been used for dehydrogenation of isobutane (Ioannides and Gavalas (1993)) and for dry reforming and partial oxidation of methane (Ioannides and Verykios (1996)). However, like palladium membranes it suffers from very low hydrogen permeability even though the selectivity for hydrogen is very high ( $\text{H}_2:\text{N}_2 \approx 2000$ ). In addition the membrane is not stable in the presence of water vapour.

Dense membrane reactors based on the flow of oxygen through the membrane are more limited in scope than those used for permeation of hydrogen. The only instances where oxygen is produced and needs to be removed from a reaction involve very high temperature decomposition of water (Cales and Baumard (1982)) and decomposition of  $\text{CO}_2$  to  $\text{CO}$  (Nigara and Cales (1986)). Rather, most applications involve the addition of oxygen to a reaction. The field is even further limited by the fact that dense metal membranes have not found application here. There are only two examples in the English literature, Gryaznov et al. (1986) and Anshits et al. (1989), which describe the use of a dense silver membrane. The membrane acts as both permeator for oxygen and catalyst for reactions between oxygen and another component. Anshits et al. (1989) investigated methane coupling while Gryaznov et al. (1986) studied oxidation of ammonia to  $\text{N}_2$  and  $\text{NO}_x$  and oxidation of ethanol to acetaldehyde. In both studies the selectivity and yield to the products is higher than if oxygen is co-fed.

Solid oxide membranes such as yttria-stabilized zirconia (YSZ), calcia-stabilized zirconia (CSZ), and magnesia-stabilized zirconia (MSZ) are well known oxide ion conductors. As such they have been natural materials for oxide ion conducting membrane reactors. Both the examples listed above ((Cales and Baumard (1982) and Nigara and Cales (1986)) used CSZ tubular reactors. The earliest example of a dense oxide conducting membrane reactor for use in hydrocarbon reactions is given by Di Cosimo et al. (1986b) for the ODHD of propylene, as mentioned earlier in this chapter. A  $\text{Bi}_2\text{O}_3\text{-La}_2\text{O}_3$  catalyst was used as a membrane in disk form with oxygen containing gas fed to one side of the membrane and propylene containing gas fed to the other side. Although propylene conversion is low (3.2%) the selectivity to dimers is 78% which is significantly higher than the 39% experienced in this system when oxygen and propylene are co-fed. The authors clearly indicate that the lattice oxygen plays the primary role in the selective oxidation and that the flux of oxygen is the limiting step for this system. Azgui et al. (1995) attempted to duplicate these results but found much higher conversion of propylene with a somewhat lower selectivity. They also found that activity declined somewhat with time on stream. Closer examination of their membrane after reaction indicated that the membrane had micron size pores and cracks on the surface and the authors surmised that the much higher conversion rate was due to molecular diffusion of oxygen through these imperfections. This study clearly shows how difficult, yet how important, is the construction of defect free and stable membranes.

Within the patent literature Hazbun (1988, 1989) discloses membrane reactor systems that consist of a thin dense YSZ layer, doped with  $\text{CeO}_2$  or  $\text{TiO}_2$ , to help increase the oxide conduction characteristics supported on a porous oxide conductor (YSZ). Catalysts for various reactions are supported in the pores of the porous layer. Claims are made that this membrane reactor (with the appropriate catalyst) can be used for oxidation of ethylene or propylene to their respective oxides, oxidative dehydrogenation of 1-butene to butadiene, and oxidative coupling of methane (OCM). The results given in the patents seem to be very promising, but there has been no further published work.

All other published information on dense oxide conducting membrane reactors have involved reactions between methane and oxygen. A series of papers published by Fujimoto and co-workers detail the development of lead oxide (PbO) dense membrane systems for OCM. Omata et al. (1989) describe a PbO/MgO membrane supported on a porous alumina tube. Nozaki et al. (1992) studied PbO-K<sub>2</sub>O membranes supported on dense oxide conductors (YSZ, MSZ, CSZ), bismuth based dense membranes supported on silica-alumina porous tubes, and PbO-MgO membranes on porous alumina. They found that the latter system still produced the highest activity and selectivity (>90% to hydrocarbon products). The high activity is likely due to the fact that this system had the lowest resistance to oxygen transport (thin dense film, porous support). Nozaki et al. (1993) and Nozaki and Fujimoto (1994) provide a more detailed evaluation of the kinetics of the reactions and the role played by the transported oxide ions. They conclude that the reactions are indeed limited by the rate of oxide ion conduction and that the conduction can be accurately modeled. It is clear, however, that greater oxygen flux rates will be necessary to facilitate their use on anything but a laboratory scale. Wang and Lin (1995) have modeled OCM in a dense oxide membrane reactor assuming the catalytic surface to have the same properties as a Li/MgO catalyst and have predicted that 70% yields of C<sub>2</sub> hydrocarbons are possible. This value is well above the presently achievable value of ~25% in a conventional reactor.

More recently Balachandran et al. (1995) have studied the use of Sr-Co-Fe-O and La-Sr-Co-Fe-O dense membranes for partial oxidation of methane to synthesis gas. In this study a rhodium based reforming catalyst is used. At admittedly low methane flow rates the methane conversion is consistently in excess of 98% with approximately 90% hydrogen atom selectivity to hydrogen and 92% carbon atom selectivity to CO. These are very encouraging results.

As a final note on dense membranes it must be noted that oxide ion and proton conductors have been more successfully used in fuel cell or electrochemical applications. That is, in applications where transport is facilitated by an electromotive force (Eng and Stoukides (1991)). This area of application of membrane reactors is not covered in this

survey of the literature as the focus for this project is pressure driven transport of species rather than EMF driven transport. For information on these topics readers are referred to Saracco and Specchia (1994). Perhaps the primary drawback of dense membranes is the low permeability they afford. Most often the reaction is limited by how much material can be passed through the membrane. In cases of selective oxidation where a solid oxide is acting as both membrane and catalyst, the limited flow of oxygen leads to over-reduction of the oxide surface. The over reduction often leads to decreased catalyst activity, further decreased flux, or both.

### 2.2.2 Porous Membranes

One natural way to overcome the low permeability of dense membranes is to use porous membranes for membrane reactor applications. Whereas work on palladium membrane reactors has received considerable attention over the past 25-30 years, work on porous membrane reactors, with a few notable exceptions, has really only been in vogue for about 10 years with many advances coming very recently. Unlike dense membranes, porous membranes generally are permeable to more than one species. However, it is usually only one species that is being preferentially added or removed. In almost all cases this species is either hydrogen or oxygen, which is the same as for dense membranes.

Research work to date has used porous membranes for the selective removal of hydrogen from a reactor, but not addition of hydrogen. Early work by Kameyama and co-workers on decomposition of  $H_2S$  carried out with a VYCOR membrane (Kameyama et al. (1981)) or a  $\gamma$ -alumina membrane (Kameyama et al. (1983)) and Shindo et al. (1981) on decomposition of HI using a porous VYCOR membrane indicated that conversions well in excess of equilibrium conversion could be achieved if hydrogen could be selectively removed from the reaction. The dehydrogenation of cyclohexane to benzene is a very popular example. Shinji et al. (1982) studied the reaction using a VYCOR membrane reactor with a  $Pt/Al_2O_3$  catalyst and could achieve a 80% conversion of cyclohexane at 215°C and 1 atm. The equilibrium conversion at these conditions is approximately 35%.

Itoh et al. (1988) carried out the same experiment at slightly lower temperatures and found very much the same sort of results. Sun and Khang (1988) worked at 270°C and 1.9 atm feed pressure and tested the VYCOR membrane reactor in two configurations. The first configuration had the Pt catalyst deposited in the pores of the VYCOR and the second configuration had the untreated membrane packed with a Pt/VYCOR catalyst (pellets). At high space times (long contact with catalyst - low flow rate) both configurations had greater conversion than equilibrium ( $C_{eq} = 26\%$ ) with the first configuration giving better results ( $C = 56\%$ ) than the second configuration ( $C = 40\%$ ). At low space times conversions for both configurations were about the same as equilibrium. This difference clearly points out that enough partial pressure driving force must be present to help selectively remove one component. When the space time is low and there is not enough extent of reaction to build up a sufficient amount of hydrogen in the reactor, the hydrogen permeation rate is not large enough to significantly shift the equilibrium.

Other popular and practical applications involving hydrogen removal are industrially relevant hydrocarbon dehydrogenation reactions. The dehydrogenation of ethylbenzene to styrene is an example. Wu et al. (1990) examined the reaction in an alumina membrane reactor using a  $Fe_2O_3/Al_2O_3$  catalyst and found that conversions could surpass equilibrium conversion by 15-25% in the temperature range of 600-660°C. However, coking was a problem and the steam added to help suppress coke formation caused the pores of the multi-layer alumina membrane to grow. This growth increased permeability but decreased selectivity of the membrane and hence decreased the conversion. Ethane dehydrogenation has been shown to be possible in a Pt impregnated anodic alumina disk membrane reactor (Furneaux et al. (1987)). This patent disclosure, however, is little more than proof of concept. The research group at the University of Southern California (USC) have carried out work using a multi-layer alumina membrane (Membralox). The work began with a study of steam reforming of methane (Tsotsis et al. 1992, 1993) and was expanded to include ethane (Champagnie et al. (1990,1992), Tsotsis et al. (1993)) and propane dehydrogenation (Ziaka et al. (1993a,b)). Patents were granted for the work

on steam reforming (Minet and Tsotsis (1991, 1993)) and ethane dehydrogenation (Minet et al. (1993)).

The studies for all three reactions were carried out to prove that the concept would work and to identify the effects on the system of key variables such as temperature, reactor pressures, contact time, reactor length and sweep (purge) gas ratio. In all three cases the conditions tested were not representative of typical industrial conditions. The steam reforming work, using a NiO on calcium aluminate catalyst in a packed bed in the membrane reactor, proved that an increase in conversion of about 10% over the equilibrium limit is possible but the tests were carried out at very high steam to methane ratios. Ethane dehydrogenation was tested using two different catalyst configurations: (1) Pt on alumina particles packed inside the membrane and (2) Pt supported on  $\gamma$ -alumina (membrane). The tests were carried out at relatively low conversion levels (<15%) but the membrane reactor could produce conversions nearly double the equilibrium limit with very high selectivity (98%+) to ethylene given the right conditions. Propane dehydrogenation tests used only the packed, supported Pt catalyst and produced results very similar to those of ethane dehydrogenation.

The work by the USC group clearly demonstrated some of the benefits of porous membrane reactors for dehydrogenation reactions. However, it also clearly showed some of the drawbacks. The first key problem is that for the alkane dehydrogenation reactions the lower hydrogen content around the catalyst causes the catalyst to coke and lose activity. The problem is so severe that hydrogen must be added to the alkane feed just to make the system operable. The second key problem is that all species (not just hydrogen) permeate across the membrane so high levels of per pass conversion may not even be possible due to alkane loss across the membrane. The third problem is that a sweep gas must be used to keep the hydrogen partial pressure low on the permeate side of the reactor. The mixing of an inert gas with the hydrogen and other permeated components will cause the separation costs to rise dramatically if it is applied on the industrial scale.

Oxygen permeation situations using porous membrane reactors are even more limited than those involving hydrogen. In this case all examples involve the permeation of oxygen into the reactor to react with a hydrocarbon and most of the work in this field has occurred in the last five years. It is this work that is most closely related to the research presented in this thesis.

A series of papers by Santamaría and co-workers describe the development of a porous ceramic membrane reactor (Lafarga et al. (1994)) and its application to oxidative coupling of methane (Coronas et al. (1994)), oxidative dehydrogenation of ethane (Coronas et al. (1995)) and oxidative dehydrogenation of butane (Téllez et al. (1997)). A very similar study has been carried out by Tonkovich and coworkers who studied OCM (Tonkovich et al. (1996b)) and oxidative dehydrogenation of ethane (Tonkovich et al. (1995, 1996a)). The membranes used by both of these research groups were multi-layered alumina membranes which had to be altered or treated to decrease the oxygen permeability. The Santamaría group deposited silica in the membrane pores to decrease permeability while the Tonkovich group used either an enamel to completely block a portion of the membrane surface or sputter coated silica on to the membrane surface to decrease permeability. In all cases a bulk heterogeneous catalyst packed into the reactor was used for these studies. The Santamaría group used lithium doped MgO and Tonkovich used samarium and lithium doped MgO. The former group found the membrane reactor to be of little advantage for ODE but that it did provide an advantage (selectivity and yield) over a standard reactor for OCM and butane dehydrogenation. The latter group found the opposite to be true - no advantage for OCM but a significant advantage for ODE. The difference between the two findings can be explained by differences in the membranes and in the operating parameters. However, both groups agreed that the membranes gave stable performance over time.

Studies by Pantazidis et al. (1995) and Capannelli et al. (1996) investigating oxidative dehydrogenation of propane and by Borges et al. (1995) investigating OCM took a slightly different approach. In all three of these studies a catalyst was supported on the wall (in the pores) of an alumina membrane. Pantazidis et al. (1995) used either a



vanadium-magnesium or nickel catalyst, Capannelli et al. (1996) used a vanadium catalyst and Borges et al. (1995) used LaOCl supported on the membrane. Pantazidis et al. (1995) used membranes with different pore sizes and found that only the mesopore (very small pores) membranes had any positive effect. Capannelli et al. (1996) found the membrane reactor to give only modest improvement over a packed bed reactor and Borges et al. (1995) stated, that despite some catalyst instability problems, beneficial effects from the membrane reactor were observed.

The work that is perhaps most closely related to this thesis research is the work of Ramachandra et al. (1996). This paper presents research on OCM using a porous VYCOR membrane reactor. This is the only example of hydrocarbon-oxygen reactions being carried out in a porous membrane reactor where the reactor is not constructed primarily of alumina. Ramachandra et al. (1996) used bulk  $\text{Sm}_2\text{O}_3$  packed into the reactor as a catalyst and found that at any particular temperature the VYCOR reactor gave a slightly higher selectivity, but had lower conversion, than a normal plug flow reactor. In the end there is little difference in yield between the two configurations. However, for a specific conversion level, the VYCOR reactor had consistently higher selectivity to  $\text{C}_2$  products. The details of the reactor design and how they compare with the reactors developed as part of this research will be presented in chapter 4 of this thesis.

The work to date involving the use of porous membrane reactors for hydrocarbon-oxygen reactions has focused on a limited number of reactions and has shown mixed results as far as the suitability of the reactor systems for those reactions. The work, however, is in its infancy and perhaps the best lessons to draw from the work revolve around how to best design and built the reactors. Often these have been the most challenging problems. These issues will be discussed in greater depth in Chapter 4 when information on the design and construction of the membrane reactors for this research is presented.

To complete the survey of the literature on porous membrane reactors one more topic needs to be briefly broached. All the work that has been presented is based on reaction occurring in a catalyst bed or perhaps on the walls of a membrane reactor. The reactants

and products are free to permeate across the membrane as partial pressures and modes of diffusion dictate. There is a body of work using membrane reactors where reactants are fed through the pores of the membrane (either co-currently or countercurrently) and the reaction is confined exclusively to the pores. The intent is to prevent one or more species either exiting the reactor or mixing with other species anywhere but in the pores. A few examples of this approach are Slood et al.(1992) who investigated reaction of  $\text{H}_2\text{S}$  with  $\text{SO}_2$  to produce liquid sulfur, Zaspalis et al. (1991) who investigated reduction of  $\text{NO}$  to nitrogen and  $\text{N}_2\text{O}$  with oxygen and ammonia, and Furneaux et al. (1987) who demonstrated the concept using the hydrogenation of ethylene. Although this idea does not seem to be directly related to the present research, the concept is useful in explaining how a membrane can promote side reactions even though the main reaction may be occurring in a catalyst bed contained within the reactor.

## **Chapter 3**

### **Experimental Equipment and Methods**

A discussion of the experimental equipment and experimental methods used for this research can be divided into two major subjects. The design and construction of an appropriate membrane reactor system was a major aspect of this research and will be covered in depth in Chapter 4. In this chapter the rest of the experimental and analysis equipment, analysis methods, data analysis methods and experimental procedures will be discussed.

#### **3.1 Experimental Equipment**

##### **3.1.1 Reactor System (excluding membrane reactor)**

A general schematic representation of the reactor system with the membrane reactor and effluent analysis gas chromatograph is depicted in Figure 3.1.

The major constituents of the system are the feed gas supply system, the feed gas metering and control system, the furnace and the instrumentation and data collection system.

##### **3.1.2 Feed Gas Supply**

The three feed gases that are normally used are helium (as a diluent), propylene and oxygen. All gases were supplied by Praxair Canada Inc. from their packaged gas plant (Edmonton, AB). All gases were used as received without further purification. The

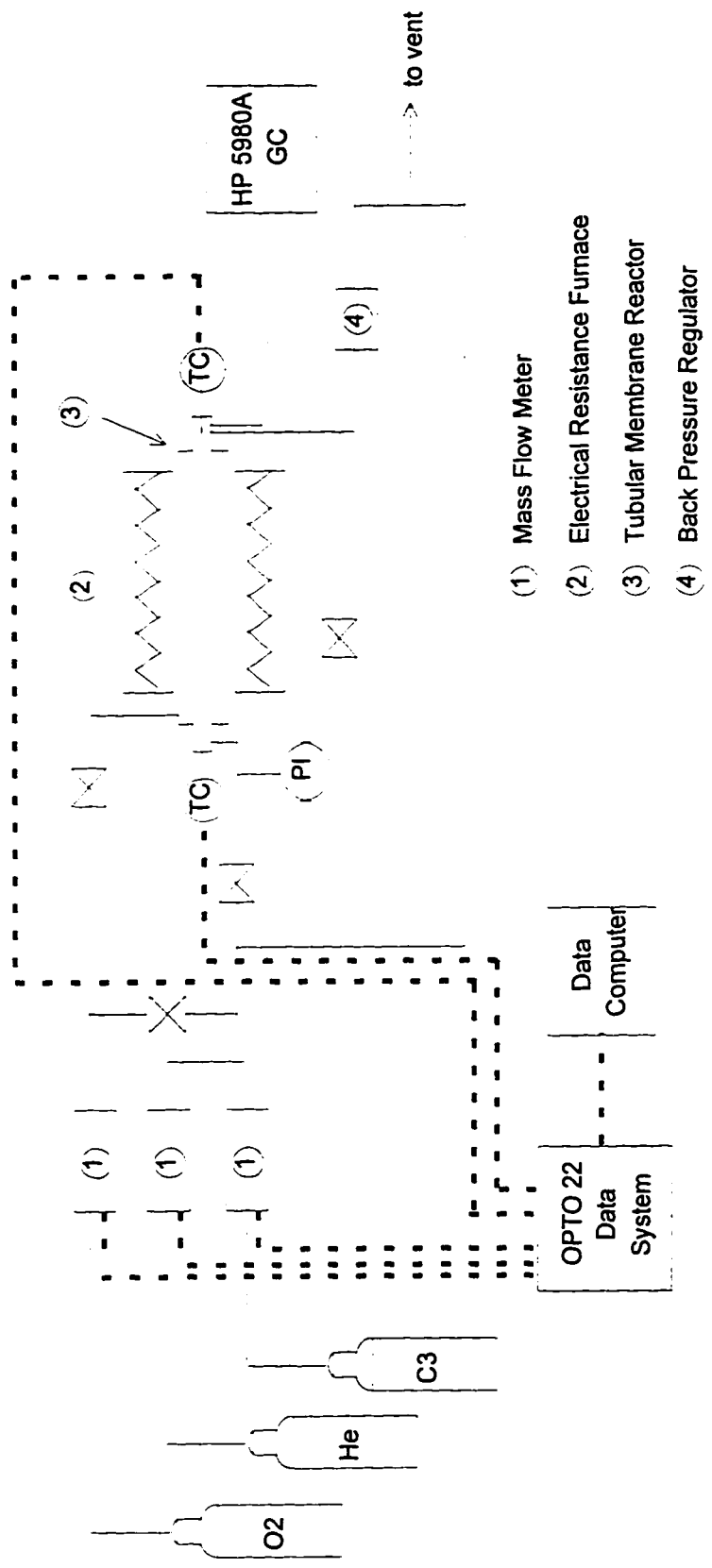


Figure 3.1 Schematic Drawing of Experimental Equipment

helium was “pre-purified” (PP) grade and was supplied in T size cylinders. Numerous helium cylinders were required over the course of the research. The oxygen use was considerably lower than that of helium and required only a single T size cylinder of ultra high purity (UHP) grade oxygen to be used. The propylene use required only one FX size cylinder of CP grade propylene. This material was provided in liquid form in a cylinder which was designed with a top, vapour draw off point. The analysis of the propylene is given in Table 3.1.

Table 3.1 - Analysis of Propylene Feed Gas

Component	Molar Comp.
Methane	5 ppm
Ethane	272 ppm
Propane	0.408 %
Propylene	99.56 %

All three feed cylinders were equipped with Matheson model 3122 high purity, dual stage brass regulators and set to provide gas to the metering system at approximately 275 kPag. The body of the propylene regulator was wrapped in fibre tape and then by approximately 60 cm of electrical resistance heating tape connected to a variable voltage regulator. The heating tape voltage was adjusted to keep the regulator body at about 45°C. The reason for providing the heating was that the vapour draw off system in the supply cylinder was prone to transporting small slugs of liquid propylene into the regulator. The liquid would often vapourize in the low pressure side of the regulator causing pressure fluctuations. The pressure fluctuations dramatically affect the stability of the flow rate from the propylene flowmeter. If the regulator is kept warm, the liquid vapourizes very quickly (before it reaches the low pressure side) and pressure fluctuations are not encountered.

### 3.1.3 Feed Gas Metering and Control

The experimental program required that the flow rates of the three feed gases would generally be in three different flow ranges. These ranges are shown in Table 3.2.

Table 3.2 - Typical Operating Ranges for Feed Gases

Feed Gas	Typical Operating Range (sccm)*
Helium	80-250
Propylene	10-50
Oxygen	3-20

\* for the sake of clarity throughout the rest of the thesis, sccm is  $\text{cm}^3/\text{min}$  (gas volume at 101.3 kPa and 0°C)

The flow range and the degree of variability within the range for each of the feed gases is different and as a result different types of meters are best suited for each application. On a practical note, one of the key attributes of equipment used in a research laboratory is flexibility. As research programs develop there are often changing requirements for the equipment, or if a project is completed/abandoned then it is best if expensive equipment can then be used for other purposes. As a result the flow meters/controllers used for the propylene and oxygen streams were older but very flexible pieces of equipment. A new flow meter and controller was purchased for the helium stream.

The propylene and oxygen meters are Vacuum General UltraFlo UC series mass flow sensors and controllers accompanied by Vacuum General model 80-55 flow command and display modules. The helium meter is a Matheson model 8272-0422 mass flow transducer coupled to a Matheson model 8270 mass flow controller and display unit. Both types of meters work on the same principle and it is as follows. As gas flows into the meter it encounters a large tube with a large concentric flow restrictor that leaves the gas with only a narrow annular flow path. The annular flow path ensures that the flow regime will be laminar and that the pressure drop across the path is linear with respect to total gas flow. While most of the gas traverses this annular flow path, a very small percentage of the gas bypasses through a capillary sensing tube. The capillary tube is wound with two self heated resistance thermometers hooked to a bridge circuit. If there is no flow through the capillary the two thermometers each put the same amount of heat into the capillary tube and measure the same temperature. Thus no voltage is generated across the bridge (corresponding to zero flow). As flow begins in the capillary some of

the heat is carried down stream by the gas causing a temperature gradient which is picked up by the two thermometers and generates a voltage difference between them. The signal is amplified and linearized resulting in flow being directly proportional to the measured voltage. The measured voltage is compared to a setpoint by the controller and a small internal solenoid valve is adjusted to regulate the flow.

For a fixed flow rate of gas, the extent of the temperature gradient in the capillary tube depends on the properties of the gas. Thus, the meter must be calibrated based on which gas will pass through the meter. The measurable flow range depends on the size of the annular flow space (main flow path). A greater annular space allows for greater flow. The key difference between the Vacuum General and Matheson meters is that these two parameters (calibration for different gases and annular flow space) are adjustable in the Vacuum General (VG) product making it a great deal more flexible in its potential uses. The "gas calibration value" is an adjustable potentiometer on the display unit and the annular opening is adjusted by changing the concentric flow restriction element. VG has elements that allow 0-1 sccm, 0-10 sccm, 0-100 sccm, 0-1 slm, and 0-10 slm. A 0-10 sccm element was used in the oxygen meter and a 0-100 sccm element was used in the propylene meter. It must be noted that the meters produce a standard 0-5 vdc signal for the stated range for a gas with a "calibration factor" of 1, such as air, but the meter still produces a linear voltage to flow signal over the range 0-10 vdc. That is, they can accurately read up to twice the stated range. For gases with a lower calibration factor they are capable of reading only some fraction of the range. For propylene with a calibration factor of 0.41 the standard range with the 0-100 sccm element would be 0-41 sccm of propylene. Reading to the full voltage range of 10 volts, a 0-82 sccm propylene range is possible. The Matheson meter (helium) came from the factory calibrated for 0-250 sccm helium. These parameters are not adjustable on the Matheson meter.

The meters were calibrated to ensure that the output voltage (and also the corresponding digital display) and the measured mass flow rate were proportional to one another for all three meters. The calibration equations are shown in Table 3.3. The "X" value corresponds to the value of the digital output display. For the VG display this output is 0-

1000 (nominally) and can read to 2000. For the Matheson display the output is 0-250 (which is supposed to correspond directly to the flow rate).

Table 3.3 - Flow Meter Calibration Equations

Feed Gas Meter	Calibration equation	$r^2$
Helium	$\text{sccm} = -0.000181X^2 + 1.08803X - 2.601$	0.999998
Propylene	$\text{sccm} = 0.099591X - 0.5705$	0.99996
Oxygen	$\text{sccm} = 0.007969X - 0.1309$	0.99997

As noted in the table the helium meter had a slight non-linear relationship between flow and output signal. However, all the calibrations were accurate within the  $\pm 1\%$  guaranteed by the manufacturers over a range from 10% of full scale (i.e. 0-1000 is the full scale on the Vacuum General meters) to the maximum value at which the meter is used in this research. In almost all cases, except at the very low flow rates, the predictions are within  $\pm 0.4\%$  of the measured values.

The controllers all exhibited steady flow rate performance while on line. The helium meter exhibited no zero or baseline drifting and zeroed rapidly and to exactly the same value every time that helium pressure was applied to the meter/controller. The Vacuum General meters, however, had some zeroing problems. As long as flow was maintained to these meters the performance was steady. When gas pressure was applied to either meter the display (with zero flow) goes dramatically negative in the propylene meter or stays very positive with the oxygen meter. Over approximately a one hour period the propylene meter would come back to the appropriate zero point. The oxygen meter, however, would often have to be re-zeroed. The zeroing potentiometer, fortunately, was located on the front of the display unit. Although there was no concern about the accuracy of the flow rates during the experiments, these idiosyncrasies of the VG meters made them a little tougher with which to work.



### 3.1.4 Electrical Resistance Tube Furnace

A temperature of approximately 500°C was required for testing the reactors and catalysts in this study. An electrically heated tube furnace was selected as the most viable choice for the heat source. This choice was based on the need to easily install and remove the reactor and the desirability of being able to physically see the reactor and/or catalyst under reaction conditions. For these reasons options such as a sand bath or molten metal bath were not considered.

The furnace selected was a Lindberg/Blue M “Mini-Mite” 1100°C horizontal tube furnace. The furnace has a 30.5 cm heated zone (one zone heating) capable of holding a 2.54 cm process tube. The furnace is controlled by an internal tunable PID controller which controlled the temperature based on a single thermocouple located just above the refractory lining at the 15.25 cm point (middle) of the furnace. The controller was programmable allowing the input of two sets of ramp, temperature and dwell setpoints.

In all experiments the catalyst was contained within a 5 cm long zone at the middle of the furnace. In the absence of flow and reaction the temperature within this zone varied by only 3°C at the temperatures typically used in this study. An unshielded thermocouple placed at the centre of the furnace (centred axially and radially) read approximately 10-13°C higher than the temperature read by the furnace controller thermocouple. When the centre thermocouple is highly shielded, that is, inside the membrane reactor assembly, it read within 1-2°C of the controller thermocouple. Thus it is clear that radiative heat transfer from the heating elements had some effect on the process temperature, but the effect was consistent and predictable. For a small portion of the experimental work (see Chapter 8) the furnace control was altered so that the centre thermocouple (within a catalyst bed) was used as the controlled process variable.

### 3.1.5 Instrumentation and Data Collection

Six process variables were continuously measured in this experimental system. The three feed gas flow rates from their respective mass flow controllers were recorded. Two reactor temperatures (immediately before the catalyst bed and the mid-bed or mid-reactor temperature) were measured with type K thermocouples and recorded. The thermocouples have 1.59 mm diameter SS sheaths and were further sheathed in 3mm OD, 2mm ID quartz. The thermocouples and sheaths were inserted axially into the reactor through appropriate Swagelok fittings. More details on the arrangement are given in Chapter 4. A reactor pressure was also continuously measured by a 0-10000 kPa Heise digital pressure gauge, but was not recorded. In the case of normal flow reactor tests (non membrane reactor tests) the inlet pressure to the reactor was measured. During membrane reactor tests the membrane reactor shell pressure was measured.

The data from the five recorded variables were received by an OPTO 22 data system and logged on an IBM PC. A 0-5 VDC signal was received from the oxygen and helium flow meters, and a 0-10 VDC signal was received from the propylene meter. The voltage signal was converted to an appropriate flow rate value by the program running the data logging computer using the equations from Table 3.3. The millivolt signals from the thermocouples were converted to temperature readings, also by the data computer program, using standard calibration curves. The recorded data were sampled every 12 seconds and recorded as averages over periods of one minute. The data recording program also accepts input data to identify the test conditions, creates the output data file and gave the output file a unique name based on the date and time.

### 3.1.6 Remaining Hardware

All the interconnecting tubing is 3.175 mm SS tubing connected with appropriate SS Swagelok fittings. All isolation valves and three way valves were 1/4 turn ball valves. The tubing running to the vent was 6.35 mm plastic tubing. The pressure in the reactor tube was controlled by means of a simple back pressure regulator which diverted some of

the reactor effluent stream around the gas chromatograph and directly to the vent. The pressure was set and maintained for all experiments at 105.5 kPa ( $\pm 1$  kPa) which was approximately 12 kPa above typical atmospheric pressure in the laboratory and ensured that approximately 100 sccm of effluent gas was directed to the GC. The effluent line (approximately 5 m in length) from the reactor exit to the GC inlet was heat traced with electrical resistance heating tape. A variable voltage transformer provided 70 volts to the heating tape. The line was heated to prevent the condensation of water in the line.

### 3.1.7 Gas Chromatograph and Analytical Method for Gaseous Streams

Prior to conducting reaction studies, it was necessary to develop a single on-line analysis technique that could be used to quantitatively analyze all of the components in the system. Development of this technique proved to be much more challenging than originally envisioned and merits some detailed discussion.

Gas chromatography (GC) was selected as the method of analysis over mass spectrometry (MS). Mass spectrometry was not a viable method in this project for a number of reasons.

1. Water is very difficult to detect.
2. MS has difficulty distinguishing between fragments with the same molecular masses. In this project two key sets of components have the same molecular masses:
  - Propane and carbon dioxide (44)
  - Ethylene and carbon monoxide (28)
3. There is no need for virtually real time analysis that MS can supply since the reaction tests are steady state tests rather than transient tests.

The GC system hardware consisted of a Hewlett Packard 5890A gas chromatograph and a HP 3396 Series II integrator. The integrator came with a BASIC language program feature which allowed some simple programming of the integrator with respect to timing of events and changing of methods. The integrator was connected to a computer on

which all data was stored electronically. The GC itself was equipped with a 10 port actuated valve which provided column sequence reversal capability, a 250  $\mu\text{L}$  sample loop, thermal conductivity detector (TCD) and flame ionization detector (FID) in series, and the capability to time program valve position changes and to temperature program the GC oven.

The GC was equipped with two 3.175 mm SS packed columns. Column 1 was 2.44 m of 100/120 mesh HayeSep DB and column 2 was 1.83 m of 80/100 mesh molecular sieve 13X. A 6.1 m section of blank 3.175 mm SS tubing was installed immediately before column 2. The carrier gas was helium at a flow rate of 29.6 ml/min. The analysis cycle required a total of 35 minutes comprised of a 23 minute GC run and 12 minutes of data analysis and hold time between runs. The method took advantage of the column reversal and temperature programming features in order to meet the analysis objectives. The FID analyzer was used to measure the hydrocarbon constituents of the effluent and the TCD to detect permanent gases and water.

The key analysis objectives were to provide adequate separation and detectability of all the components in the system in as short an analysis cycle as possible. The components ranged from permanent gases like  $\text{O}_2$  and  $\text{CO}_2$  to six carbon hydrocarbons and included water. The concentration of the various components in the reactor effluent ranged over 4 orders of magnitude (from 20% propylene to ppm levels of certain products). In previous studies involving ODHD of propylene the predominant method of reactor effluent analysis had been to remove the water, heavier hydrocarbons and oxygenates with a cold trap or by absorption in an organic solvent such as toluene. The remaining gaseous stream was analyzed by GC and the liquid products were analyzed by methods such as liquid chromatography or mass spectroscopy. Another study (Kutuzov et al. (1982)) used a complex GC method but still ignored the presence of water in the reactor effluent.

The selection of HayeSep DB as the packing for column 1 was crucial to the success of the system. This polymer facilitates very good separation of hydrocarbons particularly alkane/alkene pairs and isomers. Alkenes always elute before their analogous alkane and

an  $\alpha$ -olefin will elute before the isomeric  $\beta$ -olefin. HayeSep DB also has excellent water handling characteristics. At a sufficiently high temperature, there was very little water tailing, a characteristic that plagues many other materials that are often used for hydrocarbon separation. At higher temperatures, however, HayeSep provides little or no retention time or separation for permanent gases except CO<sub>2</sub>. Thus, a molecular sieve column was required to separate O<sub>2</sub>, CO and N<sub>2</sub> (if air is used as the oxidant in the reaction). The caveat for the molecular sieve column was that CO<sub>2</sub>, water and hydrocarbons, excluding methane, must be kept out of the column.

The column reversal feature was used to ensure that CO<sub>2</sub>, water and all the hydrocarbons were confined to the HayeSep column while the permanent gases traveled through the HayeSep column twice and the mol sieve column once. Figure 3.2 indicates how the 10 port valve and connections were set up to facilitate the column reversal feature. Operating the columns at 150°C provided rapid elution times, sharp peaks and sufficient separation for the permanent gases including CO<sub>2</sub>, water and the lighter hydrocarbons (up to C<sub>3</sub>). The GC method maintained the GC at 150°C for 7.5 minutes which was just enough time for the final compound (which is CO) in the permanent gas/water/light hydrocarbon series to elute cleanly. However, this temperature was too low to provide reasonable elution times or sharp peaks for the heavier hydrocarbons. Their adsorption on HayeSep DB at this temperature was too strong, and it was here that the temperature programming feature of the GC was utilized. The GC oven temperature was increased to 220°C after the aforementioned components had eluted. The value of this upper temperature was selected by modeling the elution times and peak widths of the heavy components (1,5-hexadiene, 1-hexene and benzene). The elution time for all components could be modeled with an Arrhenius type expression (with T being the high temperature level, in Kelvin) as in equation 3.1.

$$t_{elution} = A \exp\left(\frac{B}{T}\right) + 11 + 0.02(T - 473) \quad (3.1)$$

The last two terms are linear terms which are meant to take into account the initial lower temperature period (7.5 minutes) and the temperature ramp period between the two temperature levels. The first term represents the variation in time due to the high temperature portion of the process. It was found that the maximum rate of temperature increase between the two temperature levels that provided stable performance (no overshoot) was  $25^{\circ}\text{C}/\text{min}$ . The peak width (at half peak height) narrows at higher temperature and sharp, narrow peaks are desired. It was found that this measure of peak width could be modeled empirically for all three components in the desired temperature range by an equation of the form of equation 3.2.

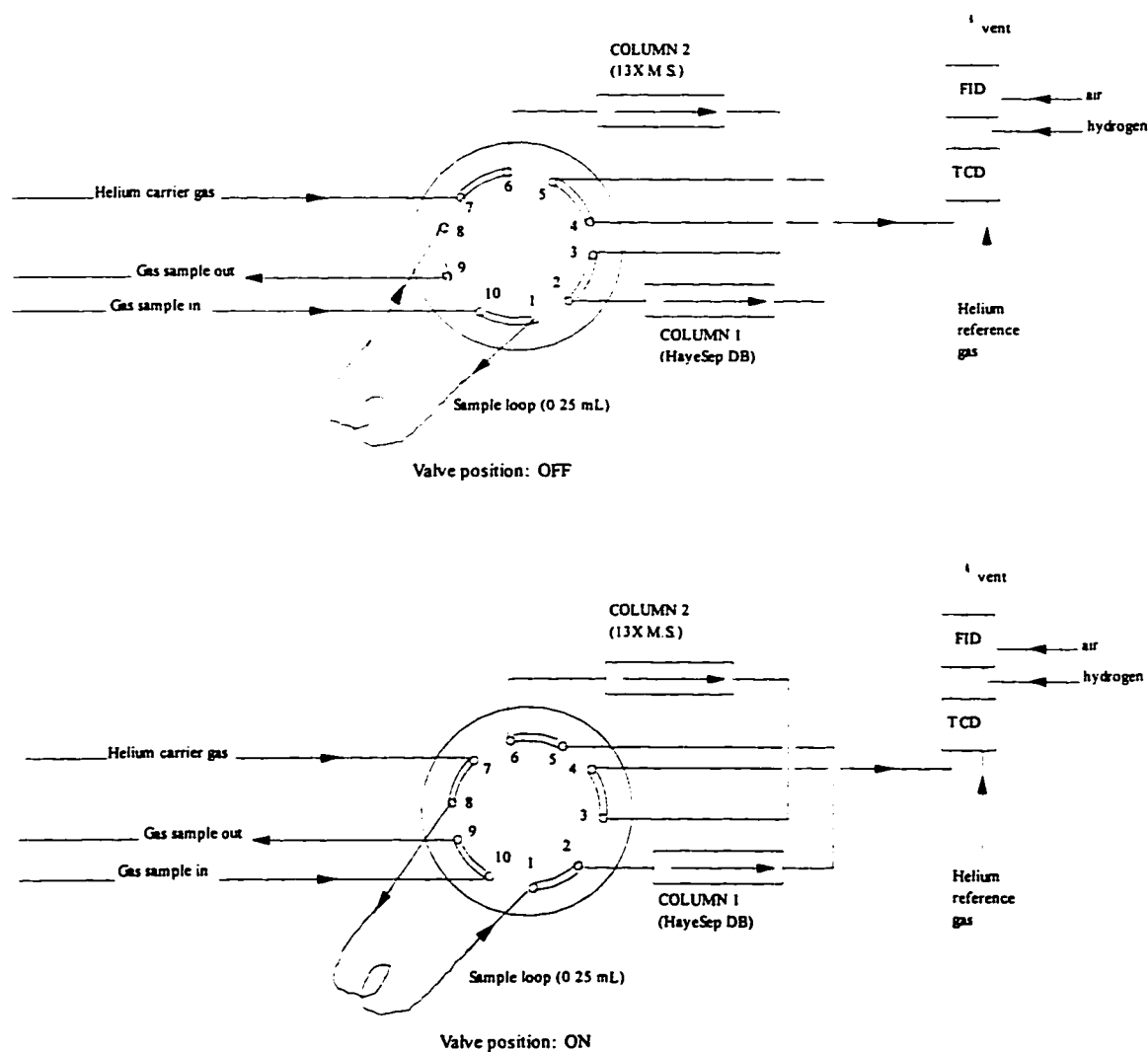


Figure 3.2 Ten Port Valve in ON and OFF Positions

$$\text{peak width} = 10^{(C \log(T) + D)} \quad (\text{with } T \text{ in K}) \quad (3.2)$$

Thus the position and width of the peaks were modeled with respect to the upper temperature level and an appropriate compromise between the competing factors of peak width, elution time and sufficient separation was found. The separation between 1,5-hexadiene and 1-hexene proved to be the key constraint and an upper temperature of 220°C best met that constraint.

This basic method is not particularly noteworthy, but it is the first time in the literature that all components of the ODHD of propylene reaction are analyzed on-line with a single method.

Two problems were encountered that required solution before the method could be applied to on-line analysis. The first problem was that in the original method propylene and oxygen co-eluted. Oxygen traveled a much further path as previously mentioned, but reached the detectors at the same time as propylene. One of the two peaks had to be moved and moved to a location (elution time) where there was sufficient room for the peak to elute cleanly. The following options were considered and tested:

1. Increase or decrease the length of one or both of the two columns to shift elution times.
2. Increase or decrease the carrier gas flow rate.
3. Add dead volume to increase the elution time of O<sub>2</sub>.

Since propylene did not travel through the mol sieve column it was expected that changes in that column would have the greatest effect in separating the propylene and oxygen elution times. Increasing the mol sieve column length caused three problems. The first problem was that the column head pressure rose to the limit of what the carrier gas regulator could supply so the carrier gas flow was barely sufficient. This first problem lead to two other problems. The high column pressure caused the water peak to flatten out and tail significantly and the release of pressure when the column reversal valve

position switch occurred had a tendency to blow out the hydrogen flame on the FID. It became clear that substantial increases in column pressure could not be tolerated. Reducing the length of the mol sieve column was attempted but the loss in peak sharpness and changes in elution times for gases other than oxygen made this approach infeasible.

An increase in carrier gas flow rate was not feasible for pressure reasons and a decrease in the rate had no substantial effect on the relative elution times. Hence adjustment of carrier gas flow could not achieve the necessary shift in elution times. As it turns out the most viable solution was to increase the elution time for O<sub>2</sub> by increasing the travel path of the oxygen. Adding the dead time was accomplished by adding at 6.1 m blank section of 3.175 mm SS tubing just before the mol sieve column. It had the effect of simply adding dead time to the O<sub>2</sub>, N<sub>2</sub> and CO elution times. Dead space is generally avoided in gas chromatography because it allows some degree of mixing and unnecessarily broadens peak widths. The peak width broadening did occur in this case, but it was not excessive and had no marked effect on the accuracy of the results.

The second problem became apparent when doing repeated analyses (run after run). There was an inconsistency in the oxygen peak area. The peak area decreased from run to run even though no changes were made to the flow rate or composition of the gas feeding the sample loop. A new steady state peak area was established after approximately 5 consecutive analyses. The new steady state value depended on the initial oxygen concentration. The problem was determined to be oxygen desorbing from the nickel sites on the stainless steel walls of the columns and the blank tubing as the temperature rose to 220°C in the analysis sequence. The subsequent sample would have some of the sample oxygen re-adsorbing on the walls at the lower temperature (150°C) decreasing the amount that could be detected at the TCD.

As with the first problem a number of options were considered. The key to solving the problem was to get sufficient oxygen back into the columns at the lower temperature to re-adsorb on the tubing before a subsequent analysis was made. Attempts were made to



dose the GC columns with pure oxygen (from the sample loop) between runs. This approach did not produce consistent results. This method was coupled with lowering the GC temperature to 50°C to try to increase the rate of oxygen re-adsorption. Again, the results were inconsistent and even if they had been consistent this method would have been extremely difficult to implement.

It was noticed that if 4-6 hours passed between runs on the GC, the oxygen peaks were consistent. This period was far too long to be practical in terms of carrying out the experimental work, but it did ultimately provide the answer to the problem. The normal carrier gas is pre-purified helium (Praxair) that contains approximately 3 ppm oxygen. It became clear that constantly adding oxygen with the carrier gas allowed re-adsorption of oxygen on the column walls to occur. In the end the best solution proved to be the use of a carrier gas with a slightly higher oxygen content (50 ppm). Even though the column walls were not completely re-coated with oxygen, the new steady state value of O<sub>2</sub> peak area was reached in only one run (no wasted analyses), was linear with respect to original sample oxygen content and was only 3% lower than the actual value. A period of approximately 12 minutes between analyses was necessary to allow the oxygen to re-adsorb. There are two potential drawbacks to this approach. The first drawback was that the higher oxygen content in the carrier gas would cause the TCD to lose sensitivity and ultimately burn out more quickly. Time, however, has shown that this was not a serious problem. The second drawback was that the higher O<sub>2</sub> concentration in the carrier gas causes a slightly higher O<sub>2</sub> concentration on the surface of the column packing materials. When the pressure changed in the GC system due to a valve position change (to affect the column reversal feature), some O<sub>2</sub> desorbed and was recorded at the TCD. This extra O<sub>2</sub> caused some slight baseline undulations. Again, however, this effect was not found to be a problem that affected the accuracy of the GC results.

A similar but less severe consistency problem has been noted with the propylene analysis. If analyses were run more or less back to back (less than 20 minutes between the end of one and the start of the next), it was observed that the propylene peak area (from integration) would always be slightly lower than expected for any analysis where the

previous analysis had used the high temperature portion (220°C) of the analysis routine. The problem was deduced to be similar to the oxygen problem where differing amounts of propylene were adsorbed on the HayeSep column wall at different temperatures. The problem was not nearly as severe as for oxygen, but since the propylene was the major hydrocarbon component, small errors in the readings would cause more pronounced uncertainties in the mass balance. As with oxygen, the propylene peak area readings decreased after the first exposure of the GC to high temperature and were steady thereafter. The readings were about 1.3% lower than would be expected.

This gas chromatography method was able to measure component concentrations from over 20 mol% of the stream down to the low ppm range for the lighter hydrocarbons. Sensitivity to the heavier hydrocarbons was limited to approximately 75 ppm due to the larger peak width of these components and sensitivity to the permanent gases was limited to approximately 500 ppm due to the lower sensitivity of the TCD in comparison with the FID. Table 3.4 indicates the elution times for all the key components for the ODHD of propylene and also indicates the elution times for a number of the minor components. Figures 3.3a/b show typical TCD and FID chromatograms respectively (note the logarithmic scale on both figures). All the components detected by the FID have traveled through the HayeSep column only. As shown on the TCD chromatogram, oxygen and carbon monoxide travel through the HayeSep column and then the column order is reversed at 1.5 minutes causing them to flow through the molecular sieve column (where they are separated) and through the HayeSep column again before being eluted. This is why they are eluted so much later than CO<sub>2</sub>.

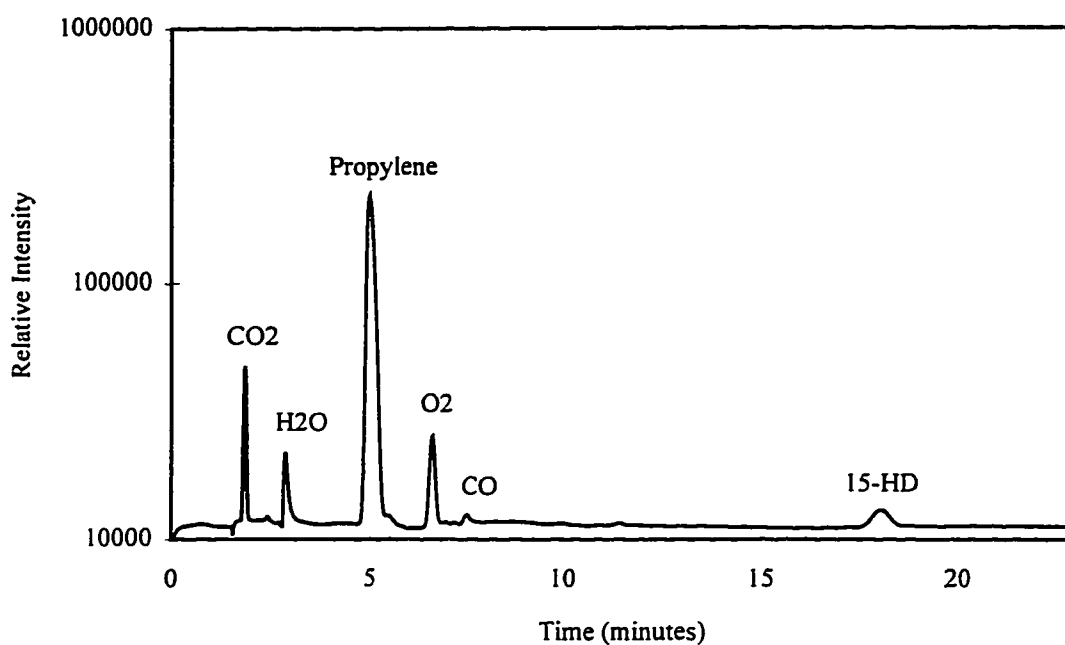


Figure 3.3a Typical TCD Chromatogram of ODHD of Propylene Reactor Effluent

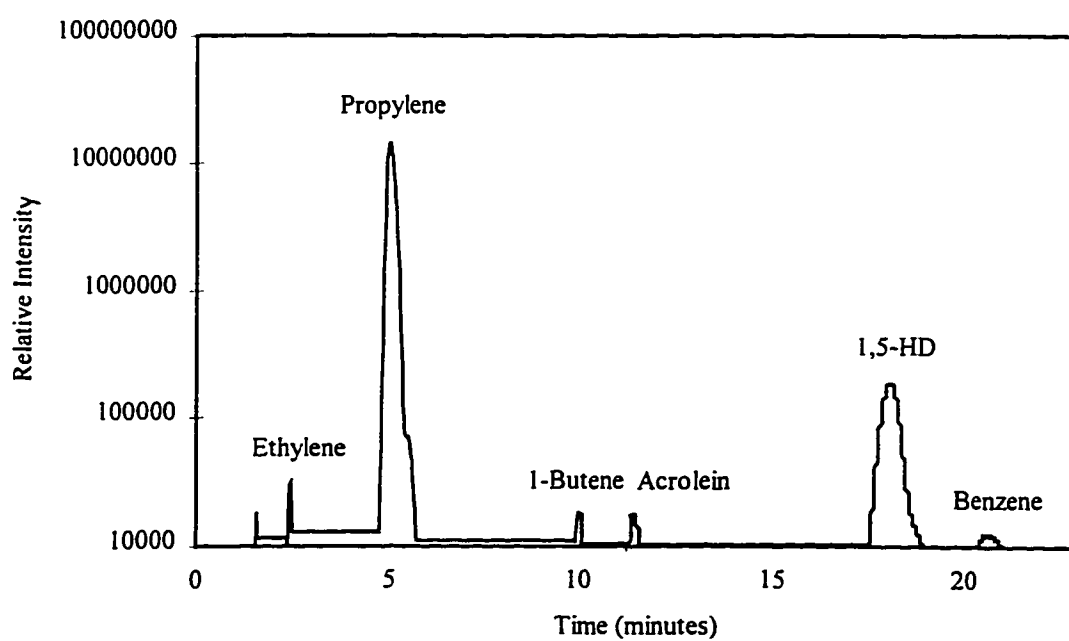


Figure 3.3b Typical FID Chromatogram of ODHD of Propylene Reactor Effluent

Table 3.4 - Elution Times for Components in Reactor Effluent

Compound	Elution time (minutes)
Methane	1.5
CO <sub>2</sub>	1.8
Ethane	2.4
Ethylene	2.7
Water	3.9
Propylene	5.0
Propane	5.5
Oxygen	6.6
Nitrogen	6.8
CO	7.3
Acetaldehyde	9.0
1-butene	10.0
trans-2-butene	10.2
cis-2-butene	10.4
Acrolein	12.5
1,5-hexadiene	18.3
1-hexene	19.2
2-hexene	20.0
Benzene	21.5

The GC has been calibrated for the various components using one of two different methods for providing a fixed gas composition to the GC. The method selected depended on the component being calibrated. Linear correlations between mole percentage of component in the gas and the measured peak area have been derived. The two gas supply methods were as follows:

- 1) Use of an analyzed calibration gas standard (either a pure gas or a mixture) which was diluted with helium to give appropriate range of compositions.

The following calibration gases were used.

- a) Primary calibration gas (Praxair) with composition given in Table 3.5.
- b) Pure oxygen
- c) Pure ethylene
- d) Pure 1-butene
- e) 2.04 mol% CO<sub>2</sub>/ balance N<sub>2</sub>

Table 3.5 - Composition of Primary Calibration Gas

Component	Mol %
Propylene	19.90
CO	5.16
CO <sub>2</sub>	5.00
1-Hexene	0.997
2-Hexene	0.325
1,5-Hexadiene	3.00
Benzene	0.499
Helium	65.119

- 2) Saturation of a flowing gas stream with a component. The component containing stream could be further diluted if necessary. This approach was used for developing the water and acrolein calibration relationships. The equipment needed to carry out this method is shown in Figure 3.4. The feed helium stream was sent through a bubbler containing the material to be evaporated (water or acrolein). This arrangement ensured that the stream was saturated at the low temperature bath conditions.

The GC calibration equations for the two detectors for each of the components along with the method used for calibration (from above), the range in which the correlation holds and the correlation coefficient are shown in Table 3.6. All the correlations show the relationship between the measured peak area and the mole percentage of the component in the stream. The correlation for the TCD is based on the TCD sensitivity being set on "HIGH". The GC composition results were routinely within 0.40% of expected values for test analyses which provided a high degree of confidence in the results and provided excellent closure of the mass balance. Formally, this GC method is an "absolute" method, without an internal standard. Changes in the pressure in the GC sample loop cause different amounts of material to enter the GC columns and hence different peak areas result. The use of a back pressure regulator (Section 3.1.6) limited the sample loop pressure variation to that caused by changes in atmospheric pressure and these changes were relatively small. Nonetheless, sampling of the feed stream (known composition) was

used as to provide the correction factors so that the problem of no internal standard was avoided. A description of the treatment of the data appears in Section 3.4.

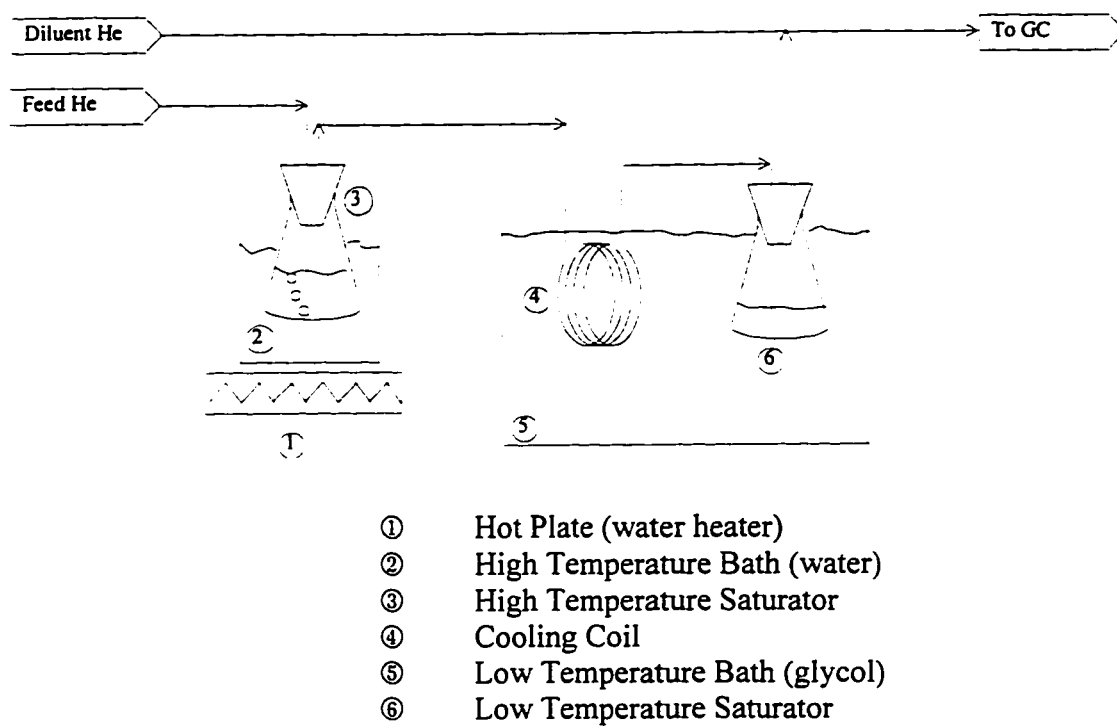


Figure 3.4 Saturator for GC Calibrations

Table 3.6 - GC Calibration Correlations

Component	Calib. Meth.	Range (mol%)	TCD Correlation mol% = a(area) + b	FID Correlation mol% = a(area) + b	Correlation Coefficient (r <sup>2</sup> )
CO	1a	0-0.42	a = 8.3645x10 <sup>-6</sup> b = -0.02376		0.99999
CO	1a	0.4-5.0	a = 8.1270x10 <sup>-6</sup> b = -0.02488		0.99984
CO <sub>2</sub>	1a,1e	0-0.4	a = 6.3094x10 <sup>-6</sup> b = -0.0217		0.99996
CO <sub>2</sub>	1a	0.4-5.0	a = 6.3377x10 <sup>-6</sup> b = -0.04213		0.99985
Propylene	1a	3-20	a = 5.21665x10 <sup>-6</sup> b = -0.08364	a = 7.85988x10 <sup>-8</sup> b = -0.066	0.99987(TCD) 0.99990(FID)
Water	2	0-3.0	a = 1.3998x10 <sup>-5</sup> b = 0.015		0.99912
Oxygen	1b	0-8.0	a = 8.70197x10 <sup>-6</sup> b = 0.00896		0.99996
Ethylene	1c	0-0.05		a = 1.174x10 <sup>-7</sup> b = -0.000741	0.9996
1-Butene	1d	0-0.05		a = 6.46x10 <sup>-8</sup> b = -0.00597	0.9999
Acrolein	2	0-0.16		a = 1.703x10 <sup>-7</sup> b = 0.00116	0.999
1,5-Hexadiene	1a	0-0.40		a = 3.9388x10 <sup>-8</sup> b = 0.000947	0.99997
Benzene	1a	0-0.04		a = 3.43x10 <sup>-8</sup> b = 0.00099	0.9996

### 3.2 Experimental Procedures (Reaction)

There were two types of reaction tests carried out during this thesis research. The first type involved testing of a catalyst in a packed bed in a normal tubular flow reactor. All such tests have been carried out in a quartz reactor. The screening tests described in Chapter 4 have been carried out in a 10 mm ID, 12 mm OD quartz reactor. All remaining packed bed, tubular reactor tests have been carried out in a 15 mm ID, 18 mm OD quartz reactor. The latter reactor dimensions were chosen to best mimic the dimensions of the membrane reactor described in Chapter 4. The second type of test involved use of the

VYCOR membrane reactor. For both the packed bed, tubular reactor tests and the membrane reactor tests a strict test protocol has been followed to assure that the effects of any external factors are minimized. The two protocols are similar but with some important differences. Both protocols are described below.

### 3.2.1 Packed Bed, Tubular Reactor Test Protocol

1. If reactor and catalyst has been previously operated without a decoking/re-calcination step being performed, then the reactor was purged with helium and heated to an appropriate decoking temperature in flowing oxygen or flowing oxygen/helium (20%/80%).
2. When calcination was complete the reactor was purged with helium and the furnace temperature set to the appropriate reaction temperature.
3. Helium, oxygen and propylene flow rates were set by adjustment of the flow controllers and checked via bubble flow meter.
4. The reactor was isolated and the feed stream was routed through the reactor bypass to the GC. Feed flow continued for 15 minutes to allow complete flushing of GC and equilibration of all tubing with the feed gas.
5. Three feed stream samples were analyzed by GC in succession. The standard GC run was set for 7.15 minutes so that both propylene and oxygen analyses were carried out and so that the GC temperature remained constant at 150°C. The GC run and processing of both TCD and FID signals required approximately 10 minutes so that 30 minutes was required for all three samples.
6. The OPTO 22 data collection program was started and 2-10 minutes of data were taken before the feed was sent to the reactor.
7. Feed was routed to the reactor. In all cases the feed composition was above the upper explosive limit (too rich in propylene) so explosive conditions were avoided as long as the reactor had been previously purged with helium.
8. The furnace setpoint and timing program and the BASIC program running the GC analysis cycles were started immediately after step 7. The first sample was taken after the reactor had been on line with reactant feed for 1 hour. As indicated in the



section describing the GC method, one complete analysis required 35 minutes. In the case of many of the screening tests only one temperature level was tested and numerous samples (up to 10) were taken. In the case of full catalyst tests (Chapters 7 & 8) four temperatures were tested over the course of an experimental day. Four samples were taken at each temperature and one hour was allowed at each temperature level to establish a steady state. In these cases, then, each temperature level required 200 minutes to complete

9. Since the furnace can only accept two setpoints at a time, the furnace program had to be reset after the first two temperatures in a four temperature test day. At the end of the final analysis at the final temperature level the reactor was allowed to cool naturally to room temperature (with reactor feed gas continuing to flow through the reactor).
10. The OPTO 22 program was terminated manually some time after the run was complete.

### 3.2.2 Membrane Reactor Test Protocol

The design of the membrane reactor is discussed in Chapter 4 and a schematic representation of the reactor is shown in Figure 4.6. The reactor had a shell and tube type design and was operated with oxygen flowing into the shell and permeating through the membrane to the tube side. The propylene feed flowed through the tube and a catalyst bed, if one was used, was packed into the tube side of the reactor.

1. If the reactor, or reactor and catalyst, had been previously operated without a decoking/re-calcination step being performed, then the tube side of the reactor was purged with helium and heated to an appropriate decoking temperature. The helium to the tube side was shut off and the shell side of the reactor was supplied with oxygen. Oxygen was flowed through the membrane and served to treat both the membrane and the catalyst in the tube (if any). Approximately 0.5 - 1 hour was allowed for this step.

2. When calcination was complete oxygen flow to the reactor was stopped and the furnace temperature was set to the appropriate reaction temperature.
3. Helium, oxygen and propylene flow rates were set by adjustment of the flow controllers and checked via bubble flow meter.
4. The reactor was isolated and the feed stream was routed through the reactor bypass to the GC. Feed flow continued for 15 minutes to allow complete flushing of GC and equilibration of all tubing with the feed gas.
5. Three feed stream samples were analyzed by GC in succession. The standard GC run was set for 7.15 minutes so that both propylene and oxygen analyses were carried out and so that the GC temperature remained constant at 150°C. The GC run and processing of both TCD and FID signals required approximately 10 minutes so that 30 minutes was required for all three samples.
6. Helium and propylene streams were routed to the vent while oxygen was routed to the shell of the reactor. The reactor shell pressure increased as oxygen flowed into the shell. Some of the oxygen also flowed out through the membrane to the tube side of the reactor which had been opened to allow flow out of the tube side to atmosphere. The oxygen pressure was allowed to rise in the shell until the flow into the shell was balanced by the flow out through the membrane. This step requires approximately 1 hour. The oxygen flowing through the membrane into the tube served to purge the tube side with oxygen. Thus the partial pressure of oxygen on the tube side was atmospheric pressure. The oxygen pressure difference across the membrane then, was simply the gauge pressure of oxygen in the shell.
7. The OPTO 22 data collection program was started and 2-10 minutes of data were taken before reactant feed was sent to the reactor.
8. The helium feed was routed to the tube side of the reactor. It was necessary to purge the tube of the oxygen so that explosive conditions in the tube were avoided. A 3-5 minute purge was all that was required. After that the propylene feed was added to the tube side.
9. The furnace setpoint and timing program and the BASIC program running the GC analysis cycles were started immediately after step 8. The first sample was taken after the reactor had been on line with reactant feed in for 90 minutes. As indicated in

the section describing the GC method, one complete analysis requires 35 minutes. For both blank reactor and full catalyst tests (Chapters 6, 7 & 8) four temperatures were tested over the course of an experimental day. Four samples were taken at each temperature and 90 minutes was allowed at each temperature level to establish a steady state before the first sample was taken. In these cases, then, each temperature level required 230 minutes to complete

10. Since the furnace can only accept two setpoints at a time, the furnace program had to be reset after the first two temperatures in a four temperature test day. At the end of the final analysis at the final temperature level the reactor was allowed to cool naturally to room temperature (with reactor feed gas continuing to flow through the reactor).
11. The OPTO 22 program was terminated manually some time after the run was complete.

### **3.3 Experimental Procedures/Equipment (Study of Catalysts)**

Analysis of some of the surface and other physical properties of various catalysts and supports has been carried out in the course of this research. These analyses provided small, but sometimes important pieces of information regarding the materials. There were no attempts to characterize catalysts or support materials in detail since the focus of this research is on the reactor, and reactor operation, rather than on catalysis. Thus, only a limited number of techniques were utilized. The equipment and methods are briefly described in the sections that follow.

#### **3.3.1 X-Ray Diffraction (XRD):**

XRD patterns were obtained with a Philips diffractometer (PW 1730 generator, PW 1050/70 vertical goniometer, 1601-14300 curved graphite monochromator) using  $\text{Cu K}\alpha_1$  and  $\text{Cu K}\alpha_2$  radiation. Samples were placed in available custom made circular sample holders and analyzed over the range of  $2\theta = 10^\circ\text{-}90^\circ$  or  $2\theta = 10^\circ\text{-}60^\circ$  at  $0.1^\circ/\text{step}$  (10 seconds per step) using 40 kV and 30 mA.

### 3.3.2 Surface Area and Pore Size Distribution:

The surface area and pore size distribution of porous material were calculated using results from nitrogen adsorption experiments on an Omnisorb 360 analyzer.

### 3.3.3 Thermogravimetric Analysis (TGA):

TGA was used to help determine what products resulted from the thermal decomposition of metal salts during calcination to make the corresponding metal oxide catalysts. These analyses were carried out on a DuPont 950 Thermogravimetric Analyzer at temperature ramp rates of 5-10°C/min in flowing nitrogen, air or oxygen.

### 3.3.4 Energy Dispersive X-Ray Analysis (EDX)

EDX was used in conjunction with a scanning electron microscope to evaluate the distribution of supported catalysts on the support materials. It did so by determining the relative abundance of the metals in the metal oxide catalysts which were “visible” on the surface of a cross section of the support material. EDX was carried out using a Hitachi S-2700 Scanning Electron Microscope equipped with an Oxford Instruments Link eXL Energy Dispersive X-Ray Analyzer.

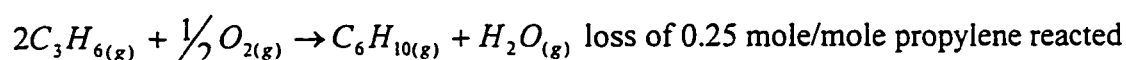
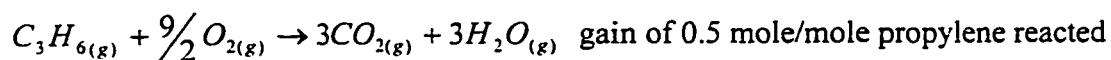
## 3.4 Experimental Procedures (Treatment of Reactor Composition Data)

The raw peak area data describing the compositions of the gas samples analyzed by the gas chromatograph were manipulated in an Excel spreadsheet to produce information regarding the conversion of the two feed components (propylene and oxygen), the carbon and oxygen mass balance closure and the carbon selectivity (in terms of propylene) to the various products. The key features of the data manipulation were:

1. The correlations relating peak area to composition (Table 3.6) were applied to the feed analysis information. Since the feed composition is known and manually

measured the results were normalized to give a correction factor for oxygen (TCD) and propylene (TCD, FID). The GC analysis often did not exactly match the measured compositions often due to small changes in atmospheric pressure that influence the mass of material in the GC sample loop. Using these correction factors is equivalent to using an internal standard such as nitrogen to determine an appropriate scaling factor.

2. Initial outlet composition information was calculated from the peak areas for the effluent analyses using the correction factors referred to in #1 (above) and using the correction in peak areas for oxygen and propylene described in section 3.1.7. All FID values were corrected by the propylene FID factor, all TCD values except oxygen and water were corrected by the propylene TCD factor, and oxygen and water were corrected by the oxygen TCD factor. The peak area corrections (section 3.1.7) were applied to all analyses except the first one at each temperature level.
3. The initial outlet composition data was further corrected to account for the change in number of moles due to reaction as per the reactions listed below. These corrected data were used to calculate conversions, selectivities and mass balance closures.



In almost all cases the carbon mass balance closure was within 1% and the oxygen balance within 3.5%. With respect to the carbon balance, coke formation was minor (if any was formed at all) in all the experiments and nothing in the literature or observed during the experimental work conducted for this thesis indicated a tendency for the catalysts to form carbonates. Carbonate formation, which has plagued a number of OCM catalysts (Raskó et al. (1991)), can go undetected if there is a problem with the carbon mass balance closure. In this research there was no gross error in carbon mass balance closure. The high degree of confidence in the accuracy of the GC results for the products (see Section 3.1.7) means that the calculation of selectivities can be made with

confidence. Since the closure of the carbon balance was well within the experimental uncertainty and there were no indications of systemic errors in the carbon balance, no attempt was made to compensate for the small imbalances. The oxygen balance was not quite as good, but uncertainty tended to be highest at the high oxygen conversion rates where the peak area correction played a larger relative role and the uncertainty in the water correlation had a larger impact. As a result, no adjustments were made for the imbalances.

## **Chapter 4**

### **Design and Construction of a Porous VYCOR Membrane Reactor**

This chapter covers the issues and experimental efforts that have gone into the design and construction of the porous VYCOR membrane reactor used for the study of ODHD of propylene in this research. The chapter begins with some background discussion on the key characteristics of porous membranes relating to their use in membrane reactors and a discussion of the membrane parameters that are available that affect the key characteristics. The research carried out to design/develop the membrane within the constraints imposed by the important characteristics for the ODHD of propylene reaction is described in some detail. A comparison of this approach to the approach taken by others in closely related research is made. Finally the method of construction of the reactor from the base membrane is described.

#### **4.1 Key Characteristics of a Porous Membrane**

There are four key characteristics of a porous membrane that can be exploited if it is to be used in a membrane reactor application.

1. Permeability
2. Selectivity
3. Inertness (Catalytic Activity) at Reaction Conditions
4. Strength and Stability at Reaction Temperature and Pressure.

In general there are five membrane variables or parameters that can be used to influence these key characteristics.

1. Membrane material
2. Membrane formation method
3. Pore size/pore size distribution
4. Ability to chemically alter the membrane
5. Membrane thickness

Although some of these concepts have been alluded to in Chapters 1 and 2, they are sufficiently important that they warrant discussion here.

#### 4.1.1 Permeability and Selectivity

The concepts of permeability and selectivity in a membrane are inseparable and are “inversely” related. Permeability is the flux (mass or molar) of material through the membrane per unit driving force (usually pressure). The selectivity is the relative permeability of a species compared to the permeability of other species. Almost without exception high permeability will lead to low (or no) selectivity and a membrane with very low permeability often is very selective to one species. The best example of the latter case is actually a dense membrane which is permeable to only one species (100% selectivity), but has a very low overall flux rate.

In a porous membrane it is the size and structure of the pores that affects the permeability and selectivity of the membrane. More precisely it is the modes of mass transport through the pores that affect permeability and selectivity. There are four transport modes that can occur across three “parallel” paths as shown schematically in Figure 4.1.



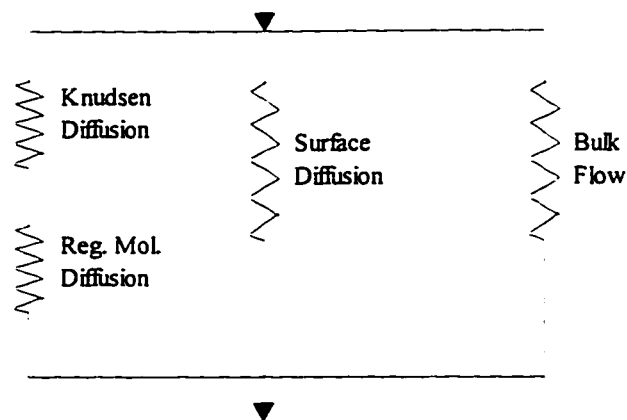


Figure 4.1 Transport Through Porous Membranes

Bulk flow is normal, total pressure driven, Poiseuille (laminar) flow in a capillary. It occurs in larger pores and results in a very high flux compared to the diffusion modes. There is, however, no separation of species. This result clearly illustrates the point that high flux leads to low selectivity. Surface diffusion occurs by having adsorbed molecules adsorb “hop” from one surface site to another. The phenomenon is driven by partial pressure differences and is most predominant at lower temperatures (<200°C). It can cause separation of species, but this generally has to happen in smaller pores (when Knudsen diffusion is occurring) to be noticed. The flux due to surface diffusion is sufficiently small that it is generally insignificant if regular molecular diffusion and/or bulk flow are occurring.

At higher temperatures where surface diffusion is much less important, two types of diffusion can occur: Knudsen diffusion and regular molecular diffusion (left hand branch of Figure 4.1). Both types of diffusion are partial pressure driven and it is the size of the pores that determines which type of diffusion is more important. Figure 4.2 illustrates the point.

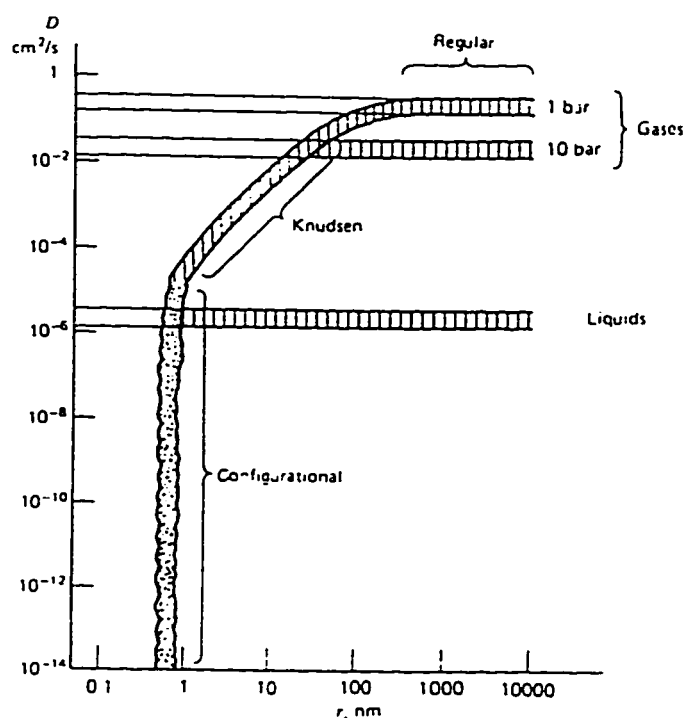


Figure 4.2 Effect of Pore Size on Diffusion Mode in Pores

From: *Chemical Reactor Design and Analysis, 2<sup>nd</sup> Ed.*, by G.F. Froment & K.B. Bischoff  
 Copyright © 1990, by John Wiley & Sons, Inc., reprinted by permission of John Wiley & Sons, Inc.

Knudsen diffusion is said to occur when the mean free path,  $\lambda$ , of the gas is greater than the diameter of the pores,  $d$ . In this case the molecules interact primarily with the walls of the pores and not with one another. Specifically values of  $d/\lambda$  less than 0.2 dictate that Knudsen diffusion will be the predominant type of diffusion occurring in the pores. From the kinetic theory of gases, the mean free path can be estimated as (Uhlhorn and Burggraaf (1991))

$$\lambda = \frac{16}{5} \mu \sqrt{(RT / 2\pi M)} / P, \quad (4.1)$$

and the Knudsen diffusion coefficient is calculated as

$$D_K = \frac{1}{3} d \sqrt{(8RT / \pi M)} = \frac{1}{3} d \bar{u} \quad (4.2)$$

where  $\bar{u}$  is the Maxwellian velocity

Since the flux is a product of  $D_K$  and the concentration gradient (assuming one dimensional flow).

$$flux = D_K \frac{dC}{dz} \quad (4.3)$$

It is most convenient to define the concentration in terms of a pressure difference across a membrane of finite thickness, so that the driving force term becomes (assuming that the gas is an ideal gas):

$$\frac{dC}{dz} = \frac{\Delta P}{\Delta z} \left( \frac{1}{RT} \right) \quad (4.4)$$

and the flux in terms of the new driving force is

$$flux = \frac{2}{3} d \sqrt{\frac{2}{\pi RTM}} \frac{\Delta P}{\Delta z} \quad (4.5)$$

It becomes clear that if Knudsen diffusion is the controlling mode of mass transport the permeation rate of a particular species, assuming no reaction in the membrane, is proportional to the partial pressure difference across the membrane and inversely proportional to the thickness of the membrane and inversely proportional to the square root of both temperature and the molecular mass of the species.

In small pores Knudsen diffusion will occur. In larger pores regular Fickian diffusion will occur, but if there is a total pressure difference across the membrane (the fairly normal situation for membrane reactors), the larger pores necessary for molecular diffusion give rise to bulk flow. Thus, in most cases the contribution of regular diffusion is not significant. The one situation where regular diffusion can play a role is for back diffusion of species out of a membrane reactor. That is, flow in the direction opposite to the main flow through the membrane. This issue will be discussed further in Chapter 6.

Permeability and selectivity for a membrane are primarily controlled by the pore size and pore size distribution of the membrane as well as the membrane thickness. The method by which the membrane is formed, in many cases, dictates what sort of membrane thickness and pore size is possible.

#### 4.1.2 Inertness of the Membrane

Unless the membrane material is catalytically active and selective for the desired reaction at the reaction conditions, it is generally desired to have a completely inert membrane. For lower temperature reactions (<200°C) membrane activity is generally not a problem since the materials used in porous membranes do not promote gas phase reactions at such low temperatures. At higher temperature, however, the problem becomes more acute. The problem is often that higher temperature reactions also involve more reactive species. For example, hydrogenation reactions often occur at relatively low temperatures and involve only a hydrocarbon and hydrogen. There is little chance a membrane will cause activity problems at these conditions. Dehydrogenation or oxidative dehydrogenation reactions, on the other hand, generally occur at temperatures in excess of 350°C (and often much higher) and involve either the presence of oxygen or a deprivation of hydrogen. In either case the possibility of the membrane being active are much higher.

At reaction conditions a ceramic or glass (silica) membrane material may be active. The inherent activity is often compounded by the large surface area of the membrane. The smaller pores necessary in a membrane to provide selectivity or to properly limit flow through the membrane give the membrane a significant specific surface area. Pores in the range of 5-50 nm often give rise to specific surface areas in the order of 100 m<sup>2</sup>/g.

Primarily there are two methods for creating "inertness" in an otherwise active membrane. The first method is to keep one or more of the reactive species away from any significant membrane surface area. An example of this approach is to flow one species (the reactive one) through the tube of a membrane reactor and have another

species permeating through the membrane at a sufficient rate to prevent any back diffusion of the reactive species into the membrane. In theory this is a good idea; in practice it may be impractical due to the flow conditions it would require.

The second method is to make the membrane catalytically inactive at the reaction conditions. There are four basic ways to try to accomplish this goal.

1. Decrease the surface area (block pores)
2. Remove the active sites
3. Chemically neutralize the active sites
4. Physically neutralize (cover) the active sites.

Thus, it is the membrane material, the size of the pores and the ability to chemically or physically alter the membrane which have the biggest impact on the catalytic activity of the membrane.

#### 4.1.3 Strength and Stability of the Membrane

It is crucial in a working membrane reactor that the membrane itself can physically withstand the reaction conditions over an extended period of time. It must be able to hold the required pressure and withstand the operating pressure without developing defects (cracks, pinholes, separation of layers in a multi-layer membrane) and without a change in pore structure. There have been significant advances in the science (art) of porous, inorganic membrane construction, both in the materials that can be used and the manner in which they are made, in the last number of years. One of the areas of advancement is work with the sol-gel method of construction and effectively using it to produce crack and pin-hole free ceramic membranes (Julbe et al. (1993), Uhlhorn et al. (1992c)).

Another key area has been development of chemical vapour deposition, chemical vapour infiltration and electrochemical vapour infiltration methods (Lin and Burggraaf (1991, 1992), Uhlhorn et al. (1992a,b)) to modify the pore size of ceramic membranes.

Materials are deposited in the pores and pore sizes consistently less than 10 Å in diameter result.

The topics of how to construct the membrane and what to make it out of are vitally important, and are the key parameters in controlling the strength and stability of the membrane at reaction conditions. However, this area of research is a huge topic on its own and is really not covered in depth in this thesis. This research investigates appropriate materials, but in the end uses commercially available membranes in the manufacture of a membrane reactor. The method of preparation of the appropriate membranes from available commercial membranes will be described later in this chapter, but the question of manufacturing methods for porous, inorganic membranes will not be discussed further.

#### **4.2 Key Characteristics for an ODHD of Propylene Membrane Reactor**

A membrane for this application must meet the following relatively stringent criteria. It must be able to structurally withstand the temperature (450°C-650°C) and pressure (up to 450 kPa(g) on the high pressure side) of the reaction and there must be a way to build a membrane reactor from the membrane. It must be relatively inert to the reactants (little catalytic activity) at the reaction conditions and it must allow the correct amount of oxygen or propylene to permeate through the membrane. As discussed in Chapter 1, based on temperature and oxygen permeability constraints, only porous, inorganic membrane reactors are to be investigated. It is presupposed that oxygen will be the primary species that permeates through the membrane. The reason for this assumption is that the stoichiometry of the ODHD of propylene reaction is 4:1 (propylene to oxygen) and the reaction order of the primary and byproduct reactions indicate that oxygen partial pressure should be kept as low as possible (this latter point will be discussed in more detail in Chapter 7). As a result, it seems logical that oxygen flow into the reaction zone should be distributed evenly and that the oxygen concentration should be kept low in the reaction zone.

### 4.3 Selection of a Membrane Material

#### 4.3.1 Screening of Potential Candidate Materials

The decision to use a porous inorganic membrane limits the choice to a ceramic, glass or other metal oxide based material. Preliminary selection of material for testing was based on inert materials typically used as catalyst supports that could also be used for membrane construction. On this basis silica,  $\alpha$ -alumina and  $\gamma$ -alumina were selected for testing.

The tests were carried out to determine the catalytic activity of the material in the presence of oxygen and propylene at typical reaction temperatures for ODHD of propylene. For all cases a standard "reaction" test based on typical operating conditions was used. The operating conditions were taken as those found to give a high selectivity with moderate conversion for ODHD of propylene over an unsupported  $\alpha$ - $\text{Bi}_2\text{O}_3$  catalyst. The preliminary  $\text{Bi}_2\text{O}_3$  testing had been carried out to verify appropriate operation of the gas chromatograph and reactor system (furnace, flow controllers, etc.). These material screening tests were carried out in a 12mm OD, 10 mm ID quartz reactor according to the tubular reactor test protocol described in Section 3.2.1. Approximately 2.0 g of each material (in a bulk form rather than in any membrane form) was used. The material was packed into the reactor with an annular thermocouple in the bed to measure bed temperature. The bed was held in place by quartz wool plugs and stainless steel screens (both inert). Each material was calcined at 660°C over night in an oxygen/helium stream. The standard reaction conditions are given in Table 4.1. Each screening test was carried out over approximately 3 hours.

Table 4.1 - Standard Reaction Conditions

Parameter	Value
Temperature (nominal)	530°C
Pressure	105.9 kPa
Flow	125 sccm
Mole % Helium	72 or 76
Mole % Propylene	20
Mole % Oxygen	8 or 4

For  $\gamma$ -alumina and silica it was necessary to increase the oxygen content of the feed gas from 4% to 8% (decreasing the helium) to attempt to test the material in a situation where oxygen consumption would be incomplete. Complete oxygen consumption indicates a high activity for combustion reactions which is not desired in this application. The increased oxygen content is necessary to determine how active the material truly is since the activity would presumably decrease when all the oxygen is consumed. In the case of  $\gamma$ -alumina, even at the higher oxygen flow rate, oxygen was completely depleted. The results of the tests are given in Table 4.2.

Table 4.2 - Membrane Material Bulk Reaction Test Results

	Material		
	$\alpha$ -alumina 3.2 mm x 3.2 mm pellets	$\gamma$ -alumina 3.2 mm x 3.2 mm pellets	silica 1.6 mm to 4.8 mm spheres
Propylene Conversion (%)	5.6	12.5	7.1
Oxygen Conversion (%)	100	100	52.5
Propylene Selectivity to (%)			
CO	25.3	21.1	38.5
CO <sub>2</sub>	71.0	67.3	41.1
Ethylene	2.7	3.2	3.7
1-Butene	0.0	6.5	1.1
Acrolein	0.0	1.0	12.0
1,5-Hexadiene	1.0	1.0 (as BZ)	3.2

The selectivities in Table 4.2 are given for measured products only and are based on percentage of converted propylene that was converted to each product. The unmeasured products, primarily coke (carbonaceous deposits) on the catalyst and tarry products



deposited on the cool reactor outlet surfaces, were apparent to varying degrees in each experiment.

There was some evidence of coke formation in each of the tests. The build up of coke and tar during the  $\gamma$ -alumina test was heavy. The closure of the carbon mass balance was extremely poor and, overall, the  $\gamma$ -alumina performed very poorly. There was little coke formation in the  $\alpha$ -alumina test. The only coke apparent visually was at the end of the bed near the exit of the reactor where the oxygen concentration would have been very low. It was assumed that oxygen either prevents coke formation or serves to oxidize the carbon and remove it. Coke formation on the silica was worse than the coke formation on  $\alpha$ -alumina. Carbon build up was apparent in all particles. The smallest spheres were completely black with coke but the larger spheres only appeared to have a central core that was black. The phenomenon in the large particles is indicative of a mass transfer problem in getting larger molecules back out of the centre of the particle, but this type of thinking does not explain why the smaller particles had uniform coke deposition.

From the results of the screening tests it is apparent that none of the investigated materials is particularly catalytically inert.  $\gamma$ -alumina is the worst choice for a membrane material likely due to its high surface area. This high  $\gamma$ -alumina activity will be troubling for the use of any alumina membrane since a layer of high surface area (small pore size) alumina is usually part of an alumina membrane. It is this layer that provides the selectivity in the permeability of various components and is the layer that most limits the overall flux through the membrane. United States Filter Corp.'s Membralox alumina membranes are an example of this type of construction where there are 3 membrane layers with pore diameters of 40 Å, 2000 Å, and 8000 Å all supported on a substrate with 15  $\mu$ m macropores. Even though the layer of the small pore material may be thin in these composite membranes, the high activity of the layer made selection of this material seem inadvisable. This type of membrane, whether Membralox or not, has been used by both the Tonkovich group and the Santamaría group. They have both used methods of attempting to decrease permeability, and as a side effect perhaps decrease activity, as described in Chapter 2. The Santamaría group has also taken to doping the membrane

with Li compound to try to decrease the membrane activity (Lafarga et al. (1994)). There are still some question about some aspects of reactor construction that also detract from the viability of this option. It is possible that an alumina membrane could be used for this application given the correct membrane design and proper treatment (doping) of the membrane to decrease the membrane activity. However, the use of  $\gamma$ -alumina is not considered further in this study. This approach could be a thrust of future work.

Although  $\alpha$ -alumina proved to be less active than  $\gamma$ -alumina it still had relatively high activity for complete combustion of the propylene. The smaller specific surface area and consequently larger average pore diameter of  $\alpha$ -alumina, 2000 Å (Tonkovich et al. (1996a)), make it somewhat unacceptable as a permselective membrane on its own. Diffusion through the pores would be by bulk diffusion and hence it would be difficult to keep the reactants substantially separated (one of the goals) in a practical membrane reactor. This problem can be partially overcome by sealing a large portion of the pores and allowing a high transmembrane pressure difference and large flux to help prevent back permeation (Tonkovich et al. (1996a)). One drawback to this approach is the difficulty in achieving uniform distribution of the permeating feed. Another drawback is that the very high flux through the membrane that would be required may not be practical given the constraints of the reaction stoichiometry. One of the key problems with alumina, in general, is that it possess both acidic and basic characteristics. Dehydroxylation above 200°C results in the appearance on the surface of  $\text{Al}^{3+}$  ions (Lewis acid) and the very strongly basic  $\text{O}^{2-}$  ions. It is the effect of the  $\text{O}^{2-}$  ions that is observed in the  $\alpha$ -alumina case as combustion reactions are highly promoted. It was not clear that any type of treatment or doping of the membrane would permanently reduce the basic characteristics of the alumina.

The results of the silica test indicated that it too is not inert to the reaction, but the results did indicate that the activity is different from that of the aluminas. The activity is not as high as for  $\gamma$ -alumina and the surface must have a more acidic nature, based on the product distribution, than  $\alpha$ -alumina. It appears as if mass transfer effects and possibly the binder used in the silica itself or an impurity may have been playing some role in the

activity. Since pure silica should be relatively inert, further investigation of a silica-based membrane was warranted.

One of the most widely known types of silica membrane is porous VYCOR glass. Porous VYCOR glass, made by the Corning Corporation (Corning code 7930), is an intermediate product produced in the process to manufacture consolidated (non-porous) VYCOR glass. VYCOR is an impervious, high silica content (96%) glass which is produced from a 70% SiO<sub>2</sub>, 23% B<sub>2</sub>O<sub>3</sub>, 7% Na<sub>2</sub>O material (typical composition). Under certain time and temperature conditions in the manufacturing process, this material separates into two distinct phases: a silica rich phase and a boric acid phase rich in alkali borate (Schnabel and Vaulont (1978)). This miscibility gap occurs between 523°C and 752°C. The boric acid phase is easily removed by leaching with a mineral acid leaving an almost pure silica matrix with a residual 3% B<sub>2</sub>O<sub>3</sub>. The pore size is not precisely controlled in the process and Corning claims that the pore size will vary between approximately 40 Å and 70 Å depending upon the thickness of the glass being manufactured. The pore size distribution, however, is very narrow with 96% percent of the pores falling within  $\pm 3$  Å of the mean pore diameter. To produce non-porous VYCOR glass the porous material is heated to a temperature greater than 1200°C. At this temperature the pore structure collapses and the glass is consolidated.

The porous VYCOR glass has a void volume of approximately 28% of the total volume and has a specific surface area of approximately 200 m<sup>2</sup>/g. This large surface area would not be beneficial for the ODHD of propylene under the best of circumstances. The small pores will promote side reactions or over-oxidation of the hydrocarbon. The problem is magnified in porous VYCOR by the surface composition. Although the glass contains only 3% B<sub>2</sub>O<sub>3</sub>, the formation process results in most or all of this residual boron being located at the surface of the pores. Hair and Chapman (1966) found that boron is 5 to 6 times more plentiful at the surface than would be assumed by bulk analysis of the glass and that 24% of the surface cations are boron. The boron will give the surface a very acidic nature.

It is not surprising, then, that when a crushed porous VYCOR sample (5.72 g) was subjected to the standard reaction test with 4% O<sub>2</sub> the results showed the VYCOR to be very active. The VYCOR became heavily coked after 10 minutes on-line and the effluent composition changed gradually with time, perhaps as a consequence of coke formation. After 2 hours on-line oxygen conversion was 100% while the conversion of propylene was 9%. The selectivity to CO<sub>2</sub> was 34%, the selectivity to CO was 51% and the balance was to a variety of cracking and isomerization products (chiefly ethylene and butenes) that are indicative of acid catalysts. It should be noted however, that even with this large amount of VYCOR tested, oxygen could still be detected in the reactor effluent even after an hour of reaction. In addition the coke was much easier to remove from the VYCOR than from the other tested materials. Although there were certainly problems to be overcome, the VYCOR showed some promise.

There are a number of compelling reasons to select VYCOR as the membrane material.

1. VYCOR comes pre-manufactured - no membranes need to be constructed - only the reactor.
2. The pore size of the VYCOR is very appropriate for the application (proper for Knudsen diffusion in the pores) and the distribution is very tight.
3. Previous work in the lab (1988) by another researcher had led to construction of a quartz-porous VYCOR tubular reactor by U of A Technical Services Glass Shop. Thus, construction of an appropriate reactor should be possible.
4. VYCOR is visually transparent and therefore it is easy to make visual observation of the reactor. Alumina would not allow this luxury.

#### 4.3.2 Treatment of Porous VYCOR

The only other known study using porous VYCOR as a membrane reactor for an oxygen/hydrocarbon reaction is Ramachandra et al. (1996). They confirmed that the VYCOR did display activity in the OCM reaction, but indicated no problems with coking and were unconcerned with latent activity.

However, in order to use the VYCOR as a membrane for the ODHD of propylene, the acidic nature of the pore surfaces must be reduced dramatically. The acidity arises from the surface boron and possibly from the surface of the silica itself. The presence of weakly acidic silanol functional groups on the surface may have some effect, although at higher temperatures (>200°C) dehydroxylation begins to occur. The silanol groups are converted to strained siloxane bridges. This process is not complete at temperatures less than 700°C, so the silica itself may contribute to the acidity in this case. To reduce acidity due to boron, the boron must be removed or neutralized, and to reduce the surface acidity of the silica the surface area should be reduced as much as possible and heated to as high a temperature as possible to convert silanol to siloxane.

In consultation with the Glass and Glass-Ceramic Core Technology group at Corning (Danielson (1995)) four methods of influencing the surface acidity of porous VYCOR were suggested.

1. Steam treatment at 750°C for several hours.
2. Impregnate dry porous glass in an ammonium fluoride solution, rinse quickly in deionized water and air dry. Heat to 750°C for several hours.
3. Impregnate dry porous glass in an ammonium fluoride solution and then immerse in 95°C water for several hours then dry.
4. Treat glass in a flowing stream of NH<sub>3</sub> at 750°C for several hours.

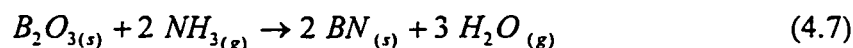
Each of these methods should affect the surface acidity by different mechanisms. The steam treatment will convert boron oxide to metaboric acid, which is volatile, by the following reaction.



This reaction should remove most or all of the surface boron from the VYCOR as long as mass transfer or reaction limits (interaction between boron and the silica surface) do not restrict the reaction. The treatment with ammonium fluoride will, Corning claims, have

two beneficial effects. First, they claim, that the  $\text{NH}_4\text{OH}$  formed when  $\text{NH}_4\text{F}$  dissociates in water will “neutralize” the acidity of the boron and second, the  $\text{HF}$  formed from  $\text{NH}_4\text{F}$  dissociation will help dissolve the smaller “spider web”-type silica filaments that are left in the pores after the VYCOR leaching process.

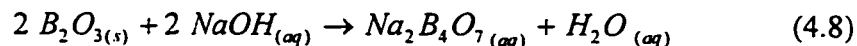
The reaction with ammonia at elevated temperatures (above  $600^\circ\text{C}$ ) will produce boron nitride, which is relatively chemically inert, by the following reaction.



Two other methods were developed independently.

5. Treat glass in  $\text{NaOH}$  solution overnight and then remove unreacted  $\text{NaOH}$  from pores by extended soaking in deionized water.
6. Treat glass in  $\text{HCl}$  solution overnight and then remove unreacted acid from pores by extended soaking in deionized water.

The treatment in a weak aqueous  $\text{NaOH}$  solution should remove boron oxide by producing aqueous borax in the reaction



and should remove the spider web silica from the pores by dissolution in the basic solution. The drawback is that the base will indiscriminately dissolve the silica in the VYCOR and will result in some structural breakdown in the glass. The treatment in hydrochloric acid may be able to remove more boron oxide by the same mechanism that Corning uses in its leaching step of the process.

All of the treatments were carried out starting with approximately 3 g of crushed VYCOR (20x30 mesh). After treatment each sample was subjected to the standard reaction test with 4%  $\text{O}_2$  in the feed. Three of the four Corning treatments (#1, 3 and 4) were tested.

The high temperature ammonium fluoride treatment (preceding point #2) was not used due to lack of success with the lower temperature  $\text{NH}_4\text{F}$  treatment. The results of the standard reaction tests on the Corning treatment samples are given in Table 4.3. All the tests showed 100% consumption of oxygen and the formation of coke. The  $\text{NH}_4\text{F}$  treatment produced results that were worse than untreated VYCOR.

Table 4.3 - Results of Standard Reaction Test from Corning Treatments

Treatment	Propylene Conv. (%)	Selectivity to $\text{CO}_2$ (%)	Selectivity to CO (%)	Selectivity to Acrolein	Comments
1	6	67	17	9	Visually coke looked heavy but, was easy to remove. There were other cracking products in small quantities.
3	10	23	20	10	Heavy coke and tar formation - only 60% of carbon can be accounted for.
4A	5	75	17	5	Uncalcined
4B	7	56	20	10	Calcined at 600°C for 15 hours

\* Selectivities are based on total propylene conversion and sum to less than 100% due to formation of unmeasured products

The results clearly indicate that none of these treatments alone is sufficient. The ammonium fluoride treatment produced no benefit. The treatment with ammonia showed promising results in that the acid characteristics and activity of the VYCOR are reduced. However the test after calcination shows a return of activity and acid characteristics. This change is likely due to boron nitride conversion back to boron oxide. This result indicates that the boron has to be removed from the VYCOR, not merely converted to another form for a treatment to be effective. The steam treatment reduced activity and acidity to some degree, an encouraging sign, but could not sufficiently reduce either.

The attempt to remove more boron by acid leaching (treatment 6) proved to be unsuccessful. It did not alter the VYCOR performance at all. Treatment with 0.038 M NaOH, however, was much more successful. VYCOR treated in this manner gives only 1.85% propylene conversion and 30.5% oxygen conversion with 55% selectivity to  $\text{CO}_2$ , 20% to CO and 25% to acrolein. There was no coke formation. In comparison to all the other treatments the NaOH treatment is dramatically better. The activity of the NaOH treated VYCOR, however, is still higher than would be desired.

In an attempt to further reduce the activity of the VYCOR the two most successful treatments (NaOH treatment and steam treatment) were combined sequentially. Treatment with steam first and in basic solution second provided no incremental benefit. NaOH treatment followed by steam treatment, however, produced outstanding results. In the standard reaction test propylene conversion was negligible and oxygen conversion was less than 5%. There was no measurable production of carbon oxides. It should be noted that the steam treatment temperature had to be limited to 600°C. The treatment of VYCOR with NaOH weakens the pores by removing the spider web silica filaments within the pores that give the pores added strength. Without these filaments the pores are much more prone to collapse under high temperature conditions. Untreated VYCOR does not even begin to experience linear shrinkage (pore collapse) until 750-800°C (Shelekhin et al. (1995)). Almost complete collapse of the pore structure of the NaOH treated VYCOR is evident at 750°C. Treatment at 600°C causes only limited pore collapse.

There is little doubt that the pore structure and surface composition of the VYCOR has been significantly altered by this dual treatment. The difference in activity is one key indicator, but the analysis of the pore size distribution and specific surface area of the VYCOR before any treatment and after the dual treatment is another clear indicator. The comparison of the two states is shown in Table 4.4.

Table 4.4 - Pore Size and Surface Area of Treated and Untreated VYCOR

	Untreated VYCOR	Dual treated VYCOR
Average pore diameter	40 Å	52 Å
Surface Area	188 m <sup>2</sup> /g	94 m <sup>2</sup> /g

While eliminating activity in the test sample is a very positive sign, it must be remembered that the membrane will experience somewhat different conditions in actual service. In service, oxygen will be diffusing through the pores at much higher concentrations than 4% and higher pressures. The higher concentration and the fact that



it is diffusing through the pores rather than diffusing into the pores may have some effect on the observed activity. These issues are addressed in Chapter 6.

#### 4.4 Construction of a Porous VYCOR Membrane Reactor

The design of the membrane reactor itself is constrained by three factors. The first factor is that to produce reliable reactor operating data from which kinetic data may be extracted, the entire reaction zone (membrane area) must be kept at a relatively constant reaction temperature. Using a tubular reactor heated by a tubular furnace means that the interfaces or connections between the membrane and non-membrane sections of the reactor will have to be able to withstand reaction temperatures since they will be in the middle of the furnace. The second factor is that the non-porous sections of the reactor need to be absolutely leak proof and inert. The third factor is the ability to form appropriate joints between metallic and non-metallic sections of the reactor. For example joints between the "shell" (usually metallic) and "tube" (non-metallic) and the tube and feed lines (metallic) must, at the very least, be able to hold pressure. Within these constraints a number of design options exist.

There are two construction methods that have evolved in porous membrane reactor design to deal with the constraints. The first method is to design the entire reactor out of the porous material and simply seal the pores in the sections which need to be non-porous. Numerous research groups have used an enamel (Lafarga et al. (1994), Tonkovich et al. (1996a)) or colloidal silica (Omata et al. (1989)) to seal the pores of an alumina membrane to create the non-porous sections. Although this method has been very successful, there is no reference in the literature of it ever being attempted with a porous glass membrane. A method of sealing porous glass which has been successful is to flow  $\text{SiH}_4$  and  $\text{O}_2$  from opposite sides of the membrane so as to react within the pore structure to form a very thin layer of  $\text{SiO}_2$  within the pores (Gavalas et al. (1989)). When the pores are completely sealed the reaction ceases. Another approach used by Ramachandra et al. (1996) is to heat treat the VYCOR section that are to be non-porous until all the pores in those sections have collapsed. In effect they made those sections

into non-porous VYCOR in the same manner that Corning does. These latter two approaches were considered but it would have to be applied after the VYCOR tubing has been completely treated. Uniform treatment of 2-3 ft sections of VYCOR tubing proved to be exceedingly difficult and there was great uncertainty as to whether heat treatment of a large section of the treated VYCOR would have produced a truly non-porous tube. Thus neither of these two approaches was attempted.

The second design method is to use only a small membrane section and physically or mechanically seal it to the non-porous sections of the reactor. Champagnie et al. (1990, 1992) have used a shell and tube design with an alumina inner tube as the membrane. They seal the membrane to the outer shell by means of graphite string and compression fittings. They, however, were investigating dehydrogenation reactions (without oxygen present) and there is some question as to whether the graphite seal could withstand high temperature and an oxygen environment. For lower temperature applications, epoxy has been used (often in construction of diffusion cells) to connect porous glass membranes to inert tubing (Okubu and Inoue (1987)).

A third possibility exists for porous glass membranes, and that is to fuse the porous glass to an inert quartz tube. Treatment of the end sections of the cylindrical porous glass membrane at high temperature will cause collapse of the pore structure and will produce a non-porous, silica glass. Quartz can be bonded to this non-porous material with regular glass working techniques. An effective method of construction for this design has been developed by the Scientific Glass Blowing - Technical Services (U of A). Within the open literature there are a few examples where the experimental apparatus is described as quartz "bonded" to porous VYCOR but no details on the type of connection are given (Shindo et al. (1983, 1984)).

Although the process to fuse untreated porous VYCOR to quartz is time consuming, difficult and delicate, the personnel with the skills exist at the University of Alberta and the results have proven to be consistently excellent. This type of bond will readily withstand the temperatures and pressures of the ODHD process and hence it was selected

as the primary method of construction. A second method using a high temperature epoxy adhesive was also investigated.

Fusing of the treated VYCOR (NaOH followed by steam treatment) to quartz proved to be much more difficult than for untreated VYCOR. In order to treat the membrane effectively, the treatment process had to precede the construction of the reactor.

Treatment of the VYCOR tends to weaken its structure to some degree and this problem became evident when the material was heated to temperatures necessary for fusion. The treated VYCOR had a high tendency to crack under this thermal stress. In addition the treated VYCOR tended to produce bubbles within the pores as it reached the fusion temperature. This problem had been encountered with untreated VYCOR but it was not extreme and the bubbles could be delicately picked out of the VYCOR before it cooled. The problem was so extreme with the treated VYCOR that the bubbles could not be removed and it was impossible to produce a strong gas tight bond between VYCOR and quartz. The glassblowers described the phenomenon as foaming. This approach had to be abandoned since reliable, repeatable construction of reactors was not possible.

The use of an adhesive to glue the membrane to quartz would certainly avoid many of the difficulties encountered when trying to fuse VYCOR to quartz in the traditional manner. Since no thermal glass working of the VYCOR would be required, the problems of cracking and foaming would be avoided and the simplicity of the construction method would likely increase the consistency of reactor quality. The problem in this application, of course, is finding an adhesive that will withstand the process temperatures and still provide a strong gas-tight seal between quartz and VYCOR. Normally this alternative would have been immediately discarded, but the glass shop had procured a high temperature adhesive, ROCKSETT, that the distributor claimed could produce a gas-tight seal at temperatures in excess of 750°C.

A preliminary tests of the adhesive was conducted by gluing two non-porous glass plates together. The adhesive produced a very strong bond between the plates even after exposure to 565°C heat with the use of very little adhesive. Given this success, a reactor

with a VYCOR membrane joined to two pieces of quartz tubing with socket joints was constructed as shown in Figure 4.3.

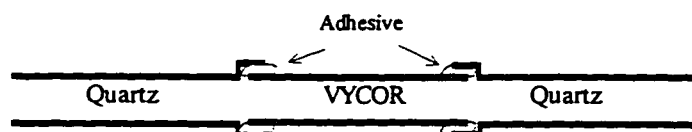


Figure 4.3 Adhesive Bonded Membrane Reactor Prototype

Although the adhesive flowed readily into the socket joints, the porous VYCOR tended to draw some liquid into the pores and upon drying the adhesive tended to bond poorly with the VYCOR at the outer lip of the socket joint. As a result a gas tight seal was difficult to achieve even though the bond between VYCOR and quartz was very strong. The gas tight seal could be restored by repeated addition of adhesive around the leaking area. The bond was capable of holding 50 kPa pressure at ambient temperature.

A much more serious problem than gas leakage developed when the prototype reactor was heated to reaction temperatures of  $\sim 530^{\circ}\text{C}$ . The epoxy turned from amber to gray in colour and dramatically changed form. Instead of the solid material present at ambient temperatures, the gray material was very porous and crumbled at the touch (at least the material that was outside the socket joint). The epoxy appeared to foam as indicated by the fact that it expanded radially inward and broke the VYCOR contained within the socket joint. Subsequent testing of the adhesive in inert and oxygen atmospheres showed that the transition in the state of the adhesive was purely a thermal phenomenon that occurred between  $325$  and  $400^{\circ}\text{C}$ . The rate of heating had a strong bearing on the degree to which the epoxy foams, but it did not change the final form of the epoxy as a porous material. Although the bond was still mechanically very strong, it was never gas-tight. It appears that the volatile material in the epoxy evaporates in the stated temperature range. Rapid evaporation leads to greater foaming. This failure meant that the use of high temperature epoxy was not a viable method of construction.

A third method of bonding VYCOR and quartz had originally been rejected because it results in a diameter restriction at the inlet and outlet to the membrane section of the reactor. There is no indication in the open literature that this method had ever been tested and there was some concern as to whether or not a proper seal could be achieved. The method depends on the radial shrinkage that tubular porous VYCOR undergoes as it is heated to form consolidated VYCOR. The process basically involves heating the VYCOR to a high enough temperature in a specific location that it “shrink wraps” itself around a quartz sleeve to form a fused joint. A simplified schematic drawing of the construction process is shown in Figure 4.4.

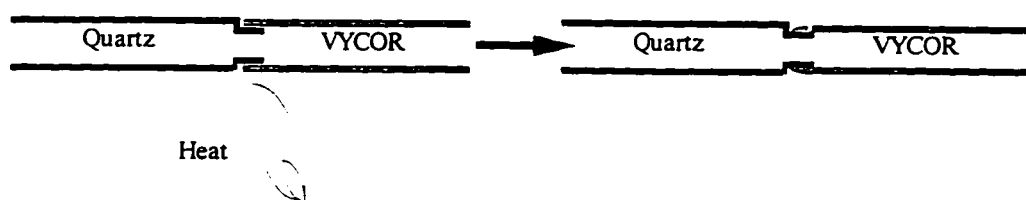


Figure 4.4 Shrink Wrap Construction Process

The small end sections of the VYCOR membrane that were consolidated to form the joint still suffered from the bubbling problem mentioned previously. However this type of socket joint provides a much larger surface area over which the joint is formed compared to the butt joint that is formed with the traditional method of glass working. In this way the bubbles are not interfering with the joint and proved not to be a problem. High strength, gas-tight connections between quartz and VYCOR could be consistently made with this method. In fact, if the original attempt to form the joint does not produce a gas tight seal, the material need only be re-heated and the joint re-worked. The only significant drawback inherent in this design is the diameter restriction of the quartz inner sleeve. Compared with the advantages that this method of construction has, the drawback is not a serious problem and hence the “shrink wrap” process was selected as the method of construction. A more detailed description of the construction process is given in Appendix A.

The VYCOR tubing used in this research comes from Corning as nominally 17 mm OD with 1.5 mm wall thickness. In reality the material dimensions are found to have some variability and are in the range 14-14.5 mm ID, 17-17.5 mm OD. The NaOH step of the treatment process is very harsh and actually removes a noticeable amount of material from the VYCOR. The result is that after treatment the tube dimensions are 14.5 mm ID, 16.5 mm OD. The quartz tubing to which it is bonded is 15 mm ID, 18 mm OD with the quartz sleeve being 12 mm ID, 14 mm OD. The total VYCOR tube portion of the reactor is 75 mm. Of this length approximately 10 mm of tubing is required on each end to make the shrink wrap joint. As a result the remaining porous tube length in the fully constructed tube section of the reactor is 55 mm. The dimensions of the assembled tube are shown in Figure 4.5.

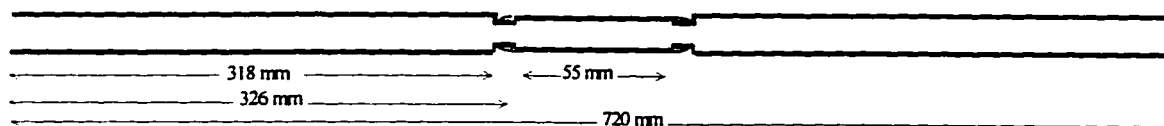


Figure 4.5 Dimensions of Membrane Reactor Tube Assembly

The final step in the construction of the reactor is a decision regarding the type of shell material to use and how to connect the tube to the shell and to the feed lines. In high temperature applications the use of stainless steel (SS) for the shell is preferred because it easily resists the temperature and will hold pressure, it is easy to work with and connect to process tubing and has very low specific surface area. For shell and tube type membrane reactors a metal (usually SS at the bench level of research) shell is most common and was selected for this application. A 25.4 mm OD 316L SS tube fitted with 25.4 mm Swagelok Tee fittings on either end forms the bulk of the shell.

This design allows all the connections between quartz (tube) and metal (tube side process lines and shell) to be made outside the furnace. As is usually the case for such connections they are made with appropriate gasket material and compression fittings. In this case two sets of 19 mm Cajon vacuum fittings with Viton o-rings are used to make the compression fitting connection to the 18 mm OD, 15 mm ID quartz tubing. One set of fittings is used for the tube to shell joints and the second set of Cajon fittings is used to

connect the inlet and outlet (tubeside) of the quartz reactor to the SS feed and effluent line tubing. Since all of these connections are made outside of the furnace, they are only subject to heating by conduction through the SS and quartz. The temperature at the shell to tube seal is well below the allowable Viton limit of 204°C. These seals are capable of withstanding a differential pressure of 450 kPa. There are a variety of other Swagelok fittings to facilitate the proper connection of the process lines and for entry of thermocouples into the reactor. Figure 4.6 is a schematic drawing showing the reactor details. Although the outlet of the shell is shown to be capped, the cap can be replaced to allow a continuous sweep flow through the shell if desired. A snug fitting quartz tube (20 mm ID, 22 mm OD) is placed along the entire length of the interior of the shell (stretching from Tee fitting to Tee fitting) to act as a sleeve and prevent any catalytic activity by the SS shell. This topic will be further discussed in Chapter 6.

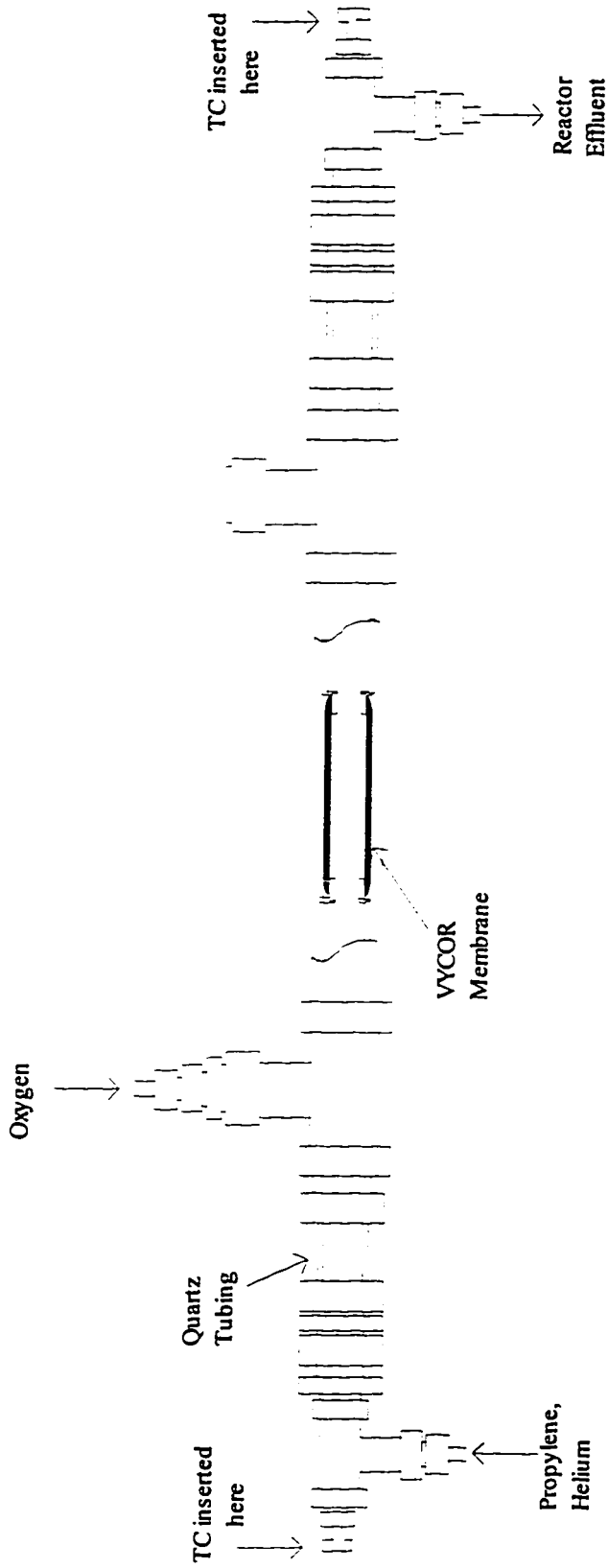


Figure 4.6 Membrane Reactor Details



## Chapter 5

### Aspects of Safety

In any research effort safety is of paramount importance. The area of “safety” encompasses numerous topics including proper construction and maintenance of the experimental equipment, safe handling and storage of feed chemicals (compressed gas cylinders in this case), safe and proper disposal of products/byproducts of the reaction, proper operation of laboratory equipment, appropriate handling and preparation of catalysts, and general lab cleanliness. It is important that all these aspects of safety are dealt with in an appropriate manner. Within the University of Alberta and the Department of Chemical and Materials Engineering guidelines exist to cover many of these issues, particularly those which are applicable to many of the research facilities. There is no need to cover these issues in any depth within this thesis. However, there is one issue surrounding equipment operation for this project which does warrant some in-depth discussion because it is an important ongoing safety issue and because it illustrates one of the advantages of using a membrane reactor compared to using a conventional reactor.

When operating any hydrocarbon/oxygen system, bench scale or industrial scale, operation inside the explosive envelope must be avoided for obvious reasons. The upper and lower explosive (or flammability) limits represent the range of concentration of hydrocarbon in an oxygen containing atmosphere at given temperature and pressure conditions over which a flame will propagate freely after ignition. The ability of the flame to propagate through a homogeneous gas mixture is affected by the relative abundance and proximity of hydrocarbon and oxygen molecules to one another and to some degree by the physical geometry of the system. Determination of the upper and

lower limits of flammability must be done experimentally as no effective method of predicting the limits is available.

Most often the flammability limits are determined at atmospheric pressure and room temperature. For propylene the limits in air and pure oxygen are given in Table 5.1.

Table 5.1 - Limits of Flammability of Propylene at Atmospheric Pressure and Room Temperature

	Lower ( $L_{25}$ )	Upper ( $U_{25}$ )
in air	2.4 vol%	11 vol%
in oxygen	2.1 vol%	53 vol%

Although the information in Table 5.1 is valuable, it does not directly apply to the situation under investigation in this study. In this study the temperatures considered are well above room temperature and the oxygen feed is highly diluted by helium. Only experimentation with conditions applicable to the test conditions would determine the explosive limits for this situation. However, the standard conditions and the propylene flammability tests using nitrogen as an inert diluent (from Jones and Kennedy (1938) as reported in Zabetakis (1965)) can be used to estimate the flammability limits for the reaction conditions. The flammability limits for most hydrocarbons widen slightly as temperature increases. It is suggested in Zabetakis (1965) that the effect of temperature on the lower and upper flammability limits can be estimated by the modified Burgess-Wheeler law by utilizing the net heat of combustion,  $\Delta H_c$  (in kcal/mol) for a substance. The modified Burgess-Wheeler law expression for the lower and upper flammability limits is shown in equations 5.1a and 5.1b.

$$\frac{L_T}{L_{25}} = 1 - \frac{0.75}{L_{25}\Delta H_c}(T - 25) \quad T \text{ in } ^\circ\text{C} \quad (5.1a)$$

$$\frac{U_T}{U_{25}} = 1 + \frac{0.75}{U_{25}\Delta H_c}(T - 25) \quad T \text{ in } ^\circ\text{C} \quad (5.1b)$$

Since the net heat of combustion for propylene is 460.4 kcal/mol, the lower and upper flammability limits in air at 530°C are 1.6 vol% and 11.8 vol%, respectively. The effect of addition of an inert diluent, nitrogen, to the air-propylene system at 26°C is shown in Figure 5.1.

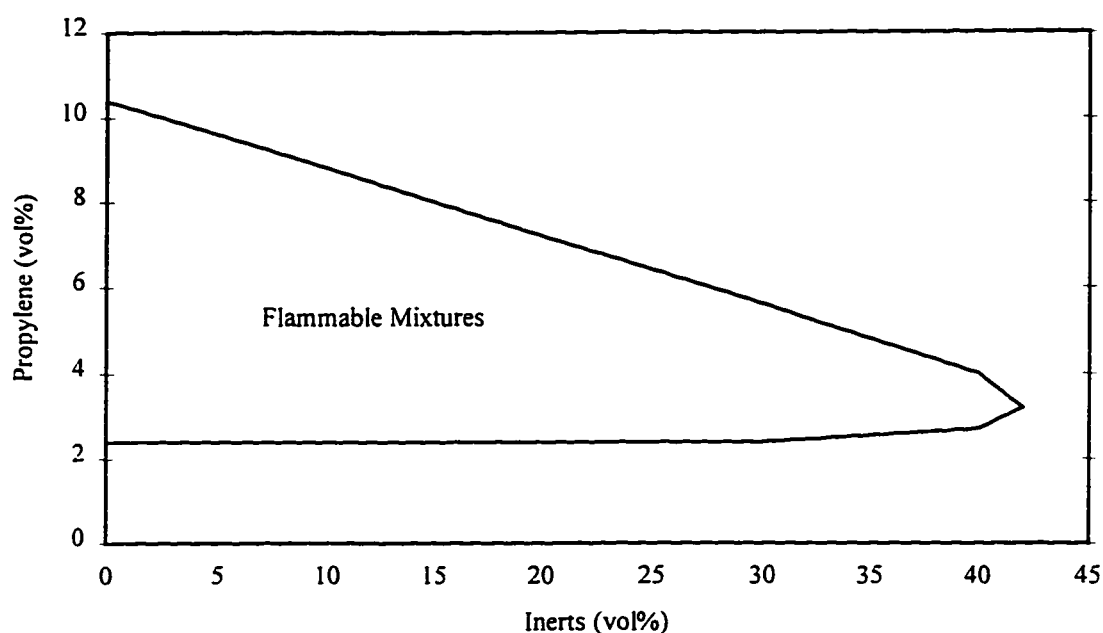


Figure 5.1 Flammability Limits for Propylene-Air-Nitrogen System at 1 atm and 26°C

In Figure 5.1 the air content in the system is 100% - propylene vol% - inert vol%. If it is assumed that nitrogen and helium behave in a similar manner in the mixture then the data from Figure 5.1 can be re-interpreted to represent the propylene-helium-oxygen system used for this study. The data, then, can be presented as a flammable region with oxygen volume percent and propylene volume percent as the parameters. The volume percentage of helium in the mixture is the balance. This data, which applies to systems in which there is lower oxygen concentration than in the standard propylene-air system, is shown in Figure 5.2. Estimates, using the modified Burgess-Wheeler law, of the explosive limits at 530°C are also shown on Figure 5.2.

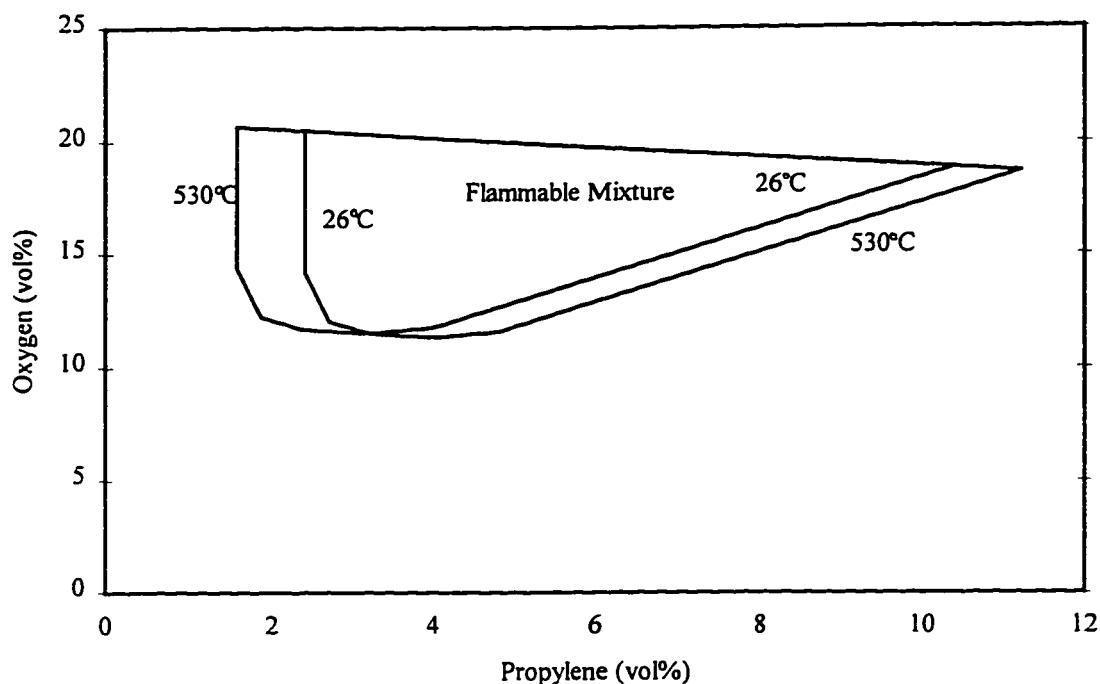


Figure 5.2 Flammability Limits for Propylene-Helium-Oxygen System at 1 atm, 26°C and 530°C

This approximation provides two important pieces of information. The first and most obvious (because it could be easily derived from the standard propylene-air system data) is that a system with propylene content greater than 11.5 vol% will not be flammable. The second piece of information is that the oxygen content must be greater than 11.5 vol% to form a flammable mixture.

The stoichiometric feed composition for the ODHD of propylene is 46% propylene in air and 80% propylene in oxygen and the reaction tends to be operated in a propylene rich environment to try to limit unwanted side reactions. Thus the “normal” operation of this process would be well above the upper flammability limit. However, the configuration of the membrane reactor allows the safe operation of the process at conditions that could normally fall within the explosive range and this is one advantage of using a membrane reactor. For example, if a high oxygen concentration is required to keep a catalyst in the membrane pores oxidized, it is possible with the membrane reactor. Alternately a reaction such as the production of maleic anhydride from butane, where the normal

stoichiometric feed is in the middle of the explosive range for both air and oxygen as the oxidant, could benefit greatly from membrane reactor technology. The existing maleic anhydride processes using either packed or fluidized bed reactor technology must operate with 1.7 mol% butane or less in the feed to avoid the explosive region.

There is also an operational safety advantage in using a membrane reactor. The hydrocarbon and oxygen are physically separated by the membrane with flow between the components regulated by the membrane. In an emergency situation (flow disruptions or control valves failing or sticking open on the oxygen system) it is much easier to prevent an explosive mixture from forming than in a conventional mixed feed reactor system. The final piece of important operating information that can be derived from the flammability limits data is how to stop/start/adjust flow rates during transient operation, primarily startup and shutdown, to avoid the formation of an explosive mixture in the reactor. In this study, the system is operated above the upper explosive limit. Safe operation would dictate that, upon start up (particularly at reaction temperatures), the reactor be purged of oxygen and that either propylene is added first or that oxygen and propylene (diluted with helium) are added simultaneously. Oxygen should never be added first. Safe operation also dictates that for shutdown situations, if one or more feed streams are to be shut off, oxygen must be removed first from the reactor to ensure that any mixtures formed are always above the upper explosive limit. These operating strategies are followed as outlined in the reactor operation protocols described in Chapter 3.

## Chapter 6

### Testing of Blank Membrane Reactors

Two of the primary reasons for selecting porous VYCOR as the membrane material for the membrane reactors in this study are that it will provide appropriate permeability to oxygen and that it is relatively inert to the reactants and the reaction conditions. In establishing the baseline performance of the membrane reactor, measurement of the permeability and activity of the membrane is necessary. The results of the evaluation of these two aspects of the membrane reactor are presented and discussed in the two major sections of this chapter.

More than one membrane reactor is used in the catalytic testing portions of this study (Chapters 7 & 8). It was possible to carry out each of the major aspects of the catalytic testing with one reactor so that the properties for the individual reactors could be appropriately applied to the corresponding test. However, for the sake of consistency it is desirable to have all the membrane reactors that are the same (same treatment, same construction procedure and same membrane dimensions) behave in the same manner. That is, within some error tolerance, the permeability and activity of each of these reactors should be the same. For the two parameters, permeability and activity, individual reactors were tested to the degree necessary to establish the information needed for the subsequent catalytic reaction tests. Thus the degree of investigation, particularly for activity, is much greater for some reactors than others. However, simple tests at identical, representative conditions were run on a variety of reactors to show that the results were consistent from reactor to reactor. The details of the blank membrane reactor tests are given in the following sections of this chapter.

## 6.1 Membrane Permeability

For the reactions involving the interaction of propylene and oxygen on the catalysts used for this study it is most appropriate to have oxygen flowing into the reactor on the shell side of the reactor (catalyst is assumed to be packed in the tube of the reactor or supported on the membrane) and permeate through the membrane into the tube of the reactor. In this way oxygen will be uniformly added to the reactor along the whole length of the reactor. The feed flow rates and temperatures used in the catalytic studies are outlined in Section 6.2 on membrane activity. However, for the sake of testing permeability it is important to test at representative conditions. The propylene/oxygen reactions take place at temperatures of approximately 500°C and require O<sub>2</sub> flow rates through the membrane between 3.75-15.0 sccm. The key questions to answer when testing the membrane reactor permeability are whether these flow rates can be achieved at reasonable pressures, whether the permeability is consistent among reactors, and whether the permeability remains stable or constant with time on-stream for individual reactors.

The weakest pressure-containing element on the shell side of the reactor is the Viton o-ring seal in the Cajon fittings. Those fittings can reliably contain a differential pressure of approximately 450 kPa but tend to develop small leaks at higher pressures. Thus, the membrane reactor permeability must be sufficiently high to allow the flow of 15 sccm of oxygen at the maximum reaction temperature with less than 450 kPa differential pressure across the o-ring. It has been assumed that Knudsen diffusion will be the dominant mode of oxygen transport through the membrane. Tests must be performed to characterize the permeation abilities of the membrane. Specifically, the tests must determine that the membrane can permeate the required amount of oxygen at reaction conditions and confirm that Knudsen diffusion is dominant

The papers by Hwang and Kammermeyer (1966) and Shindo et al. (1983) are both studies of the diffusion of permanent gases through porous VYCOR glass. Both papers present models to predict the permeability of the permanent gases through the VYCOR with contributions from both Knudsen flow and surface flow. The model of Shindo et al.

(1983) is more sophisticated and is based on data taken in the temperature range of 300-900 K. The model is given by equation 6.1.

$$Q = \frac{K}{\sqrt{MT}} \left[ \frac{1}{1 + \frac{\beta}{T} \left( \frac{e^*}{k} \right)} + \alpha \left( \exp \left( \frac{e^*}{kT} \right) - 1 \right) \right] \quad (6.1)$$

The  $\beta$ -containing term is the contribution of the Knudsen flow and is not a strong function of temperature whereas the  $\alpha$ -containing term is the contribution of surface flow and is a strong function of temperature. The parameters  $\alpha$  and  $\beta$  are constants for all gases and have the following values.

$$\alpha = 0.246$$

$$\beta = 0.606$$

The values of  $K$  and  $e^*/k$  depend on the gas in question and are given in Table 6.1 for helium and oxygen.

Table 6.1 - Constants for Equation 6.1

Component	$K$ ( $\text{mol}^{1/2} \text{kg}^{1/2} \text{K}^{1/2} \text{s}^{-1} \text{m}^{-1} \text{Pa}^{-1}$ )	$e^*/k$ (K)
Helium	$4.07 \times 10^{-11}$	108
Oxygen	$4.14 \times 10^{-11}$	247

The relative contributions of Knudsen and surface flows for both oxygen and helium are shown in Figure 6.1a for temperatures up to 900 K. Although surface diffusion does play a role, particularly for oxygen at lower temperatures, it is less than 10% of the total contribution for both components in the reaction temperature range.



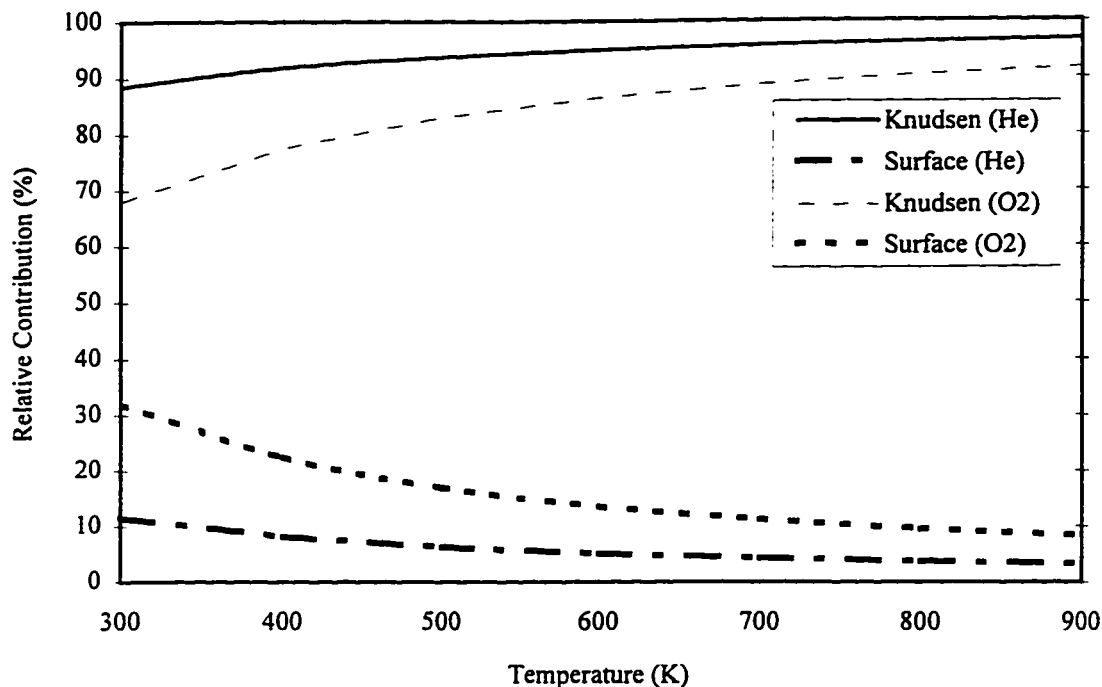


Figure 6.1a Relative Contributions of Knudsen and Surface Flow for Oxygen and Helium in VYCOR

The role that surface diffusion plays in the transport of propylene through a VYCOR membrane is much greater than the role for either helium or oxygen. Studies by Okazaki et al. (1981), Horiguchi et al. (1971) and Gilliland et al. (1958) have investigated permeation of propylene through a porous VYCOR membrane at lower temperatures (up to 50°C). All three studies found similar results, namely that at temperatures around 0°C the contribution of surface flow is approximately 3-5 times that of Knudsen diffusion. The contribution of the two modes becomes approximately equal at temperatures around 50°C. There have been no studies at higher temperatures so it is difficult to predict with certainty what role surface diffusion will have at reaction conditions (500°C). Testing of permeability of propylene in this high temperature range is impossible since the propylene reacts on the VYCOR surface. Although the work of Shindo et al. (1983) was based on permanent gases, if it is assumed that the values of  $\alpha$  and  $\beta$  still apply for propylene, then the  $\alpha$ -containing and  $\beta$ -containing terms from equation 6.1 can be used, with the estimates of the ratio surface flow to Knudsen flow from Okazaki et al. (1981),

Horiguchi et al. (1971) and Gilliland et al. (1958), to estimate  $e^*/k$ . Using a surface flow to Knudsen flow ratio of 3 at 0°C gives  $e^*/k=520$  K and using a surface flow to Knudsen flow ratio of 0.8 at 50°C gives  $e^*/k=432$  K. These values do not match exactly and may indicate that the assumption of constant  $\alpha$  and  $\beta$  for propylene may not be precisely correct. However, using an average  $e^*/k$  value of 475 K, estimates of the relative contribution of surface and Knudsen diffusion flow at higher temperatures can be made using equation 6.1. These estimates are shown in Figure 6.1b. At reaction temperatures these estimates predict the portion of flow due to surface flow to be approximately 20%.

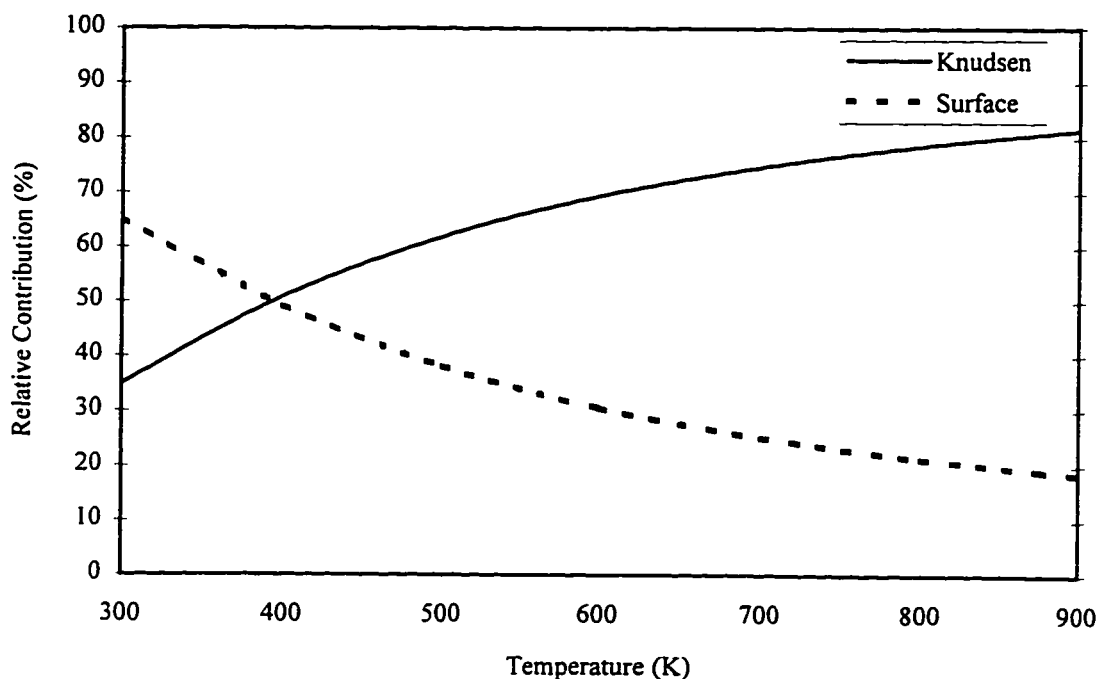


Figure 6.1b Estimates of Relative Contributions of Knudsen and Surface Flow for Propylene in VYCOR

A series of permeation tests has been conducted with a number of completely fabricated VYCOR reactors. Since fabrication must be done after the VYCOR membrane has been treated, there are no permeation results for an untreated membrane. This information is not crucial to the study, but it would have provided a more direct comparison to the results of others who have tested the untreated material for permeability and would give some further insight into the changes that the membrane treatments had caused.

Permeability tests were also conducted on a previously constructed VYCOR reactor that

had been subjected to 900°C treatment during another study. Unfortunately, as Shelekhin et al. (1995) have noted, the porous VYCOR undergoes dramatic change (pore collapse) at approximately 900°C manifested by an approximate 50% decrease in both pore volume and permeability of the membrane. Thus, comparison of the treated membrane to this reactor is of little value. The first prototype reactor in this study was constructed after undergoing NaOH treatment but the steam treatment was carried out after the reactor construction was complete. The results of the permeability tests conducted before and after steaming are shown in Figure 6.2. The steam treatment increased the permeability by approximately 20%. This increase is consistent with increased permeability found by Shelekhin et al. (1995) for heat treatment of VYCOR between 600-800°C.

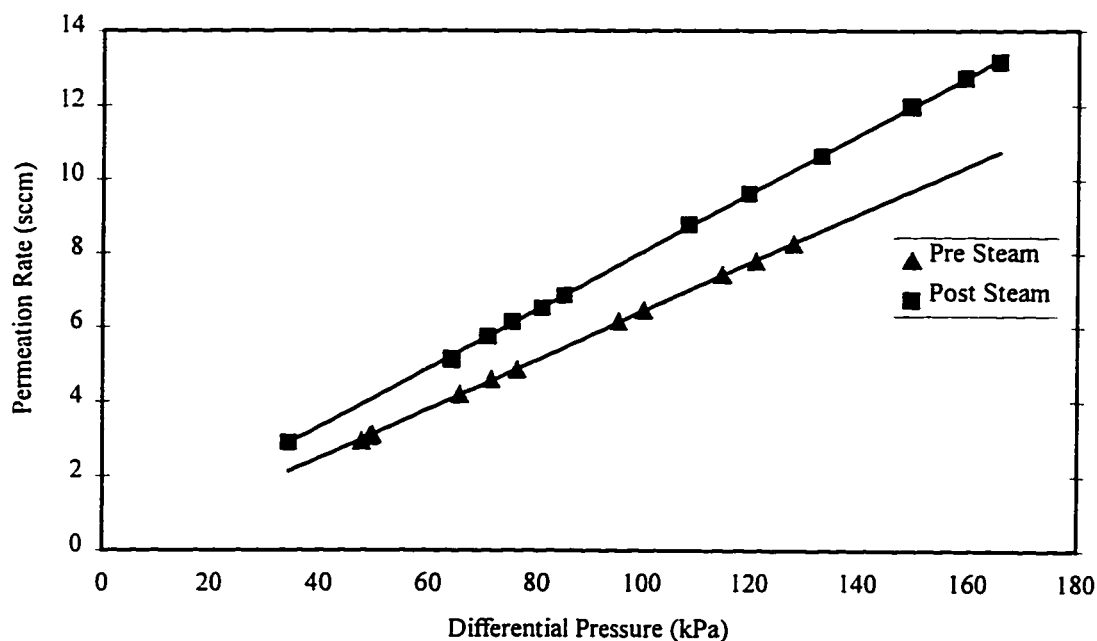


Figure 6.2 Effect of Steam Treatment on Membrane Permeability to Oxygen

The permeation tests on the treated membrane reactors have been carried out to test the permeability of all three feed components at room temperature and the permeability of the membrane to oxygen at reaction temperatures. The results for all the membranes tested were consistent indicating that the treatment and construction procedures serve to produce reactors with uniform permeability characteristics. Typical permeation rates as a function of the partial pressure difference across the membrane are shown in Figures 6.3

and 6.4. For all these tests the gases permeated across the membrane from the shell side to the tube side. The shell was first purged with the gas then the exit from the shell was sealed (Cajon fittings) and pressure was increased to the appropriate level. The tube side was also purged with the gas and then left to vent to an atmospheric bubble flow meter used to measure the gas permeation flux. In this manner, pure gases are present on both sides of the membrane and the partial pressure difference of the species is equal to the gauge pressure of the shell side.

There are two key points to be drawn from the information presented in these figures. The first point is based on the fact that the relationship between pressure and flux is linear with an intercept of approximately zero for all cases. Based on the discussion in Chapter 4, it is the case that this sort of relationship will only be true if bulk flow and normal molecular diffusion are not occurring. Bulk flow varies (approximately) as the square root of the difference in squares of the pressures on either side of the membrane. Although the driving force for molecular diffusion is partial pressure, the diffusion coefficient varies inversely with total pressure. Thus the occurrence of either phenomenon will skew the linear relationship.

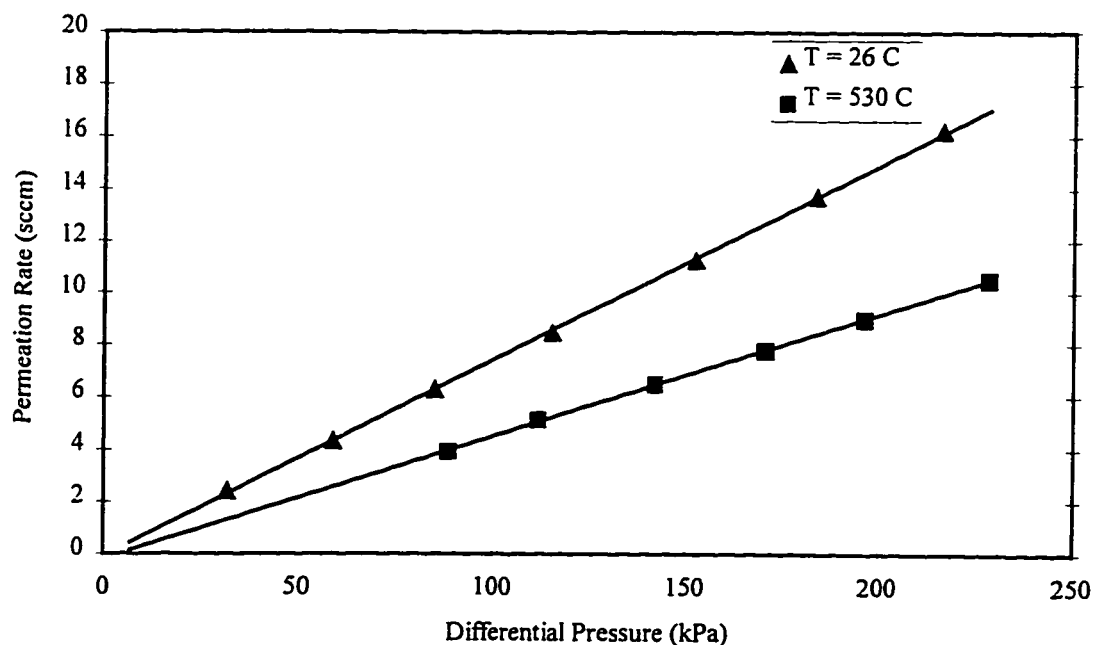


Figure 6.3 Oxygen Permeation Rates through a Fully Treated Membrane (Variation with Temperature)

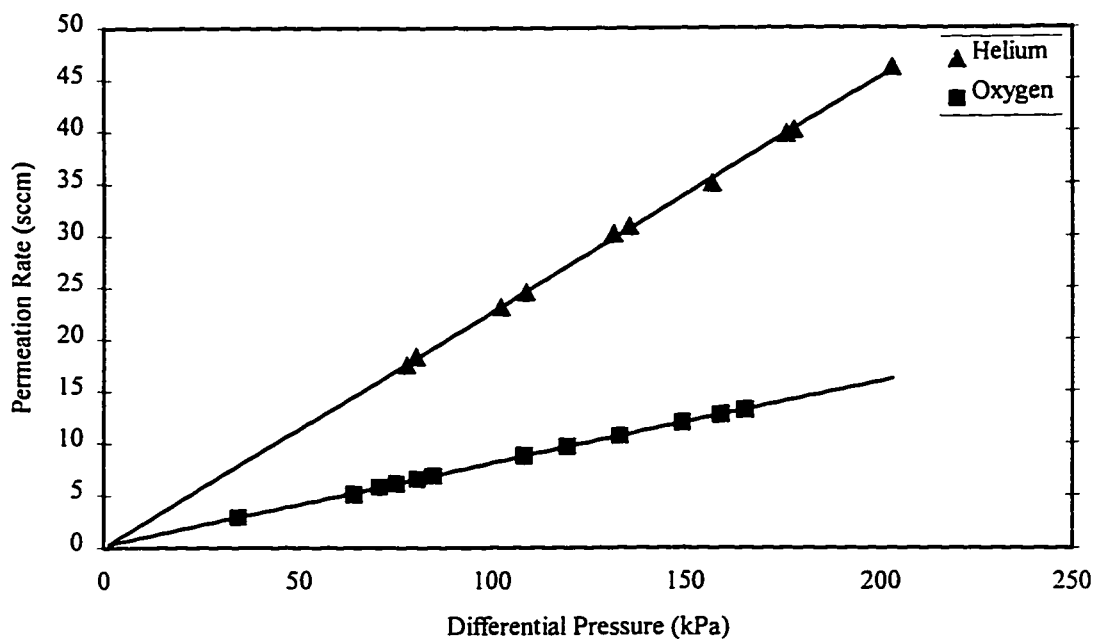


Figure 6.4 Oxygen and Helium Permeation Rates through a Fully Treated Membrane at 23°C

The second point is to determine what portion of the total flow is due to surface diffusion and what portion is due to Knudsen diffusion. The slope of the permeation curve is used to calculate the permeability, so the slopes can be used to determine if the effect of species and temperature meet the criteria of Knudsen diffusion. From Figure 6.3, for oxygen the 26°C line has a slope of 0.0750 sccm/kPa while the 530°C line has a slope of 0.04678 sccm/kPa. Knowing, from equation 4.5 that the flux varies inversely with the square root of temperature, the ratio of the permeation coefficients is

$$\frac{0.04678}{0.075} = 0.624$$

and the square root of the ratio of the temperatures is

$$\sqrt{\frac{299.15}{803.15}} = 0.610 .$$

They differ by less than 3% which indicates that either Knudsen diffusion is predominant or that the portion of the flow contributed by surface diffusion is constant at both temperatures. If it is assumed that the values of  $\alpha$  and  $\beta$  still apply for oxygen diffusion through the treated VYCOR, then equation 6.1 can be solved simultaneously at the two temperatures to give estimates of  $6.91 \times 10^{-11}$  (mol kg K)<sup>1/2</sup>/(s m Pa) for  $K$  and 35.7 for  $e^*/k$ . This value of  $e^*/k$  indicates that oxygen surface flow would contribute 3.2% of the flow at room temperature and approximately 1.1% at 800 K in the treated VYCOR membrane. Thus, it is concluded that surface flow is not playing a significant role in the permeation of oxygen in this system at any temperature. The value of  $K$  is 67% greater than the Shindo et al. (1983) value which applies to untreated VYCOR with 40 Å pores.

Results from Figure 6.4 tell a similar story. From Figure 6.4 the helium line has a slope of 0.226 sccm/kPa while the oxygen line has a slope of 0.0788 sccm/kPa. Again, from equation 4.5 for Knudsen diffusion the flux varies inversely with the square root of molecular mass of the permeating species. The ratio of the permeation coefficients is

$$\frac{0.0788}{0.226} = 0.349$$

and the square root of the ratio of the molecular masses is

$$\sqrt{\frac{4.0}{32.0}} = 0.354 .$$

These values are within 1.4% of one another, providing another very strong indication that Knudsen diffusion predominates. It can be assumed that surface flow will be less important for helium than for oxygen (based on the results presented in Figure 6.1a). Since surface flow is insignificant for oxygen in the treated membrane, it can safely be concluded that surface flow has almost no bearing on He flow in the treated membrane.

The final question to be answered is: what role does surface diffusion play in the propylene flux, particularly at high temperature? As noted earlier in this chapter it is

impossible to test at high temperature, but a test at room temperature (21°C) generated a flux coefficient of 0.115 sccm/kPa. Based on the results from helium and oxygen at this temperature a flux coefficient of 0.0672 sccm/kPa would be expected for pure Knudsen diffusion. It appears that approximately 40% of the flow at this temperature is due to surface diffusion. Okazaki et al. (1981), Horiguchi et al. (1971) and Gilliland et al. (1958) report that some 50-65% of the flux is due to surface diffusion at this temperature on untreated VYCOR. The treatment of the membrane has decreased the surface diffusion by 30-60% compared to the untreated case at room temperature. It is impossible to draw a definitive conclusion, but it appears that the effect of surface diffusion at high temperatures will be insignificant. The change in surface diffusion characteristics may be due to the decrease in surface area of the membrane. The decrease comes primarily from removal of the "spider web" silica tendrils within the pores.

There are two different values for oxygen permeation flux coefficients for two different reactors given in the preceding discussion. The values are within 5% of one another and illustrate the consistency between reactors. It is also of interest to see how these values compare to literature values for untreated VYCOR and for oxygen permeation rates in other VYCOR membrane reactor applications. For oxygen at room temperature the permeability of the treated membrane is 17.0 cm<sup>3</sup> (STP)/cm<sup>2</sup>/atm/h. The surface area of the membrane is taken as the log mean surface area. Corning literature cites a value of 4 cm<sup>3</sup> (STP)/cm<sup>2</sup>/atm/h for oxygen at room temperature across a 2 mm thick membrane. The treated membrane is only 1 mm thick, so the equivalent Corning value would be 8 cm<sup>3</sup> (STP)/cm<sup>2</sup>/atm/h. The work by Shindo et al. (1983) predicts a value of 10.7 cm<sup>3</sup> (STP)/cm<sup>2</sup>/atm/h for a 1 mm thick membrane. Ramachandra et al. (1996) list the permeability to nitrogen at room temperature of their heat treated VYCOR membrane used for OCM (thickness of 1.5 mm) as 20000 Barrer (1 Barrer = 10<sup>-10</sup> cm<sup>3</sup> (STP)/cm<sup>2</sup>/s/cm Hg). This value translates to 0.55 cm<sup>3</sup> (STP)/cm<sup>2</sup>/atm/h. Previous work from this group, Shelekhin et al. (1995), indicates that the permeability will decrease approximately 5 fold when VYCOR is treated at 900°C. If correction is made for temperature and thickness, a 1 mm thick, non heat-treated membrane would be expected to have a permeability of approximately 4.1 (STP)/cm<sup>2</sup>/atm/h for nitrogen. The oxygen value would be very similar. Although this value is slightly lower than the other reported

values, it is certainly of the correct magnitude. The important comparison to make between these literature values and the value for the treated membrane used in this research is that the treated membranes have approximately twice the permeability of untreated VYCOR membranes and approximately 30 times greater permeability than the membrane used by Ramachandra et al. (1996) in their study.

In the following section the catalytic behaviour of the membrane is described. From this discussion it becomes clear how very important a role the membrane permeability plays in its catalytic activity. The effects of changes in permeability are important and the important differences between the work by Ramachandra et al. (1996) and the present work help to illustrate the point.

## **6.2 Membrane Catalytic Activity**

As indicated in Chapter 4 the activity of treated crushed VYCOR samples during the standard reaction test is essentially zero. However, the flow conditions in the membrane reactor are somewhat different than in a tubular reactor used to test the crushed VYCOR. It had been hoped from the outset that the activity of the membrane would also be insignificant, but as the results and discussion in the following subsections indicate, this hope has not been completely fulfilled. The discussion in the following subsections will also indicate that one of the primary causes of the differences between the crushed VYCOR results and the membrane reactor results is the difference in oxygen partial pressure in the pores. In the crushed VYCOR tests the oxygen partial pressure in the VYCOR pores could not have been greater than 4-5 kPa, whereas in the membrane reactor tests the oxygen partial pressure was 15-60 times greater. In this light, the higher activity in the membrane reactor system is not that surprising.

### **6.2.1 Test Conditions**

The conditions at which the blank membrane reactor was subjected to reaction tests were developed based on appropriate operating ranges for the bulk of the kinetic testing with the bismuth oxide catalyst. The reason for this decision was that the  $\text{Bi}_2\text{O}_3$  catalysis work



represents the bulk of the reaction testing carried out in this thesis research. There are four parameters that were studied and the values of the parameters used in the study are given below.

1. propylene composition of the feed gas - (10%, 15%, 20%)
2. oxygen composition (as a percentage of the total feed gas) - (3%, 4%, 6%)
3. total feed flow rate - (125 sccm, 187.5 sccm, 250 sccm)
4. temperature - (490°C, 510°C, 530°C, 550°C)

On any particular test day the first three parameters were set and the four temperature levels were tested over the course of the day. This scheme required 27 experimental days to complete the entire set. All other parameters that could affect membrane activity were held constant. It must be noted that the changes in oxygen concentration entailed a change not only in the oxygen partial pressure in the shell and through the membrane, but also in the total pressure of the shell and the pressure gradient through the membrane. Only the partial pressures should be important, but it is not possible to separate the effect of the total pressure gradient from the partial pressure gradient, should the former have any effect.

It is also important to realize that the temperature levels tested were the nominal operating temperature of the furnace. The actual temperature as measured at the middle of the tube of the reactor was usually a few degrees lower than the stated test temperature and not necessarily the same for all tests at a particular temperature level. Although this approach to testing the effect of temperature was not ideal, it was the best available. The reaction in the blank reactor takes place within the pores of the membrane, but it was not possible to directly measure the temperature within the membrane. Given that there was little heat removed with the flowing gas, the temperature in the tube was as good a representation of the membrane temperature as was possible with this system. During reaction tests with a catalyst packed within the reactor tube the temperature would be expected to rise due to the exothermic nature of ODHD and combustion reactions. If the inner bed temperature is used to control the furnace, then the same temperature for both a blank reaction test and a catalyst reaction test will not give the same conditions in the

membrane. In the latter case the temperature in the membrane would be lower. One of the goals of determining the activity of the membrane is to be able to accurately take its activity into account when determining the role that the membrane reactor plays in facilitating the ODHD of propylene reaction. If the membrane conditions cannot be readily replicated between the two tests, then this sort of comparison could be fraught with errors. Although this approach is not perfect and still leaves room for some potential error, it appears to be the most reasonable compromise given the system constraints.

For the blank reactor tests, the tube side of the membrane portion of the reactor was packed with 20 x 30 mesh quartz chips to reduce dead volume in the reaction zone and to best simulate the conditions of a packed catalyst bed in the tube. Tests in a normal tubular reactor indicated that the crushed quartz had no catalytic activity at the test conditions. The total pressure at the inlet to the tube side of the reactor was maintained at 105 kPa  $\pm$  1 kPa and the pressure drop across the packed bed in the tube was less than 2 kPa in all cases.

### 6.2.2 Evaluation of Activity Caused by the Shell

Preliminary tests were conducted to determine if the SS shell contributed to the overall reactor activity. These tests were carried out without the inner quartz sleeve described in Chapter 4 being in place. Comparison of results using the same membrane tube portion with both new and old SS shells indicated that the "old" shell did affect the results. The products of the reaction tests were mostly combustion products (complete and incomplete combustion) with only small amounts of hydrocarbon products. The effluent from the reactor also contained the unconverted propylene and oxygen. The conversion of propylene was only marginally higher (10% more conversion, as a maximum) in the reactor using the old shell compared to the reactor with a new shell. The difference was most notable at lower temperatures. The biggest difference noted was the increase in oxygen conversion and increased selectivity to carbon dioxide as a product at the expense of carbon monoxide. The old shell was cut apart and found to have the internal surface near the membrane section of the tube covered in rust. The depletion of chromium in this

section coupled with the higher temperature exposure to the water and CO<sub>2</sub> containing gas had caused rust formation and these iron oxides acted primarily as a catalyst to promote the oxidation of CO to CO<sub>2</sub>.

Two important conclusions can be drawn from this preliminary work. The first conclusion is that the reaction of propylene in the blank reactor occurs mainly in the pores of the membrane and seems to be limited by how much propylene can enter the pores. One would expect the reaction rate in the pores to increase as the temperature increases and thereby consume all the available propylene. The SS shell could then not increase the propylene conversion. This finding has been confirmed by setting up a back pressure controlled flow system for oxygen in the shell. Some of the oxygen flowing into the shell permeated through the membrane and the balance served to keep a constant sweep of gas through the shell. This sweep gas (using a variety of sweep rates) was analyzed for propylene and only traces were found. Approximately 0.5-1.0% of the amount of propylene expected to permeate through the membrane (assuming no reaction) at the reaction temperature of 530°C was found to be present in the sweep gas. For these tests the 22 mm OD quartz inner liner described in Chapter 4 was utilized to prevent the shell from causing any reaction.

The second conclusion is that the diffusion of CO<sub>2</sub> and water within the shell was confined to a very small region around the membrane (the source of these two species entering the shell). The important point to note from this conclusion is that only a small region of the inner surface of the shell needs to be protected from contact with CO<sub>2</sub> and water to prevent the formation of the corrosion products on the shell which would increase the activity of the shell. Thus the quartz liner should be able to prevent shell activity from occurring even in the absence of a sweep flow on the shell side of the reactor.

Two methods have been considered for eliminating shell activity. The first method, and the one ultimately used, is the quartz liner. It proved to be quite successful. The second method is to replace the SS shell at regular intervals. A fresh SS shell is relatively inert but over 7-10 days of operation the shell begins to acquire some activity and within 15

days the chromium depletion problem becomes apparent by the formation of rust on the inner wall of the shell near the membrane. In the laboratory it is feasible, but cumbersome, to replace the shell. However the quartz liner is a better solution. The finding regarding the shell degradation have important ramifications if this process, or any high temperature oxidative process where combustion products will be present, is developed past the bench scale. Materials more resistant to corrosion than 316L SS will be required for construction (or cladding of construction materials) of such reactors. Such materials may significantly add to the capital cost of the process.

### 6.2.3 Results of the Reaction Tests

The results presented in this chapter are meant to demonstrate some of the key issues discovered from the testing. The full set of data is contained in Appendix B. In the previous section the four process parameters investigated in this study were given as propylene feed concentration, oxygen feed concentration, flow rate and temperature. The important process variables that are affected by these input variables are the conversion of the feed components and the selectivity to the various products. Presentation of typical results and a discussion of the observed trends follow in Sections 6.2.3.1, 6.2.3.2 and 6.2.3.3. It should be noted from the outset that one uncontrollable process parameter did vary slightly over the course of the blank reactor testing. Although three membrane reactors underwent preliminary testing to ensure that the results from different reactors would be consistent, all the data presented in this chapter come from the testing of a single reactor. During testing the permeability of this reactor increased by approximately 7% with much of the change occurring as a step change during a period when the reactor was not being operated. At the start of testing, the oxygen permeability was 1 sccm/20.1 kPa and by the end testing it had increased to 1 sccm/18.5 kPa. A discussion of why this change in permeability occurs can be found in Section 6.4. The increased permeability has been found to linearly increase the rate of feed conversion without materially affecting the selectivity to the various products. The data have been corrected for the higher permeability level. Scaling of the data was based on the measured oxygen shell pressure before the feed was added, which is a direct measure of the permeability of the membrane to oxygen.

### 6.2.3.1 Conversion of Propylene

The design of the membrane reactor system with a “dead end” shell (all gas flowing into the shell must exit through the membrane as there was no other exit) was based on making the experimental aspects of the work as uncomplicated as possible. The penalty for this type of design is that there is no way to measure the concentration (partial pressure) of the gases in the shell. This fact coupled with the fact that the kinetics of the reactions occurring in the pores are unknown means that there is no way to indisputably determine what the partial pressures of the feed and product species are in different parts of the pores. It is, however, possible to provide some simple observations and insights concerning the partial pressures of oxygen and helium within the membrane. The partial pressure of oxygen on the tube side of the membrane is very low (2-6 kPa) and on the shell side is approximately 18.5 kPa/sccm of oxygen flow rate. It decreases from one value to the other across the membrane. It is difficult to predict whether the decrease is linear with distance or whether the partial pressure decrease follows some other trajectory. Across this distance the total pressure also decreases. The shell pressure is approximately equal to the oxygen partial pressure plus the tube operating pressure of 105 kPa. The shell has no exit (other than through the membrane) and given the length of time needed for the experiments it is expected that the helium partial pressure will be the same on both sides of the membrane (in the range of 78-95 kPa depending on the reaction conditions) and that there will be no net flux of helium. Further discussion on partial pressure in the pores of some of the product species is contained in Section 6.3.

In all discussions concerning conversion, absolute conversion is defined by equation 6.2 and fractional conversion is defined by equation 6.3. In any of these cases mass or a standard gas volume measure can replace moles and give the same result.

$$\text{absolute conversion} = \text{moles in} - \text{moles out} \quad (6.2)$$

$$\text{fractional conversion} = \frac{\text{moles in} - \text{moles out}}{\text{moles in}} \quad (6.3)$$

The conversion of propylene as a function of temperature at the three oxygen “concentration” levels are shown in Figures 6.5 and 6.6. Figure 6.5 shows data for the combination of conditions which give the highest propylene feed rate (250 sccm total flow and 20% propylene in the overall feed) and Figure 6.6 shows data for the combination of conditions which minimize the propylene flow rate (125 sccm total flow and 10% propylene in the feed). On both figures the maximum flow rate of propylene through the membrane by Knudsen diffusion, assuming that one side of the membrane was maintained at the overall propylene feed concentration and the other side at zero partial pressure of propylene, is shown. The Knudsen diffusion lines assume that there is no surface diffusion occurring. The Knudsen rate decreases slightly with increasing temperature as per equation 4.5.

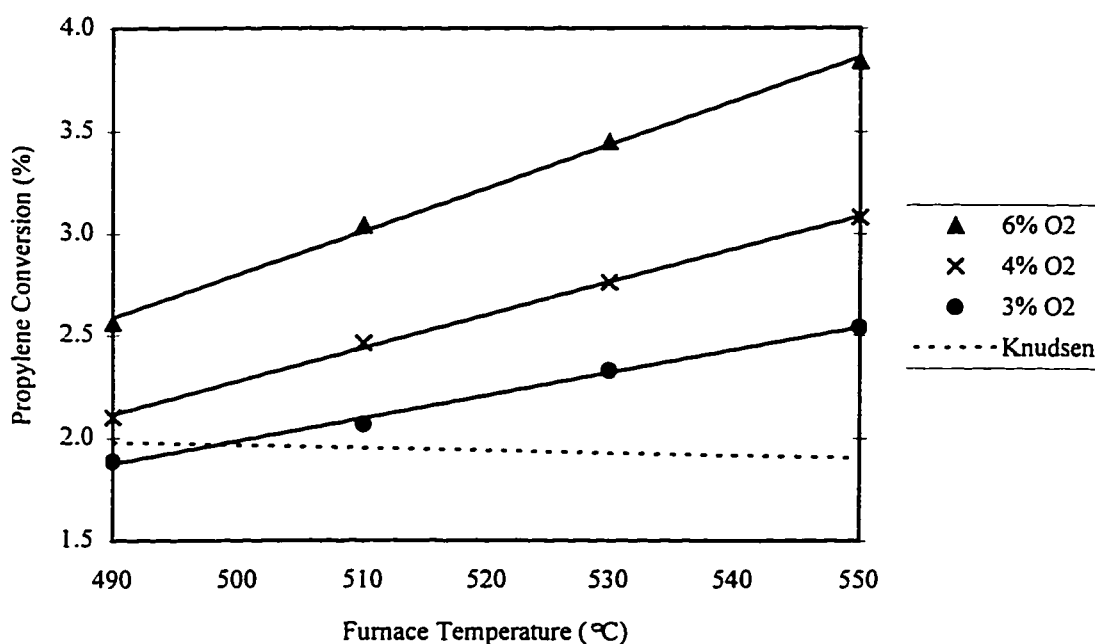


Figure 6.5 Propylene Conversion in the Blank Membrane Reactor (250 sccm Total Flow, 20% Propylene) as a Function of Temperature and Oxygen Feed Concentration

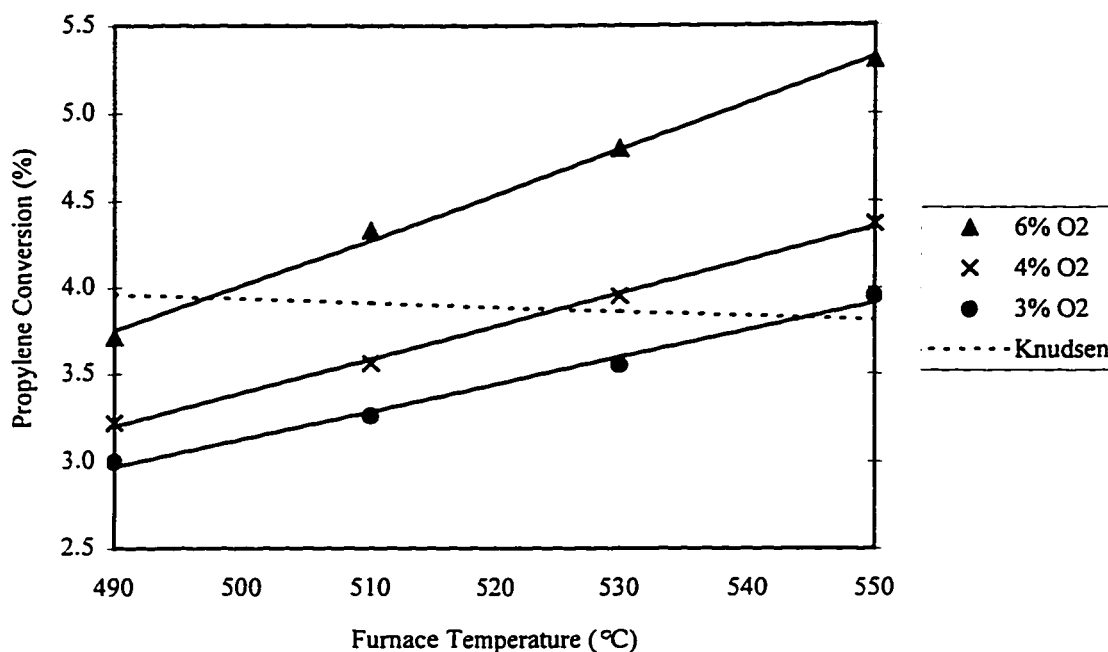


Figure 6.6 Propylene Conversion in the Blank Membrane Reactor (125 sccm Total Flow, 10% Propylene) as a Function of Temperature and Oxygen Feed Concentration

If the rate of reaction is greater than the Knudsen flow, such is the case for almost all of the conditions shown in Figure 6.5, then it must be assumed that one or both of the following phenomena is occurring. It could be that surface diffusion is playing a greater role than expected and increases the flux of propylene into the membrane. However, the surface diffusion should decrease with increasing temperature so this mechanism alone cannot explain the results. The second possibility is that the rate of reaction is high enough to consume all the propylene before it can diffuse through the entire thickness of the membrane. The result is that part of the membrane has a higher than expected propylene concentration gradient and the other part contains no propylene whatsoever. The higher gradient results in a higher Knudsen diffusion flux (see equation 4.5) and hence the higher than expected reaction rate. If it can be assumed that there is no surface diffusion and that the propylene concentration at the inner wall is the same as the feed concentration, then the degree of conversion above the Knudsen limit can be used to estimate how much of the thickness of the membrane is involved in the reaction. For the case of the 550°C point at 6% O<sub>2</sub> in Figure 6.5 the conversion is approximately double

the Knudsen limit so approximately half the membrane thickness is involved in the reaction.

For the instances when the reaction rate is less than the Knudsen limit, the propylene diffusion rate may be less than the Knudsen limit because either the propylene concentration on the tube side of the reactor is lower than the feed concentration or the propylene concentration in the shell is non-zero. The issue of the propylene concentration at the membrane wall on the tube side of the reactor is very important and will be discussed in more detail in Section 6.5.

Three important general trends must be noted based on the data in Figures 6.5 and 6.6. Clearly there is a linear relationship between propylene conversion and temperature for all oxygen concentrations in the ranges examined. Over this limited temperature range an Arrhenius expression could be used to roughly predict the linear trend, but it would likely be of limited use outside the tested temperature range. In addition it would be folly to use such an approach when it is known that diffusional limitations are occurring. The second trend is that conversion rises with increasing oxygen content in the feed. The effect is almost linear with respect to oxygen concentration (given the spacing of the lines on the two figures). The third and perhaps most telling trend is the degree of conversion with respect to oxygen pressure in the shell of the reactor (and hence the oxygen partial pressure gradient in the membrane). The oxygen shell pressure is the same for 6% oxygen at 125 sccm total flow (Figure 6.6) and 3% oxygen at 250 sccm total flow (Figure 6.5). The behaviour of the propylene conversion relative to the Knudsen limit is very similar for both of these cases. It indicates that it is actually the oxygen pressure in the membrane, rather than the overall oxygen feed composition, that most affects the conversion. This hypothesis also helps explain the observation that the conversion of propylene relative to the Knudsen limit is greater at the higher overall flow rates (Figure 6.5 vs. Figure 6.6).

The variation of propylene percentage conversion as a function of temperature and propylene feed concentration with constant oxygen flow is shown in Figures 6.7 and 6.8. Again a high total feed flow (Figure 6.7) and low total feed flow (Figure 6.8) are shown



for comparison. As with the previous set of figures the conversion increases linearly with temperature, but the fractional conversion of propylene varies only to a small degree with propylene feed concentration. Generally a lower propylene feed concentration will lead to a slightly higher fractional conversion because of the greater oxygen to propylene ratio in the pores helping to promote combustion reactions. The combustion products, as will be illustrated when product selectivity is discussed, are the primary carbon containing products. However, Figure 6.7 shows a situation where this general trend is reversed. The reversal of the general trend occurs only at higher flow rates. The small differences in fractional conversion as a function of propylene concentration means that, as a first approximation, the actual molar amount of propylene converted varies directly as the propylene feed rate at any particular total feed rate when the oxygen feed flow is constant.

The same trend with regard to conversion relative to the Knudsen limit observed in Figures 6.5 and 6.6 is observed in Figures 6.7 and 6.8. The higher oxygen partial pressure in the membrane at 4% feed oxygen with a total feed flow of 250 sccm compared with the 3% O<sub>2</sub> at 125 sccm generally results in conversions greater than the Knudsen limit.

The relationship between fractional conversion of propylene and total feed flow rate at a fixed feed composition is illustrated in Figure 6.9. As with the previous four figures the relationship between conversion and temperature is linear in this case. However, the spacing between the lines representing conversion as a function of flow rate indicates that the results are not linear with respect to flow at any fixed temperature. The lines would be equally spaced if this were to be true. If the data are presented as absolute (molar) conversion of propylene (rather than percent conversion), then the relationship is linear as shown in Figure 6.10.

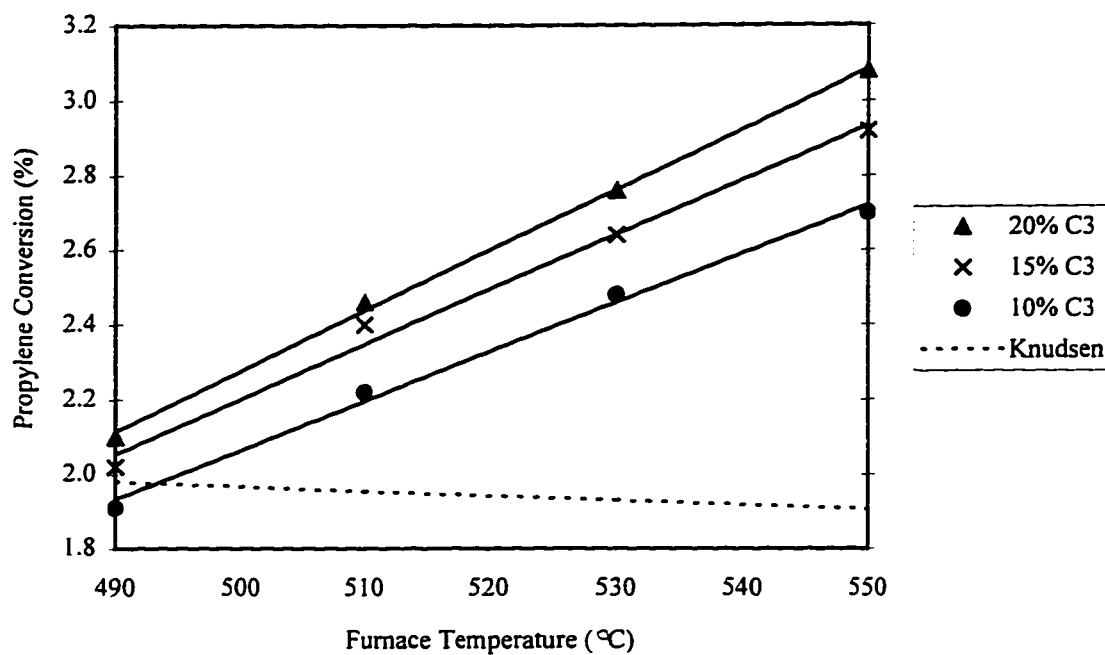


Figure 6.7 Propylene Conversion in the Blank Membrane Reactor (250 sccm Total Flow, 4% Oxygen) as a Function of Temperature and Propylene Feed Concentration

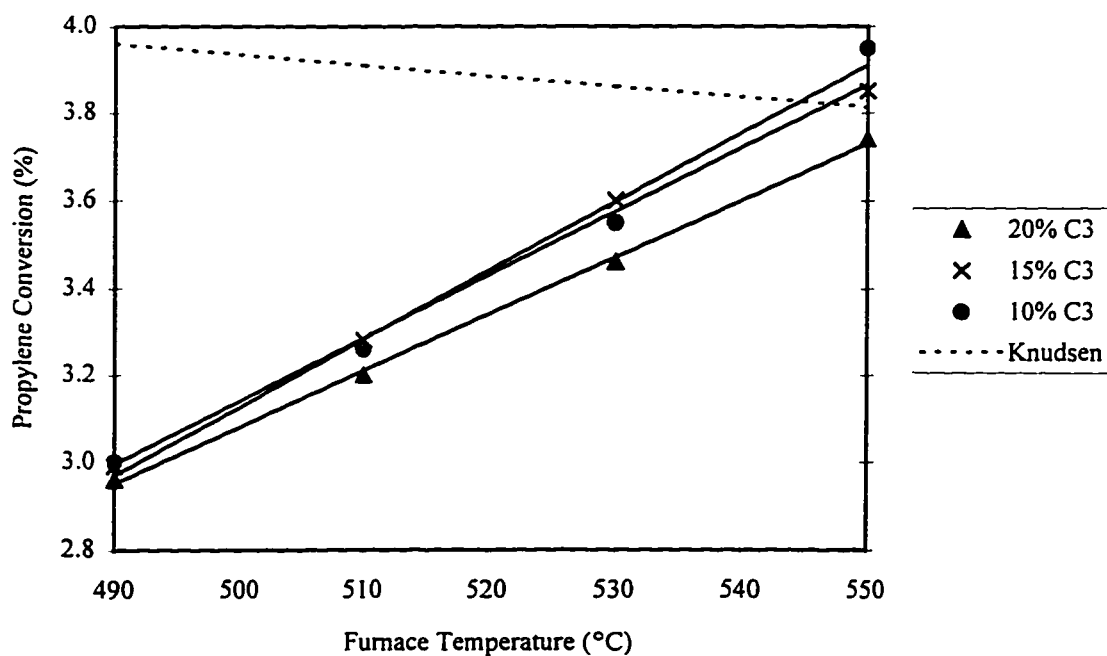


Figure 6.8 Propylene Conversion in the Blank Membrane Reactor (125 sccm Total Flow, 3% Oxygen) as a Function of Temperature and Propylene Feed Concentration

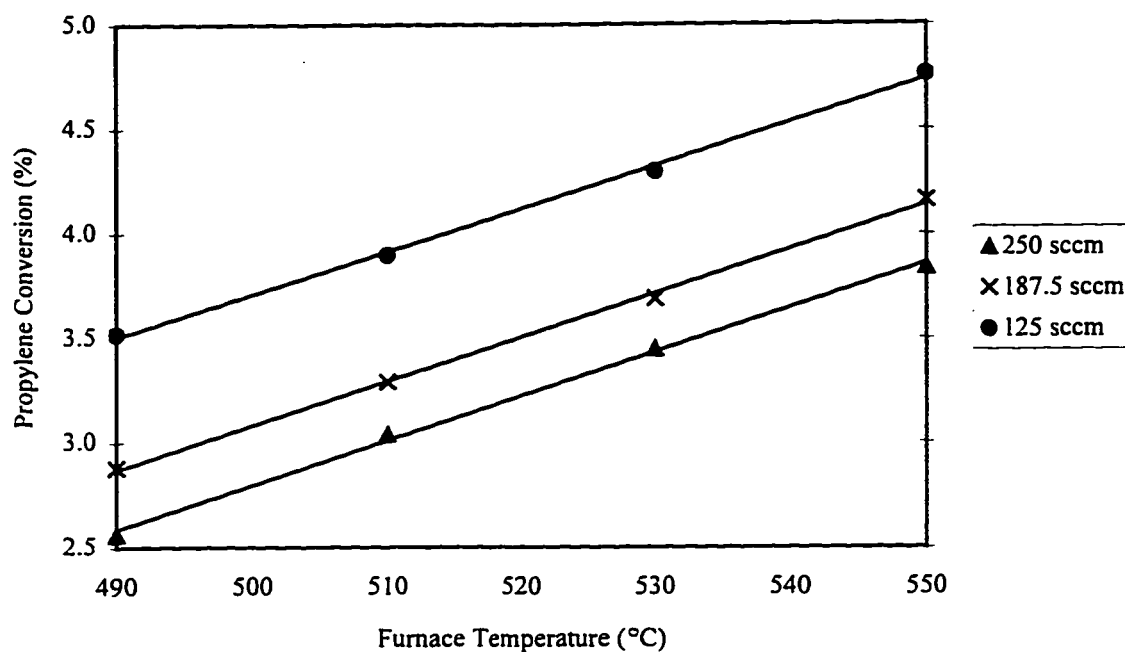


Figure 6.9 Relative Propylene Conversion in the Blank Membrane Reactor (20% Propylene, 4% Oxygen) as a Function of Temperature and Total Feed Flow Rate

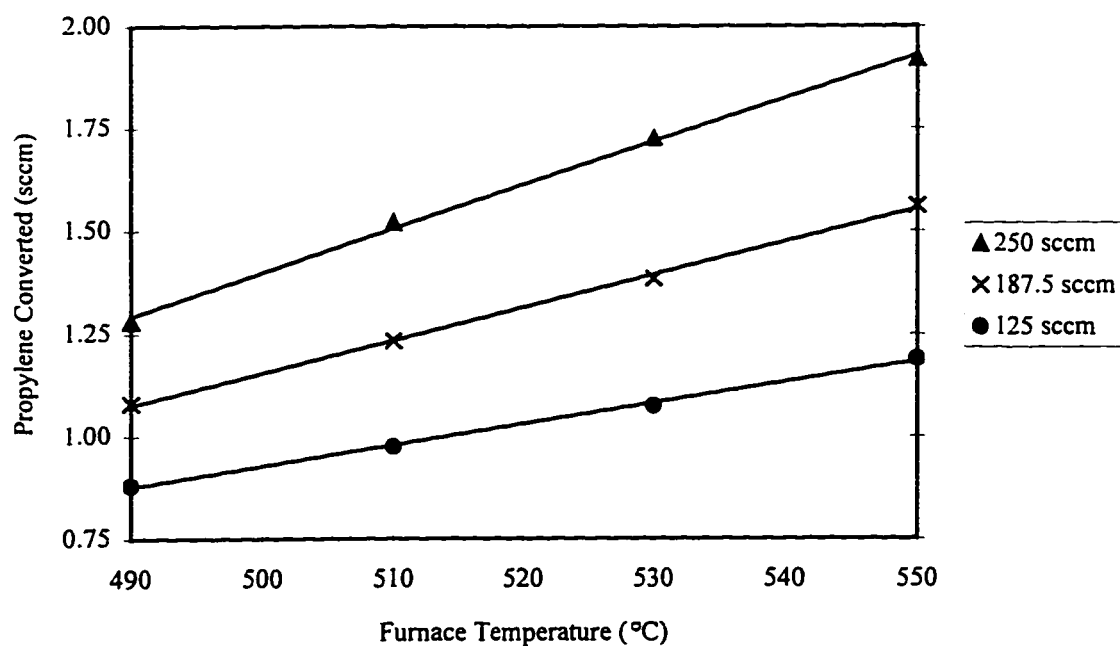


Figure 6.10 Absolute Propylene Conversion in the Blank Membrane Reactor (20% Propylene, 4% Oxygen) as a Function of Temperature and Total Feed Flow Rate

No discussion has been included here on the conversion of oxygen as a function of the key process variables. The primary reason for the omission is that it adds no new information. Oxygen is consumed primarily as propylene is converted to combustion products. Thus oxygen consumption will follow the trends of CO and CO<sub>2</sub> yields and can be calculated from propylene conversion and selectivity information. Oxygen conversion information is provided in Appendix B.

### 6.2.3.2 Selectivity to Carbon Oxides

As previously noted in this chapter the primary carbon containing products from the blank reactor testing were CO and CO<sub>2</sub>. There were smaller amounts of ethylene, acetaldehyde, acrolein and 1,5-hexadiene produced as carbon containing products and, of course, water was produced. The amounts of the secondary carbon-based products were small with the amount of acetaldehyde being particularly small. The acetaldehyde was ignored in the mass balance and selectivity calculations because there was so little of it and because it was very difficult to calibrate the GC for such low concentrations of acetaldehyde.

In this work selectivity is defined as selectivity of the converted propylene to a particular product. For example the selectivity to CO<sub>2</sub> is defined in equation 6.4.

$$S_{CO_2} = \frac{\frac{y_{CO_2}}{3}}{\frac{y_{CO_2}}{3} + \frac{y_{CO}}{3} + \frac{2y_{C_2}}{3} + y_{ACR} + 2y_{15HD}} \quad (6.4)$$

The selectivity of propylene to carbon oxides exhibited very consistent patterns with respect to the variables of temperature, feed concentrations and flow rates.

Representative data are presented in Figures 6.11a-6.16 with discussion to illustrate the observed trends.

The variation of CO and CO<sub>2</sub> selectivity as a function of temperature and oxygen feed concentration is shown in Figure 6.11a and the total CO<sub>x</sub> selectivity is shown in Figure 6.11b. Unlike conversion data the relationship between selectivities and either temperature or oxygen composition is not linear. CO selectivity decreases with increasing temperature while the CO<sub>2</sub> selectivity increases with increasing temperature and both trends are of a decidedly quadratic nature. The total selectivity to carbon oxides decreases slightly with increasing temperature as more of the hydrocarbon and oxygenate products are formed (due to the higher activation energies for the formation of these products). The slight decrease in CO<sub>x</sub> selectivity also exhibits quadratic behaviour with respect to temperature. The effect of oxygen concentration (partial pressure) on selectivity to carbon oxides is less regular. A lower oxygen to propylene feed ratio (lower oxygen partial pressure in the pores) favours CO production over CO<sub>2</sub> production as one might intuitively expect. However, the low ratio also favours higher overall CO<sub>x</sub> selectivity. This latter point may not be intuitive. It indicates that within the confines of the VYCOR pores that oxygen has a greater role in promoting the formation of the hydrocarbons and oxygenates than in promoting CO<sub>x</sub> formation. In all cases the changes in selectivity as a function of oxygen feed changes are relatively minor. Doubling the oxygen concentration typically causes less than a 10% (relative) change in CO or CO<sub>2</sub> selectivity. This trend is likely caused by the simple lack of propylene within the pores for reaction with the oxygen.

An alternate way of looking at the effect that oxygen and temperature have on CO and CO<sub>2</sub> production is to look at the product yield for each. Figure 6.12 shows sample data for CO and CO<sub>2</sub> yields. Yield is defined as the product of selectivity and propylene conversion.

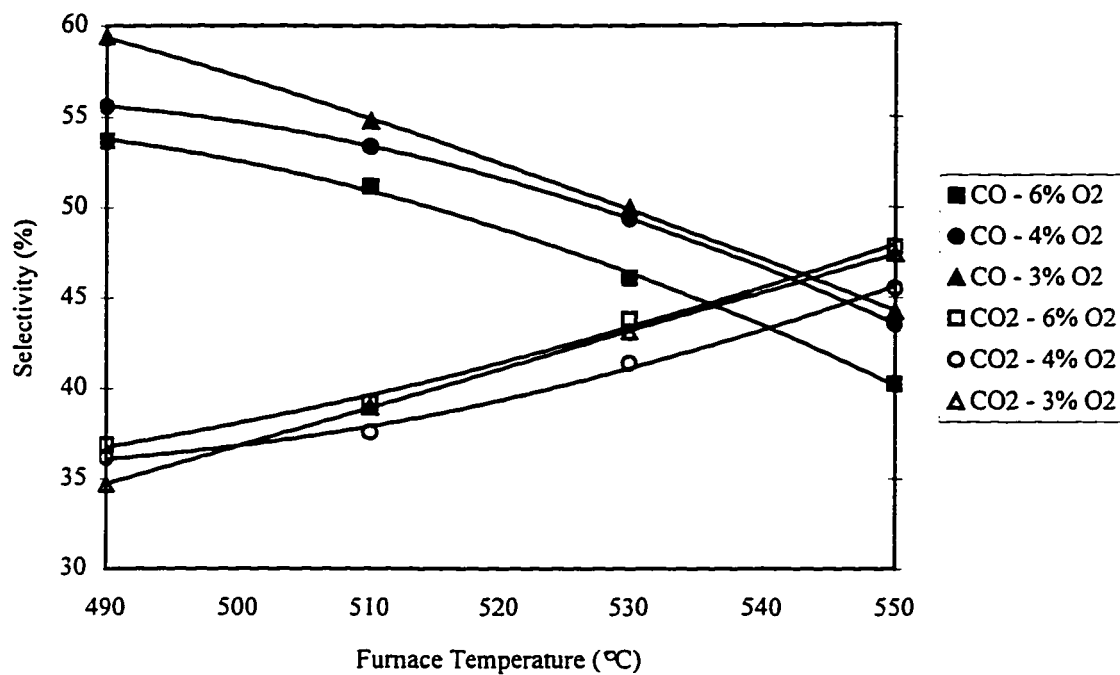


Figure 6.11a Propylene Selectivity to CO and CO<sub>2</sub> in the Blank Membrane Reactor (250 sccm Total Flow, 20% Propylene) as a Function of Temperature and Oxygen Feed Composition

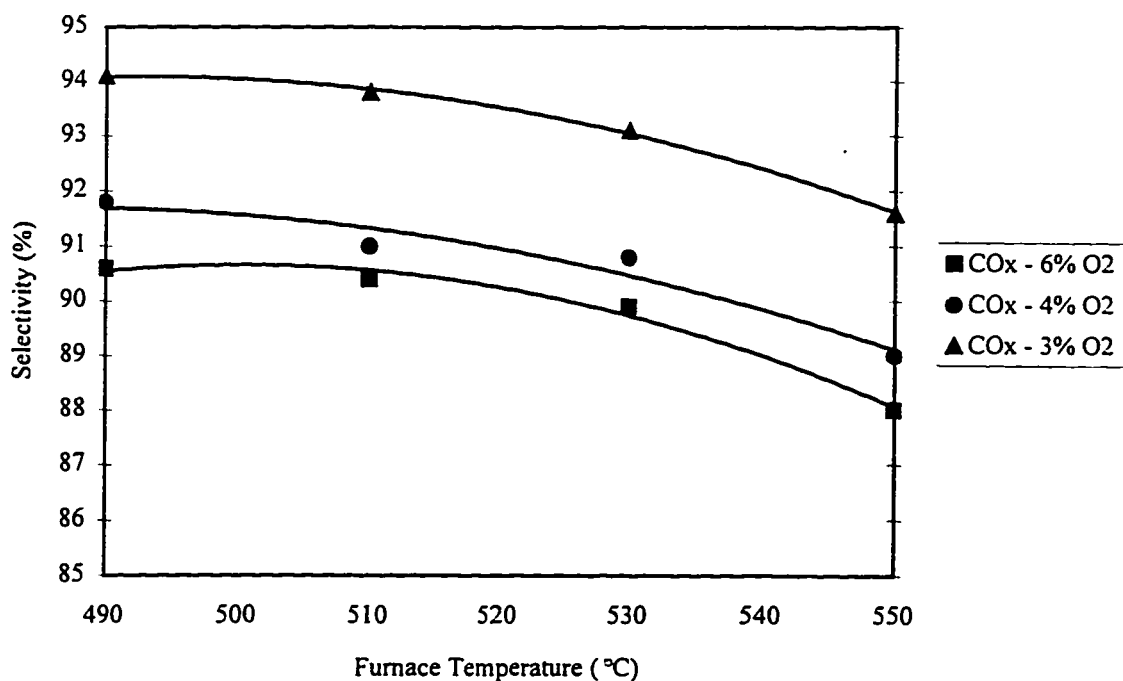


Figure 6.11b Propylene Selectivity to CO<sub>x</sub> in the Blank Membrane Reactor (250 sccm Total Flow, 20% Propylene) as a Function of Temperature and Oxygen Feed Composition

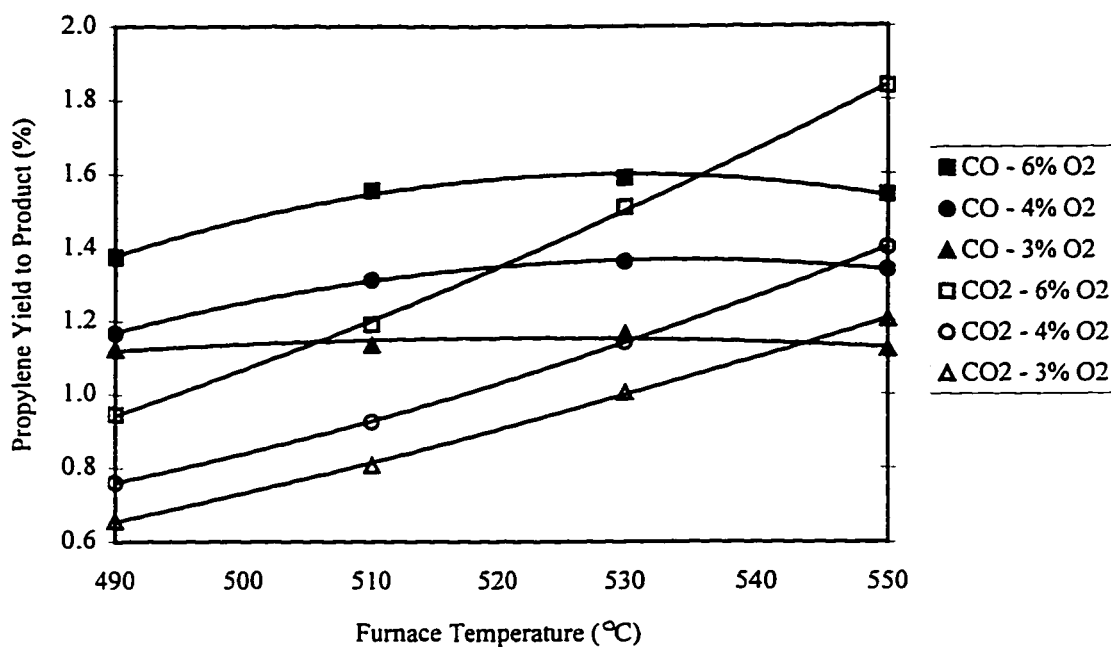


Figure 6.12 Propylene Yield to CO and CO<sub>2</sub> in the Blank Membrane Reactor (250 sccm Total Flow, 20% Propylene) as a Function of Temperature and Oxygen Feed Composition

The yield of CO<sub>2</sub> rises with temperature in a slightly quadratic fashion and increases in a roughly linear fashion with respect to the oxygen concentration. More interesting is the behaviour of the CO yield. It does not vary much with temperature and exhibits a very broad maximum at approximately 530°C. Increasing oxygen concentration increases CO yield but it is not quite linear in nature and the relationship tends to vary, as Figure 6.12 does illustrate, at different temperature levels.

The variation of CO and CO<sub>2</sub> selectivity as a function of temperature and propylene feed concentration are shown in Figure 6.13a and the total CO<sub>x</sub> selectivity is shown in Figure 6.13b. The trends exhibited in Figures 6.11a and 6.11b for changes in selectivity with respect to temperature are also exhibited in Figures 6.13a and 6.13b. In the latter case the trends tend to be more linear and the lower total feed flow rate (and consequently lower oxygen partial pressure) increases the CO selectivity and decreases the CO<sub>2</sub> selectivity when compared to the 250 sccm total flow rate case (Figure 6.11a). However the overall selectivity to carbon oxides in both cases is nearly the same.

When the propylene concentration is held constant and oxygen concentration is varied (Figure 6.11a), a higher propylene to oxygen ratio produces a greater ratio of CO to CO<sub>2</sub> selectivity. When the oxygen concentration is constant and the propylene concentration is varied, the opposite is true. Figure 6.13a illustrates this point as the selectivity to CO<sub>2</sub> is highest at the highest propylene feed concentration. The CO selectivity is also the lowest in this case, but the effect on CO selectivity of changing propylene concentration is minor. It can be safely concluded that the key variable is not the ratio of feed concentrations that is important (as it might be in a standard tubular reactor), but rather the partial pressures of the feed components in the membrane pores.

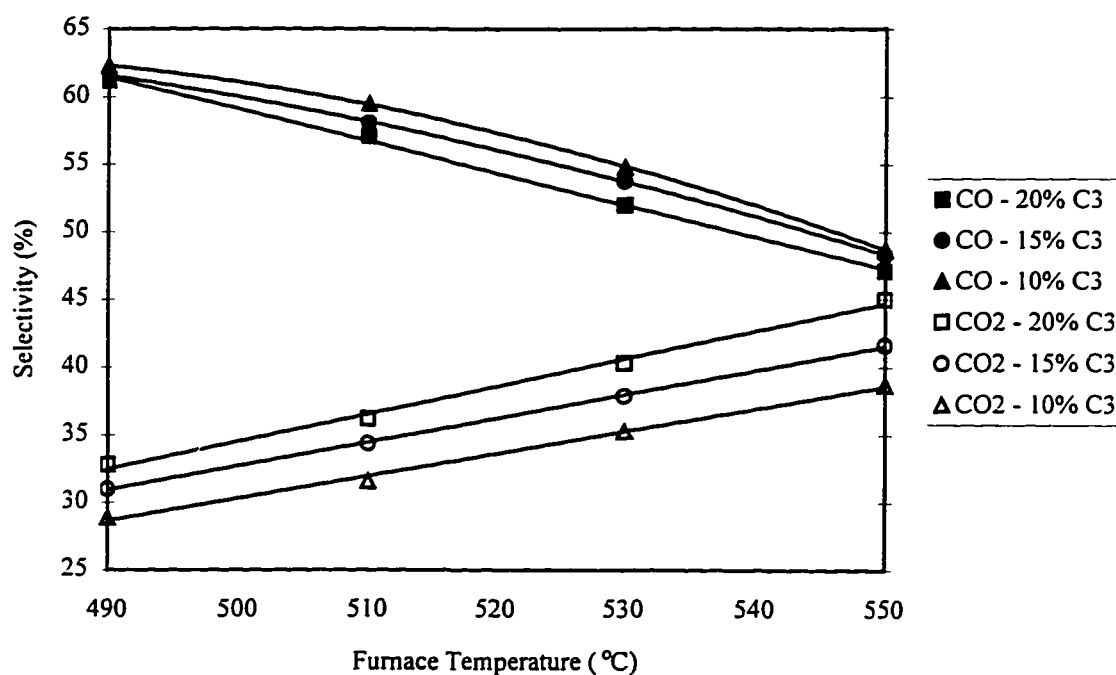


Figure 6.13a Propylene Selectivity to CO and CO<sub>2</sub> in the Blank Membrane Reactor (125 sccm Total Flow, 4% Oxygen) as a Function of Temperature and Propylene Feed Composition



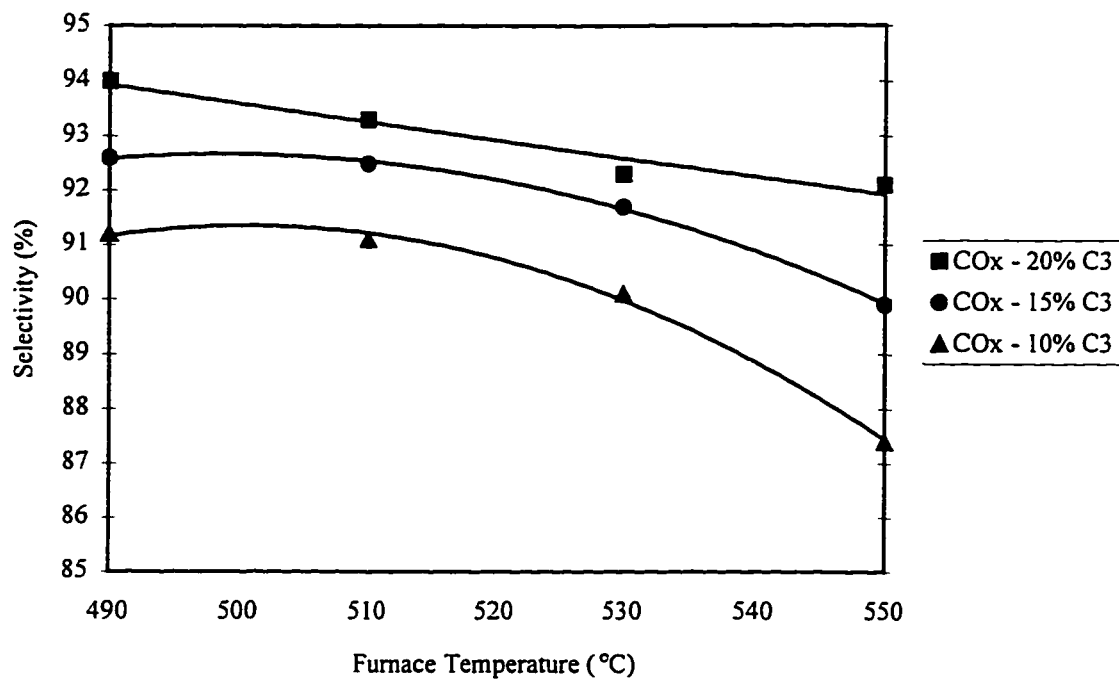


Figure 6.13b Propylene Selectivity to CO<sub>x</sub> in the Blank Membrane Reactor (125 sccm Total Flow, 4% Oxygen) as a Function of Temperature and Propylene Feed Composition

Figure 6.14 shows the relationship between CO and CO<sub>2</sub> yield and the temperature and propylene concentration parameters. At higher propylene concentrations the yield of CO<sub>2</sub> increases while the CO yield drops which mimics the selectivity information. The changes in yield with respect to temperature follow the same trends as those seen in Figure 6.12. The CO<sub>2</sub> yield increases in a roughly linear fashion with temperature while the CO yield varies little with temperature and has a maximum value at approximately 530°C.

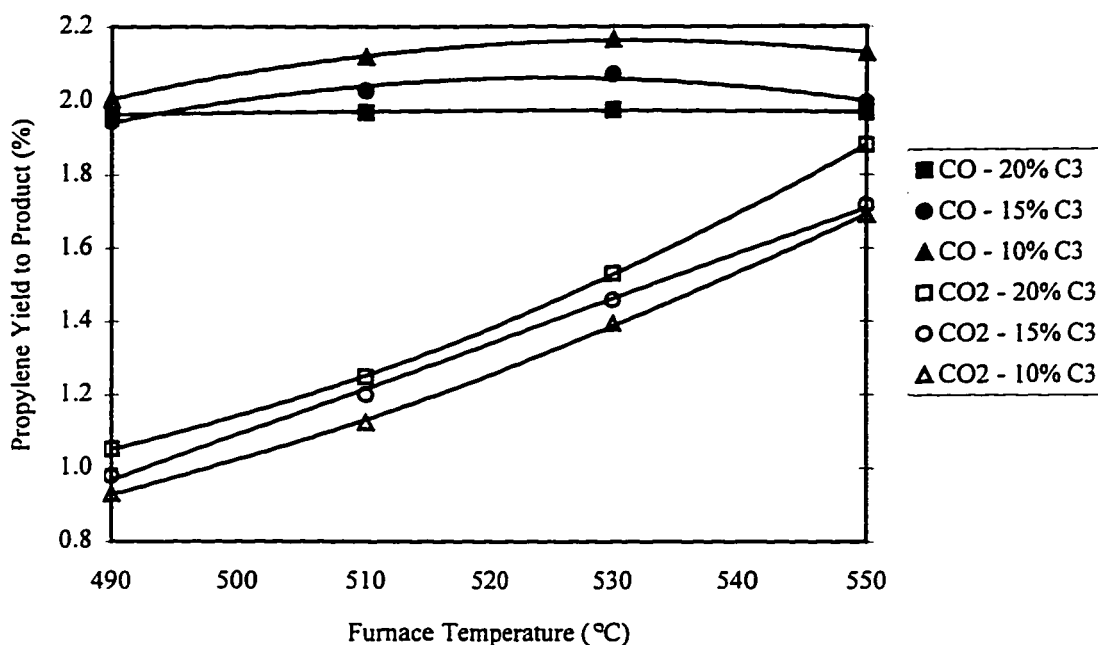


Figure 6.14 Propylene Yield to CO and CO<sub>2</sub> in the Blank Membrane Reactor (125 sccm Total Flow, 4% Oxygen) as a Function of Temperature and Propylene Feed Composition

Figures 6.15a and 6.15b illustrate the effect of total feed flow rate and temperature on carbon oxide selectivities. The trends with respect to temperature are the same as those found in Figures 6.11a,b and 6.13a,b. CO<sub>2</sub> selectivity increases in a linear fashion with temperature while CO selectivity decreases with a slightly quadratic nature with increasing temperature. The sum of the two selectivities (Figure 6.15b) results in the CO<sub>x</sub> selectivity decreasing in a slightly quadratic nature with increasing temperature. The effect of flow rate on selectivity is explained by the difference in oxygen partial pressure in the membrane. The lower overall flow rate cases have lower oxygen partial pressure in the membrane and hence the selectivity to CO increases while the selectivity to CO<sub>2</sub> decreases. This point has been alluded to when comparing the results presented in Figures 6.11a and 6.13a. The overall selectivity to CO<sub>x</sub> has very little variation due to flow rate and falls in the same range as those illustrated in Figures 6.11b and 6.13b.

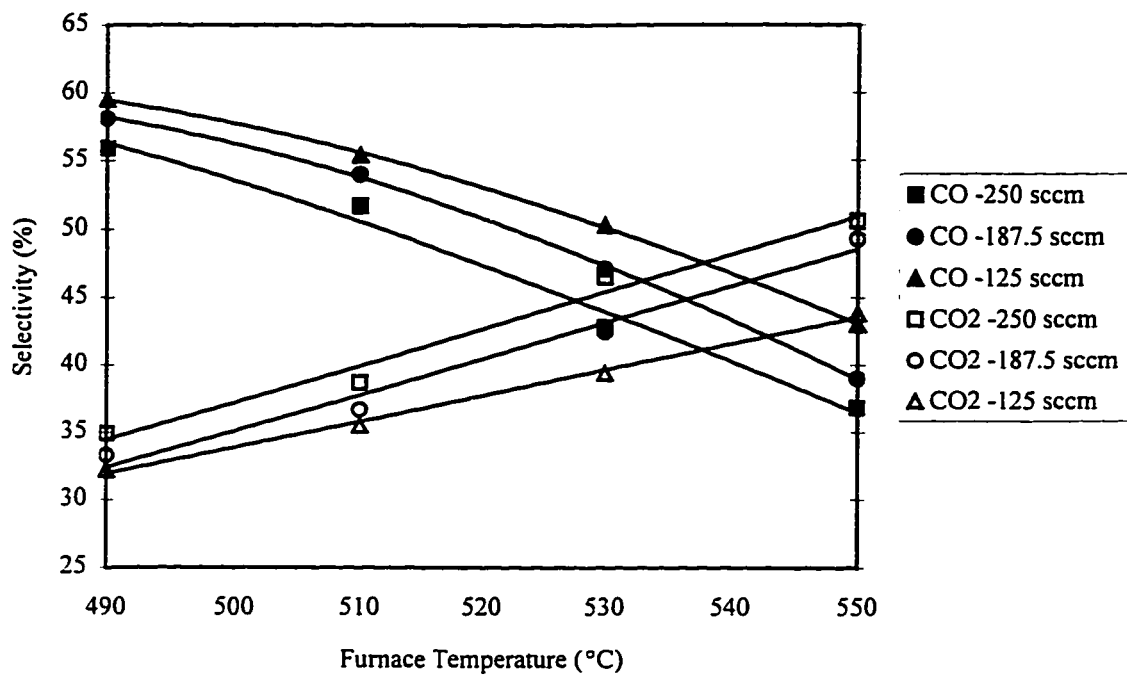


Figure 6.15a Propylene Selectivity to CO and CO<sub>2</sub> in the Blank Membrane Reactor (15% Propylene, 6% Oxygen) as a Function of Temperature and Total Feed Flow Rate

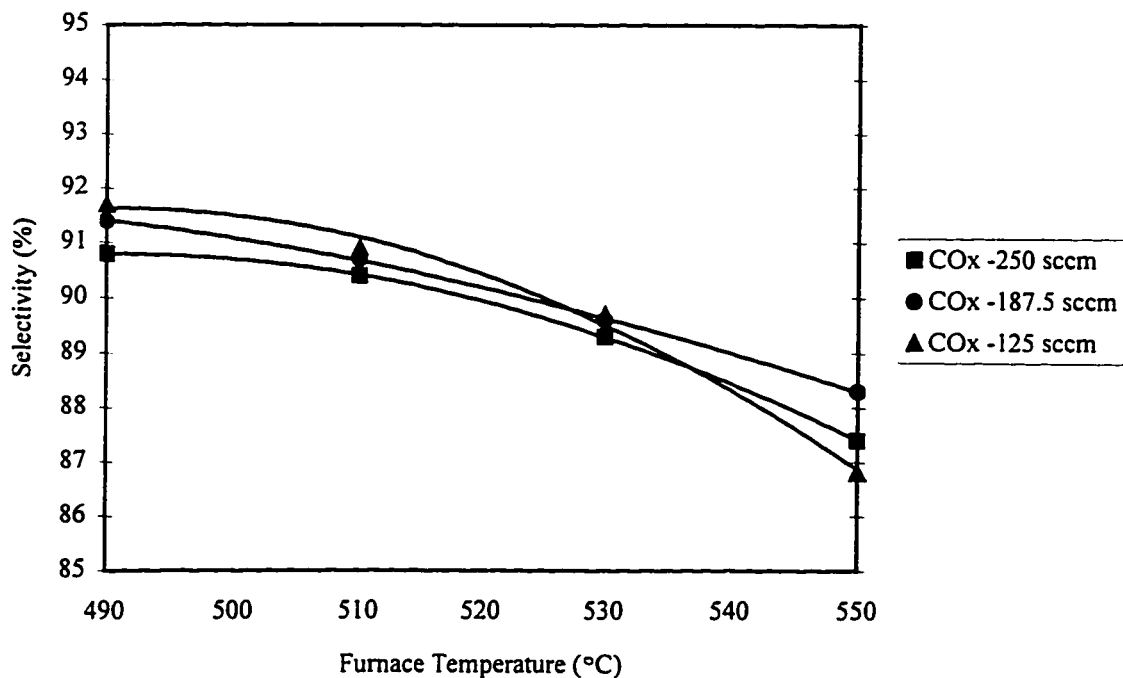


Figure 6.15b Propylene Selectivity to CO<sub>x</sub> in the Blank Membrane Reactor (15% Propylene, 6% Oxygen) as a Function of Temperature and Total Feed Flow Rate

The fractional yields of CO and CO<sub>2</sub> as a function of temperature and flow rate are illustrated in Figure 6.16. The trends with respect to temperature are the same as those illustrated on Figures 6.12 and 6.14. The only subtle difference, perhaps, is that the maximum in the CO yield seems to occur closer to 510°C than 530°C. The maximum region is so broad, though, that this difference has no material effect on the results. The fractional yields, as a function of flow rate, are highest for the lowest overall flow rate. This fact clearly illustrates that it is the propylene concentration in the tube that roughly determines the rate of diffusion into the pores. Thus, without reaction, the fraction of propylene diffusing through the membrane should double if the overall flow rate is cut in half. As Figure 6.16 shows, for a flow rate decrease from 250 sccm to 125 sccm, the fractional yield of either CO or CO<sub>2</sub> does not quite double and the reason is the difference in oxygen partial pressures between the two flow rates causes higher conversion in the higher flow rate case.

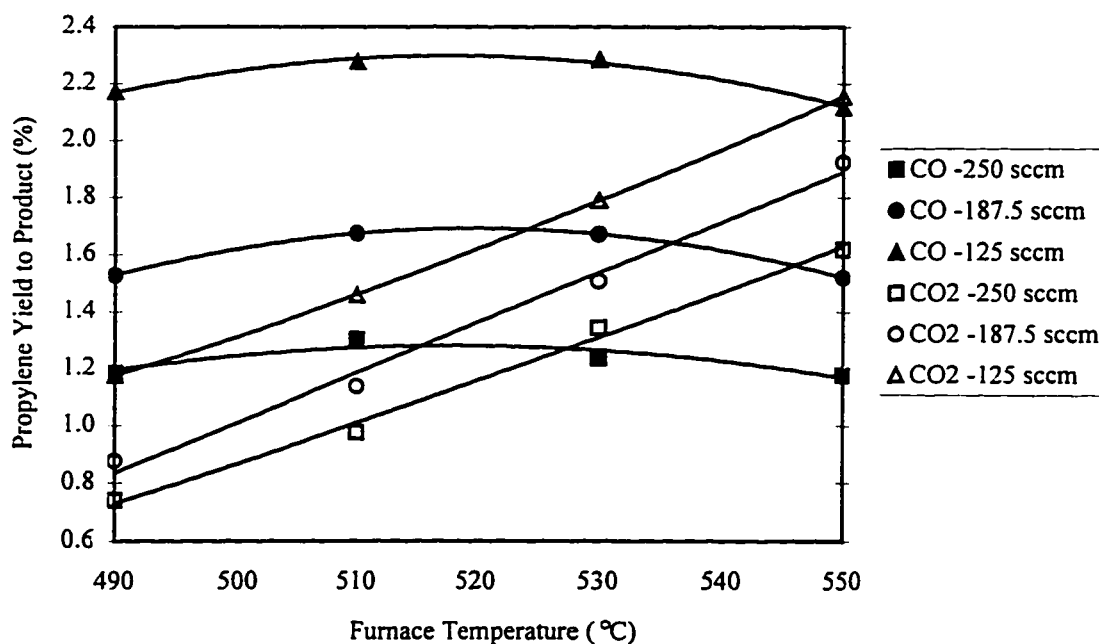


Figure 6.16 Propylene Yield to CO and CO<sub>2</sub> in the Blank Membrane Reactor (15% Propylene, 6% Oxygen) as a Function of Temperature and Total Feed Flow Rate

As it has been clearly shown, the primary carbon products of reactions in the blank membrane reactor are carbon oxides and the overall selectivity varies only slightly over

all the process parameters. However, the selectivity to the individual oxides does vary quite dramatically, particularly with respect to temperature. The reasons and mechanisms for these variations and the reasons why there is so much CO formed in the first place merit some discussion.

Within the membrane pores there is a high oxygen to propylene partial pressure ratio. If this mixture were to be present in a much less confined space in the presence of a catalyst capable of promoting combustion it is expected that the reaction of propylene would lead almost exclusively to complete combustion. However, within the confines of the pores ( $\sim 50 \text{ \AA}$  diameter) where Knudsen diffusion is the dominant form of mass transport, the interactions between propylene and oxygen are very much more limited, in both number and form, than they would be in a free volume. In Knudsen diffusion most of the collisions are between molecules and a wall. The likelihood that there will be sufficient molecular collisions at any place other than a wall to produce either CO or CO<sub>2</sub> is very low. The mechanism of the complete breakdown of propylene into carbon oxides is not known, but it is very unlikely that it will occur at one site on a pore wall. It seems much more probable that the breakdown occurs in a stepwise fashion with some intermediate hydrocarbon or oxygenate intermediates (radical or otherwise) being produced as well as carbon oxides. The intermediates then undergo further degradation along the path to combustion products. Since more oxygen is needed to produce CO<sub>2</sub> rather than CO and CO itself is a stable product, it may be reasonable to assume that most of the propylene consumed is converted to CO (as the primary combustion product) and that the CO is further converted to CO<sub>2</sub> by interaction of CO with O<sub>2</sub>. This latter reaction becomes more prevalent at higher temperatures. It is also logical to assume that if more oxygen is present in the pores (higher oxygen partial pressure), then the conversion of CO to CO<sub>2</sub> will increase and the increased selectivity to CO<sub>2</sub> seen in Figure 6.15a will be the manifestation.

The altering of expected reactions due to the confinement of species within pores helps to contribute to the safety aspects of operating the membrane reactor. It is true that somewhere within the pores there exists a region where the oxygen and propylene content are within the explosive limits (see Chapter 5). Even though combustion

reactions do occur within the pores they cannot occur in the unbounded fashion necessary to produce an explosion. There is simply no way for the reactions to propagate themselves in the manner required for explosion. This concept could be taken further, although it is not done so in this research project, to investigate processes in which there would be an advantage to operating the reaction within the pores and having the reactants approaching each other from opposite directions. The advantage could arise for safety reasons or by limiting the extent to which certain, presumably undesired, reactions can occur.

### 6.2.3.3 Selectivity of Other Product Species

The figures which have shown the total carbon oxide selectivity indicate that approximately 6-13% of the converted propylene is converted to other product species: ethylene, acrolein and 1,5-hexadiene. The variations with respect to the process variables are much smaller than those of CO and CO<sub>2</sub> and often much less interesting. All the selectivity data are in Appendix B and so a simple summary of the basic trends is presented here in Table 6.2. Over the entire data set the selectivity ranges for the three components are as follows.

Ethylene	2.1 - 3.8%
Acrolein	2.1 - 6.5%
1,5-Hexadiene	1.2 - 6.0%

Generally the selectivity to ethylene falls in a very narrow range and is not strongly affected by any of the process variables. Selectivity to all the products is most strongly influenced by the partial pressure of oxygen in the pores. The selectivity to 1,5-hexadiene shows the greatest variation as a result of all the different variables and is most strongly influenced by temperature.

Table 6.2 - Selectivity Trends for Ethylene, Acrolein and 1,5-Hexadiene in the Blank Membrane Reactor

Process Variables	Selectivity Trends			
	Temperature	Oxygen Feed Concentration	Propylene Feed Concentration	Total Feed Flow Rate
Component				
Ethylene	very gradual rise with increasing temperature	slight decrease as O <sub>2</sub> concentration increases	little effect	little effect
Acrolein	little affect although often increases at highest temperature	increases as O <sub>2</sub> concentration increases	variable but marginal effect	increases as total flow rate increases
1,5-Hexadiene	increases with increasing temperature	increases as O <sub>2</sub> concentration increases	decreases as propylene concentration increases	decreases as total flow rate increases

### 6.3 Other Aspects of Reactor Operation

Initial testing of the treated, crushed VYCOR samples (Chapter 4) showed there to be little activity and no coke formation on these samples. There are very different flow profiles and interaction between propylene and oxygen in the crushed samples compared with the membrane reactor. The flow of oxygen through the membrane and diffusion of propylene into the membrane accounts for the activity of the membrane not seen in the crushed samples. The presence of oxygen in all sections of the tubular reactor used for testing the crushed samples prevented (or removed) coke formation. In the membrane reactor system using certain sets of process variables there is little or no oxygen available inside the tube of the reactor. In these oxygen deficient regions near the inlet end of the membrane a mild deposition of carbonaceous material has been noted at the end of an entire day of tests (sequential operation at all temperatures - 490, 510, 530 and 550°C). The deposits do not seem to affect the permeability or mass balances. They are easily removed by exposure to oxygen at 530°C for a few minutes and have had no perceivable impact on the results.

There has been considerable discussion about the effect that oxygen partial pressure has on the reaction results in the reactor. However, no precise information about what the oxygen partial pressure in the membrane pores actually is, other than the simple observations provided in Section 6.2.3.1, has been provided. The reason for the omission is that the pressure varies all the way across the membrane and in many cases it is not clear whether part or all of the thickness of the membrane is involved in the series of not completely understood reactions. Without much more study of the details of reactions in the membrane no meaningful answer can be provided. This sort of study may be one fruitful path along which to continue the initial research effort covered by this thesis.

Some simple insight into the partial pressure in the pores of some of the product species is in order. However, it is even harder to predict partial pressures within the pores of the membrane of these major species, carbon oxides and water, than it is for oxygen partial pressure. In some instances the production rate of  $\text{CO}_x$  and  $\text{H}_2\text{O}$  are each approximately one third of the oxygen flux through the membrane. Since these species are formed within the membrane, there must be regions, perhaps localized, within the membrane where partial pressures of these species are significant. It becomes very difficult to predict the concentrations of the various species participating in the various reactions in the various sections of the membrane.

Some very brief experimental work has made it abundantly clear that it is partial pressure that is the important variable in the membrane. These experiments show that the presence of other species and the rates and directions of flux of these species has no bearing on the activity in the membrane. Tests of the blank membrane reactor and with a packed bed of catalyst in the reactor at 125 sccm total flow with 20 mol% propylene and 6 mol% oxygen in the feed using an undiluted oxygen feed, oxygen diluted by helium and oxygen diluted by nitrogen produce exactly the same results. Neither the total pressure in the membrane pores, the presence of nitrogen nor the direction of helium or nitrogen flux has any effect on the results.



#### 6.4 Changes in Membrane Permeability

The permeability of the membrane increased with increasing time on stream. During the reaction testing of the blank reactor the permeability of the membrane, as measured by the oxygen partial pressure difference required to produce a certain flux, increased by approximately 7%. This change was relatively small and the only discernible effect on the reaction results was an increase in total conversion of propylene by approximately 7%. This effect seems reasonable as the increase in permeability to oxygen should be accompanied by an increase in permeability to propylene which in turn will increase the amount of propylene that can react in the membrane. The small change in oxygen partial pressure is not enough to materially affect the selectivity to the various products.

There are three issues that the matter of changing permeability raise. The first issue is whether the permeability will continue to increase in the subsequent testing with a catalyst packed in the reactor tube. The answer to this question is yes and it is covered in much more detail in Chapter 7. However, since the amount of propylene conversion caused by the membrane and by the catalyst are of the same order of magnitude, changes in the conversion caused by the membrane have a noticeable effect on the results due to the catalyst alone. The effect of the membrane must be exactly known so that the effect of the catalyst can be accurately calculated. As a result further testing of the blank membrane became necessary and will be discussed in Chapter 7.

The second issue is the reason for the change in permeability. The reason or reasons for the permeability change are not indisputably known. The increase in permeability must be due to an increase in the average diameter of the pores since no new pores can be formed or from a decrease in overall membrane thickness. For this type of change to happen, one or both of the following phenomena must be occurring: (1) silica is removed from the pore walls or the inside wall of the membrane, or (2) silica chemically changes structure on the pore wall so as to not impede flow to the same extent, or, in the case of any remaining "spider web" filaments in the pores, it is removed or pushed out of the way. It seems most likely that the water combined with the high temperatures is reacting in some way with the silica and slightly changing the pore structure. It is known that

even high silica glass in the presence of water at temperatures in excess of 260°C (high pressure) will dissolve to some extent and that silica loss is experienced in the presence of high temperature steam (Filbert and Hair (1976)). The changes that cause the small percentage increase in permeability are so slight that it would be very difficult to physically measure them by means other than a simple permeability test. A more in-depth evaluation would require destructive testing of the membrane.

The third issue is finding ways of decreasing the permeability of the membrane and so decreasing the reactive nature of the membrane. If the reactivity of the membrane could be decreased by an order of magnitude, any slight changes would have little bearing on results when a catalyst would be involved. In addition, the low activity would make the membrane much more appealing for commercial application. Permeability can be decreased by one of three methods.

1. Increase membrane thickness
2. Decrease pore size
3. Decrease number of open pores

Increasing the membrane thickness only requires one to start with a thicker material. Such materials should be readily available from Corning or other manufacturers of porous glass. The key concern is whether the treatment process (hydroxide and steam) will be as effective in reducing the reactivity in a thicker membrane and whether the same construction process would be effective. Testing of this method is simple and straightforward.

Decreasing the pores size requires either a starting material with smaller pores (also available from glass manufacturers) or some method to deposit material inside the pores. Any deposited material would be best placed near the tube side wall to primarily restrict the diffusion of propylene into the pores. Either approach may yield acceptable results. Shelekhin et al. (1995) found that heat treatment would decrease permeability but that the decrease is due to complete collapse of some pores rather than a general decrease in diameter of all of the pores.

The ideas of Shelekhin et al. (1995) have been used by Ramachandra et al. (1996) to decrease permeability by collapsing pores via heat treatment. The low permeability membrane of Ramachandra et al. (1996) was discussed earlier in this chapter. It is possible to use that approach with the membranes used in this study. A simple test, heat treatment of a treated membrane at 750°C for 12 hours, resulted in a membrane with approximately 7% of the original permeability. Obviously, some temperature between 600°C (the steam treatment temperature of the membrane) and 750°C would be more appropriate. However, the lower permeability of the membrane will require a higher shell side pressure and eventually either the Cajon fittings, used in this study to seal the shell to the tube, will be unable to hold the pressure, or the membrane itself will be unable to withstand the pressure. Examination of these ideas merits additional effort.

It is also possible to decrease the number of open pores using the ideas of Gavalas et al. (1993). The reaction to form silica in the pores of VYCOR, and hence block some of the pores, could find application with the membrane reactor developed in this study. Again, however, the problem of pressure containment exists. In this case one would also have to worry about pressure containing abilities of the thin layer of deposited silica in the pores.

## **6.5 Limits to Propylene Diffusion**

It has been assumed in all the previous discussion in this chapter that the amount of propylene that can diffuse into the membrane and react is limited exclusively by the membrane. It has been assumed that the propylene concentration at the inner wall of the membrane is exactly the same as the concentration in the bulk of the tube and that no mass transfer limitations exist near or at the membrane wall. Mass transfer at the wall of a packed bed is largely an unstudied issue since walls are generally impermeable to mass, no data are directly available. So the Chilton-Colburn analogy ( $j_D$  factors) can be used to examine the problem.

The partial pressure difference of propylene across the thin film at the wall will lie in between the extremes predicted by assuming that the effect will be the same as it would be either around a particle in a packed bed or at the wall in normal pipe flow in a tube.

Following the general method presented by Froment and Bischoff (1990), the partial pressure difference across the thin film can be calculated. The Chilton-Colburn factor,  $j_D$ , is defined as

$$j_D = St_D Sc^{2/3} \quad (6.5)$$

Using the definition of Stanton number for gases as

$$St_D = \frac{Sh}{Re Sc} = \frac{k_g M_m p_{fA}}{G} \quad (6.6)$$

where  $p_{fA}$  is the film pressure factor defined as

$$p_{fA} = \frac{(P_i + \delta p_A) - (P_i + \delta p_{A_s})}{\ln \frac{(P_i + \delta p_A)}{(P_i + \delta p_{A_s})}} \quad (6.7)$$

with  $\delta$  being the change of moles on reaction (per mole of A reacted).

For very small changes in partial pressure of A across the thin film it can be shown by L'Hopital's rule that

$$p_{fA} \cong p_i + \delta p_A \quad (6.8)$$

If it is assumed that the diffusion flux and rate of reaction are equal and the definition for flux is

$$F = r = k_g a_m (\Delta p_A) \quad (6.9)$$

equations 6.5, 6.6 and 6.9 can be combined and re-arranged to solve for the pressure difference across the thin film.

$$\Delta p_A = \frac{rM_m P_{fA}}{a_m G j_D} Sc^{2/3} \quad (6.10)$$

Using two representative cases, 24 mol% propylene, balance helium and 12 mol% propylene, balance helium, for flow on the tube side of the reactor at 530°C and 105 kPa total pressure, and ignoring any impact of oxygen, the data in Table 6.3 are calculated. Physical properties are provided by the HYSIM process simulator (Peng-Robinson EOS) and diffusion coefficients are calculated by the Wilke-Lee modification of the Hirschfelder-Bird-Spotz method as presented in Treybal (1980).

Table 6.3 - Physical properties of Propylene-Helium System

	24% Propylene	12% Propylene
viscosity	0.0441 cP	0.0457 cP
density	0.2066 kg/m <sup>3</sup>	0.1348 kg/m <sup>3</sup>
mol. mass	13.142 kg/kmol	8.5752 kg/kmol
diffusion coeff.	1.34 cm <sup>2</sup> /s	1.34 cm <sup>2</sup> /s
Sc	1.593	2.53

Using the two extreme flow rates, 125 sccm and 250 sccm, and knowing that the reactor has an inside diameter of 0.015 m and that the quartz packing has an average diameter of 0.00075 m, the mass velocity, G, the Reynolds number, Re, and the particle Reynolds number, Re<sup>p</sup> are calculated and presented in Table 6.4.

Table 6.4 - Mass Velocities and Reynolds Numbers of Propylene-Helium System

	24% Propylene		12% Propylene	
	125 sccm	250 sccm	125 sccm	250 sccm
G (kg/m <sup>2</sup> s)	0.00691	0.0138	0.00451	.00902
Re	2.35	4.70	1.48	2.96
Re <sup>p</sup>	0.118	0.235	0.074	0.148

As the values in Table 6.4 indicate the flow is quite laminar for the situations described. Froment and Bischoff (1990) give a correlation for  $j_D$  in a packed bed of spheres with a void fraction of 0.37 for  $Re^p < 190$  as

$$j_D = 1.66 Re^p{}^{-0.51} \quad (6.11)$$

and Treybal (1980) indicates that for laminar flow in a tube  $Sh \approx 3.41$ . The value of  $j_D$  can be calculated from equations 6.5 and 6.6 for the latter case. Using equation 6.10 and the following assumptions,

1. the membrane is 5.5 cm in length
2. half of the reacted propylene is converted to CO and the other half to CO<sub>2</sub> giving an average increase in moles on reaction,  $\delta$ , of 1.25
3. total tube side pressure is 105 kPa
4. maximum amount of propylene converted is 1.56 sccm (Appendix B) - to be used as the extreme value,

the values for  $\Delta p$  can be calculated. They are presented in Table 6.5.

Table 6.5 - Partial Pressure Difference Across the Thin Film for the Propylene-Helium System

	24% Propylene				12% Propylene			
	125 sccm		250 sccm		125 sccm		250 sccm	
	packed bed	tube	packed bed	tube	packed bed	tube	packed bed	tube
$j_D$	4.94	1.24	3.47	0.621	6.26	1.69	4.40	0.845
$\Delta p$ (kPa)	0.032	0.128	0.023	0.128	0.030	0.113	0.022	0.113
% of bulk propylene partial pres.	0.13	0.51	0.09	0.51	0.24	0.90	0.17	0.90

In all cases the partial pressure difference of propylene across the thin film is negligible and hence the assumption that the propylene pressure at the wall is the same as in the bulk is correct. The reason that the difference is so small is that characteristic time for diffusion into and reaction in the pores is much larger than the characteristic time for diffusion across the thin film. No large concentration driving force is necessary to help facilitate the diffusion at the wall.

## 6.6 Modeling of the Results

One of the primary reasons for studying the behaviour of the blank membrane reactor is to be able to predict its contribution to the reactions when the reactor is loaded with a catalyst and used. Prediction, of course, implies some sort of model of the process, but how detailed a model and the type of model best suited for the application must be decided upon. The choice in model type is between a theoretical model and an empirical model.

A theoretical reaction model of the reactions cannot be as simple as developing Arrhenius equations for the various reactions because the rates of reaction are limited by diffusion in the pores in most cases. Thus, modeling of the diffusion processes as well as the reactions is necessary in a theoretical model. This type of full blown model, although perhaps interesting and potentially a goal of further work in this area, is not really justified given the information available to build the model and the information to be garnered from the model. A less complex approach to this sort of model is to treat the membrane as a catalyst and use the Thiele modulus-effectiveness factor method. Unfortunately the relatively simple effectiveness factor approach is meant to handle reactants diffusing concurrently into a permeable catalyst and participating in a single reaction where the kinetic parameters are known. The situation in the membrane reactor is very different. Species diffuse toward one another and react in a number of series and parallel reactions for which the true kinetic parameters are not known. It may be possible to utilize the effectiveness factor approach, but the modeling effort may be no less rigorous than a full diffusion-reaction model.

Development of a theoretical model of the system cannot be justified on the basis of the information that would be required from the model for this thesis work. Over the limited range of flow, feed concentrations and temperatures that are of interest in this study much simpler empirical models will better fit the purpose. One of the drawbacks of an empirical model is that extrapolation outside of the data set used to develop the model will often not result in reliable prediction. In this instance, however, the data collected for the blank reactor covers the ranges of all parameters of interest for the further

catalytic testing described in Chapter 7 of this thesis. As a result there is no need to extrapolate and the empirical models will suffice for this purpose. The remaining question is whether to develop a single set of empirical models to predict the yield for each of the products as a function of all of the input parameters (temperature, feed concentrations and overall flow rate) or to develop a series of simpler relationships for interpolating between available data points for each parameter individually. The former approach is really an exercise in data fitting which will produce a series of potentially non-linear models. Since the basic form will have no theoretical grounding, the models may not even accurately predict interpolated values. The latter approach, although perhaps the least compact or elegant, should provide simple, accurate results. As evidenced by the relationships illustrated in Figures 6.7-6.16, the models (one variable at a time) will be simple linear or quadratic functions. Given the relative simplicity of this method and the limited amount of interpolation needed, it is the approach selected for applying the data of this chapter to the work in Chapter 7. Since these relationships are so simple and can easily be generated from the data in Appendix B, none will be presented here.

Development of more complex and theoretically correct models to describe the behaviour of the blank reactor is one possible future research route. Work in this area may be very valuable but will likely be more applicable to other reactions or modes of membrane reactor operation than those presented in this work. Perhaps the most valuable future development work applicable to this project would be investigation of methods of decreasing the activity of the membrane to the point where it is insignificant compared to any desired catalytic reaction. A number of potential routes for this work to take have been suggested in Section 6.4.



## Chapter 7

### Reaction Tests with Bismuth (III) Oxide as a Catalyst

Most of the testing of the membrane reactor with an ODHD of propylene catalyst is carried out using  $\text{Bi}_2\text{O}_3$  as the catalyst. Presentation and discussion of the results of these tests forms one section of this chapter. In conjunction with the tests using the membrane reactor, two other sets of tests using the  $\text{Bi}_2\text{O}_3$  catalyst have also been conducted. The first series of tests, using a standard tubular reactor, were intended to investigate some potential reaction pathways for the reactions between propylene and oxygen on the catalyst and to investigate some of the kinetic parameters for these reactions. The second set of tests involved operating a tubular reactor under similar conditions to those used for the membrane reactor tests so that a direct comparison between membrane reactor operation and regular fixed bed reactor operation is available. The results of the first series of tests are presented in Sections 7.1-7.3 and the fixed bed reactor results are presented and discussed along with the membrane reactor results in section 7.4. A third section (section 7.5) contains a discussion of the attempts to support the bismuth catalyst in the pores of the membrane reactor and operate the membrane reactor with catalytically active pores.

#### 7.1 Catalyst and Reaction Parameter Evaluation

##### 7.1.1 Description of the Catalyst

Solid, unsupported  $\alpha\text{-Bi}_2\text{O}_3$  is used as the catalyst. It is supplied by the Aldrich Chemical Co. at 99.9% purity as 3-12 mm sintered pieces. The catalyst is mechanically strong witnessed by the fact that it does not suffer from attrition while in use in a fixed bed, but

it can be readily crushed by mortar and pestle. When used in reaction tests the catalyst was crushed and the 16 x 20 mesh (Tyler designations) (1 mm x 0.841 mm) fraction was screened out to be used in the catalyst bed. The catalyst bed consisted of the  $\text{Bi}_2\text{O}_3$  diluted with 20 x 30 mesh (Tyler) quartz chips. The quartz was used to ensure good heat transfer in the bed and the smaller particles helped to decrease the dimension of inter-particle spaces so as to avoid gas bypassing catalyst particles. The quartz to  $\text{Bi}_2\text{O}_3$  ratio (mass basis) was approximately 1.2 for all tests. The bed was held in place by plugs of quartz wool at the ends of the bed. An axial thermocouple was inserted into the middle of the bed. Analysis of the surface area and pore size distribution of the catalyst by B.E.T. nitrogen adsorption showed the surface area to be approximately  $0.7 \text{ m}^2/\text{g}$  and to be essentially non-porous (no appreciable micro- or meso-pores were detected). These values of these characteristics are in the expected ranges and are excellent for ODHD of propylene. The specific surface area was the same as that found by White and Hightower (1983).

#### 7.1.2 Description of the Tests

Three sets of basic tests have been conducted to evaluate the catalyst and some of the reaction parameters. The first set of tests was used to verify kinetic parameters and establish a kinetic model for the two primary reactions, formation of 1,5-hexadiene and formation of carbon dioxide. These tests were also used to investigate some of the potential reaction routes, particularly those leading to the formation of  $\text{CO}_2$  and hydrocarbon products other than 1,5-hexadiene. Experimental work on this last point is notably absent in the existing literature. The second set of tests was used to determine if there are external mass transfer limitations in the packed bed. The third test was a stability test to determine if there was a loss in activity of the catalyst with time on stream. The reaction protocol used for all these tests with the exception of the stability test is given in Section 3.2.1. The stability test follows the same general protocol except that the reactor was operated at only one temperature and the effluent was sampled only once every 12 hours.

In the course of the investigation it became clear that investigation of the reaction of 1,5-hexadiene with oxygen over the  $\text{Bi}_2\text{O}_3$  catalyst would be necessary as well as the investigation of the propylene/oxygen reactions. The results of these two subsets of the kinetic tests are given in the following sections with the propylene results presented first.

### 7.1.3 Propylene Kinetic Tests

#### 7.1.3.1 Description of the Tests

The kinetic testing was carried out using a low W/F ratio (high flow rate) to ensure that there were no heat of reaction effects and to ensure that the conversion of the feed species was low. Tests conducted with the reactor packed only with quartz chips indicate that there is no appreciable homogeneous reaction occurring under any of the test conditions and that the quartz is inert. The absolute operating pressure in the reactor in all cases was  $105 \text{ kPa} \pm 1 \text{ kPa}$ . Feed concentrations of propylene and oxygen were set so that they were generally in the same ranges used for testing of the membrane reactor. In this manner the kinetic model and parameter values should be valid for the conditions prevailing in the membrane reactor tests, but it is realized that the data may be insufficient to generate models applicable outside of these ranges. The operating parameters for the kinetic tests are given in Table 7.1. Propylene feed concentration was varied at a constant oxygen feed of 6 mol% and oxygen feed concentration was varied with the propylene feed set at 10 mol%.

Table 7.1 - Operating Parameters for Propylene Kinetic Tests over  $\text{Bi}_2\text{O}_3$

Parameter	Parameter Value(s)
Total Flow Rate	625 sccm
Amount of $\text{Bi}_2\text{O}_3$	6.4 g
Amount of diluent quartz	7.62 g
Propylene Feed Concentration	7.5, 10.0, 12.5, 15.0 mol%
Oxygen Feed Concentration	3.0, 4.0, 5.0, 6.0 mol%
Nominal Furnace Temperature	490, 510, 530, 550°C
Actual Catalyst Bed Temperature	500, 520, 540, 560°C

The difference between the bed and furnace temperature (10°C) was not experienced when conducting membrane reactor tests (see Chapter 6), but the unshielded quartz reactor suffers from this difference. As long as the actual bed temperature is known, however, the results will be perfectly valid. The test conditions were selected to minimize conversion of the reactants so that the results of the tests can be interpreted as differential results. That is, the concentrations (or partial pressures) of the feed species can be considered constant across the length of the catalyst bed. It is generally acknowledged that the assumption of differential conditions is acceptable if the conversion is less than 10%. Operation of a differential reactor is described by equation 7.1. Since the conversion criteria are met for all the tests equation 7.1 can be applied. The complete data set for these tests is given in Appendix C.

$$\frac{W}{F} = \frac{X}{-r_A} \quad (7.1)$$

### 7.1.3.2 Activation Energy Evaluation

The only species produced in any appreciable quantity were CO<sub>2</sub> and 1,5-hexadiene, the expected primary products. The data can be used to determine a number of kinetic parameters. The first parameters are the activation energies for the formation of 1,5-hexadiene and CO<sub>2</sub>. The rate of consumption of propylene for each of the two products can be derived from the data using equation 7.1. If a standard Arrhenius relationship is assumed for the reaction constant, *k*, then reaction rate equation is equation 7.2.

$$-r_{propylene} = A e^{-E/RT} f(P_{O_2}, P_{propylene}) \quad (7.2)$$

In equation 7.2 the function of feed species partial pressures is constant for any one set of feed conditions (the advantage of differential operation) and *A* is constant. These two terms can be combined into one generic constant, *C*, and equation 7.2 can be linearized to give equation 7.3.

$$\ln(-r_{\text{propylene}}) = \ln(C) - \frac{E}{R} \left( \frac{1}{T} \right) \quad (7.3)$$

The results of the kinetic tests, in the linearized Arrhenius form, are shown in Figure 7.1 for 1,5-hexadiene formation and Figure 7.2 for CO<sub>2</sub> formation.

The activation energies for the two reactions as derived from the slopes of the lines on Figures 7.1 and 7.2 are given in Table 7.2.

Table 7.2 - Measured Activation Energies for Formation of 1,5-Hexadiene and CO<sub>2</sub> from Propylene over Bi<sub>2</sub>O<sub>3</sub>

Propylene Feed Concentration (mol%)	Oxygen Feed Concentration (mol%)	1,5-Hexadiene		Carbon Dioxide	
		Activation Energy (kJ/mol)	r <sup>2</sup>	Activation Energy (kJ/mol)	r <sup>2</sup>
10	3	105.1	0.9998	76.9	0.9894
10	4	111.7	0.9993	78.1	0.9863
10	5	115.3	0.9988	77.1	0.9868
10	6	118.6	0.9986	76.8	0.9907
15	6	116.0	0.9992	76.6	0.9900
12.5	6	119.2	0.9988	79.0	0.9900
7.5	6	118.6	0.9988	79.6	0.9914

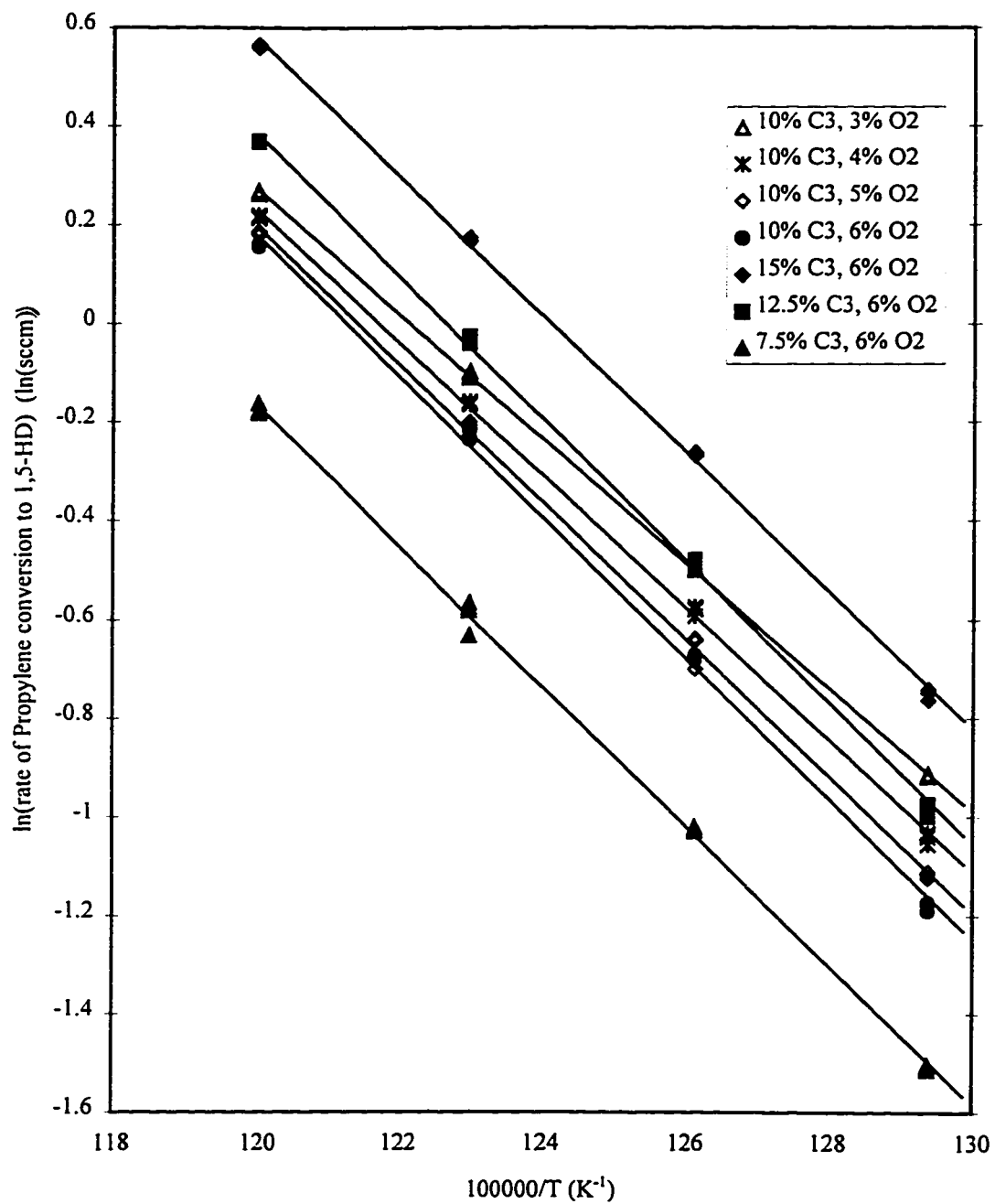


Figure 7.1 Arrhenius Plot for 1,5-Hexadiene Formation from Propylene over  $\text{Bi}_2\text{O}_3$

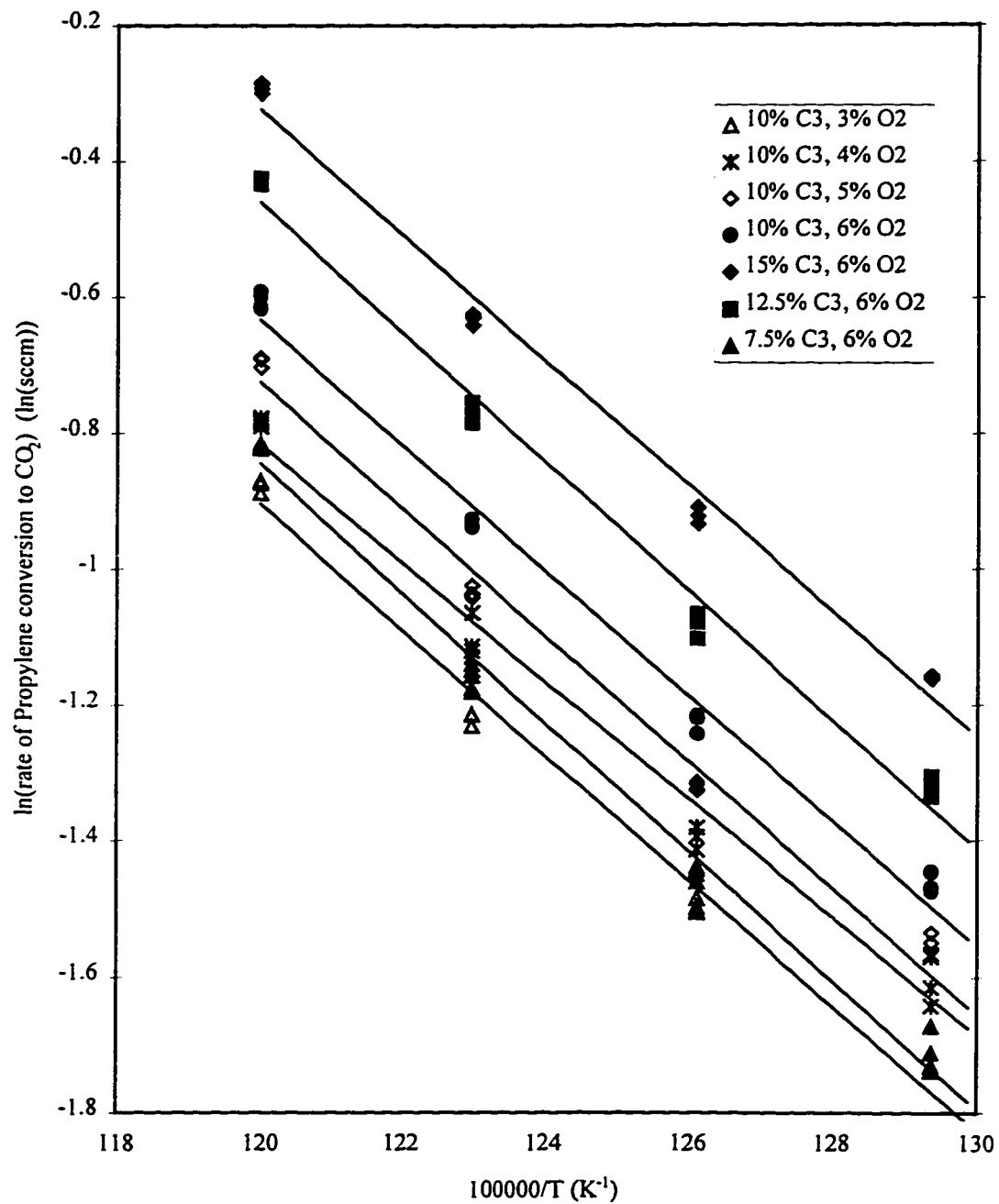


Figure 7.2 Arrhenius Plot for CO<sub>2</sub> Formation from Propylene over Bi<sub>2</sub>O<sub>3</sub>

The slightly smaller scatter in the 1,5-hexadiene data results in the correlation coefficient ( $r^2$ ) being a little closer to unity than that for the carbon dioxide data. The respective sets of correlation coefficients translate into approximately 1% standard error for the 1,5-hexadiene activation energy values and approximately 3% standard error for the CO<sub>2</sub> activation energy values. Watts (1994) indicates that linearization of a non-linear expression such as the Arrhenius equation to find parameter values is potentially fraught with errors and recommends the use of non-linear (and much more complex) statistical methods to accurately determine parameter values. Watts backs the argument by examining kinetic data from the study of propylene oxidation over bismuth molybdate to form acrolein. The results indicate that the activation energy estimates are little affected by the method used to determine them. Rather it is the estimate of the Arrhenius constant, A, which can vary greatly with small changes in activation energy, which tends to be much more accurate with non-linear methods. Although Watts (1994) indicates that non-linear statistical methods are superior, more recent work (Brauner and Shacham (1997)) indicates that the linear method is not inferior and may be superior to non-linear methods if the errors are normally distributed.

Assuming, then, that the linear estimates of activation energies are reasonable, the values can be compared to other literature values. Within the literature values of activation energy for ODHD of propylene vary. White and Hightower (1983) report a value of 92 kJ/mol, but indicate that mass transfer problems may be partially masking the true activation energy. Their evaluation of activation energy is based on overall consumption of oxygen and thus lumps both the ODHD reaction and combustion reactions into one. It seems possible that the value they have derived is not mass transfer limited but rather is simply an intermediate value between the values for 1,5-hexadiene formation and combustion reactions. The arithmetic average of the values determined in this thesis is approximately 96 kJ/mol which corresponds very well to the value of White and Hightower (1983). Massoth and Scrapicello (1971) report a value of 113 kJ/mol, Swift et al. (1971) report a value of 115 kJ/mol, and Solymosi and Bozsó (1977) report a value of 129 kJ/mol. All of these latter three values are for ODHD on Bi<sub>2</sub>O<sub>3</sub> in the absence of oxygen (simple reduction of the catalyst). The values of Massoth and Scrapicello (1971)



and Swift et al. (1971) are based on disappearance of propylene rather than the conversion of propylene to 1,5-hexadiene. Thus these values also take into account all reactions, but in these instances (no oxygen, very low conversion of propylene) the selectivity to CO<sub>2</sub> is less than 10% and hence the values derived should be good approximations of the activation energy for ODHD alone. The values in Table 7.2 for higher oxygen concentration (5-6%) are in the same range (115-119 kJ/mol), and hence correspond to the previous work very well. However, the activation energy at lower oxygen concentrations decreases below this range. The standard errors of these estimates mean that at the 95% confidence level the results should be accurate within  $\pm 2.5$  kJ/mol so that the differences resulting from the change in oxygen concentration are real. The veracity of the value of activation energy at 3% oxygen is confirmed by the experiments used to test for mass transfer limitations (Section 7.2) which show that the value is in the range 103-106 kJ/mol. The reason for the change in activation energy with oxygen concentration is not precisely known, but one possibility is that at higher oxygen concentrations more 1,5-hexadiene is converted to CO<sub>2</sub> and hence the apparent activation energy rises. This notion is discussed further in Section 7.1.4.

The activation energy for the formation of CO<sub>2</sub> is more consistent than that for 1,5-hexadiene formation. The value is approximately  $78 \pm 4.5$  kJ/mol (95% confidence level). There are no literature values available with which to compare this result. It must be noted that there is more than one route for the formation of CO<sub>2</sub>. As many other authors have indicated, CO<sub>2</sub> can be formed from any of the hydrocarbon species present within the reactor. Even though the correlation coefficients for the Arrhenius relationships for CO<sub>2</sub> are very close to unity, there is definite and consistent curvature to the data. The slope is steepest at the lowest reciprocal temperature (highest temperature). This sort of curvature is indicative of two distinct reactions occurring over the temperature range. The more highly activated reaction, occurring at higher temperatures, is assumed to be oxidation of 1,5-hexadiene. This reaction becomes more noticeable at the higher temperatures because more 1,5-hexadiene is formed at these temperatures. In these tests where the partial pressure of propylene is so much higher than any other species, it is likely that a large portion of the CO<sub>2</sub> formed comes from propylene. The

susceptibility of 1,5-hexadiene (the only other hydrocarbon with any notable concentration in the reactor) to combustion is discussed in Sections 7.1.4.3 and 7.1.4.4.

### 7.1.3.3 Kinetic Model Order (Power Law)

The form of the function of reactant partial pressures in equation 7.2, at least a power law form of the function, can also be determined from the kinetic data. The functional form, for both formation of 1,5-hexadiene and CO<sub>2</sub>, will be that of equation 7.4. The power law model is the simplest model form available to correlate the data. A more complex model, such as a Langmuir-Henshelwood model or an Eley-Rideal model, could be used. However these more complex models require testing over more extensive ranges of feed concentrations and should include some evaluation of product inhibition. Over the narrow range of concentrations (both feed and products) used for the membrane reactor studies, a more complex model than a simple power law model is not justified.

$$f(P_{O_2}, P_{propylene}) = P_{propylene}^{n_1} P_{O_2}^{n_2} \quad (7.4)$$

The results of the evaluation of the data are given in Table 7.3.

Table 7.3 - Measured Power Law Exponents for Formation of 1,5-Hexadiene and CO<sub>2</sub> from Propylene and Oxygen over Bi<sub>2</sub>O<sub>3</sub>

Temperature (°C)	1,5-Hexadiene		Carbon Dioxide	
	n <sub>1</sub>	n <sub>2</sub>	n <sub>1</sub>	n <sub>2</sub>
500	1.1	-0.33	0.80	0.43
520	1.1	-0.22	0.76	0.41
540	1.1	-0.15	0.76	0.41
560	1.0	-0.13	0.76	0.41

White and Hightower (1983) indicate for the overall consumption of oxygen (lumping together of all reactions) that the reaction is slightly greater than first order in propylene and less than first order in oxygen. The data in Table 7.3 may be in agreement. However White and Hightower (1983) do not provide selectivity information and hence it is

impossible to know what portion of the reaction is due to CO<sub>2</sub> formation and what portion to 1,5-hexadiene formation. This information is necessary to accurately assess their data. Swift et al. (1971) found the overall reaction to be first order in propylene and zeroth order in oxygen. Again this result seems possible given the data in Table 7.3. Unfortunately there is no more comprehensive data with which to compare these results.

The power law expression for CO<sub>2</sub> does not vary with temperature and is given as equation 7.5.

$$f(P_{O_2}, P_{propylene}) = P_{propylene}^{0.76} P_{O_2}^{0.41} \quad (7.5)$$

The expression for the power law for 1,5-hexadiene formation is roughly first order in propylene, as expected, but the order with respect to oxygen is negative and changes with temperature. These changes are statistically significant so some explanation is warranted. There are two possible explanations. The first explanation is that the model is some sort of Langmuir-Henshelwood type expression where the denominator is of the form of equation 7.6a for non-dissociative adsorption of oxygen (similar to that of the LH model given in equation 2.6) or equation 7.6b for dissociative adsorption of oxygen (same as equation 2.4).

$$1 + K_1 P_{propylene} + K_2 P_{O_2} \quad (7.6a)$$

$$1 + K_1 P_{propylene} + \sqrt{K_2 P_{O_2}} \quad (7.6b)$$

In either case, for the role of oxygen partial pressure to be significant in the reaction equation the propylene term would have to be small and the oxygen term would have to be at least of the order of 1. From a Langmuir adsorption point of view the latter criterion means that oxygen would have to cover approximately half the active sites (or half the sites specific for oxygen if a model like that of Trimm and Doerr (equation 2.2)

were considered). More important, however, is to note how  $K_2$  changes with temperature. The equilibrium adsorption constant relationship with respect to  $T$  is given by equation 7.7.

$$K = K^0 \exp\left(\frac{\Delta H_{ads}}{R} \left(\frac{1}{T} - \frac{1}{T_0}\right)\right) \quad (7.7)$$

An approximation the heat of adsorption of oxygen on to  $\text{Bi}_2\text{O}_3$  is given by using a slightly lower value than the value given by Gamid-Zade et al. (1979) for bond strength of oxygen on a Bi-Sn catalyst, 377 kJ/mol. In this case an estimate of 293 kJ/mol seems reasonable. Over the 60°C temperature range indicated in Table 7.3  $K_2$  will decrease by a factor of 27. Considering dissociative adsorption only, since the almost 30 fold decrease in  $K$  makes the use of a non-dissociative model unlikely and the general mechanism described in Chapter 2 assumes dissociative adsorption, a model can be constructed that roughly fits the data. Only the Mamedov model (equation 2.4) fits this general form. In order that oxygen can have an appreciable negative order using the denominator of this model (equation 7.6b), the fractional coverage of propylene must be very low (approximately 10%). For the oxygen term, if the value of  $K^0$  is set at  $2 \text{ kPa}^{-1}$  (at 500°C), the oxygen site coverage is between 50% and 75% and the variation in exponents with temperature roughly predicts the values found in Table 7.3. This analysis does not prove that the model takes such a form, but it does indicate that it may be possible. However, the low propylene surface coverage with such high oxygen surface coverage given the concentrations in the bulk, tends to argue against this form of a model. Further kinetic experiments and experiments to evaluate the catalyst surface under reaction conditions would be necessary to prove or disprove the veracity of this form of model.

The second possible explanation for the change in the value of the oxygen exponent in the 1,5-hexadiene equation involves oxidation of 1,5-hexadiene. It is possible that the reaction to form 1,5-hexadiene is truly zeroth order in oxygen, but that further consumption of the  $\text{C}_6$  via complete oxidation gives the apparent negative order in

oxygen for the propylene to 1,5-hexadiene reaction. The oxidation of 1,5-hexadiene should have a lower activation energy than the ODHD of propylene to form the 1,5-hexadiene. Thus at higher temperatures the relative effect of over oxidation of 1,5-hexadiene will be diminished. As a result one would expect the apparent order of oxygen in the reaction to become less negative at higher temperature. These changes may also help to explain the change in the measured activation energy for ODHD of propylene with changing oxygen concentration. As with the first explanation, irrefutably proving the hypothesis is very difficult. However, some testing of the interactions of oxygen and 1,5-hexadiene over  $\text{Bi}_2\text{O}_3$  could provide some insight into the problem.

#### 7.1.4 1,5-Hexadiene Tests

##### 7.1.4.1 Description of the Tests

A limited number of tests in the quartz tubular reactor using 1,5-hexadiene and oxygen (diluted in helium) have been carried out. The low vapour pressure of 1,5-hexadiene at room temperature limits the highest possible concentration of the  $\text{C}_6$  in the feed stream and limits the amount of material, even in large gas cylinders, available from the gas supplier (Praxair). As a result three aspects of the 1,5-hexadiene reactions have been investigated with a limited number of tests. These three aspects are:

1. examination of 1,5-hexadiene and oxygen conversions at conditions similar to those to be investigated in the membrane reactor portion of the study to provide insight about the extent of  $\text{C}_6$  reactions in those tests,
2. examination of possible reaction routes (homogeneous and heterogeneous),  
and
3. attempt an analysis of the kinetic model and parameters for the 1,5-hexadiene reactions.

The reaction tests were carried out using a mixture of 0.20 mol% 1,5-hexadiene in helium as the 1,5-hexadiene feed source and a separate oxygen supply which provided feed at 2-

6 mol% of the total feed stream. The full set of test conditions is given in Table 7.4. For three tests no  $\text{Bi}_2\text{O}_3$  is used. Rather, in these tests the bed consists of an equivalent volume of crushed quartz. These runs were used to determine the effect of homogeneous reactions.

Table 7.4 - Operating Parameters for 1,5-Hexadiene Reaction Tests over  $\text{Bi}_2\text{O}_3$

Parameter	Parameter Value(s)
Total Flow Rate	250 sccm
Amount of $\text{Bi}_2\text{O}_3$	2.56 g
Amount of diluent quartz	3.02 g
1,5-Hexadiene Feed Concentration	0.10 - 0.196 mol%
Oxygen Feed Concentration	2.0, 3.0, 4.0, 6.0 mol%
Nominal Furnace Temperature	490, 510, 530, 550°C
Actual Catalyst Bed Temperature	500, 520, 540, 560°C

It should be noted from the outset that none of these tests were ideal for fully evaluating the three aspects listed above. They represent a compromise between competing needs with a limited number of available runs. The small amount of 1,5-hexadiene in the feed, although it is in the proper range for simulating membrane reactor conditions, means that a significant degree of conversion is likely and hence the results, from a reaction kinetics point of view, will have to be treated as integral data rather than differential data. Use of integral data makes determination of kinetics much more challenging compared with using differential data. In addition there are many relatively important reactions occurring when 1,5-hexadiene is used as feed compared to the propylene feed cases. This fact further complicates the determination of proper kinetic models and parameters. Another example of the compromises is that there is no propylene in the feed for these tests. Propylene in the feed would be necessary to accurately simulate membrane reactor operation, but there would be no way to distinguish between the contributions to reaction of propylene and 1,5-hexadiene when determining kinetics. Thus the effect of propylene adsorption on the catalyst and how it would affect 1,5-hexadiene reactions is not taken into account so that the kinetics can be properly evaluated. Regardless of the compromises, the data will provide significant insight into the reactions involving 1,5-hexadiene.

The full data set for these experiments is contained in Appendix C with the exception of one experiment involving the reaction of 1,5-hexadiene (no oxygen) over the quartz bed. This latter experiment produced almost no reaction and will only be described qualitatively.

#### 7.1.4.2 Evaluation of Potential Mass Transfer Limitations

One key consideration when evaluating these results is the question of external mass transfer resistance. The very low 1,5-hexadiene concentration means that only a small partial pressure difference across the thin film surrounding the catalyst particle is required for the bulk and surface concentrations to be significantly different. Using the same method outlined in Chapter 6, the partial pressure change across the thin film can be calculated based on the following assumptions.

1. Catalyst particles are assumed to be perfectly spherical giving a surface area to volume ratio of  $6/d_p$
2. Catalyst particle diameter,  $d_p$ , is  $841\ \mu\text{m}$
3. Extreme cases for amount of 1,5-hexadiene reacted (0.188 mol% 1,5 hexadiene/6 mol%  $\text{O}_2$  is the most at 0.24 sccm reacted and 0.10 mol% 1,5 hexadiene/2 mol%  $\text{O}_2$  is the least at 0.065 sccm reacted) at the typical operating temperature of  $540^\circ\text{C}$  are used
4. The diffusion coefficient for diffusion of 1,5-hexadiene into the mixture of helium and oxygen is calculated by

$$\frac{1}{D_{A,m}} = \sum_i \frac{y_i}{D_{A,i}}$$

In the extreme case of the largest amount of 1,5-hexadiene reacted, the partial pressure difference across the thin film is less than 5% of the bulk partial pressure even at the end of the reactor where the conversion of 1,5-hexadiene is in excess of 50%. Although this

amount is certainly more than that calculated for the case in Chapter 6, it is not sufficient to be interpreted as an external mass transfer limitation.

#### 7.1.4.3 Heterogeneous and Homogeneous Reactions

Knowing that external mass transfer limitations do not exist, the results of the reaction tests of 1,5-hexadiene and oxygen over  $\text{Bi}_2\text{O}_3$  can be interpreted using bulk partial pressures as representative concentrations. Typical results for the variation in 1,5-hexadiene conversion and selectivity to the major products (benzene,  $\text{CO}_2$ , ethylene and propylene) with respect to temperature, 1,5-hexadiene feed concentration and oxygen feed concentration are shown in Figures 7.3, 7.4 and 7.5 respectively.

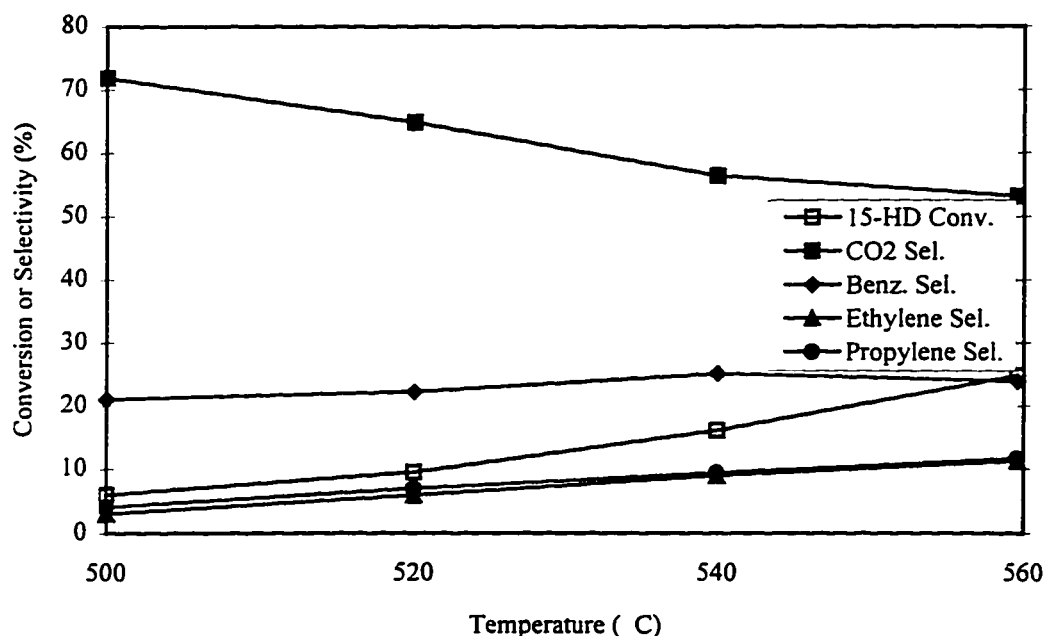


Figure 7.3 Conversion and Selectivity with respect to Temperature with 0.196 mol% 1,5-Hexadiene, 2 mol% Oxygen in Feed



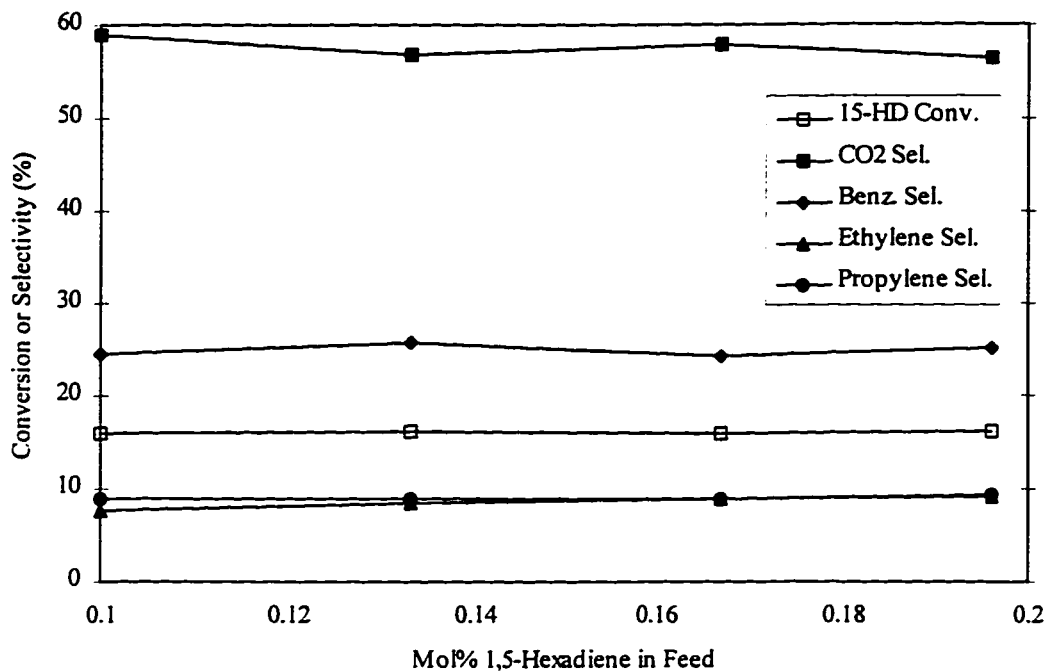


Figure 7.4 Conversion and Selectivity with respect to 1,5-Hexadiene Feed Concentration with 2 mol% Oxygen in Feed at 540°C

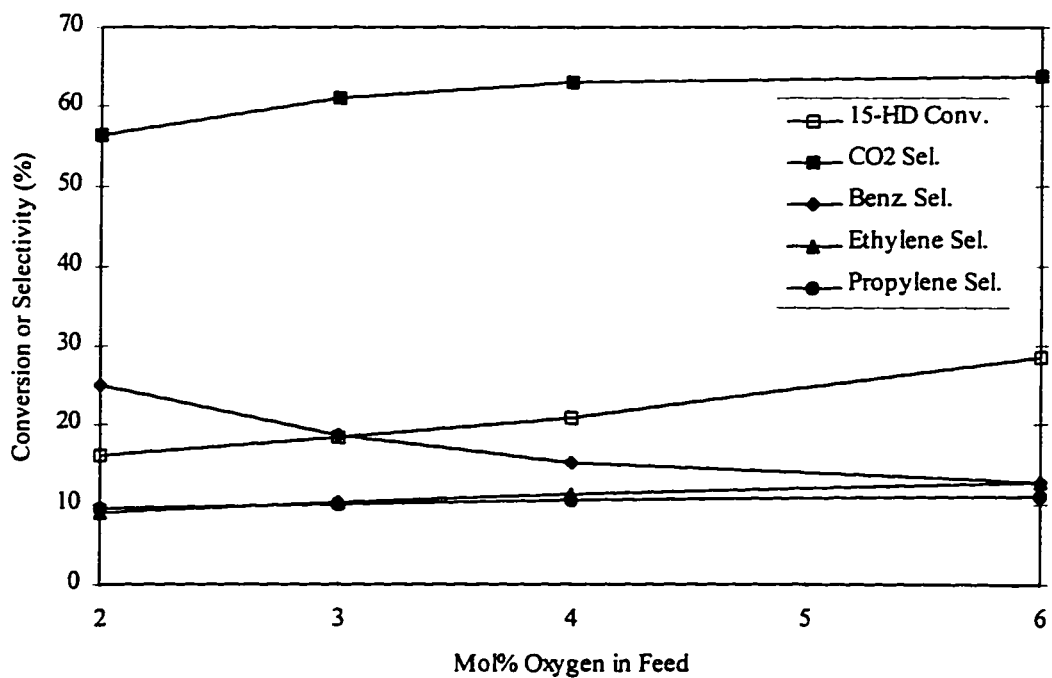


Figure 7.5 Conversion and Selectivity with respect to O<sub>2</sub> Feed Concentration with ~0.2 mol% 1,5-Hexadiene in Feed at 540°C

As would be expected an increase in temperature results in an increase in 1,5-hexadiene conversion. The selectivity to CO<sub>2</sub> drops noticeably in relation to the selectivity to all other products as the temperature increases indicating that the activation energy of the combustion reaction (or reactions) is less than that for the other reactions. Changes in feed 1,5-hexadiene partial pressure have almost no effect on either 1,5-hexadiene fractional conversion or any of the product selectivities. This fact indicates that all of the reactions, at least to a first approximation, are first order in 1,5-hexadiene. An increase in the oxygen feed concentration causes an increase in 1,5-hexadiene conversion and a mild increase in CO<sub>2</sub> selectivity, but has little effect on either ethylene or propylene selectivity. It does cause a substantial decrease in benzene selectivity. This effect could be caused by combustion of benzene at higher oxygen concentrations or by the fact that the formation of CO<sub>2</sub> is much more strongly promoted by oxygen than is benzene formation.

Three tests have been conducted without Bi<sub>2</sub>O<sub>3</sub> present. Two tests mimic the feed and test conditions of runs with Bi<sub>2</sub>O<sub>3</sub> and the third test is run without oxygen. Table 7.5 shows conversion of 1,5-hexadiene and rate of conversion of 1,5-hexadiene to key products for a Bi<sub>2</sub>O<sub>3</sub> test and a no- Bi<sub>2</sub>O<sub>3</sub> test under the same conditions.

Table 7.5 - Comparison of Catalyst and non-Catalyst Tests for 0.188 mol% 1,5-Hexadiene and 6 mol% Oxygen in the Feed

	Temperature (°C)			
	500	520	540	560
<b>Bi<sub>2</sub>O<sub>3</sub> Test</b>				
1,5-Hexadiene Conversion (%)	9.5	15.9	28.7	50.4
1,5-Hexadiene Converted to (sccm x 1000)				
CO <sub>2</sub>	32.4	50.6	86.8	142.8
Benzene	7.3	11.7	15.9	26.2
Ethylene	2.1	6.3	17.3	39.5
Propylene	2.7	6.0	14.7	28.3
<b>Non-Bi<sub>2</sub>O<sub>3</sub> Test</b>				
1,5-Hexadiene Conversion (%)	4.0	7.5	17.0	35.2
1,5-Hexadiene Converted to (sccm x 1000)				
CO <sub>2</sub>	3.9	6.8	13.4	24.6
CO	9.8	14.1	27.0	57.7
Ethylene	2.0	7.1	21.3	48.6
Propylene	2.9	7.2	17.9	34.5

Three important conclusions can be drawn from the examination of the data in Table 7.5. The first and most obvious conclusion is that the conversion of 1,5-hexadiene, at typical ODHD of propylene conditions, is due to both heterogeneous and homogenous pathways and that both are of similar magnitude. This conclusion is a little disconcerting for the ODHD of propylene process in general because it means that a significant proportion of the 1,5-hexadiene produced may be converted by homogeneous means no matter how good the catalyst is. The second conclusion is that ethylene and propylene are likely produced exclusively by homogeneous reactions. The third conclusion, and perhaps the most pertinent, is that the reaction scheme to form the various products is complex. Carbon monoxide is not produced in the catalyst tests and hence the CO formed homogeneously must be oxidized by the  $\text{Bi}_2\text{O}_3$  to  $\text{CO}_2$ , but some of the  $\text{CO}_2$  present in the catalyst test must be formed homogeneously. More ethylene and propylene are produced by the non-catalyst test than the catalyst test so some of each of these products must be converted to  $\text{CO}_2$  by  $\text{Bi}_2\text{O}_3$ . Small amounts of other components such as acrolein and 1-butene are also produced in the non-catalyst test and they too must be converted to  $\text{CO}_2$  by  $\text{Bi}_2\text{O}_3$ . Small amounts of benzene are produced homogeneously but they are only measurable at the highest temperatures. Nonetheless, it is clear that benzene is formed by a combination of heterogeneous and homogeneous routes.

A final interesting observation can be made by noting the results of the test done over quartz with no oxygen in the feed. There is little conversion of 1,5-hexadiene in this test except at the highest temperatures. At these temperatures very small amounts of propylene are produced along with carbonaceous deposits in the reactor. It can be concluded, then, that all the homogeneous pathways to gaseous carbon containing compounds rely on oxygen. This observation suggests free radical mechanisms for which oxygen serves as an initiator. The oxygen must also serve as a reactant for some of the reactions. The products of the homogeneous pathways in this case are very reminiscent of the products produced in the pores of the membrane reactor when oxygen and propylene react (as described in Chapter 6).

#### 7.1.4.4 Evaluation of Reaction Kinetics

Given the complexity of the reaction scheme, development of kinetic models from this limited data set will be difficult. The best approach is to produce crude models lumping together all possible pathways to the individual products. Unfortunately these models will not necessarily accurately represent reaction on the  $\text{Bi}_2\text{O}_3$  catalyst and may not even be applicable to a situation where large amounts of propylene are also present. The models should, however, provide some insight into some aspects of the reactions.

To derive kinetic models for the key components ( $\text{CO}_2$  and benzene) that are produced to some extent heterogeneously, some simplifying assumptions must be made so that the integral data may be used. The first assumption is that all ethylene and propylene are produced exclusively by homogeneous routes. Thus the design equation for “heterogeneous” reactions in the reactor is equation 7.8.

$$\frac{W}{F} = \int_0^x \frac{dx}{\left(-r_{15\text{HD to CO}_2} + -r_{15\text{HD to BZ}}\right)} \quad (7.8)$$

A very significant simplification of this equation could be made if both reactions are of the same order with respect to 1,5-hexadiene. As noted in the examination of Figure 7.4 (which is quite representative of all the data), to a first approximation all the reactions appear to be first order in 1,5-hexadiene. Using this assumption and the fact that oxygen conversion is small for all experiments so that the oxygen partial pressure can be considered as a constant throughout the length of the reactor, equation 7.8 can be re-written as follows.

$$\frac{W}{F} = \frac{1}{P_{1,5\text{HD}}^o \left(k_{\text{CO}_2} P_{\text{O}_2}^{n_1} + k_{\text{BZ}} P_{\text{O}_2}^{n_2}\right)} \int_0^x \frac{dx}{1-x} \quad (7.9)$$

The integral can be written analytically, so the final form of the equation is given by equation 7.10.

$$\frac{W}{F} = \frac{1}{P_{1,5HD}^0 (k_{CO_2} P_{O_2}^{n_1} + k_{BZ} P_{O_2}^{n_2})} \ln\left(\frac{1}{1-X}\right) \quad (7.10)$$

The logarithmic term is the correction factor to take into account the change in 1,5-hexadiene partial pressure across the length of the catalyst bed. This correction factor can be applied to the rate of 1,5-hexadiene conversion to each product and the information cast into the linearized Arrhenius form described by equation 7.3. The Arrhenius plots for formation of CO<sub>2</sub> and benzene are shown in Figures 7.6 and 7.7, respectively. Figure 7.7 does not include all the data to avoid overcrowding and illegibility.

The activation energies for the two reactions, as derived from the slopes of the lines on Figures 7.6 and 7.7 as well as for the runs not shown on Figure 7.7, are given in Table 7.6.

Table 7.6 - Measured Activation Energies for Formation of CO<sub>2</sub> and Benzene from 1,5-Hexadiene over Bi<sub>2</sub>O<sub>3</sub>

1,5-Hexadiene Feed Concentration (mol%)	Oxygen Feed Concentration (mol%)	Carbon Dioxide		Benzene	
		Activation Energy (kJ/mol)	r <sup>2</sup>	Activation Energy (kJ/mol)	r <sup>2</sup>
0.188	6	159	0.9911	139	0.9840
0.192	4	129	0.9901	146	0.9785
0.194	3	114	0.9920	98	0.9092
0.196	2	109	0.9975	153	0.9888
0.167	2	102	0.9933	131	0.9772
0.133	2	101	0.9920	124	0.9838
0.100	2	103	0.9889	151	0.9843

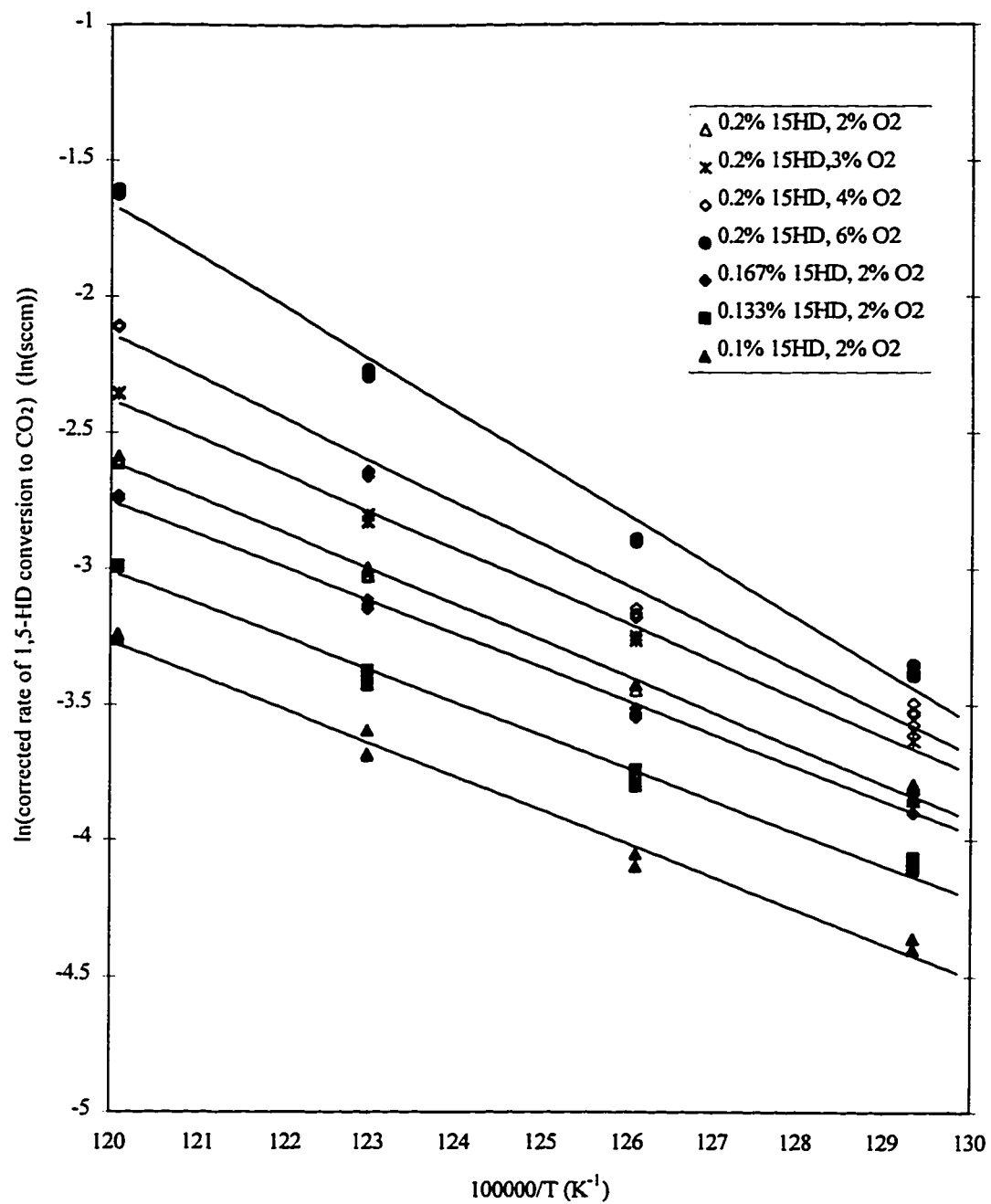


Figure 7.6 Arrhenius Plot for CO<sub>2</sub> Formation from 1,5-Hexadiene over Bi<sub>2</sub>O<sub>3</sub>

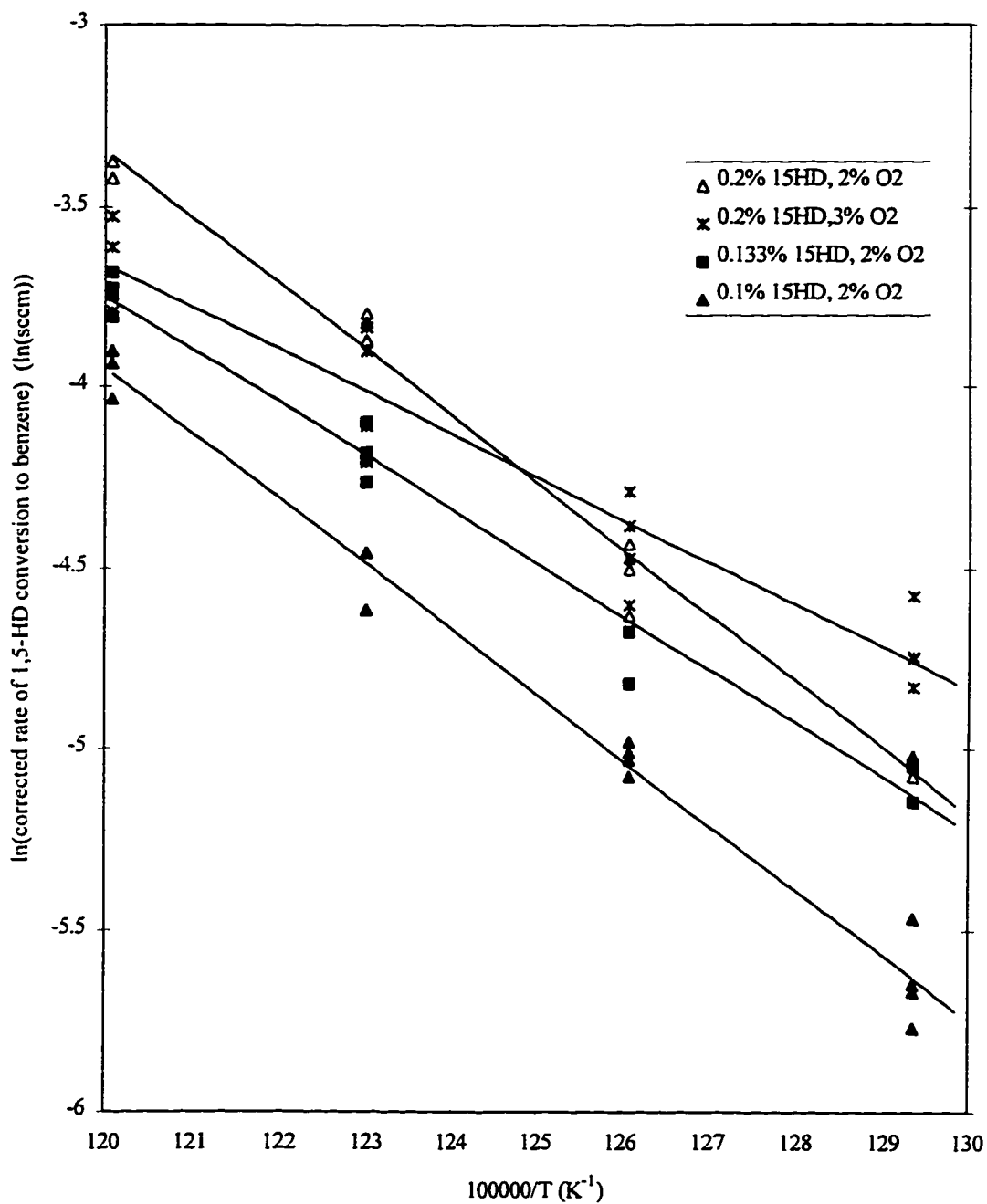


Figure 7.7 Arrhenius Plot for Benzene Formation from 1,5-Hexadiene over Bi<sub>2</sub>O<sub>3</sub>

The scatter in the data is greater for the 1,5-hexadiene data than it is for the propylene reactions (Figures 7.1 and 7.2). The greater scatter is also indicated by the somewhat lower correlation coefficients in Table 7.6 compared with those in Table 7.2. The

standard error for the activation energy estimate for the formation of  $\text{CO}_2$  is generally less than 3% and the standard error for the benzene case is generally less than 4%. The one exception in the benzene case is the shaded value in Table 7.6. The low value of the estimated activation energy and the relatively poor correlation of the data indicate that this value is an outlier.

The estimate of the activation energy for the formation of  $\text{CO}_2$  is consistent as long as the oxygen concentration does not change. However there is a real rise in activation energy as the oxygen concentration increases. The increase is likely due to the greater contribution to combustion reactions of the homogeneous routes as the oxygen content increases. The homogeneous reactions should have higher activation energies than heterogeneous routes and hence when more homogeneous reactions occur the “overall” activation energy will increase. An estimate of the homogeneous activation energy for the formation of  $\text{CO}_2$  can be derived from the non-catalyst test data of Table 7.5. A value of 186 kJ/mol is calculated and is consistent with the trend of the data in Table 7.6. That is, it is higher than any of the “heterogeneous” values. The fact that in all cases the apparent activation energy for 1,5-hexadiene combustion is in excess of the value found for propylene combustion (Section 7.1.3.2) supports the claim that 1,5-hexadiene combustion is more highly activated than propylene combustion and that 1,5-hexadiene combustion is more prevalent at higher temperatures.

The estimates of activation energy in the formation of benzene, ignoring the one outlier, are centred around 140 kJ/mol. All the values fall within the 99% confidence region around this value. The activation energy does not appear to be affected by reactant partial pressures which is the result one would expect if the reaction is purely heterogeneous. The few non-catalyst tests have indicated that a homogeneous route to the formation of benzene does exist and does play a part in the conversion, but that it is not a large part. The activation energy calculations seem to support this observation.

The only literature data available for the activation energy of 1,5-hexadiene conversion comes from a very simple pulse test, in the absence of oxygen, conducted by White and



Hightower (1983). They found that the activation energy for the consumption of 1,5-hexadiene (no products or degree of conversion are given) to be 80 kJ/mol. Their value is considerably lower than that found in this research.

The corrected conversion data can also be used to generate estimates of the exponents in a power law model of a similar form to equation 7.4. In this case the functional form of the power law is given by equation 7.11 and the estimates of the exponents are shown in Table 7.7 for each of the two primary reactions.

$$f(P_{O_2}, P_{15HD}) = P_{15HD}^{n_1} P_{O_2}^{n_2} \quad (7.11)$$

Table 7.7 - Measured Power Law Exponents for Formation of CO<sub>2</sub> and Benzene from 1,5-Hexadiene and Oxygen over Bi<sub>2</sub>O<sub>3</sub>

Temperature (°C)	Carbon Dioxide		Benzene	
	n <sub>1</sub>	n <sub>2</sub>	n <sub>1</sub>	n <sub>2</sub>
500	1.06	0.41	0.95	0.15
520	0.97	0.51	0.83	0.12
540	0.95	0.69	0.98	-0.09
560	0.96	0.91	0.85	0.13

The correlations for CO<sub>2</sub> formation are reasonably good, although not as good as those for the formation from propylene (Table 7.3). The 1,5-hexadiene exponent is not statistically different from 1 for any temperature so it appears that the assumption of first order kinetics with respect to 1,5-hexadiene is valid. The oxygen exponent increases quite dramatically with temperature and this phenomenon is likely due to the increasing role that homogeneous reactions are playing at the higher temperature. The correlations for benzene formation data are not particularly good. The oxygen exponent correlations are particularly poor and none of the results are significantly different from zero. This finding could mean that the reaction is zeroth order with respect to oxygen or it could be that the complex interplay of temperature, oxygen concentration and the mix of heterogeneous and homogeneous reactions leads to this result. More investigation is

necessary before conclusive statements can be made. The 1,5-hexadiene exponents for benzene formation are not statistically different from 1, but the fact that they are all consistently less than 1 makes the assertion that the reaction is first order in 1,5-hexadiene difficult to make. Nonetheless, it is close enough to first order that the first order approximation used to generate the corrected data is still valid.

## 7.2 External Mass Transfer Limitations Evaluation

To carry out a proper comparison of the membrane reactor with a packed catalyst bed and a regular tubular flow reactor with a packed catalyst bed, it is important to ensure that there are no external mass transfer limitations. Mass transfer limitations could mask the effect that differences in bulk partial pressures of the reactants between the two reactors are intended to create. Thus, a formal experimental evaluation has been made to determine if such mass transfer limitations exist at the flow rates used in this research. It is a very simple test involving a change in overall flow rate while maintaining constant reactant feed partial pressures and a constant W/F. From equation 7.1 it is apparent that the criteria for concluding that there are no mass transfer limitations is that the relative conversion does not change with flow rate.

The tests have been conducted with total flow rate varying from 125-625 sccm using 10 mol% propylene in the feed and a W/F ratio of 0.01024 g/sccm (total flow). Two sets of tests have been run. One set uses 3.0 mol% oxygen in the feed and the other uses 6.0 mol% oxygen in the feed. A complete summary of the conversion data is located in Appendix C. Figure 7.8 is representative of all of the data and represents the condition most likely to indicate a mass transfer limitation (highest conversion of oxygen, the limiting reactant). None of the data indicate that an external mass transfer limitation exists.

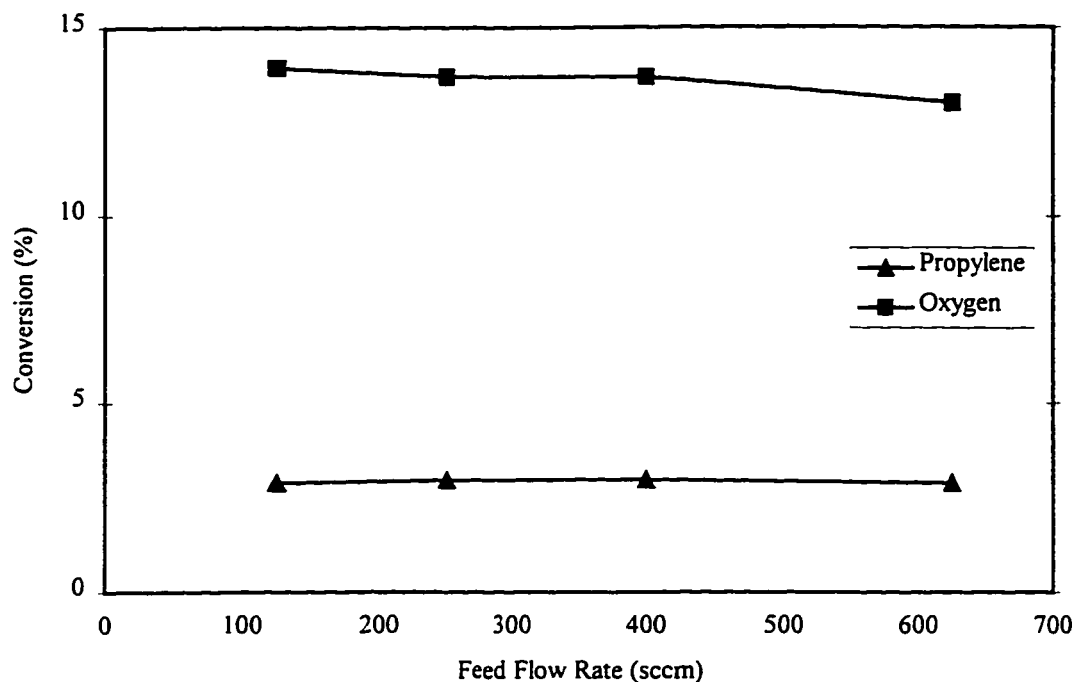


Figure 7.8 Variation in Conversion of Propylene and Oxygen over  $\text{Bi}_2\text{O}_3$  with Feed Flow Rate ( $W/F = 0.01024$ , 10 mol% Propylene and 3 mol% Oxygen in Feed)

### 7.3 Evaluation of the Stability of the Catalyst

The issue of the ability of the  $\text{Bi}_2\text{O}_3$  catalyst to maintain its activity during extended use has not been reported on elsewhere in the literature. Long term stability of the catalyst is important to this research because it means that the difficulties and possible experimental uncertainties involved with continually changing catalysts are substantially decreased. It is also important for any potential commercial application since rapid and/or continual loss of catalyst activity usually increases both capital and operating costs of a facility and generally makes steady operation of a plant more difficult.

To test for long-term stability, a fresh catalyst bed (1.28 g of  $\text{Bi}_2\text{O}_3$  and 1.52 g of quartz chips) was maintained in the quartz reactor at  $540^\circ\text{C}$  and was fed 125 sccm containing 10 mol% propylene and 3 mol% oxygen. The test duration was approximately 250 hours with reactor effluent sampled every 12 hours. The conversion of propylene and

selectivity to the two primary products, 1,5-hexadiene and  $\text{CO}_2$ , over the duration of the test are shown in Figure 7.9.

There is a noticeable variation in propylene conversion from day to night (the saw-tooth pattern) owing to small changes in laboratory ambient temperature and pressure affecting the flow meters and GC sampling loop pressure. It appears that there may have been a 50 hour induction period before the conversion and selectivities became constant, but in this experiment those changes were an artifact of the stainless steel screens in the reactor gaining some activity over the first 50 hours. That activity remained unchanged for the remainder of the run. The stainless steel screens were used only in this experiment to ensure that the catalyst bed remained tightly packed over the entire 10 day period. It is concluded from this experiment that the catalyst is indeed stable over an extended period of time. It must be noted that there was always sufficient oxygen available during this extended run to ensure that the  $\text{Bi}_2\text{O}_3$  remained fully oxidized. The issue of catalyst stability under conditions of substantial depletion of oxygen in the gas phase will be addressed in Section 7.4.3.

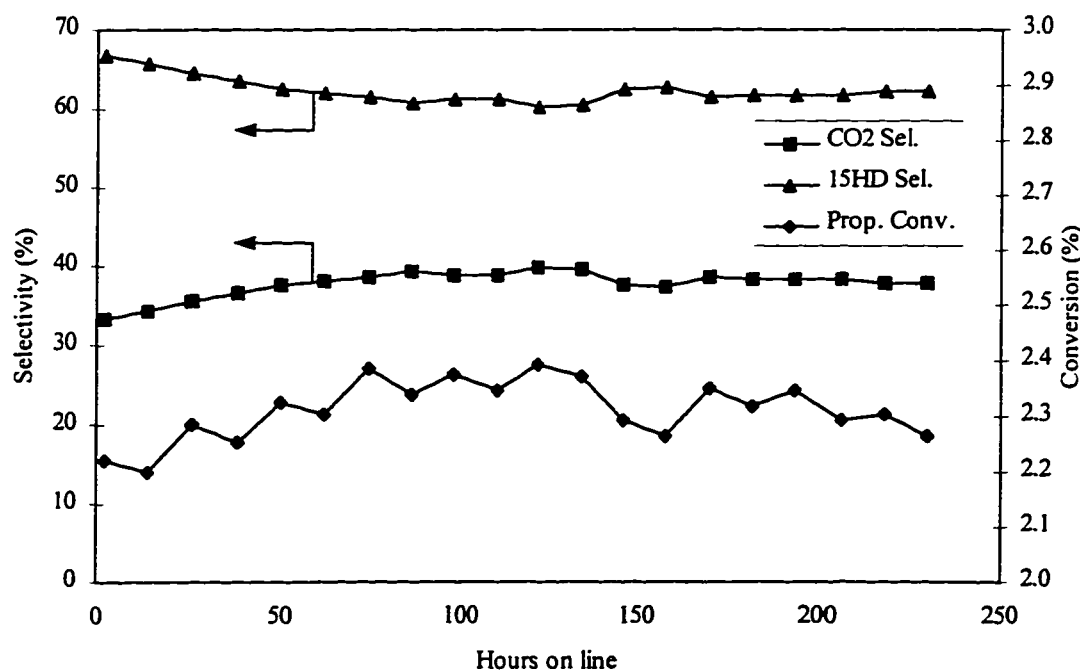


Figure 7.9 Propylene Conversion and Product Selectivities During Catalyst Stability Test (W/F = 0.01024, T=540°C, 10 mol% Propylene and 3 mol% Oxygen in Feed)

## 7.4 Membrane Reactor and Tubular Reactor Results

The comparison of the operation of the membrane reactor containing a packed bed of  $\text{Bi}_2\text{O}_3$  (termed the Inert Membrane Packed Bed Reactor (IMPBR) mode) with operation of the normal tubular reactor is the key test of the ability of the membrane reactor. The question of whether or not a distributed oxygen feed is beneficial for the ODHD reaction must be answered by this set of experiments. In addition to the direct comparison of the two types of reactors, this set of tests gives some insight into what “optimal” operating conditions for both types of reactors may be and whether the optimal conditions are the same for both types of reactor.

### 7.4.1 Description of the Experimental Regime

In the comparison of the operation of the two reactor types three sets of tests are required. Two of the sets, naturally, are runs using the membrane reactor and tubular reactor with a packed catalyst bed. The third set of tests involve re-evaluation of the reaction results in the blank membrane reactor because the activity of the membrane reactor continues to change slightly with time on stream. The reaction due to the membrane alone, when testing the membrane reactor with a packed catalyst bed, is significant. It is important to know exactly what the membrane activity is in order that the results ascribed to the catalyst can be calculated without gross error. The blank membrane activity was re-tested immediately following the completion of the tests of the membrane reactor with a catalyst bed. The partial pressure in the shell was carefully monitored in both the membrane reactor catalyst and blank tests to ensure that it was the same in both tests indicating that the permeability of the membrane (and presumably the activity) of the membrane is the same for both sets of tests. The change in membrane permeability is an ongoing, and as yet unsolved, problem with the VYCOR membrane. The operating parameters for the catalyst tests (membrane reactor and tubular reactor) are given in Table 7.8. The blank membrane reactor tests were conducted under the same conditions except that a packed bed of quartz particles was used in the place of the catalyst bed.

Table 7.8 - Operating Parameters for Membrane and Tubular Reactor Tests using  $\text{Bi}_2\text{O}_3$  Catalyst

Parameter	Parameter Value(s)
Total Flow Rate	125, 187.5, 250 sccm
Amount of $\text{Bi}_2\text{O}_3$	6.42 g
Amount of diluent quartz	7.6 g
Propylene Feed Concentration	10.0, 15.0, 20.0 mol%
Oxygen Feed Concentration	2.0, 3.0, 4.0, 6.0 mol%
Nominal Furnace Temperature	490, 510, 530, 550°C

The full 3 x 3 x 3 x 4 variable parameter study used in the original evaluation of the blank membrane reactor (Chapter 6) was not used here. The advantage in using a membrane reactor is that the oxygen feed is distributed. Situations where there will be a tremendous excess or complete consumption of oxygen in the membrane reactor tests represent unfavourable operating conditions and have not been evaluated. That is, some of the higher temperatures for a given set of feed conditions have not been evaluated because they would result in complete consumption of oxygen. Also some feed conditions have not been evaluated if tests with less oxygen in the feed (all other conditions the same) result in oxygen conversion of less than 70% at the highest temperature. Adding more oxygen would not help the membrane reactor performance and so those situations have not been tested.

#### 7.4.2 Issues Surrounding IMPBR Data

Before the results are presented three issues must be addressed. The first issue is whether oxygen is being radially well distributed in the reactor. That is, is there an oxygen mass transfer problem between the membrane wall and the middle (radially) of the catalyst bed resulting in significant radial oxygen gradients? Diffusion of oxygen at higher concentration at the tube side surface of the membrane into the bulk gas phase flowing in the tube is controlled by normal gaseous diffusion. The diffusivity of oxygen into the bulk gas can be estimated by assuming that the bulk gas will be 80% helium (balance propylene) on an oxygen-free basis. Binary diffusion coefficients can be calculated using the Wilke-Lee modification of the Hirschfelder-Bird-Spotz method (Treybal (1980)) at

reaction temperature and pressure. The effective diffusivity for oxygen into the mixture is found by equation 7.12

$$\frac{1}{D_{A,m}} = \sum_i \frac{y_i}{D_{A,i}} \quad (7.12)$$

The  $D_{A,m}$  value at 800 K and 105 kPa is 2.2 cm<sup>2</sup>/s. A theoretical analysis of the radial and axial concentration gradients in an empty (non-packed) reactor is possible by knowing the axial flow velocity, by treating the radially entering oxygen as a constant flux with assumed concentration at the inner membrane surface and by ignoring reaction. These assumptions simplify the analysis to a great extent but do not mirror reality that well. The normal operating situation, of course, has the tube packed with catalyst and analysis of this situation is much more difficult due to the mixing effect of the bed. Thus the analysis will not be exact and will only provide an indication of whether radial gradients exist.

For the purposes of estimating whether significant radial gradients will exist an analogy to transient heat conduction in an infinite rod can be drawn. The axial flow will be treated as plug flow, which is not a good assumption since  $Re \approx 1.5-5$ . Oxygen will be assumed to be constantly available at the wall (analogous to no external heat transfer limitation). If the oxygen partial pressure at the wall is 6 kPa and the steady state, uniform partial pressure in the tube is desired to be 3 kPa, the Heisler chart for a rod of infinite length can be used to determine that the time to reach uniform concentration at the middle of the tube (radially) is in the order of 0.05 s. With the superficial axial velocity in the tube being 3.5-7.0 cm/s this would indicate a “mixing length” of approximately 3.5 mm which is about 6% of the total length of the membrane. Based on this simplified analysis it appears that diffusion of oxygen into the bulk is rapid and that radial oxygen gradients in the bulk will not be severe.

The second issue is how to separate the reaction due to the catalyst and reaction due to the membrane in the membrane reactor tests. As detailed in Chapter 6 it is assumed that

all reaction caused by the membrane occurs in the membrane and hence that quantity of product can be subtracted from the total product stream to yield the products of the catalytic reaction. For all the cases tested there was less CO product in the membrane reactor test with catalyst than there was in the blank membrane reactor test. This result means that some of the CO is being oxidized to CO<sub>2</sub> on the catalyst and to properly account for propylene reaction on the catalyst the total CO<sub>x</sub> yield of the membrane reactor alone must be subtracted from the CO<sub>x</sub> production of the membrane reactor with catalysis. The balance is the CO<sub>2</sub> produced from propylene (or other hydrocarbon products) on the catalyst or from reaction of one of the products, most likely 1,5-hexadiene, with oxygen in the membrane pores. The contribution due to the latter route should not be large, and since it is difficult to accurately calculate, it is simply lumped in as part of the production on the catalyst. All other components produced on the membrane alone have their "membrane production" subtracted from the total production to provide the results for the catalyst alone.

The third issue involves the difference in the mid-bed temperature measured for the membrane reactor with catalyst tests and the blank membrane reactor tests. The former is always higher due to the additional exothermic reactions occurring in the catalyst bed. The issue is what conditions prevail in the membrane during the catalyst tests. It seems likely that the membrane temperature in the catalyst tests would be higher than that occurring in the blank tests. It could be higher by as much as the measured difference in the mid-bed temperature between the two situations, but without some method of actually measuring the membrane temperature the value is highly speculative. Perhaps the relevant question is, does the potential 1-4°C temperature difference make any difference in the measured product selectivities for the catalytic reactions? The selectivity to the various products can be calculated by assuming that the membrane temperature has risen by the equivalent of the difference between the measured mid-bed temperatures and correcting the activity of the membrane alone. This procedure increases the selectivity to 1,5-hexadiene by 1-4% depending upon the case considered. Figure 7.10 shows the corrected and uncorrected 1,5-hexadiene selectivities for the two extreme cases (largest and smallest measured differences in mid-bed temperatures). The mid-bed temperature



referred to on this figure and all subsequent figures is the catalyst bed temperature. For the largest temperature difference case (as depicted in Figure 7.10) the increase in selectivity is not insignificant, however, there is no way to confirm that the membrane temperature actually rises by the full difference in the measured bed temperatures. As a result a conservative approach has been adopted and all further results are presented with no temperature correction to ensure that the results are not overstated.

The conversion of propylene during the catalyst tests of the membrane reactor was due to both catalyst and membrane. Much effort has been spent characterizing the membrane activity because it must be accurately accounted for to determine the catalyst behaviour. This is true only because the activity of the membrane is high relative to the activity of the catalyst. Figure 7.11 shows the portion of total propylene conversion in the membrane reactor tests with catalyst that is due to the membrane. The two cases presented represent the extremes in the range of all the tests. It is very clear that the fraction of the conversion due to the membrane decreases as the temperature increases and does so in a linear fashion. The conversion due to the catalyst increases much more rapidly with temperature than does the conversion due to the membrane. The reason for this phenomenon is that the membrane reaction is largely limited by Knudsen diffusion whereas the catalytic reactions increase with temperature as their Arrhenius-law forms dictate. However, even at the highest temperatures the contribution of the membrane conversion is in excess of 40%. These data serve to reinforce the notion that for both laboratory and potential commercial applications of this sort of membrane reactor technology, efforts to stabilize and reduce the activity of the membrane are of vital importance.

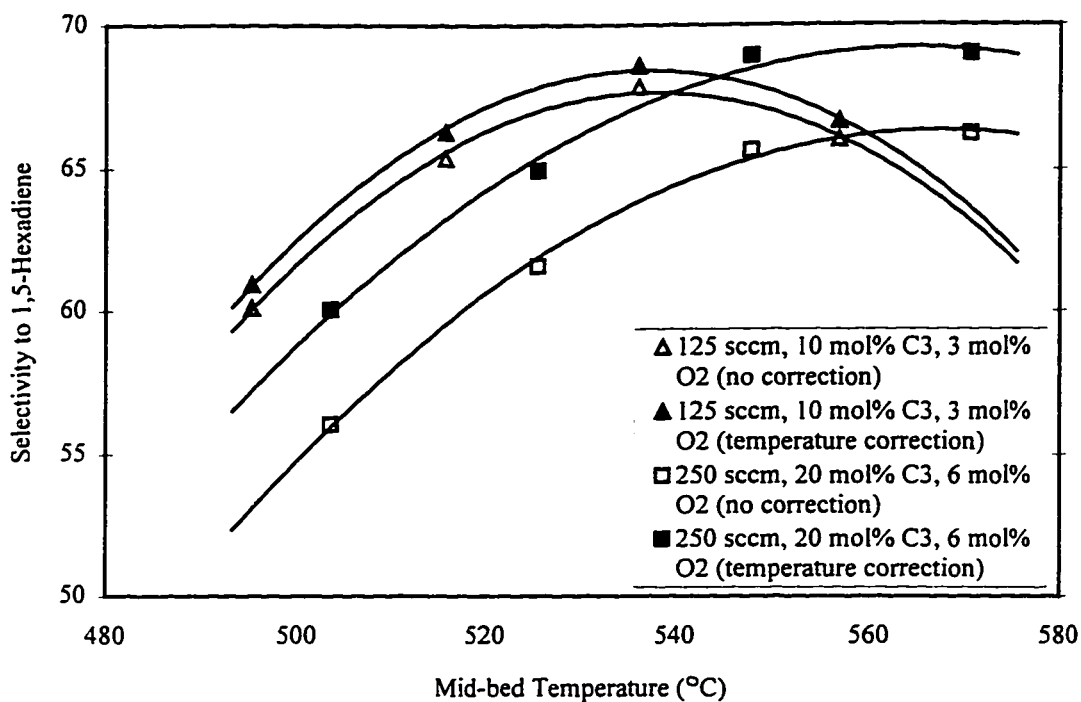


Figure 7.10 Effect of Membrane Temperature Correction on 1,5-Hexadiene Selectivity

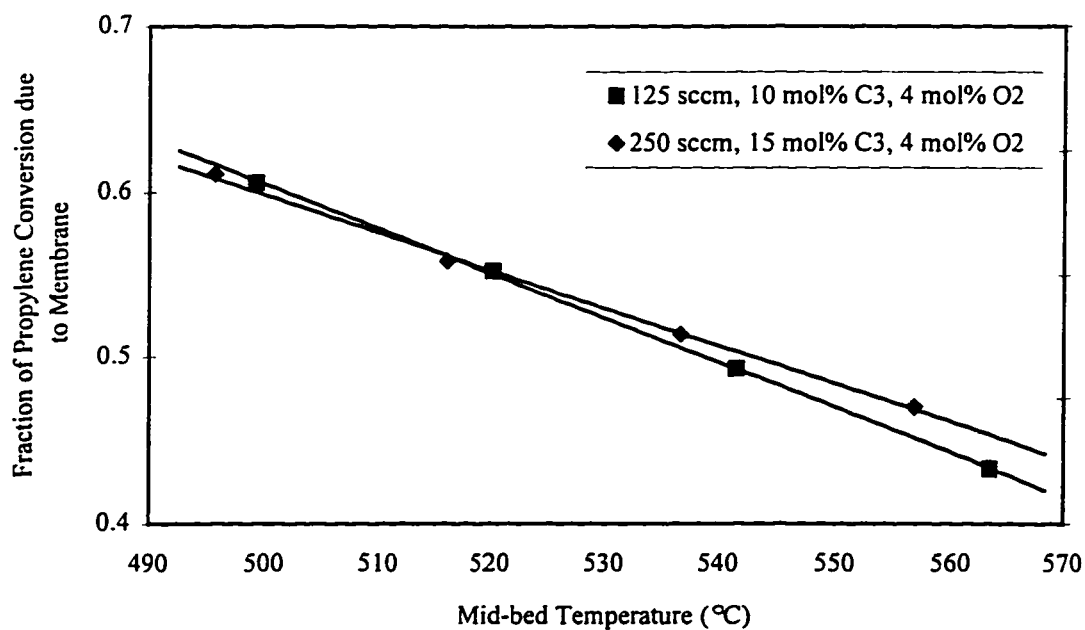


Figure 7.11 Fraction of Propylene Conversion due to Membrane Reactions during Membrane Reactor with Catalyst Tests

### 7.4.3 Comparison of IMPBR and Tubular Reactor Operation

A complete summary of all data is included in Appendix C. Each table gives conversion and selectivity data for each of the three tests (membrane reactor with catalyst, blank membrane reactor and tubular reactor) carried out for each case. The information presented in the body of the thesis is a small but representative subset of the whole data set. It is meant to convey an understanding of how the two reactor configurations function with respect to one another and how the various operating parameters affect their respective performance without overloading the reader with data.

The variables selected for measuring performance of the reactors are the selectivity of propylene conversion to 1,5-hexadiene, selectivity to total C<sub>6</sub> products and selectivity to carbon dioxide. The reason for this selection is twofold. The first reason is that the selectivity will best show the differences between the two configurations. The lower overall oxygen concentration in the membrane reactor should decrease CO<sub>2</sub> production while having little effect on 1,5-hexadiene production. The result should be a higher selectivity to 1,5-hexadiene. The second reason is that the catalyst charge used for the membrane tests and that used for the tubular reactor tests came from different batches from the catalyst supplier. The two samples, unfortunately, have somewhat different activity levels with the material used in the tubular reactor tests having higher activity. As a result of this difference, comparison of product yields cannot be made on a completely consistent basis.

The other effect of the difference in catalyst activity is that more C<sub>6</sub> products are produced in the tubular reactor tests than in the membrane reactor tests. The argument made earlier in this chapter is that oxidation of C<sub>6</sub> products, particularly 1,5-hexadiene, contributes significantly to the formation of CO<sub>2</sub>. Higher concentration of the C<sub>6</sub> material in the tubular reactor cases will likely lead to a higher rate of oxidation of these materials, but to what degree is not precisely known. The 1,5-hexadiene selectivity values garnered from the kinetic tests (discussed earlier in this chapter) indicate 1,5-hexadiene selectivity (which is also the total C<sub>6</sub> selectivity for these tests) of ~68% at the highest temperatures

and ~62% at the lowest temperatures in most cases. The 1,5-hexadiene concentrations in the kinetic tests are significantly lower than in the membrane reactor and tubular reactor tests, and commensurately, the selectivity to 1,5-hexadiene is noticeably higher. The differences between the 1,5-hexadiene concentrations in the membrane reactor and tubular reactor cases are not so large and thus the effect on selectivity should not be large. Comparison of the tubular reactor results to the kinetic test results adds weight to the argument that the over-oxidation of C<sub>6</sub> material is important for situations involving significant conversion of propylene. These situations would be prevalent in commercial applications involving ODHD of propylene and represent one of the significant challenges in this and many other oxidative dehydrogenation and coupling reactions. That challenge is how to operate a reactor system effectively when a product is more prone to oxidation than the reactant hydrocarbon. None of the previous literature on ODHD of propylene clearly addresses this problem of degradation of the products as the product concentration increases.

It must be noted from the outset that none of the reactor situations investigated were studied under completely isothermal conditions. The use of a single zone resistance furnace and a catalyst bed that is approximately 50 mm in length inevitably results in some temperature non-uniformity across the bed. Figure 7.12 shows some typical temperature profiles in the bed for the two reactor configurations and the blank membrane reactor. The temperature differences are not great but isothermal conditions do not exist. The saving grace is that the temperature profiles are fairly uniform from case to case and are predictable. In all the membrane reactor tests the temperature at the ends of the bed are the same as the nominal oven temperature  $\pm 1^\circ\text{C}$  while for the tubular reactor tests the temperatures at the edges of the bed are  $10^\circ\text{C}$  greater than the nominal oven temperature ( $\pm 1^\circ\text{C}$ ). All the mid-bed temperatures are reported in Appendix C.

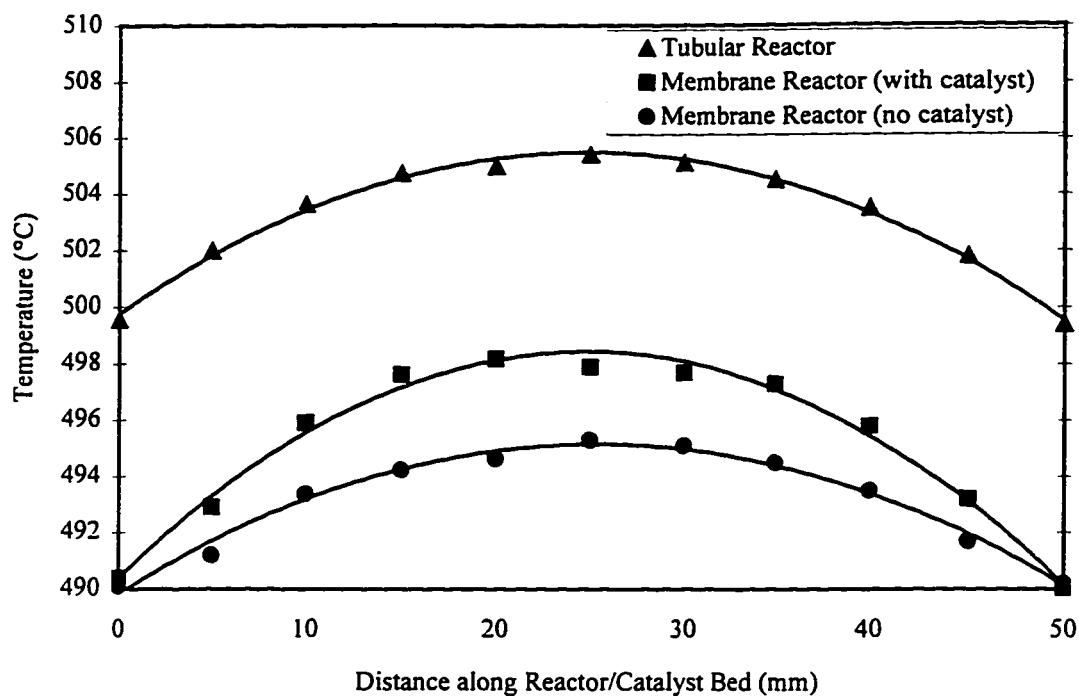


Figure 7.12 Catalyst Bed Temperature Profiles (250 sccm Total Flow, 15 mol% Propylene and 3 mol% Oxygen in Feed, 490°C Nominal Furnace Temperature)

There is no presentation, in this chapter, of the results of the combined effect of the membrane reactor and the catalyst bed. Even though this information represents the actual operating result of the membrane reactor, it is not included except as raw data in the appendix. It has been conceded that the membrane activity must be reduced before the membrane reactor could be used in any commercially practical situation, so evaluation of the two effects together, at this point, is not worthwhile. In general the combination performed better at conditions which increased the reaction on the catalyst (high selectivity to  $C_6$ 's) to a greater extent than the reaction in the membrane (very low selectivity to  $C_6$ 's). In most cases, in reference to Figure 7.11, temperature has the greatest effect and high  $C_6$  selectivity occurred at the highest operating temperature. A higher overall flow rates also increased the selectivity to 1,5-hexadiene, but to a much smaller extent than temperature.

The two reactor configurations, membrane reactor and tubular reactor, have been evaluated with respect to the four operating parameters, temperature, propylene feed concentration, oxygen feed concentration and overall flow rate, and are compared to one another. The information presented for the membrane reactor is the effect of the catalyst alone in all cases. The values for selectivity to the products of the catalyst alone in the membrane reactor are derived from the data in Appendix C. Selectivity and conversion data are used to calculate the actual yield (moles) of each product for both membrane reactor without catalyst and membrane reactor with catalyst. The former is subtracted from the latter to give the product yields due to the catalyst alone. The yield data is then used to calculate selectivity to the products. As noted in section 7.4.2 CO is converted to CO<sub>2</sub> on the catalyst, but the catalyst itself forms no appreciable amounts of CO during ODHD of propylene. Thus, the production of CO<sub>2</sub> from propylene or ODHD of propylene products by the catalyst must be calculated as the difference between the CO<sub>x</sub> yield in the membrane reactor with catalyst and the CO<sub>x</sub> yield in the membrane reactor alone.

A study of the kinetic expressions for the key reactions indicates that temperature and oxygen concentration are likely to have the greatest effect on the selectivity to C<sub>6</sub> products for both reactor configurations and that the lower overall oxygen concentration in the membrane reactor configuration than in the tubular reactor configuration should result in higher C<sub>6</sub> selectivity than does the tubular reactor. The effect on selectivity of the operating parameters is presented using representative data on the figures that follow. Figure 7.13 shows the effect of temperature.

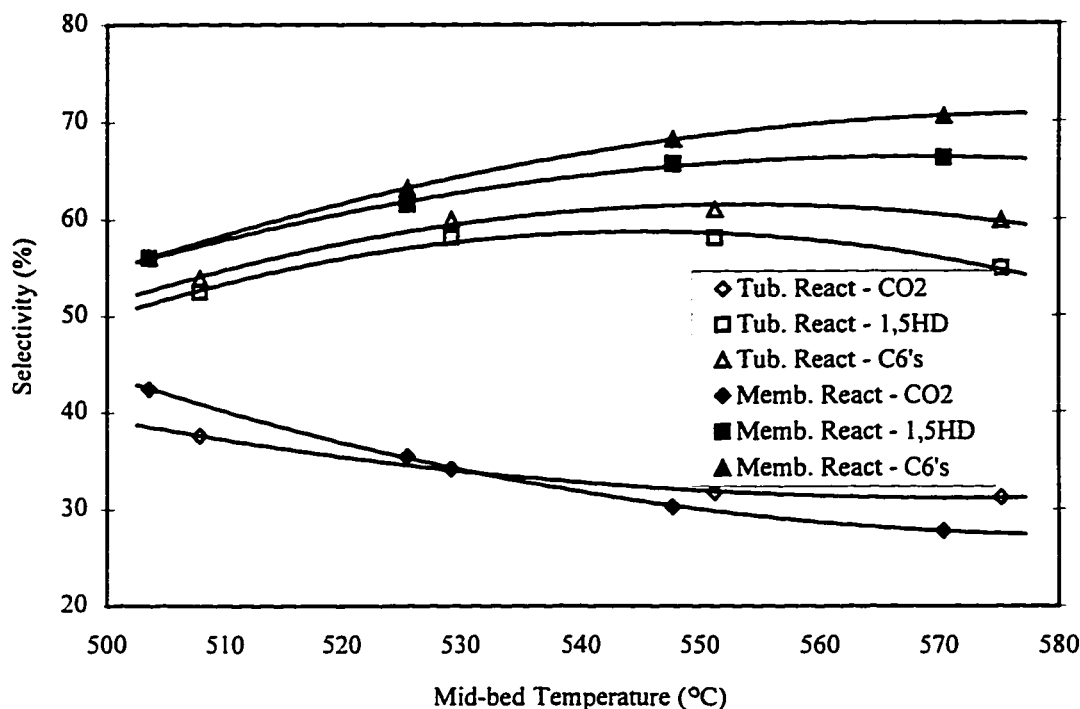


Figure 7.13 Product Selectivity for Membrane and Tubular Reactor Configurations as a Function of Temperature (250 sccm Total Flow, 20 mol% Propylene and 6 mol% Oxygen in Feed)

The selectivity to 1,5-hexadiene does rise with increasing temperature for both configurations but is maximized for the tubular reactor around 540°C. The selectivity to total C<sub>6</sub> products reaches a maximum in the tubular reactor at approximately 550°C. The membrane reactor, on the other hand, does not reach a maximum for either of these selectivity values within the range of temperatures tested, but it does look like a maximum will occur for both values around 580-590°C. The maximum will be very broad. It should also be noted that the membrane reactor outperforms the tubular reactor in terms of selectivity to desired products and the gap between the two widens as the temperature increases.

The effect of oxygen feed concentration (or flow rate) on product selectivity is shown in Figure 7.14. The selectivity to the desired products is highest at the lowest oxygen concentration which is exactly as one would have expected. Again the membrane reactor

outperforms the tubular reactor and the difference is most notable at the lowest oxygen concentration. At the higher oxygen concentrations (feed rates) there is significantly more oxygen flowing into the bed in the membrane reactor than is necessary for reaction so the membrane reactor, in these cases, begins to behave much like a regular tubular reactor with a consistently high oxygen concentration. Hence there is less difference in performance between the two configurations at the higher oxygen concentrations.

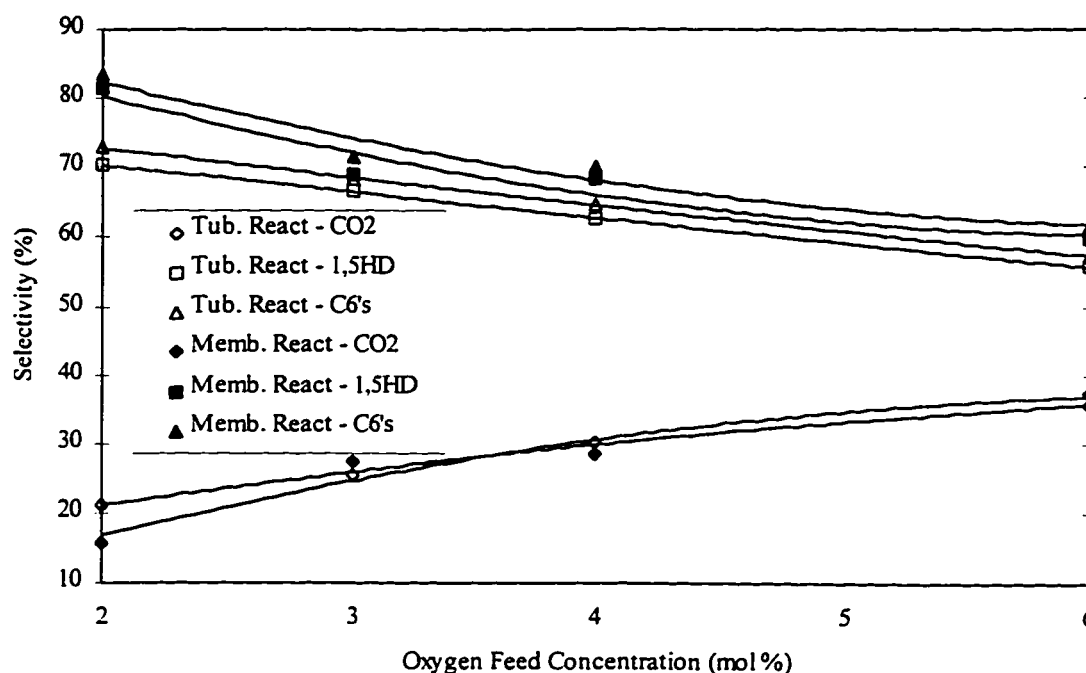


Figure 7.14 Product Selectivity for Membrane and Tubular Reactor Configurations as a Function of Oxygen Feed Concentration (250 sccm Total Flow, 20 mol% Propylene in Feed, Mid-bed Temperature is 520°C)

The effect of propylene feed concentration to the reactor is shown in Figure 7.15. The membrane reactor selectivity to the desired products is approximately 7% (absolute) higher than the tubular reactor, but the effect of the propylene concentration is relatively minor. Selectivity to 1,5-hexadiene increases only marginally with increasing propylene concentration for both configurations. The increase is less than would be expected from calculations using the kinetic expressions for propylene conversion to 1,5-hexadiene and CO<sub>2</sub> derived in Section 7.1.3.3. This discrepancy may be partially due to a greater degree



of over oxidation of the C<sub>6</sub> products when the C<sub>6</sub> product concentrations are highest (at the greatest propylene concentration).

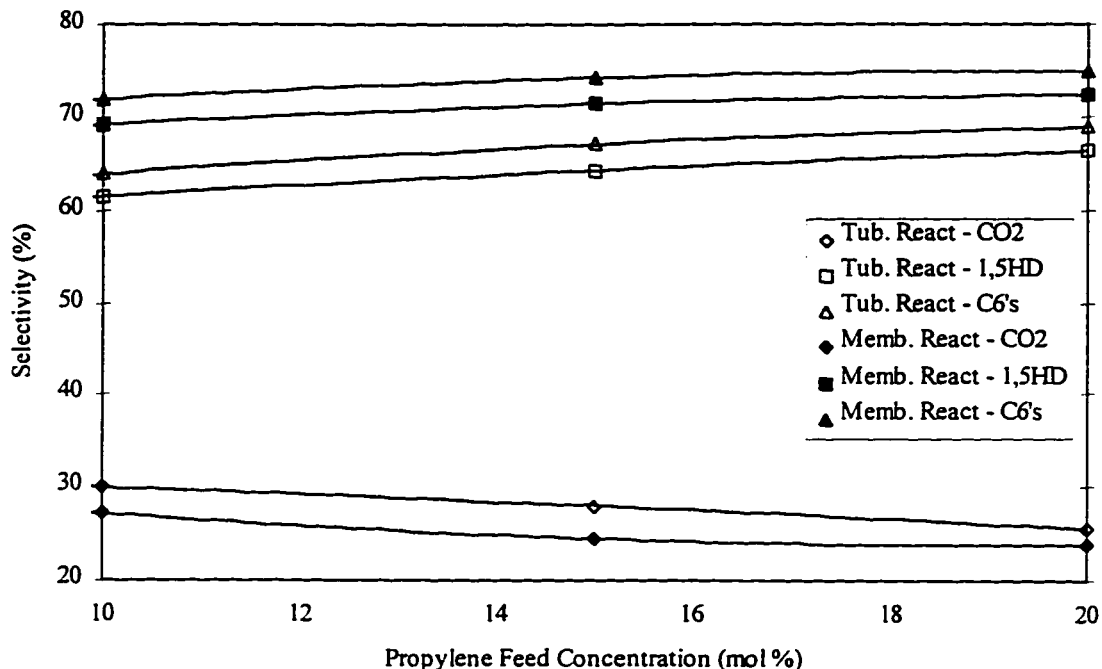


Figure 7.15 Product Selectivity for Membrane and Tubular Reactor Configurations as a Function of Propylene Feed Concentration (187.5 sccm Total Flow, 3 mol% in Oxygen Feed, Mid-bed Temperature is 520°C)

An example of how selectivity varies with respect to total flow rate is shown in Figure 7.16. The trends depicted in this figure indicate that the effect of flow rate is not large. The changing flow rate is really a variation of the W/F ratio, and the change in W/F will result in there being different conversion levels for each different flow rate. Different fractional conversion levels will result, potentially, in very different average oxygen and C<sub>6</sub> product concentrations in the catalyst bed for the different flow rates. In fact the change in these average concentrations as a function of flow can vary from case to case depending on the feed conditions and operating temperature. In general, however, the higher flow rates (lower W/F) increase selectivity to the desired products for the tubular reactor, while the opposite is true for the membrane reactor. For the tubular reactor, the lower 1,5-hexadiene concentration at the higher flow rates is serving to lessen the effect of C<sub>6</sub> oxidation and hence the selectivity to the C<sub>6</sub> products rises. It is the higher overall

oxygen concentration at the higher flow rates which is having a greater effect on the behaviour of the membrane reactor. The higher  $O_2$  concentration is promoting combustion reactions and the result is a loss in  $C_6$  selectivity. A much less complicated conclusion that can be drawn from Figure 7.16 is the same one as can be drawn from the previous three figures. The membrane reactor configuration consistently produces a higher selectivity to the desired  $C_6$  products than does the tubular reactor.

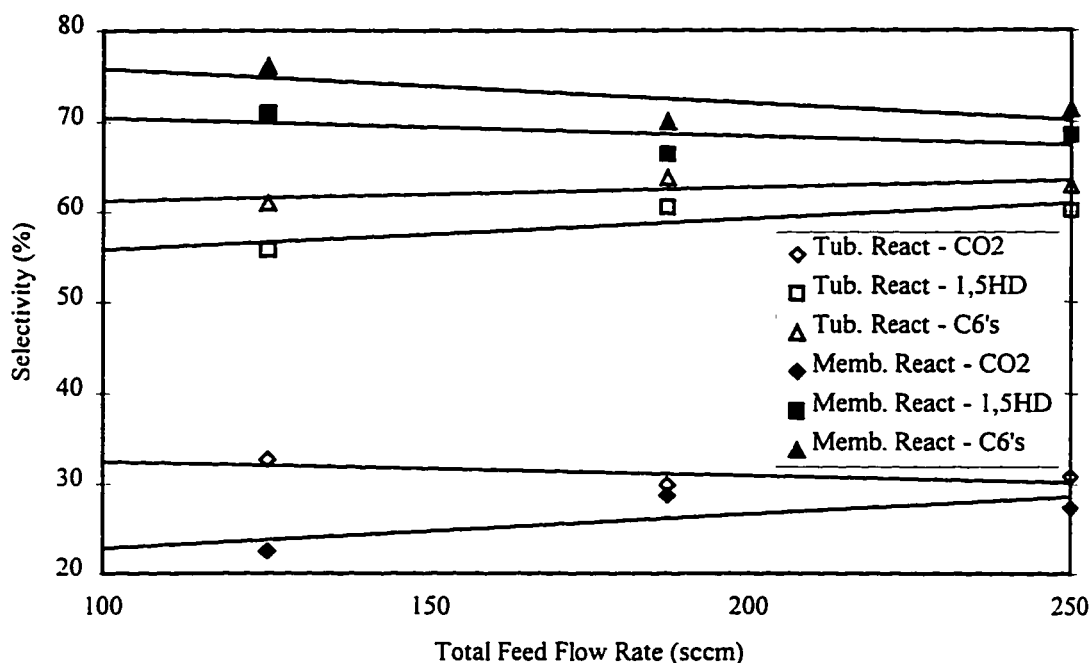


Figure 7.16 Product Selectivity for Membrane and Tubular Reactor Configurations as a Function of Total Feed Flow Rate (15 mol% Propylene and 4 mol% in Oxygen Feed, Mid-bed Temperature is 540°C)

The evaluation of the two reactor configurations leads to some general comments about the relative performance of each and about what conditions are necessary to optimize the selectivity to the desired  $C_6$  products. It is clear that the membrane reactor configuration consistently gives higher selectivity to the desired products than the regular tubular reactor. Although there are some small uncertainties in the absolute values of the improvements due to the temperature correction, difference in catalyst activity and reaction of  $C_6$  product in the membrane (as discussed earlier in this section), there is little doubt that the membrane reactor configuration is beneficial for production of 1,5-hexadiene and benzene in the ODHD of propylene when compared to a standard tubular

flow reactor configuration. Improvements of 6-12% (absolute or 10-20% relative) in the selectivity to 1,5-hexadiene are achieved by using the membrane reactor. Admittedly there needs to be more development work on the membrane reactor itself. However, the results provide proof of concept for the idea that limiting the oxygen concentration in the reactor will help promote selectivity to 1,5-hexadiene by reducing oxidation of propylene and the hydrocarbon products to CO<sub>2</sub> and that this effect can be achieved using a porous membrane reactor.

The conditions that will produce the maximum selectivity to 1,5-hexadiene in the membrane reactor are a combination of the highest possible propylene feed concentration, an operating temperature of approximately 580°C and an oxygen feed rate set so that there is little or no excess oxygen in the reactor effluent. If all the oxygen is consumed as it is added, then the effective concentration of oxygen throughout the whole catalyst bed is nearly zero. The conditions that maximize 1,5-hexadiene selectivity in the tubular reactor are similar but have some subtle but important differences. The propylene concentration should be as high as possible, but the operating temperature should be approximately 540°C to prevent excessive over-oxidation of the product to CO<sub>2</sub>. The oxygen feed concentration should be set to ensure that there is little or no excess O<sub>2</sub> in the reactor effluent, but in this case it will not result in a nearly zero O<sub>2</sub> concentration throughout the catalyst bed. In both cases low conversion of propylene (low C<sub>6</sub> concentration in the catalyst bed) will help increase 1,5-hexadiene selectivity, but in practical situations this would lead to very low product yield and necessitate a very high degree of recycle in the system. The operating cost of a plant with such a significant recycle would be very high and difficult to justify economically.

Although proof of the concept has been established, more comprehensive work to further investigate the parameters and to better understand some of the intricacies of the membrane reactor operation may be justified. A better understanding of the diffusion process for the distributed component, oxygen in this case, into the catalyst bed would indicate whether there are mass transfer limitations within the bed. This understanding, in turn, may shed light on one other phenomenon that has been noted. When the bismuth

oxide catalyst is operated at conditions of low oxygen concentration and high temperature for extended periods of time there is a permanent decrease in activity of the catalyst. The situations involving the membrane reactor when this occurs are those which result in very high conversion of the feed oxygen (low flow rate and high propylene concentration). This effect had been anticipated so the tests that might damage the catalyst were carried out last. Swift et al. (1971) has noted a similar loss in catalyst activity under periodic operating conditions. The reduction in activity could be a serious problem in any practical application because the best operating conditions dictate that a nearly zero oxygen level in the catalyst bed be maintained.

### **7.5 Supporting $\text{Bi}_2\text{O}_3$ in the Pores of the VYCOR Membrane Reactor**

A membrane reactor with catalytically active walls is a commonly envisioned mode of operation called a catalytic membrane reactor (CMR). The VYCOR itself is clearly not a good catalyst for the ODHD of propylene, but if a good catalyst can be supported in the pores, interesting results may be achieved. There are three specific advantages to this type of catalyst configuration. The first advantage is that one can achieve a much higher active area to catalyst mass ratio than can be achieved using bulk catalysts. This design is of particular advantage when very high surface area is desired or when the catalyst is very expensive (platinum/palladium). Although neither instance is true in this study, the highly dispersed catalyst in the membrane pores would be much less likely to experience the reduction and subsequent loss in activity suffered by the bulk catalyst. The second advantage is that all of the reaction will ideally occur on the catalyst. Ideally the catalyst will be supported in a thin band within the membrane and on the inner wall of the membrane. If reactant flows are set such that the desired reaction can go virtually to completion within this reaction region, the amount of homogeneous mixing of reactants and products and potential undesired side reaction (combustion) can be, ideally, limited. The third advantage is that the membrane will act as an effective heat sink (by conduction) and should help ensure isothermal operation. The primary drawback of this configuration for ODHD of propylene is that much of the reaction will occur in the pores of the membrane. The reaction will be mass transfer limited (propylene flow into the

membrane) and the tremendous VYCOR surface area may adversely affect results by promoting the combustion of products. Drawbacks aside, the concept merits investigation.

#### 7.5.1 Preparation of the Membrane with Supported Catalyst

The preparation of the bismuth oxide catalyst supported on the VYCOR membrane provides a number of challenges. Preliminary testing conducted during the reactor design and construction phase of the project indicated that the catalyst would have to be added to the membrane after the VYCOR to quartz connections are made. The oxide catalysts caused the VYCOR membrane to foam (literally) in the locations exposed to the temperature necessary to collapse the VYCOR membrane around the quartz sleeve. It has proven to be impossible to bond the VYCOR to quartz if the VYCOR is contaminated by the catalyst. This constraint is not difficult to overcome, but it does limit the ways in which catalyst can be added to the membrane and makes the addition more physically cumbersome.

In addition to the construction constraint, three other factors have to be considered when developing the catalyst addition method.

1. Distribution of the catalyst should be even across the wall area of the membrane in the reaction zone.
2. Catalyst should be kept at, or as near as possible, to the inner surface of the membrane.
3. The method of addition should have no deleterious effect on the membrane performance.

A precipitation method of catalyst deposition is not readily applicable in this situation. Thus, an impregnation method is required. For any impregnation method a suitable solvent for the catalyst or catalyst pre-cursor is required and an appropriate method for application of the solution to the membrane is also required. Two application methods

have been considered. The first method is drop-wise addition of the solution from a micropipet to the inner surface of the membrane. This method is easy to employ but may not provide uniform catalyst distribution and may not minimize the extent to which the catalyst will travel into the membrane structure. The degree to which these problems will manifest themselves depends upon the solvent used. The second method is an incipient wetness method in which the solution is uniformly sprayed onto a warm/hot membrane inner surface causing the solvent to rapidly evaporate. This method is more difficult to use because of the need for an effective spraying device which can be used within the physical confines of the reactor. However, it should be very effective in producing a uniform catalyst distribution and in producing an egg-shell type of supported catalyst where the catalyst is supported at or very near the surface of the membrane. Given the difficulty in finding an appropriate spraying device, the latter method was to be considered only if the drop-wise addition method failed. Champagnie et al. (1992) considers the problem of catalyst addition to the membrane from a solution but does not draw any conclusions as to which of these two methods is better.

Bismuth oxide is insoluble except in strong acids. There is some concern that the use of an acid as the solvent may re-introduce some of the acidic characteristics to the membrane. Preliminary tests of glacial acetic acid treated VYCOR membrane material indicated that the acid may have had some effect, but the tests were not conclusive. Nonetheless, for safety reasons, the use of a strong acid is not desirable. To avoid this problem altogether, bismuth nitrate pentahydrate ( $\text{Bi}(\text{NO}_3)_3 \cdot 5\text{H}_2\text{O}$ ), which is soluble in solvents other than strong acids, was selected as a catalyst precursor. The nitrate is supposed to be soluble in organic solvents such as acetone and glycerol. Using acetone as a solvent has been investigated, but problems were encountered due to residual water in the acetone. The small amount of water remaining in the acetone reacts with the nitrate to form the hydroxide,  $\text{Bi}(\text{OH})_3$ , which is completely insoluble.

Glycerol, however, is an excellent solvent for a number of reasons and preparation of a supported catalyst with 6.3 mg of  $\text{Bi}(\text{NO}_3)_3 \cdot 5\text{H}_2\text{O}$  in approximately 0.75 mL of glycerol was undertaken. Bismuth nitrate readily dissolved in this minimum amount of warm

glycerol and the warm glycerol was easily added to the membrane in a drop-wise fashion. The glycerol was not noticeably drawn into the pores at all as it was added to the membrane surface. Rotating the reactor allowed the solution to coat the entire inner membrane surface (otherwise some material would pool at the lower surface). The method to complete the catalyst precursor application was to gently heat the reactor to approximately 150-200°C, under constant rotation, and purge inert gas through the tube. The glycerol became much less viscous at these conditions and flowed freely on the membrane surface. Under the heat and purge conditions the glycerol evaporated/decomposed and was drawn into the pores to some degree. When all the glycerol had left the surface there was a visually uniform catalyst layer left on the membrane. It is difficult to determine the depth of penetration of the catalyst within the membrane without using a cross section of the membrane which involves breaking the membrane. One approximate method is to observe a cross section of the membrane using scanning electron microscopy (SEM) and use energy dispersive x-ray analysis (EDX) to identify the concentration of bismuth in various parts of the cross section. This method relies on the ability to produce a relatively smooth surface to observe. Any attempt to polish the surface would likely spread or smear the catalyst. No attempt to quantify the catalyst distribution was made before it was certain that an effective catalyst could be properly formed from the precursor.

It was assumed that the supported bismuth nitrate could be converted to bismuth oxide by thermal decomposition. The literature clearly indicates that this conversion is possible but gives a range of temperatures, 530-700°C, over which it will occur.

Thermogravimetric analyses (TGA) of bulk bismuth nitrate decomposition in both inert and air atmospheres showed that the conversion to  $\text{Bi}_2\text{O}_3$  was complete between 550°C and 590°C, and thus a calcining temperature of 600°C in an oxygen atmosphere was selected. It would be desirable to conduct TGA on bismuth nitrate supported on VYCOR to determine a precise transition temperature and ensure that bismuth nitrate is being converted to bismuth oxide. However, it is difficult to conduct a meaningful TGA on a bismuth-loaded VYCOR sample because any changes in the large quantity of VYCOR would mask the changes in the much lower concentration bismuth component.

### 7.5.2 Testing of Supported Bismuth

The uncalcined membrane has an opaque (white) appearance which should become yellowish in colour (colour of  $\text{Bi}_2\text{O}_3$ ) as the bismuth nitrate is converted to bismuth oxide. However, initial attempts at calcining the membrane reactor resulted in no noticeable colour change. An initial reaction test of the calcined membrane indicated some significant problems. The initial test (125 sccm, 20 mol% propylene and 4 mol% oxygen in the feed, 530°C) provided some very unexpected results. Coke deposition on the inside of the membrane was heavy and, based on other tests, rapid. The reaction results for a 2 hour test are given in Table 7.9. Selectivity values are based on measured products only.

Table 7.9 - Bismuth Loaded "Catalytic Membrane Reactor" Initial Reaction Test

	Start of run	End of run
Propylene conversion	3.2 %	3.9 %
Oxygen conversion	40 %	83 %
CO <sub>2</sub> selectivity	44 %	70 %
CO selectivity	31 %	27 %
Acrolein selectivity	16 %	*
1,5-Hexadiene selectivity	9 %	*

\* Other 3 % is a variety of hydrocarbon products

The results clearly show that the addition of the bismuth to the membrane caused a change in activity and selectivity compared to the blank reactor (see Appendix B). It was primarily the oxygen conversion that increased since the propylene activity is largely controlled by Knudsen diffusion. There was significantly greater selectivity to all products except CO (the difference was most notable at the end of the run), and the unstable (time varying) results were not experienced during blank reactor testing. The bismuth addition caused the formation of products, including coke, that were strongly indicative of an acid catalyst. Both the reaction and visual evidence suggest that one of three things happened.



1. Bismuth nitrate was not properly decomposing on the VYCOR and bismuth oxide is not being formed.
2. The bismuth loading on the VYCOR was too low and the bismuth really acted as a dopant to the  $\text{SiO}_2$  in the membrane rather than as a catalyst.
3. Some substance other than pure  $\text{Bi}_2\text{O}_3$  (likely a bismuth-silica compound) was formed.

To pinpoint the problem, further tests were conducted on treated crushed VYCOR samples. The first test involved calcining VYCOR-supported bismuth at various temperatures between 600 and 800°C in inert and oxygen containing atmospheres to ascertain whether a higher calcining temperature was required to completely convert the supported bismuth nitrate to bismuth oxide. No change was noted except at higher temperatures (>750°C) where the VYCOR became largely consolidated. The second set of tests was used to determine the effect of bismuth loading. Increasing the bismuth loading on the VYCOR only accentuated the coking and high conversion problems. These two sets of tests indicated that neither calcination temperature nor bismuth loading were causing the problems. It must be concluded, then, that a substance other than  $\text{Bi}_2\text{O}_3$  is being formed on the VYCOR. X-ray diffraction (XRD) testing of the calcined bismuth supported on crushed VYCOR clearly indicated crystalline structures on the otherwise amorphous silica of the VYCOR. The XRD pattern, shown in Figure 7.17, however, does not match the pattern of  $\text{Bi}_2\text{O}_3$ . The pattern has similarities to bismuth-silicon oxides.

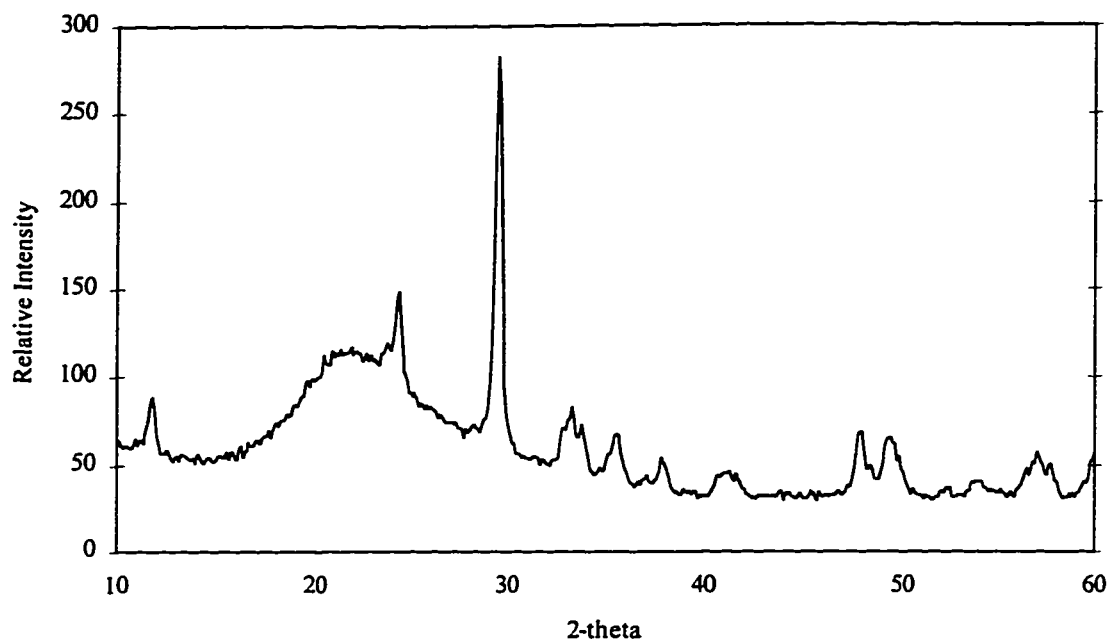


Figure 7.17 X-ray Diffraction Pattern for High Temperature Bismuth on VYCOR

Knowing that  $\text{Bi}_2\text{O}_3$  is not being formed on the surface leads to one final avenue of exploration - is the method of catalyst precursor addition and/or calcination method responsible for formation of the bismuth-silicon oxides? An alternative approach for producing  $\text{Bi}_2\text{O}_3$  from bismuth nitrate is to reduce the nitrate to bismuth metal and then re-oxidize to  $\text{Bi}_2\text{O}_3$ . A procedure to reduce the supported bismuth nitrate using hydrogen at as low a temperature as possible and then re-oxidize in oxygen, again at as low a temperature as possible, has been developed. The supported bismuth nitrate was heated to  $225^\circ\text{C}$  in flowing  $\text{H}_2$  for 2 hours. The temperature had to be kept below the melting point of bismuth metal ( $271^\circ\text{C}$ ). The material was re-oxidized in pure oxygen at  $225^\circ\text{C}$  for 1.5 hours. The reduction step resulted in a change of the colour of the bismuth-coated VYCOR from the white of supported bismuth nitrate to black. XRD analysis of this sample produced no peaks. This result is consistent with highly dispersed bismuth metal on the VYCOR surface. The re-oxidation step caused the black VYCOR to become a very deep yellow colour. This colour is very similar to that of bulk bismuth oxide and very different from any colour that had been produced with oxidizing bismuth nitrate on VYCOR. The XRD analysis of this sample shows only a minor shoulder on the main

silica pattern. The shoulder occurs at approximately the position of the main  $\text{Bi}_2\text{O}_3$  peak. Again, the lack of significant peaks may simply be indicative of a very highly dispersed (small crystallite) catalyst. Although the XRD and visual evidence is not conclusive, it seems likely that bismuth oxide can be successfully formed on the surface of VYCOR at relatively low temperatures.

The final part of the test procedure was to slowly heat the  $\text{Bi}_2\text{O}_3$ -VYCOR to temperatures in excess of the normal reaction temperature in 10% oxygen. The VYCOR turned from yellow to white and the final bismuth-coated membrane looked very similar to the previous high temperature samples. X-ray diffraction results confirmed that this material was the same as the material produced by the normal calcination method. The transition between bismuth oxide and the bismuth-silicon oxides appeared (visually) to occur between 325 and 375°C and was certainly complete at 400°C.

These tests indicate that a substance other than  $\text{Bi}_2\text{O}_3$  is the thermodynamically stable component when intimate interaction between VYCOR and  $\text{Bi}_2\text{O}_3$  occurs at temperatures in excess of 400°C. Comparison of the XRD results to known patterns for bismuth-silicon oxide components shows that a single identifiable compound is present. It is  $\text{Bi}_2\text{SiO}_5$  (a 1:1 mixture of bismuth oxide and silica). The standard XRD patterns for bismuth silicate in the range  $2\theta = 10^\circ$ - $60^\circ$  is shown in Figure 7.18 overlaid on the experimental bismuth-VYCOR pattern.

It is unclear whether this compound would be formed in every situation in which  $\text{SiO}_2$  and  $\text{Bi}_2\text{O}_3$  interact or whether it is limited to  $\text{Bi}_2\text{O}_3$ -VYCOR interaction. Bismuth has been supported on crushed quartz using the standard method starting with the bismuth nitrate precursor and calcining at 625°C in 15%  $\text{O}_2$ . In this case a yellow substance, colour identical to bulk  $\text{Bi}_2\text{O}_3$ , was produced on the quartz substrate. The substance did not bind very well to the quartz, as one would expect with a non-porous substrate. A simple reaction test indicated only a very low conversion of propylene (since the quantity of  $\text{Bi}_2\text{O}_3$  was very small), but selectivity greater than 70% to 1,5-hexadiene. While these test results would indicate that the interaction between  $\text{Bi}_2\text{O}_3$  and  $\text{SiO}_2$  is prevalent only

on VYCOR, an XRD analysis of the quartz supported  $\text{Bi}_2\text{O}_3$  showed that in addition to  $\text{Bi}_2\text{O}_3$  (the little bit that had not flaked off the surface),  $\text{Bi}_2\text{SiO}_5$  and sillenite,  $\text{Bi}_{12}\text{SiO}_{20}$ , were also present on the quartz surface. It was only the very low surface area of the quartz that prevented these other components from coming into play in the reaction test.

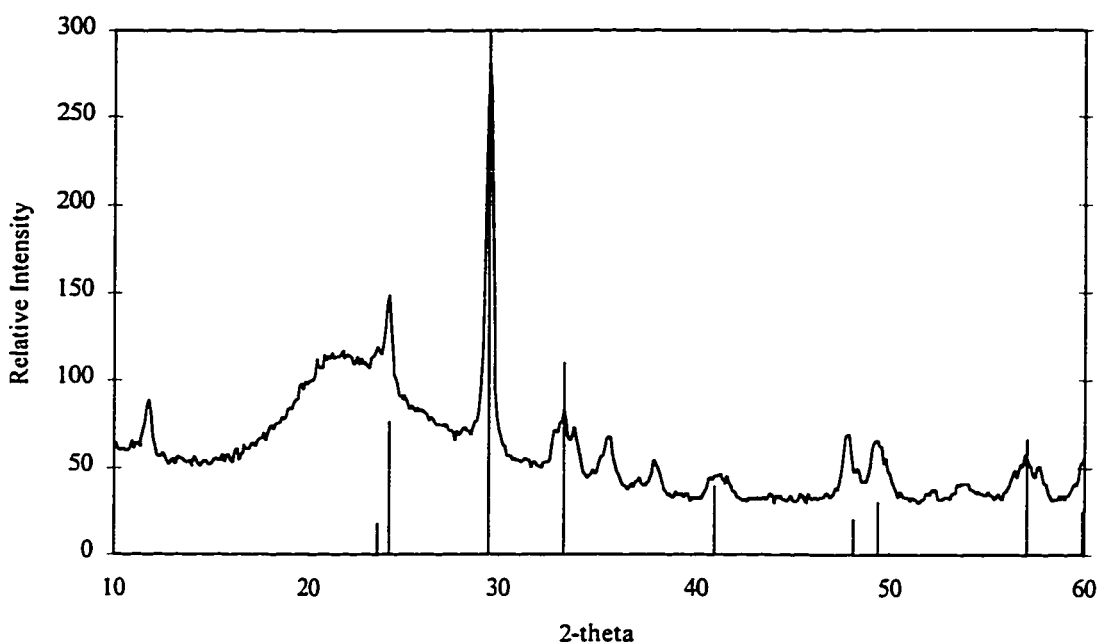


Figure 7.18 Comparison of Standard XRD Pattern for Bismuth Silicate ( $\text{Bi}_2\text{SiO}_5$ ) with Experimental Bismuth-VYCOR Pattern

Ultimately the results of the testing of  $\text{Bi}_2\text{O}_3$  supported on VYCOR lead to the conclusion that an effective bismuth catalyst that can withstand operation at temperatures in excess of  $400^\circ\text{C}$  cannot be made. Although this is a disappointing result from a reactor operations point of view, the reasons for the problems are clearly understood. Various literature sources indicate that  $\text{Bi}_{12}\text{SiO}_{20}$  is formed when silica and bismuth oxide are heated to  $800^\circ\text{C}$ , but the formation at lower temperatures and the formation of  $\text{Bi}_2\text{SiO}_5$  are unexpected and represent a new finding. From an examination of the Russian literature, there are indications that  $\gamma\text{-Bi}_2\text{O}_3$  (one of the higher temperature phases) will form stable phases with many oxides (Batog et al. (1973)) including all the others that could have been used as membranes for this project ( $\text{ZnO}$  and  $\text{Al}_2\text{O}_3$ ). It seems very possible, then, that any other membrane choice would have led to the same conclusion

and that support of a useful bismuth oxide catalyst for ODHD of propylene on any oxide membrane is unlikely to be successful.

The failure of the efforts to develop a supported bismuth catalyst means that the issue of whether or not the CMR configuration is reasonable for ODHD of propylene has not yet been addressed. The efforts to find another suitable ODHD catalyst that could be supported on the VYCOR membrane and a brief investigation of the catalyst in CMR mode are discussed in Chapter 8.

## Chapter 8

### Investigation of Catalytic Membrane Reactor Mode of Operation using Indium (III) Oxide

In order that the Catalytic Membrane Reactor (CMR) mode of operation for ODHD of propylene in the VYCOR membrane reactor be evaluated two tasks must be successfully completed. The first task is to find an appropriate ODHD of propylene catalyst that can be supported on the VYCOR membrane. The failure to support  $\text{Bi}_2\text{O}_3$  also casts some doubt on the ability to support other similar catalysts. Very few examples involving work with supported catalysts exist in the related literature. In those studies that do report investigation of supported catalysts (Swift et al. (1971), Trimm and Doerr (1971, 1972)) the supported catalyst is always made by mechanical mixing of the oxide (or precursor) with the support. In the situation to be investigated in this study, a typical highly dispersed supported catalyst will need to be produced using an impregnation method. The only examples of this type of supported catalyst for ODHD of propylene are briefly reported in the patent literature (Friedli (1970, 1973)).

The problems with supporting  $\text{Bi}_2\text{O}_3$  on the membrane also mean that the comparison of the CMR mode to a regular tubular reactor and to operation with the catalyst bed inside the membrane reactor tube will not be as rigorous as it could have been. The second task, then, is to carry out an experimental regimen that will indicate whether CMR mode is an appropriate mode of operation for ODHD of propylene. The goal of this experimental regime is not to cover all the operating parameters to the same depth as the work presented in Chapter 7. Instead, the aim is to provide some indication of the appropriateness of the membrane reactor technology used in the CMR mode. As a result the experimental programme is not nearly as extensive as the one presented in Chapter 7.

## 8.1 Finding an Appropriate Catalyst

The comparison of various single oxide catalysts presented in Table 2.1 indicates that there are a number of other potential ODHD of propylene catalysts that can be investigated. Four potential catalysts stand out: PbO, SnO<sub>2</sub>, Tl<sub>2</sub>O<sub>3</sub> and In<sub>2</sub>O<sub>3</sub>. The lead oxide catalyst was not investigated in this study as Greene et al. (1970) indicated that supporting this oxide on a highly siliceous material and operating at temperatures in excess of 500°C will not be successful. The problem stems from PbO causing flux of the siliceous material. The investigation of the remaining catalysts is discussed in the following sections.

### 8.1.1 Tin (IV) Oxide

Although SnO<sub>2</sub> is a viable unsupported catalyst for ODHD of propylene (Solymosi and Bozsó (1977)), the use of SnO<sub>2</sub> in supported form has proven to be problematic. No successful method has been found during this study to deposit the material on a catalyst support. Attempts to decompose Sn(IV) salts in oxygen at high temperature, a standard technique for producing supported metal oxide catalysts, lead to the formation of SnO rather than SnO<sub>2</sub>. Tin (IV) oxide itself is only soluble in strong bases, so dissolving the oxide and trying to impregnate with that sort of solution will lead to deposition of the metal ion from the base as well as the Sn<sup>4+</sup> ion. The likelihood of the formation of a mixed oxide seems high. The exception to this problem is dissolution in very strong NH<sub>4</sub>OH. Preliminary testing indicated that SnO<sub>2</sub> will not dissolve in NH<sub>4</sub>OH and hence the attempts to support SnO<sub>2</sub> were terminated.

### 8.1.2 Thallic Oxide

Early literature concerning the ODHD of propylene (Trimm and Doerr (1970, 1971)) indicated that thallic oxide (Tl<sub>2</sub>O<sub>3</sub>) is a very intriguing catalyst for this reaction. At operating temperatures just slightly below the standard temperatures for ODHD of propylene on Bi<sub>2</sub>O<sub>3</sub>, Trimm and Doerr (1970) reported that at conditions of low oxygen

concentration the selectivity to 1,5-hexadiene is 78% and rises as the oxygen concentration is further decreased. The key problem with this operating condition is that thallic oxide is thermally unstable particularly in reducing atmospheres (high concentration of propylene, low concentration of oxygen) and tends to rapidly deactivate. The mechanism involves the reduction of thallic oxide to thallos oxide ( $Tl_2O$ ) which has very poor catalytic properties and is much more volatile than thallic oxide. Cubicciotti and Keneshea (1967) have studied the vapourization of thallic oxide under various temperature and oxygen atmosphere conditions. Specifically, they studied the thallic oxide-thallos oxide equilibrium system as shown in equation 8.1.



At 800 K, for example, the partial pressure of  $Tl_2O$  in equilibrium with  $Tl_2O_3$  given an oxygen partial pressure of 0.1 atm is  $1.2 \times 10^{-7}$  atm and rises to  $1.2 \times 10^{-6}$  atm with an oxygen partial pressure of 0.01 atm. In addition to the normal equilibrium problem, the fact that  $Tl_2O_3$  is reduced to the more volatile  $Tl_2O$  in the course of the reaction means that the loss of the catalyst out of the reactor through sublimation is always a potential problem.

The degree to which deactivation and evaporation of the catalyst will occur must be evaluated as a part of the decision as to whether or not  $Tl_2O_3$  is an appropriate catalyst. Simple reaction tests in the tubular reactor with unsupported  $Tl_2O_3$  indicate that it did have a very high initial activity, but that the catalyst deactivated quite rapidly (over an hour) and that the selectivity to 1,5-hexadiene was never greater than 40%. In addition, the build up of a yellowish deposit on the cool walls of the quartz reactor was indicative of thallos salts (Trimm and Doerr (1971)) meaning that catalyst was leaving the reactor by sublimation. The amount of thallium leaving the reactor is a discouraging result, particularly if it is applied to supported catalysts. There would be very little thallic oxide supported on the VYCOR and if it easily sublimates off the support and out of the reactor then the use of the supported catalyst will be difficult or impossible.



To determine if  $Tl_2O_3$  supported on VYCOR would remain on the support under reaction conditions a 16 wt%  $Tl_2O_3$  on crushed VYCOR catalyst (not on a VYCOR membrane) was prepared. The preparation involved dissolving the  $Tl_2O_3$  in nitric acid and impregnating the VYCOR with the acid solution. The acid was evaporated at  $75^\circ C$  and then the supported material is calcined in oxygen at  $350^\circ C$  for 2 hours. XRD analysis indicated that  $Tl_2O_3$  was the thallium species present on the surface of the VYCOR. Two tests were conducted with separate batches of the supported catalyst. In the first test the catalyst was packed into a tubular reactor and subjected to a temperature of  $600^\circ C$  in flowing  $O_2$  (5 sccm) for 12 hours. All the thallic oxide was removed from the VYCOR in this test. Although the temperature was above typical reaction temperatures, the very high oxygen partial pressure should have compensated to some degree and reduced the  $Tl_2O_3$  loss. This result indicated that the supported  $Tl_2O_3$  would not be viable. The second test was a reaction test in the tubular reactor packed with the crushed VYCOR/ $Tl_2O_3$  catalyst at  $530^\circ C$ . Although the catalyst initially had very high activity and a selectivity to  $C_6$  products (1,5-hexadiene and benzene) of approximately 50%, the activity and  $C_6$  selectivity declined sharply over a one hour test period. Signs of both coke formation and catalyst loss were visually apparent and decoking/recalcining the catalyst at  $530^\circ C$  in pure oxygen lead to even further catalyst loss.

If the  $Tl_2O_3$  were to be supported on the walls of the VYCOR membrane it is possible that it would see a much higher oxygen partial pressure than it does in the tubular reactor trials. The higher oxygen partial pressure might help to lessen the loss of catalyst during the tests, but it seems likely that the continual loss of catalyst is unavoidable. No consistent results can be achieved from a CMR which suffers from continual catalyst loss and replenishment of catalyst between tests, or use of a new reactor for each test is far too onerous to be practical. In addition to potential problems with consistency, thallium compounds are very toxic materials. Thallic oxide itself is readily absorbed through the skin and can cause severe medical problems in the gastrointestinal tract, skin, nervous system, eyes and cardiovascular system. The LD50 value (rats, oral) is 44 mg/kg and the time weighted average (TWA) exposure limit is  $0.1 \text{ mg(Tl)}/\text{m}^3$ . The fact that the material cannot be isolated within the reactor only serves to accentuate potential health problems.

Thus, for both operational and safety reasons the use of a supported thallic oxide catalyst was not continued.

### 8.1.3 Indium (III) Oxide

Trimm and Doerr (1972) have investigated the use of indium oxide as a ODHD of propylene catalyst and have indicated that "indium oxide is a good catalyst for the oxidation of propylene to 1,5-hexadiene and to benzene". The work indicated that the selectivity to benzene tended to be higher than the selectivity to 1,5-hexadiene, particularly at higher levels of conversion (higher W/F), and that there was also significant formation of acrolein. Although this catalyst does not primarily produce 1,5-hexadiene, it does seem to be a reasonable catalyst.

Closer examination of the results of Trimm and Doerr (1972) reveals that indium oxide may not be as good a catalyst as was stated in their paper. The selectivity of the ODHD reaction to total C<sub>6</sub> products over bulk In<sub>2</sub>O<sub>3</sub> is approximately 17% with the balance of conversion resulting in the formation of CO<sub>2</sub>. This high degree of combustion leads to the potential for a significant rise in temperature across the catalyst bed. Trimm and Doerr (1972) refer to this problem but do not indicate the magnitude of the temperature rise. Their investigation of a supported In<sub>2</sub>O<sub>3</sub> catalyst (mechanical mixture with a pumice support) gave two distinct results. At very low conversion levels, levels at which products cannot be reliably detected by the equipment used in this work, only 1,5-hexadiene and acrolein are formed. At higher conversion levels the selectivity to non-combustion products is low and the non-combustion products consist mainly of acrolein except at the highest conversion levels when benzene is prevalent. The selectivity to CO<sub>2</sub> is usually in excess of 60% and rises to greater than 85% at high conversion. Although it is not mentioned by Trimm and Doerr, temperature rise in the catalyst bed was likely a problem. These results indicate that In<sub>2</sub>O<sub>3</sub> is far from an ideal catalyst for ODHD of propylene but is one of the few catalysts that may be stable and can be supported on the VYCOR membrane.

A supported  $\text{In}_2\text{O}_3$  catalyst must be produced from a precursor indium salt because the crystalline form of  $\text{In}_2\text{O}_3$  is not soluble in any solvent. Indium nitrate pentahydrate ( $\text{In}(\text{NO}_3)_3 \cdot 5\text{H}_2\text{O}$  - 99.99% purity - metals basis) supplied by Aesar Chemicals was used in this study. This material is readily soluble in water and decomposes at sufficiently high temperatures in an oxygen environment to  $\text{In}_2\text{O}_3$ . Deposition of the precursor on the VYCOR membrane requires a modification of the deposition method described for bismuth nitrate described in Chapter 7. Water is drawn into the pores of the VYCOR much more rapidly at room temperature than is the glycerol used for bismuth deposition. Adding the aqueous indium solution to the VYCOR membrane would likely result in uneven catalyst distribution. The necessary modification of the method was to pre-wet the membrane with deionized water until it was saturated. By doing so the indium solution was not drawn into the pores as it was dropped on to the membrane surface and the method of slowly heating the membrane while rotating and purging it was just as effective in this case as with the bismuth precursor. The only difference was that the membrane needed only be heated to approximately  $75^\circ\text{C}$  for the method to work. The membrane was calcined at  $520^\circ\text{C}$  in a 20%  $\text{O}_2$  stream to decompose the nitrate. Preliminary work, focusing on the deposition of the indium on crushed VYCOR, indicated that this calcination temperature was sufficient. XRD analysis of the crushed sample indicated only one small peak (other than the amorphous pattern caused by the VYCOR), and it was located at the value of the primary  $\text{In}_2\text{O}_3$  peak. These results, along with the visual observation that the colour of the supported material was the same yellow colour as bulk  $\text{In}_2\text{O}_3$ , indicate that  $\text{In}_2\text{O}_3$  was the species on the VYCOR surface but that it was very highly dispersed.

Knowing that  $\text{In}_2\text{O}_3$  can successfully be supported on VYCOR is a big step towards being able to use  $\text{In}_2\text{O}_3$  as the catalyst to demonstrate the application of CMR mode applied to ODHD of propylene. The second step is to see if the supported catalyst will still behave as an ODHD of propylene catalyst and to find an appropriate alternate operating configuration to compare to the CMR mode. Preliminary work with  $\text{In}_2\text{O}_3$  supported on crushed VYCOR showed that the catalyst maintained activity, but that the primary non-combustion product was acrolein and that some carbonaceous material was formed

during the course of the tests. The carbonaceous material turned the VYCOR completely black, but it did not seem to affect activity and it was easily removed by exposure to oxygen (no propylene) at 520°C. Although it would be preferential to have no coke formation and to produce 1,5-hexadiene so that a more direct comparison to the bismuth oxide work would be possible, the supported  $\text{In}_2\text{O}_3$  should be sufficient for evaluation of the CMR mode.

It would be most preferable to compare CMR mode to a tubular reactor containing bulk  $\text{In}_2\text{O}_3$  as the catalyst. This comparison would most closely parallel the work described in this chapter and that described in Chapter 7. Testing of 18 x 20 mesh bulk  $\text{In}_2\text{O}_3$  diluted with quartz chips using 250 sccm total flow with 20% propylene and 6% oxygen in the feed at nominal operating temperatures between 410-475°C in a quartz tubular reactor gave very discouraging results. A temperature rise across the catalyst bed in excess of 30°C was experienced and selectivity to total  $\text{C}_6$  products was less than 22% in cases which produce any significant conversion of propylene. These results are consistent with those found by Trimm and Doerr (1972) except that far more 1,5-hexadiene than benzene is formed. The catalyst showed no signs of coke formation and provided little or no activity in the absence of oxygen. However, the large degree of non-isothermality in the reactor would make comparison of the results to those of the CMR mode very difficult and hence, for purposes of this study, the use of unsupported  $\text{In}_2\text{O}_3$  was not considered.

Since unsupported  $\text{In}_2\text{O}_3$  cannot be used in the tubular reactor, some form of supported  $\text{In}_2\text{O}_3$  must be used for the comparison to CMR mode. Knowing that high surface area catalysts are often deleterious to ODHD reactions, a low surface area, supported catalyst is desired. Attempts to support  $\text{In}_2\text{O}_3$  on corundum by simple mechanical mixing (in a manner similar to that described by Trimm and Doerr (1972)) has proven unsuccessful as the  $\text{In}_2\text{O}_3$  tends to flake off or not adhere in the first place. This result brings into question how Trimm and Doerr were able to support up to 70 wt%  $\text{In}_2\text{O}_3$  on pumice. The indium nitrate precursor can be supported on other very low surface area carriers such as corundum or Norton SA 5018 silica/ $\alpha$ -alumina carrier to give catalysts in excess of 5 wt%  $\text{In}_2\text{O}_3$  by an impregnation method. The carriers themselves are not completely inert

at reaction temperatures, and the supported catalysts, even at a 1 wt%  $\text{In}_2\text{O}_3$  loading are far too active. Reaction tests with these catalysts resulted in highly non-isothermal catalyst beds, rapid and heavy coke formation and the coke caused the activity to change with time. XRD analyses of the supported catalysts indicated peaks that could not be attributed to either  $\alpha$ -alumina or  $\text{In}_2\text{O}_3$ . It is possible that an indium-alumina compound was formed, and this compound would make support of indium oxide on an alumina membrane very difficult. This problem is the same sort of problem encountered when bismuth oxide was supported on VYCOR (Chapter 7).

The best remaining option is to use  $\text{In}_2\text{O}_3$  supported on crushed VYCOR. It is not the ideal catalyst, but it is feasible and it may provide a better comparison to the CMR mode by also taking into account some of the activity the VYCOR pores will cause.

## **8.2 Comparison of CMR Mode to a Tubular Reactor using an $\text{In}_2\text{O}_3$ Catalyst**

### **8.2.1 Description of Operating Conditions**

The same operating parameters used to study the blank membrane reactor (Chapter 6), and for making the operating mode comparisons using bismuth oxide as a catalyst (Chapter 7), were used for this part of the study. The primary difference was that, other than operating temperature, the variables were only tested at two levels. That is, a 2x2x2 study (8 runs) was carried out at four temperature levels. The test values of the various parameters are shown in Table 8.1. This limited study will elucidate trends in the operation but will not provide definitive correlations for the effect of the operating parameters on conversion and selectivity to products for the two different operating configurations. The goal of this part of the study is simply to determine whether CMR is potentially a feasible operating mode for the ODHD of propylene process.

Table 8.1 - Operating Parameters for Membrane and Tubular Reactor Tests using  $\text{In}_2\text{O}_3$  Catalyst

Parameter	Parameter Value(s)
Total Flow Rate	125 and 250 sccm
Mass of Membrane/Crushed VYCOR	6.11 g
Catalyst Loading	1 wt%
Propylene Feed Concentration	10.0 and 20.0 mol%
Oxygen Feed Concentration	3.0 and 6.0 mol%
Nominal Furnace Temperature	430, 450, 470, 490°C

Both the membrane reactor and the supported catalyst were prepared by first pre-wetting the VYCOR to saturation then adding the catalyst precursor. In order to best mimic the VYCOR characteristics of the membrane reactor in the supported catalyst, a fully treated VYCOR membrane that was not made into a reactor was crushed and used as the support. Crushing, unfortunately, does not yield particles all within a very narrow size distribution, and all the VYCOR material needs to be used to get the same amount of VYCOR as is in the membrane reactor. Although the size distribution is broad compared to that of the catalyst materials described in Chapter 7, it should still provide an adequate basis for comparison of CMR to tubular reactor modes. The size distribution of the crushed VYCOR is given in Table 8.2.

Table 8.2 - Size Distribution of Crushed VYCOR used for  $\text{In}_2\text{O}_3$  Support

Size Range (Tyler Mesh)	Mass (g)
20 x 30	2.98
30 x 40	1.22
40 x 70	1.16
< 70	0.75

The distribution of the supported  $\text{In}_2\text{O}_3$  on both the crushed VYCOR and on the membrane of the membrane reactor is potentially an important parameter in this study. The effect of catalyst distribution is not studied as part of this research work, but it may warrant study in the future. It is important, however, to document, as much as possible, the catalyst distribution used for this study. From the XRD work that has been completed

on the supported catalyst, it can be concluded that the  $\text{In}_2\text{O}_3$  was very highly dispersed on the VYCOR. It is very difficult, however, to determine how far into the VYCOR particles the  $\text{In}_2\text{O}_3$  had penetrated. The distribution can be determined by EDX if a good cross-sectional sample of a representative pellet can be produced. Producing such a sample has proven to be exceedingly difficult and the EDX analysis has not been carried out. For the membrane reactor no XRD analysis has been completed but there is no reason to believe that the dispersion should be dramatically different on the membrane than on the crushed VYCOR samples. Completing an EDX analysis of a cross section of the membrane requires the destruction of the membrane reactor to obtain a piece of membrane on which to carry out the analysis. At the conclusion of reaction testing such an analysis was carried out. The EDX analysis is the jagged white line on the scanning electron micrograph shown in Figure 8.1. The indium concentration peaks just inside the inner membrane wall and decreases to essentially zero within 0.45 mm of the inner wall. The dark vertical line on the micrograph marks the limit of  $\text{In}_2\text{O}_3$  penetration.

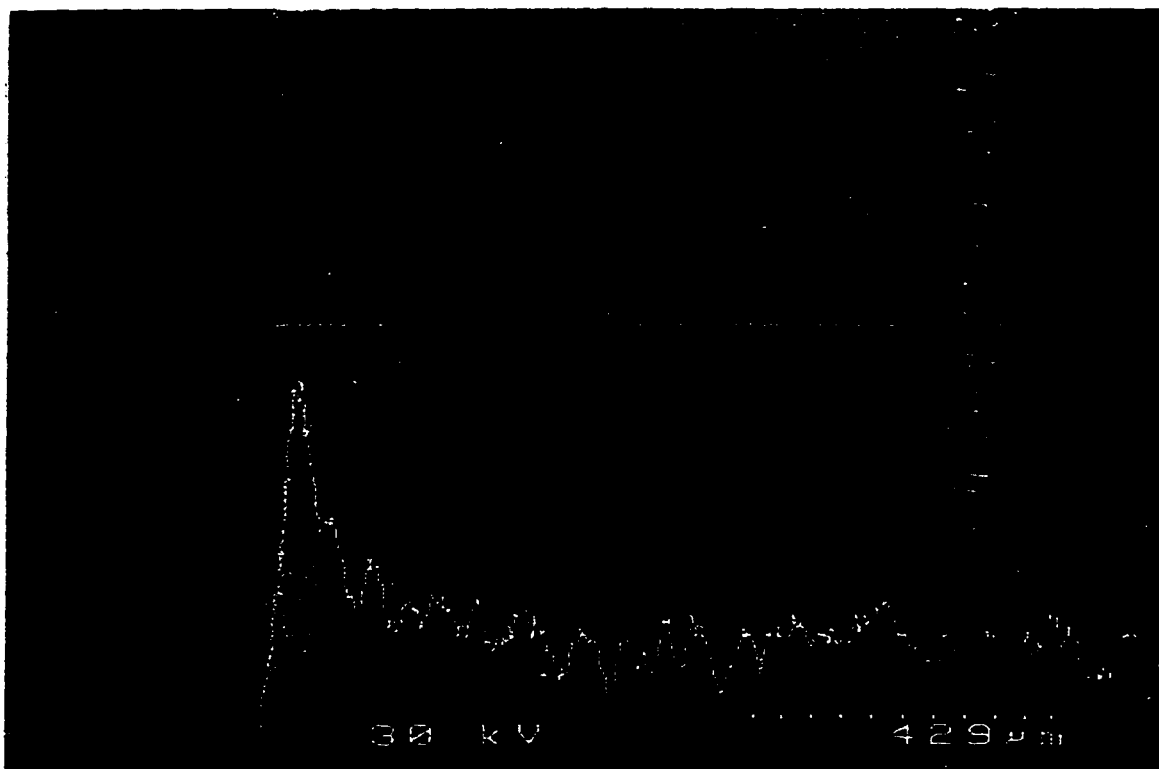


Figure 8.1 EDX analysis for Indium on Scanning Electron Micrograph of Membrane Cross Section

The catalytic membrane reactor was operated without any packing material on the tube side of the membrane. A thermocouple was inserted to measure the temperature at the axial and radial centre of the tube side space of the membrane section. For the tubular reactor the same thermocouple, placed in the middle of the catalyst bed, was used to control the furnace rather than using the furnace internal thermocouple. This approach had to be utilized in this instance because two factors tend to cause changes in the measured catalyst activity. The first factor was the relatively high selectivity to combustion products that resulted in significant heat production in the catalyst bed. The second factor was a continuous drop in intrinsic activity of the catalyst over a 7 day period of operation. As the activity decreased, the catalyst bed temperature decreased (the oven thermocouple did not detect these changes adequately enough to compensate for them) and the result was an even greater apparent drop in activity. Figure 8.2 illustrates the real drop in activity at one constant mid-bed temperature over the initial seven day period. A complete summary of the activity testing data is contained in Appendix D. After this initial period the activity was very stable.

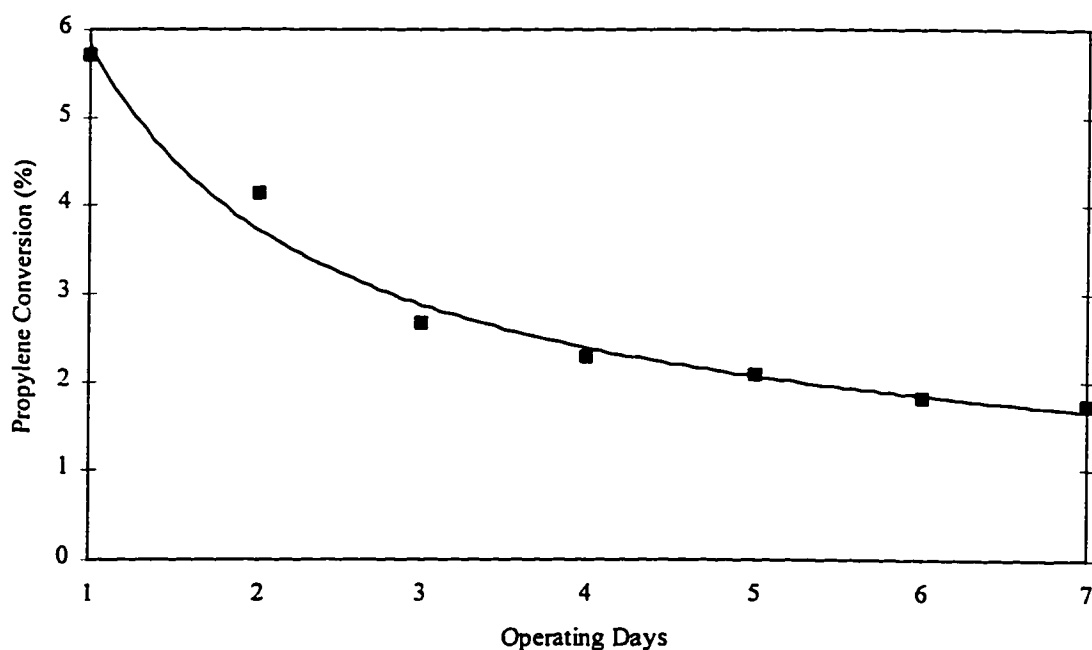


Figure 8.2 Changes in Propylene Conversion over the 1 wt%  $\text{In}_2\text{O}_3$  on Crushed VYCOR Catalyst at 480°C (7 Day Period)



The same sort of change in activity occurred on the catalytic membrane reactor but it was less noticeable because the membrane itself accounted for some of the reaction. In both cases the reaction tests were carried out only after the catalyst activity had stabilized.

### 8.2.2 Discussion of Reaction Test Results

The full data summaries for both the CMR mode tests and the tubular reactor tests are contained in Appendix D. The data presented in this section are representative of the general trends found in the complete data set.

There are some general trends common to both the CMR and the tubular reactor. The selectivity to either ethylene or 1,5-hexadiene (the only detectable, non-combustion products other than acrolein) was small. In all cases it was less than 4% for either species and tends to decrease with decreasing temperature. The selectivity to acrolein was different for the two different modes but in both cases it decreases with an increase in temperature.

In tubular reactor mode neither the total flow rate nor the feed concentrations of either oxygen or propylene had any significant impact on the selectivity to the different products. The absolute conversion of propylene increased with increasing total flow rate. These trends are entirely consistent with the reaction being mass transfer limited on the supported catalyst. From the discussion on Knudsen diffusion limitations into porous VYCOR it should be clear that a mass transfer limited reaction is exactly what should be expected.

The membrane reactor behaved in many of the same general ways as the blank membrane reactor (Chapter 6) with respect to the process parameters. Higher propylene feed concentration resulted in greater total conversion and increased the selectivity to CO and acrolein over CO<sub>2</sub> (less over-oxidation of CO and acrolein). Higher oxygen feed concentrations (higher O<sub>2</sub> partial pressure in the membrane pores) resulted in an increase in selectivity to CO<sub>2</sub> at the expense of CO and acrolein. An increase in total flow rate

was accompanied by a higher oxygen partial pressure in the membrane and hence the results were affected in the same way as an increase in oxygen feed concentration.

Unfortunately the lowest temperature at which the blank membrane reactor was tested (Chapter 6) was approximately 490°C, which is the upper end of the temperature range used for the indium loaded membrane. Thus direct comparison between the blank and catalyst loaded membrane is difficult. Even if a full data set existed in the proper temperature range for the blank reactor, the “effect” of the membrane itself could not be subtracted from the total reaction as has been done for the bismuth oxide catalyst bed inside the membrane reactor. There is simply no way to decouple the effect of the membrane alone from that of the catalyst alone. There are two fundamental differences between operation with the indium catalyst on the membrane and the blank membrane. The first difference is that the ratio of CO<sub>2</sub> selectivity to CO selectivity is much higher in the indium-loaded membrane than would be expected at these lower temperatures in the blank membrane. The second difference is that total activity of the indium-loaded membrane is higher than would be expected from the blank reactor. Both of these differences indicate that the indium oxide supported in the membrane pores is promoting combustion reactions (and preferentially complete combustion).

The comparison between the CMR mode and the tubular reactor mode will indicate whether CMR mode is potentially viable for ODHD of propylene reactions. The key indicators are the overall activity (measured by conversion of propylene), the selectivity to the various major products and the yield of the desired product (in this case acrolein). The comparison of propylene conversion is shown in Figure 8.3

The conversion in CMR mode is always greater than the tubular reactor mode within this temperature range. The ratio of the conversions decreases as the temperature increases indicating that proportionally more conversion is due to the catalyst as the temperature rises in the CMR mode. For the conditions shown in Figure 8.3 it is possible to operate at a higher temperature because oxygen conversion is less than 50% for both modes. However, as shown in Figure 8.4, the selectivity to acrolein decreases at higher

temperature. The selectivity values for all the main products ( $\text{CO}_2$ ,  $\text{CO}$  and acrolein) are illustrated for the two configurations in Figure 8.4.

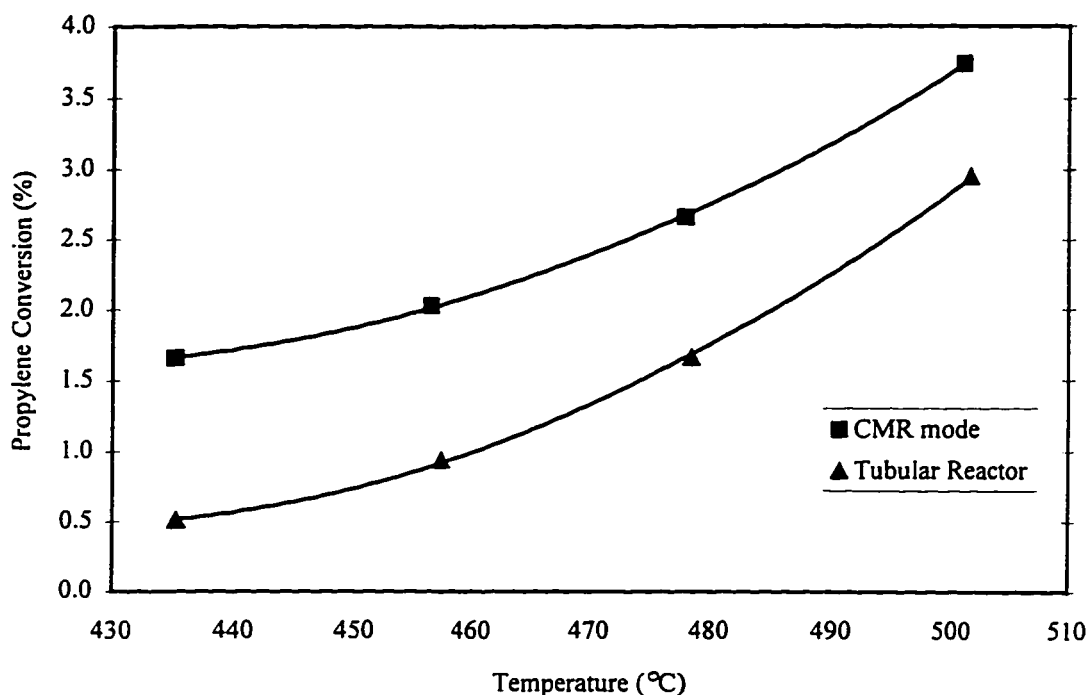


Figure 8.3 - Comparison of Propylene Conversion Between Operating Modes (250 sccm Total Flow, 20 mol% Propylene and 6 mol% Oxygen in Feed)

The most marked differences between the two operating modes are the dramatically higher selectivity to acrolein and the much lower total selectivity to carbon oxides in the tubular reactor. The membrane plus catalyst in CMR mode causes much of the propylene entering the membrane pores to be converted (eventually) to combustion products. This problem is the primary downfall of the CMR mode in this instance. Even though the tubular reactor has lower overall conversion, the higher selectivity to acrolein gives that configuration higher overall yield to acrolein. This phenomenon is illustrated by Figure 8.5.

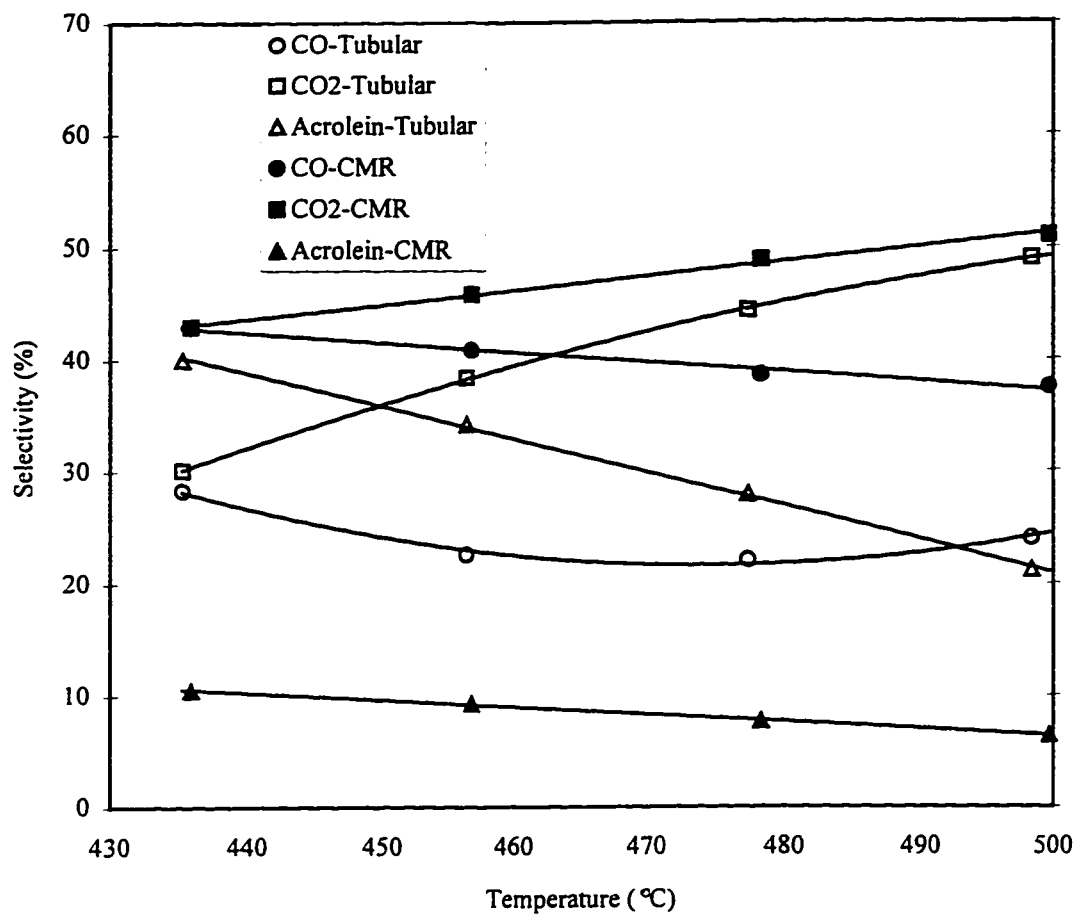


Figure 8.4 Comparison of Key Product Selectivities Between Operating Modes (125 sccm Total Flow, 20 mol% Propylene and 6 mol% Oxygen in Feed)

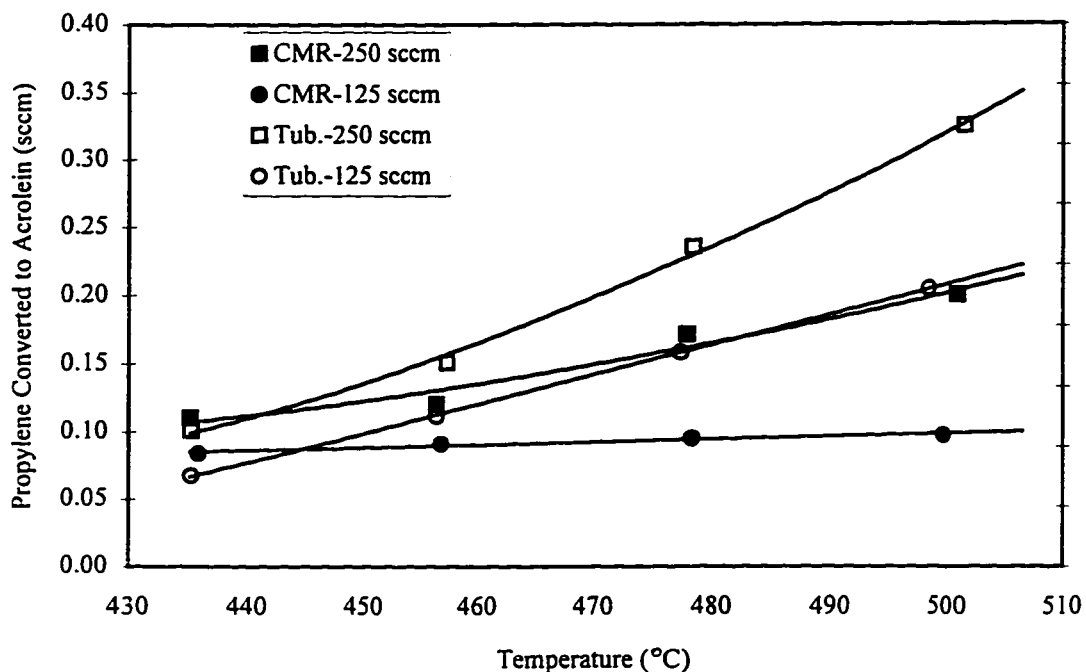


Figure 8.5 Comparison of Propylene Conversion to Acrolein Between Operating Modes (20 mol% Propylene and 6 mol% Oxygen in Feed)

The conversion of propylene to combustion products and the over conversion of acrolein to combustion products in the pores of the membrane reactor make it a less desirable operating configuration than a standard tubular reactor. Although the formation of acrolein is a partial oxidation reaction rather than an ODHD reaction, the problems would be very similar in ODHD of propylene. 1,5-Hexadiene will also be highly susceptible to over oxidation in the pores so the partial oxidation reaction is a reasonable alternative model to illustrate the potential problems. The problem with the membrane is two fold. The higher oxygen partial pressure in the membrane pores (compared to the pores of the tubular reactor catalyst) is promoting the combustion reactions. The higher oxygen partial pressure is an unavoidable trait of the membrane reactor. The second cause of the problem is the activity inherent to the pores of the membrane. This trait is a function of the membrane itself (pore size, structure and material) and could be altered by further treatment of the VYCOR or by using a different membrane material.

It appears that the use of CMR mode for ODHD of propylene is not appropriate. The CMR mode for oxidative reactions would better utilized when high partial pressures of oxygen are desirable, when more complete oxidation of a hydrocarbon species is desired or in situations when a lower operating temperature can be utilized to carry out the reaction. The lower temperature will help decrease the inherent membrane activity. However, in all these cases a simple tubular reactor would function just as well and should be easier to operate. The advantage that the CMR would have in these situations is that reaction will be confined to the pores and possible explosive mixture problems could be avoided. Further research is required to determine if an appropriate situation for the use of the CMR mode in an oxidative reaction exists.

## Chapter 9

### Conclusions and Recommendations

There are basically three elements of research on various aspects of the oxidative dehydrodimerization of propylene that come together to make up this thesis: (1) design, development and construction of the experimental equipment (focused on the membrane reactor itself), (2) evaluation of some of the kinetic aspects of the catalysts (mainly  $\text{Bi}_2\text{O}_3$ ), and (3) evaluating membrane reactor technology for ODHD of propylene. The conclusions and recommendations arising from this research effort are outlined in the following sections using the three basic elements as the structure for presenting the material.

#### 9.1 Conclusions

##### 9.1.1 Equipment

A single, on-line gas chromatography method, developed in the course of this research, is now available to analyze all the reactant and product species of the ODHD of propylene. The method allows analysis of a wide range of compositions and since it accurately provides analysis for all the components, there is great confidence in the overall mass balance.

The core of the work on equipment design has been on the development of a porous VYCOR membrane reactor that can be used for ODHD of propylene. A new method of treatment of porous VYCOR by sequential treatment in an aqueous sodium hydroxide solution then treatment in flowing steam at elevated temperature drastically reduces the propylene oxidation activity of the porous VYCOR. There is some physical degradation

of the membrane witnessed by the increase in mean pore diameter and a visible decrease in membrane thickness, but the degradation is not severe and does not pose any operational problems. This treatment is necessary to operate in the propylene/oxygen environment at typical ODHD of propylene reaction temperatures without excessive conversion of propylene on the membrane itself. There is, however, potential for further reducing the intrinsic activity of the membrane.

Traditional glass working techniques, particularly glass welding, are difficult to use with porous VYCOR due to its porous nature, but they are not impossible to use. Unfortunately the treated VYCOR used in this research is even more difficult to work with than regular porous VYCOR and glass welding of the treated material is impossible. As a result, a new construction method has been developed called the "shrink wrap" method. The method utilizes the natural consolidation that porous VYCOR undergoes as it is heated to cause the tube diameter of a VYCOR tube to decrease and tightly bond to an inner quartz sleeve.

To design a standard shell and tube type membrane reactor an effective method of sealing the quartz tube to the metal shell must be used. For this work a rubber o-ring joint which is placed outside of the heated zone is used. It is essential to keep the seal cool in order that it does not suffer from thermal degradation or from chemical attack by oxygen at high temperatures. This type of seal is capable of withstanding a differential pressure of 450 kPa, but future work or any potential commercial application may require a more robust sealing system.

The membrane reactor has been designed to allow oxygen to flow through the pores of the membranes so that the oxygen feed into the reactor is evenly distributed along the total length of the reactor. When the membrane reactor is operated in membrane reactor mode (oxygen flowing through the membrane into the tube where a propylene containing stream is flowing), the reactor does have some residual propylene oxidation activity. This activity is not present when crushed samples of the membrane material are tested in a flowing stream containing oxygen and propylene. The VYCOR pore surfaces will



cause reaction at ODHD of propylene temperatures and it is the different partial pressures of propylene and oxygen in the membrane reactor set up compared to the crushed samples that facilitates the activity. The degree of activity is directly related to the permeability of the membrane and the permeability is controlled by Knudsen diffusion. The primary propylene oxidation reactions that occur in the membrane are combustion to CO and CO<sub>2</sub>. CO<sub>2</sub> production is favoured at higher temperatures and oxygen and propylene partial pressures. The activity is undesired and tends to increase with time on stream as a result of an increase in overall membrane permeability. The exact reasons for the increases in activity and methods of eliminating the activity changes have not yet been identified.

### 9.1.2 Catalysts

Most of this research work has been focused on Bi<sub>2</sub>O<sub>3</sub> as an ODHD of propylene catalyst. Kinetic expressions and parameters have been developed for the two primary reactions that occur between propylene and oxygen on Bi<sub>2</sub>O<sub>3</sub> namely production of 1,5-hexadiene and CO<sub>2</sub>. The work on production of 1,5-hexadiene confirms the findings of other researchers, but raises some interesting questions about the over-oxidation of 1,5-hexadiene and the role that that reaction may play in the overall process. The development of the kinetic power-law expression for CO<sub>2</sub> production from propylene has not previously been reported. This work indicates that the reaction is 0.76 order in propylene, 0.41 order in oxygen and has a measured activation energy of 78 kJ/mol.

The questions surrounding the oxidation of 1,5-hexadiene have been partially answered by research that is also unique to this thesis. Conversion of 1,5-hexadiene to both CO<sub>2</sub> and benzene is found to occur by both homogeneous and heterogeneous routes in the temperature range of interest in this study. Benzene is produced predominantly by the heterogeneous route and that reaction appears to be first order in 1,5-hexadiene and have a measured activation energy of 140 kJ/mol. The production of CO<sub>2</sub> is more evenly divided between homogeneous and heterogeneous routes with the former being more important at higher oxygen concentration levels. The overall production of CO<sub>2</sub> is

approximately first order in propylene, but this research work has not been able to accurately determine either oxygen order or the true activation energies for either the homogeneous or heterogeneous routes. It is abundantly clear, however, that a significant portion of the CO<sub>2</sub> produced in the ODHD of propylene is a result of oxidation of 1,5-hexadiene. This finding is the reason that selectivity to 1,5-hexadiene from ODHD of propylene decreases as propylene conversion increases. It also presents a significant practical problem for any ODHD of propylene catalyst or process. That is, if high selectivity can only be maintained at low conversion, such a process can never be economically viable.

The long term stability of the Bi<sub>2</sub>O<sub>3</sub> catalyst under reaction conditions is described for the first time in this work. Under conditions of abundant oxygen the catalyst activity and selectivity remain unchanged over a 250 hour period. However, in situations where oxygen is very nearly depleted the catalyst suffers from an irreversible loss in activity. This finding represents a particular challenge to the operation of a membrane reactor in which low oxygen concentration in the catalyst bed is the goal. A lower catalyst activity may be one of the tradeoffs necessary for reasonable membrane reactor operation.

### 9.1.3 Evaluation of Membrane Reactor Technology

The use of membrane reactor technology for ODHD of propylene has been evaluated in two operating modes and compared with the results obtained in a standard tubular reactor with a fixed catalyst bed. One operating mode is the Inert Membrane Packed Bed Reactor which has been evaluated using Bi<sub>2</sub>O<sub>3</sub> as the catalyst. In this work the membrane itself is not completely inert, as discussed in Section 9.1.1, and accounts for between 40-65% of the total conversion of propylene. When the membrane reactions are discounted, the IMPBR configuration consistently gives 1,5-hexadiene and total C<sub>6</sub> product selectivities that are 6-12% (absolute or 10-20% relative) higher than those of a tubular reactor. These are substantial gains in selectivity. The 1,5-hexadiene selectivity will be maximized by operating at approximately 580°C with the highest possible propylene concentration and conditions which ensure that there is little or no excess oxygen. These

results are proof of concept for the use of membrane reactor technology for ODHD of propylene.

Membrane reactor technology has also been evaluated in Catalytic Membrane Reactor (CMR) mode. The  $\text{Bi}_2\text{O}_3$  catalyst could not be used for this evaluation. It has been discovered during this investigation that the bismuth oxide interacts with the silica in VYCOR to produce bismuth-silicon oxides which are of no catalytic value to this process. As a result CMR mode has been evaluated using  $\text{In}_2\text{O}_3$  as a catalyst. The evaluation shows that CMR mode is inferior to the standard tubular reactor. The pores of the VYCOR, in which the catalyst is placed, simply cause too much non-selective oxidation of feed and products for CMR mode to be practical.

## 9.2 Recommendations

### 9.2.1 Membrane Reactor Development

The VYCOR membrane reactor used for this study has been sufficient for proving that membrane reactor technology can be of value for ODHD of propylene. However, there is room for improvement of the design of the reactor itself and further work in the following areas is recommended.

1. Investigation of the causes and methods for mitigation of changes in permeability of the membrane reactor with time in service.
2. Reducing the activity and hence extent of propylene conversion in the pores of the membrane reactor.
3. Development of designs or construction methods that will allow for significantly greater pressure on the shell side of the membrane reactor.
4. Investigation of the mechanisms for the reactions in the pores of the membrane reactor.

The most important of these recommendations, from a practical point of view, is the reduction in the activity of the membrane. For the VYCOR reactor to be used in any

practical situation outside of the laboratory the activity must be reduced so that the membrane is almost completely inert.

### 9.2.2 Study of $\text{Bi}_2\text{O}_3$ as a Catalyst

The most outstanding issue from both a theoretical and practical point of view is the understanding of how ODHD products, primarily 1,5-hexadiene, react, both homogeneously and heterogeneously, after formation. This work has indicated that a significant portion of the  $\text{CO}_2$  produced in the ODHD of propylene over  $\text{Bi}_2\text{O}_3$  is produced by oxidation of 1,5-hexadiene. It has also cast some light on the general pathways and kinetics of such reactions. There is, however, still much left to understand and more work is recommended, particularly on degradation of 1,5-hexadiene under typical ODHD of propylene conditions (temperatures, pressures and concentrations of feeds and products). Understanding these reactions will help determine if operating the ODHD reaction at high conversion is even practical.

### 9.2.3 Membrane Reactor Operation

The investigation of the IMPBR mode operation with  $\text{Bi}_2\text{O}_3$  should be continued and extended particularly to situations in which there is little excess oxygen in the system and situations with much higher propylene concentrations than tested in this work. These results will indicate how high the selectivity to the desired products can be. It is also recommended that a model of the process, covering reaction both on the catalyst and in the membrane pores, be developed. At present, such a model would be primarily of theoretical interest, but should commercial application be found for the reactor, it would then be of great practical interest.

It is clear that the CMR mode is not a practical operating mode for ODHD of propylene and this course of research should be pursued no further. However, there may be other oxidative reactions that could benefit from use of the VYCOR reactor in either IMPBR or CMR mode and efforts should be undertaken to determine if such reaction systems exist.

## REFERENCES

- Andrews, J. and Bonnifay, P., The IFP Dimersol process for dimerization of propylene into isohexenes, in *Industrial and Laboratory Alkylations*, ed. by L.F. Albright and A.R. Goldsby, ACS Symp. Ser. **55**, 328-340 (1977)
- Anshits, A.G., Shigapov, A.N., Vereshchagin, S.N. and Shevnin, V.N., Oxidative conversion of methane into C<sub>2</sub> hydrocarbons on silver membrane catalysts, *Kinet. and Catal.*, **30**, 1103 (1989)
- Armor, J.N., Catalysis with permselective inorganic membranes, *Appl. Cat. A*, **49**, 1-25 (1989)
- Azgui, S., Guillaume, F., Taouk, B. and Bordes, E., Competition between molecular and anionic diffusion of oxygen in a catalytic membrane reactor for oxidation reaction, *Cat. Today*, **25**, 391-395 (1995)
- Baker, R.W., Membrane technology, in *Kirk-Othmer Encycl. of Chem. Tech.* 4<sup>th</sup> ed., **16**, 135-193 (1995)
- Balachandran, U., Dusek, J.T., Mieville, R.L., Poeppel, R.B., Kleefisch, M.S., Pei, S., Kobylinski, T.P., Udovich, C.A. and Bose, A.C., Dense ceramic membranes for partial oxidation of methane to syngas, *Appl. Cat.*, **133**, 19-29 (1995)
- Batog, V.N., Pakhomov, V.I., Safronov, G.M. and Fedorov, P.M., Nature of phases with  $\gamma$ -bismuth trioxide structure (sillenite phase), *Izv. Akad. Nauk. SSSR, Neorg. Mater.*, **9**, 1576-1578 (1973)
- Bhave, R.R. (ed.), *Inorganic Membranes: Synthesis, Characteristics and Applications*, Van Nostrand Reinhold, New York (1991)
- Bozik, J.E., Ondrey, J.A. and Swift, H.E., Process for coupling lower olefins, *United States Patent 3,730,957* (1973a)
- Bozik, J.E., Ondrey, J.A. and Swift, H.E., Process for coupling propylene and isobutylene, *United States Patent 3,761,536* (1973b)
- Borges, H., Giroir-Fendler, A., Mirodatos, C., Chanaud, P. and Julbe, A., Catalytic membrane reactor for oxidative coupling of methane. Part II - Catalytic properties of LaOCl membranes, *Cat. Today*, **25**, 377-383 (1995)
- Brauner, N. and Shacham, M., Statistical analysis of linear and non-linear correlation of the Arrhenius equation constants, *Chem. Eng. & Proc.*, **36**, 243-249 (1997)

- Cales, B. and Baumard, J.F., Production of hydrogen by direct thermal decomposition of water with the aid of a semipermeable membrane, *High Temp.-High Press.*, **14**, 681-686 (1982)
- Capanelli, G., Carosini, E., Cavani, F., Monticelli, O. and Trifiro, F., Comparison of the catalytic performance of  $V_2O_5/\gamma-Al_2O_3$  in the oxidehydrogenation of propane to propylene in different reactor configurations: i) packed-bed reactor, ii) monolith-like reactor and iii) catalytic membrane reactor, *Chem. Eng. Sci.*, **51**, 1817-1826 (1996)
- Champagnie, A.M., Tsotsis, T.T., Minet R.G. and Webster, I.A., A high temperature catalytic membrane reactor for ethane dehydrogenation, *Chem. Eng. Sci.*, **45**, 2423-2429 (1990)
- Champagnie, A.M., Tsotsis, T.T., Minet R.G. and Wagner, E., The study of ethane dehydrogenation in a catalytic membrane reactor, *J. Catal.*, **134**, 713-730 (1992)
- Coronas, J., Menédez, M. and Santamaría, J., Methane oxidative coupling using porous ceramic membrane reactors - II. Reaction studies, *Chem. Eng. Sci.*, **49**, 2015-2025 (1994)
- Coronas, J., Menédez, M. and Santamaría, J., Use of a ceramic membrane reactor for the oxidative dehydrogenation of ethane to ethylene and higher hydrocarbons, *Ind. Eng. Chem. Res.*, **34**, 4229-4234 (1995)
- Cubicciotti, D. and Keneshea, F.J., Thermodynamics of vaporization of thallic oxide, *J. Phys. Chem.*, **71**, 808-814 (1967)
- D'Alessandro, A.F. and Mitchell, M.M., Process for the catalytic conversion of olefins to aromatics, *United States Patent 3,830,866* (1974)
- Danielson, P.S., Glass and Glass-Ceramic Core Technology Group, Corning Inc. Ph. 607-974-3308, Private communication, March 3, 1995 (1995)
- Di Cosimo, R., Burrington, J.D. and Grasselli, R.K., Process for effecting oxidative dehydrodimerization, *United States Patent 4,571,443* (1986a)
- Di Cosimo, R., Burrington, J.D. and Grasselli, R.K., Oxidative dehydrodimerization of propylene over a  $Bi_2O_3-La_2O_3$  oxide ion-conductive catalyst, *J. Catal.*, **102**, 234-239 (1986b)
- Driscoll, D.J. and Lunsford, J.H., Kinetic isotope effect in the partial oxidation of propylene over  $Bi_2O_3$ , *J. Phys. Chem.*, **87**, 301-303 (1983)
- Eng, D. and Stoukides, M.J., Catalytic and electrocatalytic methane oxidation with solid oxide membranes, *Catal. Rev. Sci. Eng.*, **33**, 375-412 (1991)

- Ermilova, M.M., Orekhova N.V., Morozova, L.S. and Skakunova, E.V., *Membr. Katal.*, **70** (1985)
- Fenton, T.P., Fischer-Tropsch routes to olefins, *Proc. 8<sup>th</sup> Ethylene Prod. Conf. (vol. 5)*, 591-596 (1996)
- Filbert, A.M. and Hair, M.L., Surface chemistry and corrosion of glass, in *Advances in Corrosion Science and Technology*, ed. by M.G. Fontana and R.W. Staehle, **5**, 1-54 (1976)
- Friedli, H.R., Production of 1,5-hexadienes by catalytic oxidative dehydrodimerization of C<sub>3</sub>-C<sub>4</sub> alkenes, *United States Patent 3,494,972* (1970)
- Friedli, H.R., Oxydehydrodimerization of propylene and isobutylene, *United States Patent 3,769,361* (1973)
- Froment, G.F. and Bischoff, K.B., *Chemical Reactor Design and Analysis*, 2nd ed., Wiley, New York (1990)
- Furneaux, R.C., Davidson, A.P. and Ball, M.D., Porous anodic aluminum oxide membrane catalyst support, *Eur. Patent Appl. 0,244,970* (1987)
- Gamid-Zade, E.G., Mamedov, E.A. and Rizaev, R.G., Oxidative dehydrodimerization of propylene on an oxidic bismuth-tin catalyst. I - Interaction of propylene and oxygen with the catalyst surface, *Kinet. Catal.*, **20**, 328-331 (1979)
- Gavalas, G.R., Megiris, C.E. and Nam, S.W., Deposition of H<sub>2</sub>-permselective SiO<sub>2</sub> films, *Chem. Eng. Sci.*, **44**, 1829-1835 (1989)
- Gilliland, E.R., Baddour, R.F. and Russell, J.L., Rates of flow through microporous solids, *AIChE J.*, **4**, 90-96 (1958)
- Gillot, J., The developing use of inorganic membranes: a historical prospective, in *Inorganic Membranes: Synthesis, Characteristics and Applications*, ed. by R.R. Bhave, Van Nostrand Reinhold, New York, 1-8 (1991)
- Gobina, E. and Hughes, R., Ethane dehydrogenation using a high-temperature catalytic membrane reactor, *J. Memb. Sci.*, **90**, 11-19 (1994)
- Gobina, E., Hou, K. and Hughes, R., Ethane dehydrogenation in a catalytic membrane reactor coupled with a reactive sweep gas, *Chem. Eng. Sci.*, **50**, 2311-2319 (1995)
- Gobina, E. and Hughes, R., Reaction assisted hydrogen transport during catalytic dehydrogenation in a membrane reactor, *Appl. Catal. A*, **137**, 119-127 (1996)
- Graham, T., *Phyl. Trans. Roy. Soc. (London)*, **156**, 399 (1866)

- Greene, P.A., Buyalos, E.J. and Scheirer, D.E., Dehydrodimerization process, *United States Patent 3,494,956* (1970)
- Gryaznov, V.M., Smirnov, V.S. and Slin'ko, M.G., Heterogeneous catalysis with reagent transfer through the selectively permeable catalysts, *Proc. 5th Int. Congr. Catal.*, **2**, 1139-1147 (1973)
- Gryaznov, V.M. and Slin'ko, M.G., Selectivity in catalysis by hydrogen porous membranes, *Faraday Discuss. Chem. Soc.*, **72**, 73-93 (1981)
- Gryaznov, V.M., Vedernikov, V.I. and Gul'yanova, S.G., Participation of oxygen, having diffused through a silver membrane catalyst, in heterogeneous oxidation processes, *Kinet. and Catal.*, **27**, 129-133 (1986)
- Hair, M.L. and Chapman, I.D., Surface composition of porous glass, *J. Amer. Ceram. Soc.*, **49**, 651-654 (1966)
- Hazbun, E.A., Ceramic membrane for hydrocarbon conversion, *United States Patent 4,791,079* (1988)
- Hazbun, E.A., Ceramic membrane and use thereof for hydrocarbon conversion, *United States Patent 4,827,071* (1989)
- Hsieh, H.P., Inorganic membrane reactors, *Cat. Rev.: Sci. and Engg.*, **33**, 1-70 (1991)
- Horiguchi, Y., Hudgins, R.R. and Silveston, P.L., Effect of surface heterogeneity on surface diffusion in microporous solids, *Can. J. Chem. Eng.*, **49**, 76-87 (1971)
- Hwang, S-T. and Kammermeyer, K., Surface diffusion in microporous media, *Can. J. Chem. Eng.*, **44**, 82-89 (1966)
- Ioannides, T. and Gavalas, G.R., Catalytic isobutane dehydrogenation in a dense silica membrane reactor, *J. Memb. Sci.*, **77**, 207-220 (1993)
- Ioannides, T. and Verykios, X.E., Application of a dense silica membrane reactor in the reactions of dry reforming and partial oxidation of methane, *Catal. Lett.*, **36**, 165-169 (1996)
- Itoh, N., A membrane reactor using palladium, *AIChE J.*, **33**, 1576-1578 (1987)
- Itoh, N., Shindo, Y., Haraya, K. and Hakuta, T., A membrane reactor using microporous glass for shifting equilibrium of cyclohexane dehydrogenation, *J. Chem. Eng. Japan*, **21**, 399-404 (1988)
- Itoh, N. and Govind, R., Development of a novel oxidative palladium membrane reactor, *AIChE Symp. Ser. 268*, **85**, 10-17 (1989)



- Itoh, N., Simulation of bifunctional palladium membrane reactor, *J. Chem. Eng. Japan*, **23**, 81-87 (1990)
- Jones, A.L., Olefin conversion process, *United States Patent 3,786,109* (1974)
- Jones, G.W. and Kennedy, R.E., Extinction of propylene flames by diluting with nitrogen and carbon dioxide and some observations on the explosive properties of propylene, *U.S. Bur. Mines Report of Investig. 3395* (1938)
- Julbe, A., Guizard, C., Larbot, A., Cot, L. and Giroir-Fendler, A., The sol-gel approach to prepare candidate microporous inorganic membranes for membrane reactors, *J. Memb. Sci.*, **77**, 137-153 (1993)
- Kaliberdo, L.M., E.A., Tselyutina, M.I., Vaabel', A.S., Kalikhman, V.M. and Shvetsov, B.N., The role of the catalyst lattice oxygen and the gas-phase oxygen in the oxidative dehydrodimerization of propene, *Russ. J Phys. Chem.*, **53**, 843-845 (1979)
- Kameyama, T., Dokiya, M., Fujishige, M., Yokokawa, H. and Fukuda, K., Possibility for effective production of hydrogen from hydrogen sulfide by means of a porous Vycor glass membrane, *Ind. Eng. Chem. Fund.*, **20**, 97-99 (1981)
- Kameyama, T., Dokiya, M., Fujishige, M., Yokokawa, H. and Fukuda, K., Production of hydrogen from hydrogen sulfide by means of selective diffusion membrane, *Int. J. Hydrogen Ener.*, **8**, 5-13 (1983)
- Keller, G.E. and Bhasin, M.M., Synthesis of ethylene via oxidative coupling of methane, I. Determination of active catalysts, *J. Catal.*, **73**, 9-19 (1992)
- Kutuzov, V.M., Tselyutina, M.I., Kaliberdo, L.M. and Vaabel', A.S., Gas-chromatographic analysis of the mixtures of reaction products from the oxidative dehydrodimerization of propylene, *Russ. J. Analyt. Chem.*, **37**, 422-424 (1982)
- Lafarga, D., Santamaría, J., and Menédez, M., Methane oxidative coupling using porous ceramic membrane reactors - I. Reactor development, *Chem. Eng. Sci.*, **49**, 2005-2013 (1994)
- Lewis, K.E. and Steiner, H., Kinetics and mechanism of thermal cyclisation of hexa-1,cis-3,5-triene to cyclohexa-1,3-diene, *J. Chem. Soc.*, 3080 (1964)
- Lin, Y.S. and Burggraaf, A.J., Modelling and analysis of CVD processes in porous media for ceramic composite preparation, *Chem. Eng. Sci.*, **46**, 3067-3080 (1991)
- Lin, Y.S. and Burggraaf, A.J., CVD of solid oxides in porous substrates for ceramics membrane modification, *AIChE J.*, **38**, 445-454 (1992)

- Lipsig, J., Olefin dehydrodimerization, *United States Patent 3,631,216* (1971)
- Mamedov, E.A., Gamid-Zade, E.G. and Rizaev, R.G., Mechanism of oxidative dehydrodimerization of propylene over Bi-Sn oxide catalysts, *React. Kinet. and Catal. Lett.*, **8**, 227-233 (1978a)
- Mamedov, E.A., Vislovskii, V.P. and Aliev, V.S., Role of oxide catalyst acidity in the partial oxidation and oxidative dehydrodimerization of propylene, *Kinet. Catal.*, **19**, 629-632 (1978b)
- Mamedov, E.A., Principles of oxidative dehydrodimerization of olefins on oxide catalysts, *React. Kinet. and Catal. Lett.*, **11**, 11-14 (1979)
- Mamedov, E.A., Gamid-Zade, E.G., Agaev, F.M. and Rizaev, R.G., Oxidative dehydrodimerization of propylene over a bismuth-tin oxide catalyst, *Kinet. Catal.*, **20**, 333-337 (1979)
- Mamedov, E.A., Oxidative dehydrodimerization and cyclisation reactions of unsaturated hydrocarbons in the presence of oxide catalysts, *Russ. Chem. Rev.*, **50**, 291-304 (1981)
- Mamedov, E.A., Keulks, G.W. and Ruzsala, F.A., The oxidative dehydrodimerization of propylene over Bi-Sn oxide catalysts - III. Reduction and temperature programmed reoxidation of the catalyst, *J. Catal.*, **70**, 241-248 (1981)
- Mamedov, E.A. and Pankrat'ev, Y.D., Bond energy of the surface oxygen and activity of oxide catalysts in the oxidative dehydrodimerization of propylene, *Kinet. Catal.*, **23**, 772-776 (1982)
- Mamedov, E.A., Mechanism of oxidative dehydrodimerization of hydrocarbons on oxide catalysts, *Kinet. Catal.*, **25**, 741-746 (1984)
- Martir, W. and Lunsford, J.H., The formation of gas-phase  $\pi$ -allyl radicals from propylene over bismuth oxide and  $\gamma$ -bismuth molybdate catalysts, *J. Am. Chem. Soc.*, **103**, 3728-3732 (1981)
- Massoth, F.E. and Scapiello, D.A., Kinetics of bismuth oxide reduction with propylene, *J. Catal.*, **21**, 225-238 (1971)
- Minet, R.G. and Tsotsis, T.T., Steam reforming process for manufacture of hydrogen, carbon monoxide and carbon dioxide using ceramic membrane catalyst support, *United States Patent 4,981,676* (1991)
- Minet, R.G. and Tsotsis, T.T., Process and apparatus containing a catalytic ceramic membrane for manufacture of hydrogen, carbon monoxide and carbon dioxide by steam reforming of hydrocarbons, *United States Patent 5,229,102* (1993)

- Minet, R.G., Tsotsis, T.T. and Champagnie, A.M., Process for the production of ethylene from ethane, *United States Patent 5,202,517* (1993)
- Modler, R., Anderson, E. and Yoshida, Y., Linear Alpha-Olefins – CEH Marketing Research Report, *Chemical Economics Handbook*, SRI International (1997)
- Nagamoto, H. and Inoue, H., The hydrogenation of 1,3-butadiene over a palladium membrane, *Bull. Chem. Soc. Japan*, **59**, 3935-3939 (1986)
- Nigara, Y. and Cales, B., Production of carbon monoxide by direct thermal splitting of carbon dioxide at high temperature, *Bull. Chem. Soc. Japan*, **59**, 1997-2002 (1986)
- Nozaki, T., Hashimoto, S., Omata, K. and Fujimoto, K., Selective oxidative coupling of methane with membrane reactor, *Chem. Eng. Sci.*, **47**, 2945-2950 (1992)
- Nozaki, T., Yamazaki, O., Omata, K. and Fujimoto, K., Oxidative coupling of methane with membrane reactors containing lead oxide, *Ind. Eng. Chem. Res.*, **32**, 1174-1179 (1993)
- Nozaki, T. and Fujimoto, K., Oxide ion transport for selective oxidative coupling of methane with new membrane reactor, *AIChE J.*, **40**, 870-877 (1994)
- Okazaki, M., Tamon, H. and Toei, R., Interpretation of surface flow phenomenon of adsorbed gases by hopping model, *AIChE J.*, **27**, 262-270 (1981)
- Okubu, T. and Inoue, H., Surface diffusion on modified surface of porous glass, *J. Chem. Eng. Japan*, **20**, 590-597 (1987)
- Omata, K.S., Hashimoto, H., Tominaga, H. and Fujimoto, K., Oxidative coupling of methane using a membrane reactor, *Appl. Catal.*, **52**, L1-L4 (1989)
- Pantazidis, A., Dalmon, J.A. and Mirodatos, C., Oxidative dehydrogenation of propane on catalytic membrane reactors, *Cat. Today*, **25**, 403-408 (1995)
- Pillai, S.M., Ravindranathan, M. and Sivaram, S., Dimerization of ethylene and propylene catalyzed by transition-metal complexes, *Chemical Reviews*, **86**, 353-399 (1986)
- Ramachandra, A.M., Lu, Y., Ma, Y.H., Moser, W.R. and Dixon, A.G., Oxidative coupling of methane in porous Vycor membrane reactors, *J. Memb. Sci.*, **116**, 253-264 (1996)
- Ramaroson, E., Blanchard, G., Che, M. and Tatibouët, J.M., Oxidative dimerization of propene to 1,5-hexadiene on Bi-Zn-O catalysts, *Cat. Lett.*, **15**, 393-400 (1992)

- Raskó, J., Periera, P., Somorjai, G.A. and Heinemann, H., The catalytic low temperature oxydehydrogenation of methane. Temperature dependence, carbon balance and effects of catalyst composition, *Cat. Lett.*, **9**, 395-402 (1991)
- Saracco, G. and Specchia, V., Catalytic inorganic membrane reactors: Present experience and future opportunities, *Cat. Rev.: Sci. and Engg.*, **36**, 305-384 (1994)
- Schnabel, R. and Vaulont, W., High pressure techniques with porous glass membranes, *Desalination*, **24**, 249-272 (1978)
- Seiyama, T., Sakamoto, T. and Egashira, M., New catalytic aromatization of lower olefins over bismuth phosphate catalyst, *J. Catal.*, **2**, 407-409 (1970)
- Seiyama, T., Yamazoe, N. and Egashira, M., Allylic oxidations of olefins over metal or metal oxide catalysts, *Proc. 5th Int. Congr. Catal.*, **2**, 997-1010 (1972a)
- Seiyama, T., Egashira, M., Sakamoto, T. and Aso, I., Oxidative dehydroaromatization - II. Oxidation of propylene over binary oxide catalysts containing bismuth or tin, *J. Catal.*, **24**, 76-81 (1972b)
- Seiyama, T., Uda, T., Mochida, I. and Egashira, M., Oxidative dehydroaromatization - III. The mechanism of oxidative dehydrodimerization process of C<sub>3</sub>-C<sub>4</sub> olefins over Bi<sub>2</sub>O<sub>3</sub>-SnO<sub>2</sub> catalyst, *J. Catal.*, **34**, 29-34 (1974)
- Sheintuch, M. and Dessau, R.M., Observations, modeling and optimization of yield, selectivity and activity during dehydrogenation of isobutane and propane in a Pd membrane reactor, *Chem. Eng. Sci.*, **51**, 535-547 (1996)
- Shelekhin, A.B., Pien, S. and Ma, Y.H., Permeability, surface area, pore volume and pore size of Vycor glass membrane heat-treated at high temperatures, *J. Memb. Sci.*, **103**, 39-43 (1995)
- Shindo, Y., Obata, K., Hakuta, T., Yoshitome, H., Todo, N. and Kato, J., Permeation of hydrogen through a porous Vycor glass membrane, *Adv. Hydrogen Ener.*, **2**, 325-333 (1981)
- Shindo, Y., Hakuta, T., Yoshitome, H. and Inoue, H., Gas diffusion in microporous media in Knudsen's regime, *J. Chem. Eng. Japan*, **16**, 120-126 (1983)
- Shindo, Y., Hakuta, T., Yoshitome, H. and Inoue, H., Separation of gases by means of a porous glass membrane at high temperatures, *J. Chem. Eng. Japan*, **17**, 650-652 (1984)
- Shinji, O., Misono, M. and Yoneda, Y., The dehydrogenation of cyclohexane by the use of a porous glass reactor, *Bull. Chem. Soc. Japan*, **55**, 2760-2764 (1982)

- Shu, J., Grandjean, B.P.A., van Neste, A. and Kaliaguine, S., Catalytic palladium-based membrane reactors: A review, *Can. J. Chem. Eng.*, **69**, 1036-1060 (1991)
- Sing, K.S.W., Everett, D.H., Haul, R.A.W., Moscou, L., Pierotti, R.A., Rouquerol, J. and Siemieniewska, T., Reporting physisorption data for gas/solid systems with special reference to the determination of surface area and porosity, *Pure and Appl. Chem.*, **57**, 603-619 (1985)
- Sloot, H.J., Smolders, C.A., van Swaaij, W.P.M. and Versteeg, G.F., High temperature membrane reactors for catalytic gas-solid reactions, *AIChE J.*, **38**, 887-900 (1992)
- Sokolovskii, V.D. and Bulgakov, N.N., Prediction of the catalytic action of oxide catalysts in allyl oxidation of propylene, *React. Kinet. and Catal. Lett.*, **6**, 65-72 (1977)
- Sokolovskii, V.D. and Mamedov, E.A., Oxidative coupling of hydrocarbons, *Cat. Today*, **14**, 331-486 (1992)
- Solymosi, F. and Bozsó, F., The oxidative dehydrodimerization and aromatization of propylene on SnO<sub>2</sub>-Bi<sub>2</sub>O<sub>3</sub> binary oxides, *Proc. 6th Int. Congr. Catal.*, **1**, 365-375 (1977)
- Sun, Y.M. and Khang, S.J., Catalytic membrane for simultaneous chemical reaction and separation applied to a dehydrogenation reaction, *Ind. Eng. Chem. Res.*, **27**, 1136-1142 (1988)
- Swift, H.E., Bozik, J.E. and Ondrey, J.A., Dehydrodimerization of propylene using bismuth oxide as the oxidant, *J. Catal.*, **21**, 212-224 (1971)
- Téllez, C., Menéndez, M. and Santamaría, J., Oxidative dehydrogenation of butane using membrane reactors, *AIChE J.*, **43**, 777-784 (1997)
- Tonkovich, A.L.Y., Secker, R.B., Reed, E.L., Roberts, G.L. and Cox, J.L., Membrane reactor/separator: A design for bimolecular reactant addition, *Sep. Sci. Tech.*, **30**, 1609-1624 (1995)
- Tonkovich, A.L.Y., Zilka, J.L., Jimenez, D.M., Roberts, G.L. and Cox, J.L., Experimental investigations of inorganic membrane reactors: a distributed feed approach for partial oxidation reactions, *Chem. Eng. Sci.*, **51**, 789-806 (1996a)
- Tonkovich, A.L.Y., Jimenez, D.M., Zilka, J.L. and Roberts, G.L., Inorganic membrane reactors for the oxidative coupling of methane, *Chem. Eng. Sci.*, **51**, 3051-3056 (1996b)
- Treybal, R.E., *Mass Transfer Operations*, 3rd ed., McGraw-Hill, New York (1980)

- Trimm, D.L. and Doerr, L.A., The catalytic oxidation of propene to hexa-1,5-diene and to benzene, *J. Chem. Soc. - Chem. Comm.*, 1303 (1970)
- Trimm, D.L. and Doerr, L.A., The catalytic oxidative dimerization of propylene, *J. Catal.*, **23**, 49-53 (1971)
- Trimm, D.L. and Doerr, L.A., The catalytic oxidative dimerization of propylene to benzene, *J. Catal.*, **26**, 1-10 (1972)
- Tsotsis, T.T., Champagnie, A.M., Vasileiadis S.P., Ziaka, Z.D. and Minet R.G., Packed bed catalytic membrane reactors, *Chem. Eng. Sci.*, **47**, 2903-2908 (1992)
- Tsotsis, T.T., Champagnie, A.M., Vasileiadis S.P., Ziaka, Z.D. and Minet R.G., Enhancement of reaction yield through the use of high temperature membrane reactor, *Sep. Sci. Tech.*, **28**, 397-2908 (1993)
- Uemiya, S., Sato, N., Ando, H. and Kikuchi, E., The water-gas shift reaction assisted by a palladium membrane reactor, *Appl. Catal.*, **67**, 223-230 (1991a)
- Uemiya, S., Sato, N., Ando, H., Matsuda, T. and Kikuchi, E., Steam reforming of methane in a hydrogen-permeable membrane reactor, *Ind. Eng. Chem. Res.*, **30**, 585-589 (1991b)
- Uhlhorn, R.J.R. and Burggraaf, A.J., Gas separations with inorganic membranes, in *Inorganic Membranes: Synthesis, Characteristics and Applications*, ed. by R.R. Bhave, Van Nostrand Reinhold, New York, 155-176 (1991)
- Uhlhorn, R.J.R., Keizer, K. and Burggraaf, A.J., Gas transport and separation with ceramic membranes. Part I: Multilayer diffusion and capillary condensation, *J. Memb. Sci.*, **66**, 259-269 (1992a)
- Uhlhorn, R.J.R., Keizer, K. and Burggraaf, A.J., Gas transport and separation with ceramic membranes. Part II. Synthesis and separation properties of microporous membranes., *J. Memb. Sci.*, **66**, 271-287 (1992b)
- Uhlhorn, R.J.R., Huis in't Veld, M.H.B.J., Keizer, K. and Burggraaf, A.J., Synthesis of ceramic membranes. Part 1 Synthesis of non-supported and supported gamma-alumina membranes without defects, *J. Mater. Sci.*, **27**, 527-537 (1992c)
- Vaabel', A.S., *USSR Patent 411066* (1974a)
- Vaabel', A.S., Kaliberdo, L.M., Dubenkova, L.B. and Kuvakina, P.R., Dehydrodimerization of propylene on bismuth-phosphorus oxide catalysts, *Neftekhim.*, **14**, 598-604 (1974b)

- Vermel', Y.Y., Kabakova, B.V. and Stukova, R.N., Oxidation of propylene with silver catalysts, *Neftekhim.*, **13**, 88-93 (1973)
- Wang, L., Duan, Y. and Zhao, Q., Catalytic behavior of Bi-containing binary oxides in the oxidative dehydrodimerization of propylene, *Ranliao Huaxue Xuebao*, **16**, 59-67 (1988)
- Wang, L., Duan, Y. and Zhao, Q., Kinetics of oxidative dehydrodimerization of propylene over bismuth-cerium binary oxide catalysts, *Yingyong Huaxue*, **6**, 69-72 (1989)
- Wang, W. and Lin, Y.S., Analysis of oxidative coupling of methane in dense oxide membrane reactors, *J. Memb. Sci.*, **103**, 219-233 (1995)
- Watts, D.G., Estimating parameters in nonlinear rate equations, *Can. J. Chem. Eng.*, **72**, 701-710 (1994)
- White, M.G. and Hightower, J.W., Properties of bismuth oxide catalysts for oxidative dehydrogenation dimerization of propylene, *AIChE J.*, **27**, 545-551 (1981)
- White, M.G. and Hightower, J.W., Oxidative dehydrogenation dimerization of propylene over bismuth oxide: kinetic and mechanistic study, *J. Catal.*, **82**, 185-195 (1983)
- Wu, J.C.S., Gerdes, T.E., Pszezolkowski, J.L., Bhave, R.R. and Liu, P.K.T., Dehydrogenation of ethylbenzene to styrene using commercial ceramic membranes as reactors, *Sep. Sci. Tech.*, **25**, 1489-1510 (1990)
- Zabetakis, M.G., *Flammability Characteristics of Combustible Gases and Vapours*, U.S. Bureau of Mines Bulletin 627 (1965)
- Zaman, J. and Chakma, A., Inorganic membrane reactors, *J. Memb. Sci.*, **92**, 1-28 (1994)
- Zaspalis, V.T., van Praag, W., Keizer, K., van Ommen, J.G., Ross, J.H.R. and Burggraaf, A.J., Reactor studies using vanadia modified titania and alumina catalytically active membranes for the reaction of nitrogen oxide with ammonia, *Appl. Catal.*, **74**, 249-260 (1991)
- Zhao, R., Itoh, N. and Govind, R., Novel oxidative membrane reactor for dehydrogenation reactions, in *Novel Materials in Heterogeneous Catalysis (ACS Symp. Ser. 437)*, Baker, R.T.K. and Murrell, L.L. (eds), 216-230 (1990)
- Ziaka, Z.D., Minet, R.G. and Tsotsis, T.T., Propane dehydrogenation in a packed bed membrane reactor, *AIChE J.*, **39**, 526-529 (1993a)
- Ziaka, Z.D., Minet, R.G. and Tsotsis, T.T., A high temperature catalytic membrane reactor for propane dehydrogenation, *J. Memb. Sci.*, **77**, 221-232 (1993b)

**Appendix A**  
**Working with Porous VYCOR Glass**



## **1. Introduction**

Porous VYCOR glass (Corning Code 7930) is used in this research as a membrane material for membrane reactors. The use of porous VYCOR as a membrane material in membrane reactors is not particularly widespread, although it is becoming more common. The use of porous VYCOR that has been chemically and/or physically treated to alter the membrane properties is less common and explicit information on glass working techniques for porous VYCOR are almost non-existent in the open literature. Even the Corning Corporation does not seem to be a storehouse of information on the latter point.

The material in this appendix is intended as formal documentation of some of the tips, tricks and techniques for working with porous VYCOR that have been garnered during the course of this thesis research project. Many of the points of information and techniques may seem to be very simple, but they either involve areas not previously explored in research available in the open literature or simply have not been documented when research has been carried out. During this research, the learning curve with respect to working with the VYCOR material has been particularly steep. It is hoped that this documentation will help others in the field when they are presented with similar situations.

## **2. Physical Aspects of Working with Porous VYCOR**

Porous VYCOR has reasonable mechanical strength, but it is not nearly as resistant to cracking and breakage as a normal quartz glass. The reason, of course, is the extensive and very fine pore structure that gives the material an overall porosity of approximately 28%. Cracks propagate much more freely in porous VYCOR and this problem is exacerbated by either thermal or mechanical stress on the material. If a crack develops, the affected portion cannot simply be cut off or removed by torch as per other standard glass working techniques.

At issue here is how to best stabilize porous VYCOR and how to be able to cut the material whether it is to prevent crack propagation or simply because a smaller piece of material is required. Corning suggests that porous VYCOR be stored in de-ionized water to prevent contamination. However, they fail to mention that when the pores are filled with water the mechanical strength and stability of the material is much higher than when it is dry. It has been found that soaking the VYCOR in de-ionized water is necessary before any room temperature cutting operation can occur, but that this treatment gives the VYCOR the necessary strength to undergo the mechanical rigours of the cutting process. Corning indicates that rapid wetting (or drying) of large pieces of porous VYCOR will often lead to breakage of the pieces. The experience in this research indicates otherwise. Approximately metre long pieces of VYCOR are routinely completely and rapidly submersed in aqueous media with no problems with breakage. The process of water infiltration into the pores takes 0.5-1 hour for pieces of this size. The process is complete when gas bubbles can no longer be seen coming from the VYCOR.

Cutting of unwetted VYCOR is almost impossible. Cutting of wetted VYCOR is still a delicate operation, but with proper care not to impart any undue mechanical stress on the glass it is highly successful. The recommended cutting tool is a circular glass cutting wheel using a silicon carbide blade. The piece being cut must be fully supported on both sides of the cut and must be firmly held in place as it passes through the blade. Any "chattering" or movement of the glass laterally with respect to the blade increases the chances of shattering the glass.

### **3. Techniques for the Treatment of Porous VYCOR in Aqueous Media and in Superheated Steam**

Part of the development work in this project involved finding effective methods for treating the VYCOR membrane to change its surface acidity characteristics. Ultimately this work led to the treatment in sodium hydroxide followed by treatment with high temperature steam as described in Chapter 4. Many potential treatments involve treating the membrane in an aqueous medium. As noted in section 2 of this appendix the

VYCOR can be rapidly submerged in water without deleterious effects. However, for a treatment where some chemical reaction is to be carried out between the VYCOR surfaces (pores) and a species in the aqueous medium to be successful a number of guidelines must be followed. Diffusion of species into the VYCOR pores is not rapid owing to the small pore size. Thus sufficient time is necessary to allow any such diffusion to occur. Typically 16 hours has been allowed for the treatments described in this thesis. Getting any residual chemical back out of the pores is an even more time consuming process. The removal of residual NaOH from the pores of the VYCOR during the treatment process described in Chapter 4 takes almost 7 days and requires frequent replacement of the water used to remove the hydroxide.

In this research the treatment and washing steps take place as batch processes (in a beaker). To help enhance the rate of diffusion however, it is necessary that all VYCOR surfaces are equally exposed to the medium and that the medium is not stagnant. In this research the VYCOR tubes are suspended in the aqueous medium ensuring that there is minimal contact between the VYCOR and the string or wire used to suspend it (so that none of the surface is prevented from having access to the medium). The medium is constantly stirred by means of a magnetic stirrer. Failure to do both steps can result in incomplete or non-uniform treatment. On a larger scale some sort of continuous flow system in which the VYCOR is placed will likely work well.

The hydroxide treatment used in the research takes place at room temperature. Other treatments in boiling media have been suggested, but working under these conditions presents other problems. The fine, but extensive, pore structure of the VYCOR tends to promote explosive boiling in water. Experience in this research effort has indicated that the sort of boiling, particularly in confined spaces such as a beaker, will likely result in damage to the VYCOR pieces.

Drying of wetted VYCOR must occur slowly. The VYCOR can be air dried or dried in a flowing gas stream. For this research the bulk of the drying occurred at room temperature (the process takes several hours), but Corning indicates that drying at

temperatures up to 60°C is feasible. Rapid drying can lead to cracking of the glass due to thermal stress. One can tell when the material is sufficiently dry by visual observation. When VYCOR is fully wetted (submerged) it is clear. As it is removed from water and begins to dry it becomes white (opaque) and remains so until most of the water is removed. When the VYCOR is finally at or close to equilibrium with the surrounding air it becomes clear again.

The treatment in superheated steam is relatively simple. The same rules apply as in aqueous media. The entire VYCOR surface must be exposed to the steam and the steam must not be stagnant. In this research steaming occurs in a flowing system in which saturated steam is fed through a holding tube in which the VYCOR piece is placed. The holding tube is inside a process furnace so the furnace serves to superheat the steam. The VYCOR is placed on small wads of quartz wool to ensure that a significant surface area is not directly touching the wall of the holding tube. The important thing to bear in mind is that conditions must be maintained so that no subcooled liquid can contact the VYCOR. This was occasionally a problem in the small furnace used for this research. The effect is that the VYCOR cracks due to a combination of thermal shock and rapid expansion of the water as it is drawn into the pores and vapourized.

#### **4. The Shrink Wrap Construction Method**

Thermal glass working using porous VYCOR is delicate a business at the best of times and working with the treated material used in this research is particularly difficult. Many of the problems have been outlined in Chapter 4. The success of the shrink wrap technique came after extensive experimentation and numerous failures. It is a relatively simple procedure and should be easily completed by anyone who is skilled in the art and techniques of glass blowing. The key to the procedure (and really to any glass blowing procedures involving porous VYCOR) is to minimize thermal stress on the VYCOR. This point cannot be stressed enough - it is thermal stress that most often leads to failure.

The shrink wrap technique is outlined below.

- A. On one side of the glass lathe the quartz piece (with the inner sleeve section already prepared) is placed and on the other side the VYCOR piece is placed (supported on another piece of quartz if necessary).
- B. A quartz heat shield is placed around the VYCOR piece and the lathe is turned on.
- C. The VYCOR is heated first to approximately 300°C by application of a natural gas/air flame to the outside of the heat shield. The heat shield basically serves to make the inner section of the shield behave as a furnace in which the VYCOR can be heated without exposing it to direct flame. This process takes about 10 minutes.
- D. The second heating step is completed using a natural gas/oxygen flame on the outside of the heat shield. This step must be carried out carefully so that the VYCOR is not heated too rapidly or to too high a temperature. The aim is to heat the VYCOR to approximately 600°C. This temperature is about as high as the treated VYCOR can comfortably be heated without danger of changing the pore structure of the material. Success in this step really depends on the experience of the glass blower.
- E. When the VYCOR is appropriately heated the flame and heat shield are quickly removed. It is essential that the following steps occur rapidly so that the VYCOR is not allowed to cool. Allowing the VYCOR to cool will dramatically increase the potential for thermal stresses to crack the VYCOR.
- F. Slide the quartz sleeve (which should also be pre-heated to some degree) into the VYCOR in preparation for sealing the joint. The lathe must remain on to ensure that the two pieces are perfectly aligned.
- G. Rapidly heat the section of VYCOR that must be collapsed around the quartz sleeve by direct contact with a natural gas/oxygen flame. The collapse of the VYCOR will occur naturally and very rapidly. Shaping tools are not necessary and besides, they often lead to cracking (cold tools). No more direct flame than is necessary should be used and it should only be applied to

the limited area of the VYCOR which needs to be collapsed. Bubbling of the VYCOR will occur at its edge but it should have no effect on the joint.

- H. Joints must be manufactured one at a time and the full procedure should be repeated for each joint.

## **Appendix B**

### **Blank Membrane Reactor Reaction Data**

## List of Tables in Appendix B

Table B1 - Blank Membrane Reactor Test Data (250 sccm Total Feed Flow Rate, 20 mol% Propylene and 6 mol% Oxygen in Feed).....	251
Table B2 - Blank Membrane Reactor Test Data (250 sccm Total Feed Flow Rate, 20 mol% Propylene and 4 mol% Oxygen in Feed).....	252
Table B3 - Blank Membrane Reactor Test Data (250 sccm Total Feed Flow Rate, 20 mol% Propylene and 3 mol% Oxygen in Feed).....	253
Table B4 - Blank Membrane Reactor Test Data (250 sccm Total Feed Flow Rate, 15 mol% Propylene and 6 mol% Oxygen in Feed).....	254
Table B5 - Blank Membrane Reactor Test Data (250 sccm Total Feed Flow Rate, 15 mol% Propylene and 4 mol% Oxygen in Feed).....	255
Table B6 - Blank Membrane Reactor Test Data (250 sccm Total Feed Flow Rate, 15 mol% Propylene and 3 mol% Oxygen in Feed).....	256
Table B7 - Blank Membrane Reactor Test Data (250 sccm Total Feed Flow Rate, 10 mol% Propylene and 6 mol% Oxygen in Feed).....	257
Table B8 - Blank Membrane Reactor Test Data (250 sccm Total Feed Flow Rate, 10 mol% Propylene and 4 mol% Oxygen in Feed).....	258
Table B9 - Blank Membrane Reactor Test Data (250 sccm Total Feed Flow Rate, 10 mol% Propylene and 3 mol% Oxygen in Feed).....	259
Table B10 - Blank Membrane Reactor Test Data (187.5 sccm Total Feed Flow Rate, 20 mol% Propylene and 6 mol% Oxygen in Feed).....	260
Table B11 - Blank Membrane Reactor Test Data (187.5 sccm Total Feed Flow Rate, 20 mol% Propylene and 4 mol% Oxygen in Feed).....	261
Table B12 - Blank Membrane Reactor Test Data (187.5 sccm Total Feed Flow Rate, 20 mol% Propylene and 3 mol% Oxygen in Feed).....	262
Table B13 - Blank Membrane Reactor Test Data (187.5 sccm Total Feed Flow Rate, 15 mol% Propylene and 6 mol% Oxygen in Feed).....	263
Table B14 - Blank Membrane Reactor Test Data (187.5 sccm Total Feed Flow Rate, 15 mol% Propylene and 4 mol% Oxygen in Feed).....	264



## List of Tables in Appendix B (cont'd)

Table B15 - Blank Membrane Reactor Test Data (187.5 sccm Total Feed Flow Rate, 15 mol% Propylene and 3 mol% Oxygen in Feed).....	265
Table B16 - Blank Membrane Reactor Test Data (187.5 sccm Total Feed Flow Rate, 10 mol% Propylene and 6 mol% Oxygen in Feed).....	266
Table B17 - Blank Membrane Reactor Test Data (187.5 sccm Total Feed Flow Rate, 10 mol% Propylene and 4 mol% Oxygen in Feed).....	267
Table B18 - Blank Membrane Reactor Test Data (187.5 sccm Total Feed Flow Rate, 10 mol% Propylene and 3 mol% Oxygen in Feed).....	268
Table B19 - Blank Membrane Reactor Test Data (125 sccm Total Feed Flow Rate, 20 mol% Propylene and 6 mol% Oxygen in Feed).....	269
Table B20 - Blank Membrane Reactor Test Data (125 sccm Total Feed Flow Rate, 20 mol% Propylene and 4 mol% Oxygen in Feed).....	270
Table B21 - Blank Membrane Reactor Test Data (125 sccm Total Feed Flow Rate, 20 mol% Propylene and 3 mol% Oxygen in Feed).....	271
Table B22 - Blank Membrane Reactor Test Data (125 sccm Total Feed Flow Rate, 15 mol% Propylene and 6 mol% Oxygen in Feed).....	272
Table B23 - Blank Membrane Reactor Test Data (125 sccm Total Feed Flow Rate, 15 mol% Propylene and 4 mol% Oxygen in Feed).....	273
Table B24 - Blank Membrane Reactor Test Data (125 sccm Total Feed Flow Rate, 15 mol% Propylene and 3 mol% Oxygen in Feed).....	274
Table B25 - Blank Membrane Reactor Test Data (125 sccm Total Feed Flow Rate, 10 mol% Propylene and 6 mol% Oxygen in Feed).....	275
Table B26 - Blank Membrane Reactor Test Data (125 sccm Total Feed Flow Rate, 10 mol% Propylene and 4 mol% Oxygen in Feed).....	276
Table B27 - Blank Membrane Reactor Test Data (125 sccm Total Feed Flow Rate, 10 mol% Propylene and 3 mol% Oxygen in Feed).....	277

Table B1 - Blank Membrane Reactor Test Data  
 (250 sccm Total Feed Flow Rate, 20 mol% Propylene and 6 mol% Oxygen in Feed)

Total Flow Rate =		250 sccm											
Feed Concentrations (%)													
Propylene =		20											
Oxygen =		6											
Temperature (furnace) (°C)		490.0		510.0		530.0		550.0					
Temperature (reactor bed)(°C)		490.1		510.7		530.8		550.5					
Propylene conversion (%)		2.56		3.04		3.45		3.84					
Oxygen conversion (%)		26.9		32.7		38.4		42.3					
Propylene Selectivity (%)													
CO		53.7	1.375	2.062	51.2	1.556	2.335	46.1	1.590	2.386	40.2	1.544	2.316
CO <sub>2</sub>		36.9	0.945	1.417	39.2	1.192	1.788	43.8	1.511	2.267	47.8	1.836	2.753
C <sub>2</sub>		2.7	0.069	0.052	2.9	0.088	0.066	3.0	0.104	0.078	3.1	0.119	0.089
Acrolein		4.6	0.118	0.059	4.3	0.131	0.065	4.1	0.141	0.071	5.1	0.196	0.098
1,5-HD		2.1	0.054	0.013	2.4	0.073	0.018	3.0	0.104	0.026	3.8	0.146	0.036
Propylene converted (sccm)		1.28		1.52		1.73		1.92		2.16		2.316	
Oxygen converted (sccm)		4.04		4.91		5.76		6.35		6.96		7.53	

Table B2 - Blank Membrane Reactor Test Data  
(250 sccm Total Feed Flow Rate, 20 mol% Propylene and 4 mol% Oxygen in Feed)

Total Flow Rate =		250 sccm	
Feed Concentrations (%)			
Propylene =	20		
Oxygen =	4		
Temperature (furnace) (°C)	490.0	510.0	530.0
Temperature (reactor bed)(°C)	488.4	508.6	528.4
Propylene conversion (%)	2.10	2.46	2.76
Oxygen conversion (%)	33.2	38.9	44.8
			3.08
			50.7
Propylene Selectivity (%)			
CO	55.6	1.168	1.751
		1.314	1.970
CO <sub>2</sub>	36.2	0.760	1.140
		0.925	1.387
C <sub>2</sub>	2.7	0.057	0.043
		0.071	0.054
Acrolein	3.5	0.074	0.037
		0.093	0.047
1,5-HD	2.0	0.042	0.011
		0.057	0.014
		2.3	0.019
		2.7	0.019
		3.3	0.102
		43.5	1.340
		45.5	1.401
		3.2	0.099
		4.5	0.139
		3.3	0.102
		2.045	2.010
		1.714	2.102
		0.062	0.074
		0.048	0.069
		0.019	0.025
Propylene converted (sccm)			
		1.23	1.38
Oxygen converted (sccm)		3.89	4.48
			1.54
			5.07

Table B3 - Blank Membrane Reactor Test Data  
(250 sccm Total Feed Flow Rate, 20 mol% Propylene and 3 mol% Oxygen in Feed)

Total Flow Rate =		250 sccm										
Feed Concentrations (%)												
Propylene =		20										
Oxygen =		3										
Temperature (furnace) (°C)		490.0		510.0		530.0		550.0				
Temperature (reactor bed)(°C)		490.0		510.0		529.6		549.5				
Propylene conversion (%)		1.89		2.07		2.33		2.54				
Oxygen conversion (%)		42.4		47.0		53.2		58.8				
Propylene Selectivity (%)												
CO		59.4	1.123	1.684	1.702	1.134	1.165	50.0	1.748	44.2	1.123	1.684
CO <sub>2</sub>		34.7	0.656	0.984	1.211	0.807	1.004	43.1	1.506	47.4	1.204	1.806
C <sub>2</sub>		2.3	0.043	0.033	0.034	0.046	0.049	2.1	0.037	2.2	0.056	0.042
Acrolein		2.3	0.043	0.022	0.026	0.052	0.068	2.9	0.034	3.8	0.097	0.048
1,5-HD		1.3	0.025	0.006	0.008	1.5	0.031	1.9	0.011	2.4	0.061	0.015
Propylene converted (sccm)		0.95		1.04		1.17		1.27				
Oxygen converted (sccm)		3.18		3.53		3.99		4.41				

Table B4 - Blank Membrane Reactor Test Data  
 (250 sccm Total Feed Flow Rate, 15 mol% Propylene and 6 mol% Oxygen in Feed)

Total Flow Rate = 250 sccm												
Feed Concentrations (%)												
Propylene =	15											
Oxygen =	6											
Temperature (furnace) (°C)	490.0	510.0	530.0	550.0								
Temperature (reactor bed)(°C)	488.7	509.1	528.9	548.8								
Propylene conversion (%)	2.12	2.52	2.89	3.20								
Oxygen conversion (%)	17.7	21.1	25.0	27.4								
Propylene Selectivity (%)	Propylene Yield to Product (%)	Product Effluent Flow (sccm)	Propylene Yield to Product (%)	Product Effluent Flow (sccm)	Propylene Yield to Product (%)	Product Effluent Flow (sccm)						
CO	55.9	1.185	1.333	51.7	1.303	1.466	42.8	1.237	1.392	36.8	1.178	1.325
CO <sub>2</sub>	34.9	0.740	0.832	38.7	0.975	1.097	46.5	1.344	1.512	50.6	1.619	1.822
C <sub>2</sub>	2.5	0.053	0.030	2.6	0.066	0.037	2.7	0.078	0.044	3.0	0.096	0.054
Acrolein	4.6	0.098	0.037	4.1	0.103	0.039	4.1	0.118	0.044	4.4	0.141	0.053
1,5-HD	2.1	0.045	0.008	2.9	0.073	0.014	3.9	0.113	0.021	5.2	0.166	0.031
Propylene converted (sccm)		0.80	0.95			1.08						1.20
Oxygen converted (sccm)		2.66	3.17			3.75						4.11

Table B5 - Blank Membrane Reactor Test Data  
(250 sccm Total Feed Flow Rate, 15 mol% Propylene and 4 mol% Oxygen in Feed)

Total Flow Rate =		250 sccm											
Feed Concentrations (%)													
Propylene =	15												
Oxygen =	4												
Temperature (furnace) (°C)	490.0	510.0	530.0	550.0									
Temperature (reactor bed)(°C)	488.1	508.1	527.6	547.3									
Propylene conversion (%)	2.02	2.40	2.64	2.92									
Oxygen conversion (%)	25.5	30.4	34.3	38.0									
Propylene Selectivity (%)													
	Propylene Yield to Product (%)	Product Effluent Flow (sccm)	Propylene Yield to Product (%)	Product Effluent Flow (sccm)									
CO	57.8	1.168	1.314	1.485	55.0	1.320	1.485	48.0	1.267	1.426	40.1	1.171	1.317
CO <sub>2</sub>	34.5	0.697	0.784	1.013	37.5	0.900	1.013	43.5	1.148	1.292	49.2	1.437	1.616
C <sub>2</sub>	2.5	0.051	0.028	0.032	2.4	0.058	0.032	2.5	0.066	0.037	2.6	0.076	0.043
Acrolein	3.6	0.073	0.027	0.031	3.4	0.082	0.031	3.6	0.095	0.036	5.1	0.149	0.056
1,5-HD	1.6	0.032	0.006	0.008	1.7	0.041	0.008	2.4	0.063	0.012	3.0	0.088	0.016
Propylene converted (sccm)	0.76		0.90		0.99		1.10						
Oxygen converted (sccm)	2.55		3.04		3.43		3.80						

Table B6 - Blank Membrane Reactor Test Data  
(250 sccm Total Feed Flow Rate, 15 mol% Propylene and 3 mol% Oxygen in Feed)

Total Flow Rate =		250 sccm						
Feed Concentrations (%)								
Propylene =	15							
Oxygen =	3							
Temperature (furnace) (°C)	490.0	510.0	530.0					
Temperature (reactor bed)(°C)	489.1	509.1	548.8					
Propylene conversion (%)	1.78	2.00	2.47					
Oxygen conversion (%)	30.3	34.5	43.3					
Propylene Selectivity (%)								
CO	57.2	1.145	1.202	49.0	1.213	43.2	1.067	1.200
CO <sub>2</sub>	35.8	0.637	0.717	39.7	0.893	43.6	0.959	1.312
C <sub>2</sub>	2.4	0.043	0.024	2.2	0.044	2.3	0.051	0.033
Acrolein	2.9	0.052	0.019	3.0	0.060	3.0	0.066	0.044
1,5-HD	1.7	0.030	0.006	1.7	0.034	2.1	0.046	0.012
Propylene converted (sccm)	0.67		0.75		0.83		0.93	
Oxygen converted (sccm)	2.27		2.59		2.90		3.25	





Table B8 - Blank Membrane Reactor Test Data  
(250 sccm Total Feed Flow Rate, 10 mol% Propylene and 4 mol% Oxygen in Feed)

Total Flow Rate =		250 sccm								
Feed Concentrations (%)										
Propylene =	10									
Oxygen =	4									
Temperature (furnace) (°C)	490.0	510.0	530.0	550.0						
Temperature (reactor bed)(°C)	488.0	508.0	527.5	547.5						
Propylene conversion (%)	1.91	2.22	2.48	2.70						
Oxygen conversion (%)	16.2	19.2	21.8	24.3						
Propylene Selectivity (%)										
	Propylene Yield to Product (%)	Product Effluent Flow (sccm)	Propylene Yield to Product (%)	Product Effluent Flow (sccm)						
CO	59.9	1.144	0.858	0.914	44.9	1.114	0.835	36.4	0.983	0.737
CO <sub>2</sub>	31.2	0.596	0.447	0.583	44.4	1.101	0.826	50.9	1.374	1.031
C <sub>2</sub>	2.4	0.046	0.017	0.020	2.4	0.053	0.022	2.6	0.070	0.026
Acrolein	4.1	0.078	0.020	0.025	4.1	0.102	0.025	4.6	0.124	0.031
1,5-HD	2.4	0.046	0.006	0.009	4.2	0.104	0.013	5.5	0.149	0.019
Propylene converted (sccm)	0.48		0.56		0.62		0.68			
Oxygen converted (sccm)	1.62		1.92		2.18		2.43			

Table B9 - Blank Membrane Reactor Test Data  
(250 sccm Total Feed Flow Rate, 10 mol% Propylene and 3 mol% Oxygen in Feed)

Total Flow Rate =		250 sccm	
Feed Concentrations (%)			
Propylene =	10		
Oxygen =	3		
Temperature (furnace) (°C)	490.0	510.0	530.0
Temperature (reactor bed)(°C)	488.0	508.1	547.5
Propylene conversion (%)	1.85	2.08	2.54
Oxygen conversion (%)	21.4	24.6	30.5
Propylene Selectivity (%)			
	Propylene Yield to Product (%)	Propylene Yield to Product (%)	Propylene Yield to Product (%)
	Product Effluent Flow (sccm)	Product Effluent Flow (sccm)	Product Effluent Flow (sccm)
CO	61.0	1.129	0.846
		57.0	1.186
CO <sub>2</sub>	31.5	0.583	0.437
		35.5	0.738
C <sub>2</sub>	2.4	0.044	0.017
		2.3	0.048
Acrolein	3.1	0.057	0.014
		3.0	0.062
1,5-HD	2.0	0.037	0.005
		2.2	0.046
		51.5	1.185
		44.0	1.118
		40.5	0.932
		46.8	1.189
		2.3	0.053
		2.4	0.061
		3.2	0.074
		3.5	0.089
		2.5	0.058
		3.3	0.084
Propylene converted (sccm)	0.52		
Oxygen converted (sccm)	1.85		
		0.58	0.64
		2.06	2.29

Table B10 - Blank Membrane Reactor Test Data  
 (187.5 sccm Total Feed Flow Rate, 20 mol% Propylene and 6 mol% Oxygen in Feed)

Total Flow Rate =		187.5 sccm											
Feed Concentrations (%)													
Propylene =		20											
Oxygen =		6											
Temperature (furnace) (°C)		490.0		510.0		530.0		550.0					
Temperature (reactor bed)(°C)		489.1		509.1		528.5		548.2					
Propylene conversion (%)		2.88		3.29		3.69		4.16					
Oxygen conversion (%)		31.6		36.7		41.6		47.6					
Propylene Selectivity (%)													
CO		56.1	1.616	1.818	51.4	1.691	1.902	46.2	1.703	1.916	38.9	1.618	1.821
CO <sub>2</sub>		36.3	1.045	1.176	40.8	1.342	1.510	45.5	1.677	1.887	50.4	2.097	2.359
C <sub>2</sub>		2.3	0.066	0.037	2.3	0.076	0.043	2.5	0.092	0.052	2.6	0.108	0.061
Acrolein		3.6	0.104	0.039	3.4	0.112	0.042	3.3	0.122	0.046	4.9	0.204	0.076
1,5-HD		1.7	0.049	0.009	2.1	0.069	0.013	2.6	0.096	0.018	3.2	0.133	0.025
Propylene converted (sccm)		1.08		1.23		1.38		1.56		1.71		1.86	
Oxygen converted (sccm)		3.56		4.13		4.68		5.24		5.80		6.36	

Table B11 - Blank Membrane Reactor Test Data  
(187.5 sccm Total Feed Flow Rate, 20 mol% Propylene and 4 mol% Oxygen in Feed)

Total Flow Rate =		187.5 sccm										
Feed Concentrations (%)												
Propylene =		20										
Oxygen =		4										
Temperature (furnace) (°C)		490.0		510.0		530.0		550.0				
Temperature (reactor bed) (°C)		488.0		508.0		527.6		547.3				
Propylene conversion (%)		2.35		2.69		3.03		3.40				
Oxygen conversion (%)		40.9		45.8		51.4		59.1				
Propylene Selectivity (%)												
CO	58.9	1.384	1.557	54.2	1.458	1.640	48.2	1.460	1.643	43.1	1.465	1.649
CO <sub>2</sub>	34.8	0.818	0.920	39.8	1.071	1.204	43.8	1.327	1.493	48.7	1.656	1.863
C <sub>2</sub>	2.3	0.054	0.030	2.1	0.056	0.032	2.1	0.064	0.036	2.2	0.075	0.042
Acrolein	2.7	0.063	0.024	2.4	0.065	0.024	4.0	0.121	0.045	3.6	0.122	0.046
1,5-HD	1.3	0.031	0.006	1.5	0.040	0.008	1.9	0.058	0.011	2.4	0.082	0.015
Propylene converted (sccm)												
		0.88		1.01		1.14		1.28				
Oxygen converted (sccm)												
		3.07		3.44		3.86		4.43				

Table B12 - Blank Membrane Reactor Test Data  
(187.5 sccm Total Feed Flow Rate, 20 mol% Propylene and 3 mol% Oxygen in Feed)

Total Flow Rate =		187.5 sccm										
Feed Concentrations (%)												
Propylene =		20										
Oxygen =		3										
Temperature (furnace) (°C)		490.0		510.0		530.0		550.0				
Temperature (reactor bed)(°C)		488.0		508.0		527.4		547.2				
Propylene conversion (%)		2.26		2.41		2.70		3.00				
Oxygen conversion (%)		49.8		54.8		60.5		68.7				
Propylene Selectivity (%)												
CO		60.9	1.376	1.548	56.7	1.366	1.537	51.3	1.385	46.3	1.389	1.563
CO <sub>2</sub>		33.4	0.755	0.849	37.6	0.906	1.019	41.4	1.118	46.3	1.389	1.563
C <sub>2</sub>		2.3	0.052	0.029	2.2	0.053	0.030	2.2	0.059	2.4	0.072	0.041
Acrolein		2.3	0.052	0.019	2.1	0.051	0.019	3.4	0.092	2.8	0.084	0.032
1,5-HD		1.1	0.025	0.005	1.4	0.034	0.006	1.7	0.046	2.2	0.066	0.012
Propylene converted (sccm)		0.85		0.90		0.90		1.01		1.13		
Oxygen converted (sccm)		2.80		3.08		3.08		3.40		3.86		

Table B13 - Blank Membrane Reactor Test Data  
(187.5 sccm Total Feed Flow Rate, 15 mol% Propylene and 6 mol% Oxygen in Feed)

Total Flow Rate =		187.5 sccm									
Feed Concentrations (%)											
Propylene =		15									
Oxygen =		6									
Temperature (furnace) (°C)		490.0		510.0		530.0		550.0			
Temperature (reactor bed)(°C)		488.3		508.5		528.0		548.0			
Propylene conversion (%)		2.63		3.10		3.55		3.90			
Oxygen conversion (%)		21.7		25.7		29.5		32.7			
Propylene Selectivity (%)											
		Propylene Yield to Product (%)	Product Effluent Flow (sccm)	Propylene Yield to Product (%)	Product Effluent Flow (sccm)	Propylene Yield to Product (%)	Product Effluent Flow (sccm)	Propylene Yield to Product (%)	Product Effluent Flow (sccm)	Propylene Yield to Product (%)	Product Effluent Flow (sccm)
CO	58.1	1.528	1.289	54.0	1.412	47.1	1.411	39.0	1.521	1.283	1.283
CO <sub>2</sub>	33.3	0.876	0.739	36.7	0.960	42.5	1.273	49.3	1.923	1.622	1.622
C <sub>2</sub>	2.4	0.063	0.027	2.5	0.033	2.7	0.040	2.9	0.113	0.048	0.048
Acrolein	4.1	0.108	0.030	4.0	0.035	4.0	0.040	4.0	0.156	0.044	0.044
1,5-HD	2.1	0.055	0.008	2.8	0.012	3.7	0.018	4.8	0.187	0.026	0.026
Propylene converted (sccm)			0.74		0.87		1.00		1.10		1.10
Oxygen converted (sccm)			2.44		2.89		3.32		3.68		3.68

Table B14 - Blank Membrane Reactor Test Data  
(187.5 sccm Total Feed Flow Rate, 15 mol% Propylene and 4 mol% Oxygen in Feed)

Total Flow Rate =		187.5 sccm	
Feed Concentrations (%)			
Propylene =	15		
Oxygen =	4		
Temperature (furnace) (°C)	490.0	510.0	530.0
Temperature (reactor bed)(°C)	488.0	508.1	527.7
Propylene conversion (%)	2.46	2.73	3.10
Oxygen conversion (%)	31.3	35.3	40.0
			3.46
			44.4
Propylene Selectivity (%)			
CO	59.5	1.464	1.235
CO <sub>2</sub>	33.4	0.822	0.693
C <sub>2</sub>	2.4	0.059	0.025
Acrolein	3.0	0.074	0.021
1,5-HD	1.7	0.042	0.006
Propylene converted (sccm)			0.69
Oxygen converted (sccm)			2.35
			0.77
			2.65
			0.87
			3.00
			0.97
			3.33
			1.287
			1.343
			0.034
			0.044
			0.015
			1.526
			1.592
			0.080
			0.156
			0.107
			44.1
			46.0
			2.3
			4.5
			3.1
			1.321
			1.096
			0.029
			0.026
			0.010
			50.5
			41.9
			2.2
			3.0
			2.4
			1.566
			1.299
			0.068
			0.093
			0.074
			1.502
			1.032
			0.060
			0.082
			0.055
			55.0
			37.8
			2.2
			3.0
			2.0
			1.267
			0.871
			0.025
			0.023
			0.008
			1.267
			0.871
			0.025
			0.023
			0.008
			1.502
			1.032
			0.060
			0.082
			0.055
			55.0
			37.8
			2.2
			3.0
			2.0
			1.267
			0.871
			0.025
			0.023
			0.008
			1.267
			0.871
			0.025
			0.023
			0.008
			1.502
			1.032
			0.060
			0.082
			0.055
			55.0
			37.8
			2.2
			3.0
			2.0
			1.267
			0.871
			0.025
			0.023
			0.008
			1.267
			0.871
			0.025
			0.023
			0.008
			1.502
			1.032
			0.060
			0.082
			0.055
			55.0
			37.8
			2.2
			3.0
			2.0
			1.267
			0.871
			0.025
			0.023
			0.008
			1.267
			0.871
			0.025
			0.023
			0.008
			1.502
			1.032
			0.060
			0.082
			0.055
			55.0
			37.8
			2.2
			3.0
			2.0
			1.267
			0.871
			0.025
			0.023
			0.008
			1.267
			0.871
			0.025
			0.023
			0.008
			1.502
			1.032
			0.060
			0.082
			0.055
			55.0
			37.8
			2.2
			3.0
			2.0
			1.267
			0.871
			0.025
			0.023
			0.008
			1.267
			0.871
			0.025
			0.023
			0.008
			1.502
			1.032
			0.060
			0.082
			0.055
			55.0
			37.8
			2.2
			3.0
			2.0
			1.267
			0.871
			0.025
			0.023
			0.008
			1.267
			0.871
			0.025
			0.023
			0.008
			1.502
			1.032
			0.060
			0.082
			0.055
			55.0
			37.8
			2.2
			3.0
			2.0
			1.267
			0.871
			0.025
			0.023
			0.008
			1.267
			0.871
			0.025
			0.023
			0.008
			1.502
			1.032
			0.060
			0.082
			0.055
			55.0
			37.8
			2.2
			3.0
			2.0
			1.267
			0.871
			0.025
			0.023
			0.008
			1.267
			0.871
			0.025
			0.023
			0.008
			1.502
			1.032
			0.060
			0.082
			0.055
			55.0
			37.8
			2.2
			3.0
			2.0
			1.267
			0.871
			0.025
			0.023
			0.008
			1.267
			0.871
			0.025
			0.023
			0.008
			1.502
			1.032
			0.060
			0.082
			0.055
			55.0
			37.8
			2.2
			3.0
			2.0
			1.267
			0.871
			0.025
			0.023
			0.008
			1.267
			0.871
			0.025
			0.023
			0.008
			1.502
			1.032
			0.060
			0.082
			0.055
			55.0
			37.8
			2.2
			3.0
			2.0
			1.267
			0.871
			0.025
			0.023
			0.008
			1.267
			0.871
			0.025
			0.023
			0.008
			1.502
			1.032
			0.060
			0.082
			0.055
			55.0
			37.8
			2.2
			3.0
			2.0
			1.267
			0.871
			0.025
			0.023
			0.008
			1.267
			0.871
			0.025
			0.023
			0.008
			1.502
			1.032
			0.060
			0.082
			0.055
			55.0
			37.8
			2.2
			3.0
			2.0
			1.267
			0.871
			0.025
			0.023
			0.008
			1.267
			0.871
			0.025
			0.023
			0.008
			1.502
			1.032
			0.060
			0.082
			0.055
			55.0
			37.8
			2.2
			3.0
			2.0
			1.267
			0.871
			0.025
			0.023
			0.008
			1.267
			0.871
			0.025
			0.023
			0.008
			1.502
			1.032
			0.060
			0.082
			0.055
			55.0
			37.8
			2.2
			3.0
			2.0
			1.267
			0.871
			0.025
			0.023
			0.008
			1.267

Table B15 - Blank Membrane Reactor Test Data  
(187.5 sccm Total Feed Flow Rate, 15 mol% Propylene and 3 mol% Oxygen in Feed)

Total Flow Rate =		187.5 sccm											
Feed Concentrations (%)													
Propylene =		15											
Oxygen =		3											
Temperature (furnace) (°C)		490.0		510.0		530.0		550.0					
Temperature (reactor bed)(°C)		487.9		507.6		527.2		547.0					
Propylene conversion (%)		2.47		2.72		3.05		3.37					
Oxygen conversion (%)		42.0		46.2		51.7		58.1					
Propylene Selectivity (%)													
CO		62.1	1.534	1.294	1.294	57.6	1.567	1.322	52.2	1.592	47.2	1.591	1.342
CO <sub>2</sub>		31.7	0.783	0.661	0.661	36.2	0.985	0.831	40.4	1.232	44.4	1.496	1.262
C <sub>2</sub>		2.4	0.059	0.025	0.025	2.2	0.060	0.025	2.2	0.067	2.2	0.074	0.031
Acrolein		2.4	0.059	0.017	0.017	2.4	0.065	0.018	3.1	0.095	3.6	0.121	0.034
1,5-HD		1.4	0.035	0.005	0.005	1.6	0.044	0.006	2.1	0.064	2.6	0.088	0.012
Propylene converted (sccm)		0.69		0.77		0.86		0.95					
Oxygen converted (sccm)		2.36		2.60		2.91		3.27					



Table B16 - Blank Membrane Reactor Test Data  
(187.5 sccm Total Feed Flow Rate, 10 mol% Propylene and 6 mol% Oxygen in Feed)

Total Flow Rate =		187.5 sccm									
Feed Concentrations (%)											
Propylene =		10									
Oxygen =		6									
Temperature (furnace) (°C)		490.0		510.0		530.0		550.0			
Temperature (reactor bed)(°C)		487.3		507.5		527.3		547.1			
Propylene conversion (%)		2.90		3.34		3.80		4.12			
Oxygen conversion (%)		16.6		19.1		22.0		24.2			
Propylene Selectivity (%)											
		Propylene Yield to Product (%)		Propylene Yield to Product (%)		Propylene Yield to Product (%)		Propylene Yield to Product (%)		Product Effluent Flow (sccm)	
CO		58.5		53.4		44.4		35.8		0.830	
CO <sub>2</sub>		32.5		37.1		45.6		52.1		1.207	
C <sub>2</sub>		2.5		2.5		2.3		2.7		0.031	
Acrolein		4.5		4.0		3.8		4.2		0.032	
1,5-HD		2.0		3.0		4.0		5.2		0.020	
Propylene converted (sccm)		0.54		0.63		0.71		0.77			
Oxygen converted (sccm)		1.87		2.15		2.48		2.72			

Table B17 - Blank Membrane Reactor Test Data  
(187.5 sccm Total Feed Flow Rate, 10 mol% Propylene and 4 mol% Oxygen in Feed)

Total Flow Rate =		187.5 sccm																																										
Feed Concentrations (%)																																												
Propylene =																							10																					
Oxygen =																							4																					
Temperature (furnace) (°C)																							490.0		510.0		530.0		550.0															
Temperature (reactor bed)(°C)																							487.2		507.1		526.7		546.5															
Propylene conversion (%)																							2.52		2.85		3.22		3.59															
Oxygen conversion (%)																							21.5		24.6		28.4		31.4															
Propylene Selectivity (%)																																												
CO																							60.8		1.532		0.862		56.3		1.605		0.903		51.6		1.662		0.935		41.3		1.483	
CO <sub>2</sub>																							31.8		0.801		0.451		35.7		1.017		0.572		39.9		1.285		0.723		47.1		1.691	
C <sub>2</sub>																							2.4		0.060		0.017		2.3		0.066		0.018		2.2		0.071		0.020		2.3		0.083	
Acrolein																							3.0		0.076		0.014		3.2		0.091		0.017		3.4		0.109		0.021		5.5		0.197	
1,5-HD																							2.0		0.050		0.005		2.5		0.071		0.007		2.9		0.093		0.009		3.8		0.136	
Propylene converted (sccm)																									0.47								0.53						0.60				0.67	
Oxygen converted (sccm)																									1.61						1.85								2.13				2.36	

Table B18 - Blank Membrane Reactor Test Data  
(187.5 sccm Total Feed Flow Rate, 10 mol% Propylene and 3 mol% Oxygen in Feed)

Total Flow Rate =		187.5 sccm													
Feed Concentrations (%)															
Propylene =		10													
Oxygen =		3													
Temperature (furnace) (°C)		490.0		510.0		530.0		550.0							
Temperature (reactor bed)(°C)		487.2		507.0		526.6		546.3							
Propylene conversion (%)		2.30		2.50		2.85		3.20							
Oxygen conversion (%)		25.6		29.0		32.8		36.6							
Propylene Selectivity (%)															
CO		61.4	1.412	0.794	0.812	0.812	57.8	1.444	0.812	53.4	1.522	0.856	47.3	1.514	0.851
CO <sub>2</sub>		30.7	0.706	0.397	0.486	0.486	34.6	0.864	0.486	38.7	1.103	0.620	42.4	1.357	0.763
C <sub>2</sub>		2.5	0.058	0.016	0.016	0.016	2.3	0.058	0.016	2.2	0.063	0.018	2.2	0.070	0.020
Acrolein		3.3	0.076	0.014	0.015	0.015	3.3	0.083	0.015	3.1	0.088	0.017	4.9	0.157	0.029
1,5-HD		2.1	0.048	0.005	0.005	0.005	2.1	0.053	0.005	2.6	0.074	0.007	3.2	0.102	0.010
Propylene converted (sccm)				0.43		0.47		0.53		0.53		0.53		0.60	
Oxygen converted (sccm)				1.44		1.63		1.85		1.85		1.85		2.06	

Table B19 - Blank Membrane Reactor Test Data  
(125 sccm Total Feed Flow Rate, 20 mol% Propylene and 6 mol% Oxygen in Feed)

Total Flow Rate =		125 sccm																					
Feed Concentrations (%)																							
Propylene =		20																					
Oxygen =		6																					
Temperature (furnace) (°C)																							
		490.0				510.0				530.0				550.0									
Temperature (reactor bed)(°C)																							
		488.1				508.1				527.7				547.5									
Propylene conversion (%)																							
		3.52				3.90				4.30				4.76									
Oxygen conversion (%)																							
		37.8				42.6				48.1				52.9									
Propylene Selectivity (%)																							
		57.6		2.028		1.521		53.3		2.079		1.559		48.4		2.081		1.561		42.5		1.517	
CO		34.6		1.218		0.913		38.5		1.502		1.126		42.6		1.832		1.374		46.4		1.656	
CO <sub>2</sub>		2.4		0.084		0.032		2.3		0.090		0.034		2.4		0.103		0.039		2.5		0.045	
C2		3.4		0.120		0.030		3.3		0.129		0.032		3.4		0.146		0.037		4.7		0.056	
Acrolein		2.0		0.070		0.009		2.6		0.101		0.013		3.2		0.138		0.017		3.9		0.023	
1,5-HD																							
Propylene converted (sccm)																							
		0.88				0.98				1.08				1.19				1.08				1.19	
Oxygen converted (sccm)																							
		2.84				3.20				3.61				3.97				3.61				3.97	



Table B21 - Blank Membrane Reactor Test Data  
(125 sccm Total Feed Flow Rate, 20 mol% Propylene and 3 mol% Oxygen in Feed)

Total Flow Rate =		125 sccm											
Feed Concentrations (%)													
Propylene =		20											
Oxygen =		3											
Temperature (furnace) (°C)		490.0		510.0		530.0		550.0					
Temperature (reactor bed)(°C)		488.0		507.9		527.5		547.3					
Propylene conversion (%)		2.96		3.20		3.46		3.74					
Oxygen conversion (%)		62.0		67.7		74.6		82.7					
Propylene Selectivity (%)													
CO		63.3	1.874	1.405	1.435	59.8	1.914	1.435	55.7	1.927	50.9	1.904	1.428
CO <sub>2</sub>		30.1	0.891	0.668	0.792	33.0	1.056	0.792	36.5	1.263	40.8	1.526	1.144
C <sub>2</sub>		3.3	0.098	0.037	0.042	3.5	0.112	0.042	3.6	0.125	3.8	0.142	0.055
Acrolein		2.1	0.062	0.016	0.018	2.3	0.074	0.018	2.4	0.083	2.4	0.090	0.022
1,5-HD		1.2	0.036	0.004	0.006	1.4	0.045	0.006	1.8	0.062	2.1	0.079	0.010
Propylene converted (sccm)		0.74		0.80		0.87		0.87		0.87		0.94	
Oxygen converted (sccm)		2.33		2.54		2.80		2.80		2.80		3.10	

Table B22 - Blank Membrane Reactor Test Data  
(125 sccm Total Feed Flow Rate, 15 mol% Propylene and 6 mol% Oxygen in Feed)

Total Flow Rate =		125 sccm	
Feed Concentrations (%)			
Propylene =	15		
Oxygen =	6		
Temperature (furnace) (°C)	490.0	510.0	530.0
Temperature (reactor bed)(°C)	488.2	508.1	527.7
Propylene conversion (%)	3.65	4.11	4.54
Oxygen conversion (%)	29.7	32.8	36.9
			4.92
			40.5
Propylene Selectivity (%)			
CO	59.5	2.172	1.222
CO <sub>2</sub>	32.2	1.175	0.661
C2	2.5	0.091	0.026
Acrolein	3.5	0.128	0.024
1,5-HD	2.3	0.084	0.008
Propylene converted (sccm)	0.68		0.77
Oxygen converted (sccm)	2.23		2.46
			0.85
			2.77
			0.92
			3.04
			1.190
			1.212
			0.037
			0.051
			0.023
			43.0
			43.8
			2.7
			5.5
			5.0
			2.116
			2.155
			0.133
			0.271
			0.246
			1.285
			1.006
			0.033
			0.031
			0.017
			2.284
			1.789
			0.118
			0.168
			0.182
			50.3
			39.4
			2.6
			3.7
			4.0
			1.281
			0.821
			0.028
			0.027
			0.012
			2.277
			1.459
			0.099
			0.144
			0.127
			55.4
			35.5
			2.4
			3.5
			3.1
			1.281
			0.821
			0.028
			0.027
			0.012
			2.277
			1.459
			0.099
			0.144
			0.127
			55.4
			35.5
			2.4
			3.5
			3.1
			1.281
			0.821
			0.028
			0.027
			0.012
			2.277
			1.459
			0.099
			0.144
			0.127
			55.4
			35.5
			2.4
			3.5
			3.1
			1.281
			0.821
			0.028
			0.027
			0.012
			2.277
			1.459
			0.099
			0.144
			0.127
			55.4
			35.5
			2.4
			3.5
			3.1
			1.281
			0.821
			0.028
			0.027
			0.012
			2.277
			1.459
			0.099
			0.144
			0.127
			55.4
			35.5
			2.4
			3.5
			3.1
			1.281
			0.821
			0.028
			0.027
			0.012
			2.277
			1.459
			0.099
			0.144
			0.127
			55.4
			35.5
			2.4
			3.5
			3.1
			1.281
			0.821
			0.028
			0.027
			0.012
			2.277
			1.459
			0.099
			0.144
			0.127
			55.4
			35.5
			2.4
			3.5
			3.1
			1.281
			0.821
			0.028
			0.027
			0.012
			2.277
			1.459
			0.099
			0.144
			0.127
			55.4
			35.5
			2.4
			3.5
			3.1
			1.281
			0.821
			0.028
			0.027
			0.012
			2.277
			1.459
			0.099
			0.144
			0.127
			55.4
			35.5
			2.4
			3.5
			3.1
			1.281
			0.821
			0.028
			0.027
			0.012
			2.277
			1.459
			0.099
			0.144
			0.127
			55.4
			35.5
			2.4
			3.5
			3.1
			1.281
			0.821
			0.028
			0.027
			0.012
			2.277
			1.459
			0.099
			0.144
			0.127
			55.4
			35.5
			2.4
			3.5
			3.1
			1.281
			0.821
			0.028
			0.027
			0.012
			2.277
			1.459
			0.099
			0.144
			0.127
			55.4
			35.5
			2.4
			3.5
			3.1
			1.281
			0.821
			0.028
			0.027
			0.012
			2.277
			1.459
			0.099
			0.144
			0.127
			55.4
			35.5
			2.4
			3.5
			3.1
			1.281
			0.821
			0.028
			0.027
			0.012
			2.277
			1.459
			0.099
			0.144
			0.127
			55.4
			35.5
			2.4
			3.5
			3.1
			1.281
			0.821
			0.028
			0.027
			0.012
			2.277
			1.459
			0.099
			0.144
			0.127
			55.4
			35.5
			2.4
			3.5
			3.1
			1.281
			0.821
			0.028
			0.027
			0.012
			2.277
			1.459
			0.099
			0.144
			0.127
			55.4
			35.5
			2.4
			3.5
			3.1
			1.281
			0.821
			0.028
			0.027
			0.012
			2.277
			1.459
			0.099
			0.144
			0.127
			55.4
			35.5
			2.4
			3.5
			3.1
			1.281
			0.821
			0.028
			0.027
			0.012
			2.277
			1.459
			0.099
			0.144
			0.127
			55.4
			35.5
			2.4
			3.5
			3.1
			1.281
			0.821
			0.028
			0.027
			0.012
			2.277
			1.459
			0.099
			0.144
			0.127
			55.4
			35.5
			2.4
			3.5
			3.1
			1.281
			0.821
			0.028
			0.027
			0.012
			2.277
			1.459
			0.099
			0.144
			0.127
			55.4
			35.5
			2.4
			3.5
			3.1
			1.281
			0.821
			0.028
			0.027
			0.012
			2.277
			1.459
			0.099
			0.144
			0.127
			55.4
			35.5
			2.4
			3.5
			3.1
			1.281
			0.821
			0.028
			0.027
			0.012

Table B23 - Blank Membrane Reactor Test Data  
(125 sccm Total Feed Flow Rate, 15 mol% Propylene and 4 mol% Oxygen in Feed)

Total Flow Rate =		125 sccm									
Feed Concentrations (%)											
Propylene =		15									
Oxygen =		4									
Temperature (furnace) (°C)	490.0	510.0	530.0	550.0							
Temperature (reactor bed)(°C)	487.8	507.7	527.4	547.2							
Propylene conversion (%)	3.16	3.49	3.85	4.13							
Oxygen conversion (%)	38.7	42.2	46.2	51.0							
Propylene Selectivity (%)											
		Propylene Yield to Product (%)	Product Effluent Flow (sccm)	Propylene Yield to Product (%)	Product Effluent Flow (sccm)	Propylene Yield to Product (%)	Product Effluent Flow (sccm)	Propylene Yield to Product (%)	Product Effluent Flow (sccm)	Propylene Yield to Product (%)	Product Effluent Flow (sccm)
CO	61.6	1.947	1.095	58.1	2.028	1.141	53.8	2.071	1.165	48.3	1.122
CO <sub>2</sub>	31.0	0.980	0.551	34.4	1.201	0.675	37.9	1.459	0.821	41.6	0.966
C <sub>2</sub>	2.6	0.082	0.023	2.4	0.084	0.024	2.4	0.092	0.026	2.5	0.029
Acrolein	2.8	0.088	0.017	2.7	0.094	0.018	2.9	0.112	0.021	4.0	0.031
1,5-HD	2.0	0.063	0.006	2.4	0.084	0.008	3.0	0.116	0.011	3.6	0.014
Propylene converted (sccm)			0.59			0.65			0.72		0.77
Oxygen converted (sccm)			1.94			2.11			2.31		2.55



Table B24 - Blank Membrane Reactor Test Data  
(125 sccm Total Feed Flow Rate, 15 mol% Propylene and 3 mol% Oxygen in Feed)

Total Flow Rate =		125 sccm									
Feed Concentrations (%)											
Propylene =		15									
Oxygen =		3									
Temperature (furnace) (°C)		490.0		510.0		530.0		550.0			
Temperature (reactor bed)(°C)		487.7		507.5		527.1		547.0			
Propylene conversion (%)		2.99		3.28		3.60		3.85			
Oxygen conversion (%)		48.4		52.5		57.6		64.0			
Propylene Selectivity (%)											
CO		62.7	1.875	1.055	1.124	1.998	60.9	1.998	1.138	51.7	1.120
CO <sub>2</sub>		30.4	0.909	0.511	0.594	1.056	32.2	1.056	0.719	39.7	0.860
C <sub>2</sub>		3.0	0.090	0.025	0.027	0.095	2.9	0.095	0.029	3.0	0.032
Acrolein		2.3	0.069	0.013	0.014	0.075	2.3	0.075	0.021	2.8	0.020
1,5-HD		1.6	0.048	0.004	0.005	0.056	1.7	0.056	0.008	2.8	0.010
Propylene converted (sccm)		0.56		0.62		0.68		0.72			
Oxygen converted (sccm)		1.82		1.97		2.16		2.40			

Table B25 - Blank Membrane Reactor Test Data  
(125 sccm Total Feed Flow Rate, 10 mol% Propylene and 6 mol% Oxygen in Feed)

Total Flow Rate =		125 sccm										
Feed Concentrations (%)												
Propylene =	10											
Oxygen =	6											
Temperature (furnace) (°C)	490.0	510.0	530.0	550.0								
Temperature (reactor bed)(°C)	487.7	507.6	527.2	547.1								
Propylene conversion (%)	3.71	4.33	4.80	5.30								
Oxygen conversion (%)	20.3	23.5	26.4	28.7								
Propylene Selectivity (%)												
	Propylene Yield to Product (%)	Product Effluent Flow (sccm)	Propylene Yield to Product (%)	Product Effluent Flow (sccm)								
CO	60.3	2.237	0.839	57.2	2.477	0.929	49.8	2.390	0.896	39.9	2.115	0.793
CO <sub>2</sub>	30.4	1.128	0.423	32.7	1.416	0.531	38.5	1.848	0.693	44.9	2.380	0.892
C <sub>2</sub>	2.6	0.096	0.018	2.5	0.108	0.020	2.6	0.125	0.023	2.7	0.143	0.027
Acrolein	4.4	0.163	0.020	4.3	0.186	0.023	4.4	0.211	0.026	6.5	0.345	0.043
1,5-HD	2.3	0.085	0.005	3.3	0.143	0.009	4.7	0.226	0.014	6.0	0.318	0.020
Propylene converted (sccm)	0.46		0.54		0.60		0.60					
Oxygen converted (sccm)	1.52		1.76		1.98		2.15					





## Appendix C

### Reaction Data for Tests Involving $\text{Bi}_2\text{O}_3$

## List of Tables in Appendix C

Table C1 -	Data for Evaluation Kinetics of ODHD of Propylene on $\text{Bi}_2\text{O}_3$ (15 mol% propylene, 6 mol% oxygen).....	283
Table C2 -	Data for Evaluation Kinetics of ODHD of Propylene on $\text{Bi}_2\text{O}_3$ (12.5 mol% propylene, 6 mol% oxygen).....	284
Table C3 -	Data for Evaluation Kinetics of ODHD of Propylene on $\text{Bi}_2\text{O}_3$ (10 mol% propylene, 6 mol% oxygen).....	285
Table C4 -	Data for Evaluation Kinetics of ODHD of Propylene on $\text{Bi}_2\text{O}_3$ (7.5 mol% propylene, 6 mol% oxygen).....	286
Table C5 -	Data for Evaluation Kinetics of ODHD of Propylene on $\text{Bi}_2\text{O}_3$ (10 mol% propylene, 5 mol% oxygen).....	287
Table C6 -	Data for Evaluation Kinetics of ODHD of Propylene on $\text{Bi}_2\text{O}_3$ (10 mol% propylene, 4 mol% oxygen).....	288
Table C7 -	Data for Evaluation Kinetics of ODHD of Propylene on $\text{Bi}_2\text{O}_3$ (10 mol% propylene, 3 mol% oxygen).....	289
Table C8 -	Data for Reaction of 1,5-Hexadiene and Oxygen on $\text{Bi}_2\text{O}_3$ (0.188 mol% 1,5-hexadiene, 6 mol% oxygen).....	290
Table C9 -	Data for Reaction of 1,5-Hexadiene and Oxygen on $\text{Bi}_2\text{O}_3$ (0.192 mol% 1,5-hexadiene, 4 mol% oxygen).....	291
Table C10 -	Data for Reaction of 1,5-Hexadiene and Oxygen on $\text{Bi}_2\text{O}_3$ (0.194 mol% 1,5-hexadiene, 3 mol% oxygen).....	292
Table C11 -	Data for Reaction of 1,5-Hexadiene and Oxygen on $\text{Bi}_2\text{O}_3$ (0.196 mol% 1,5-hexadiene, 2 mol% oxygen).....	293
Table C12 -	Data for Reaction of 1,5-Hexadiene and Oxygen on $\text{Bi}_2\text{O}_3$ (0.167 mol% 1,5-hexadiene, 2 mol% oxygen).....	294
Table C13 -	Data for Reaction of 1,5-Hexadiene and Oxygen on $\text{Bi}_2\text{O}_3$ (0.133 mol% 1,5-hexadiene, 2 mol% oxygen).....	295
Table C14 -	Data for Reaction of 1,5-Hexadiene and Oxygen on $\text{Bi}_2\text{O}_3$ (0.100 mol% 1,5-hexadiene, 2 mol% oxygen).....	296

## List of Tables in Appendix C (cont'd)

Table C15 - Summary of Propylene and Oxygen Conversion for Mass Transfer Tests on $\text{Bi}_2\text{O}_3$ (W/F = 0.01024 g cat/sccm, 10 mol% Propylene and 3 mol% Oxygen in Feed).....	297
Table C16 - Summary of Propylene and Oxygen Conversion for Mass Transfer Tests on $\text{Bi}_2\text{O}_3$ (W/F = 0.01024 g cat/sccm, 10 mol% Propylene and 6 mol% Oxygen in Feed).....	297
Table C17 - Membrane and Tubular Reactor Results Summary using $\text{Bi}_2\text{O}_3$ as Catalyst (250 sccm Total Feed Flow Rate, 10 mol% Propylene and 3 mol% Oxygen in Feed).....	298
Table C18 - Membrane and Tubular Reactor Results Summary using $\text{Bi}_2\text{O}_3$ as Catalyst (250 sccm Total Feed Flow Rate, 15 mol% Propylene and 3 mol% Oxygen in Feed).....	299
Table C19 - Membrane and Tubular Reactor Results Summary using $\text{Bi}_2\text{O}_3$ as Catalyst (250 sccm Total Feed Flow Rate, 15 mol% Propylene and 4 mol% Oxygen in Feed).....	300
Table C20 - Membrane and Tubular Reactor Results Summary using $\text{Bi}_2\text{O}_3$ as Catalyst (250 sccm Total Feed Flow Rate, 20 mol% Propylene and 2 mol% Oxygen in Feed).....	301
Table C21 - Membrane and Tubular Reactor Results Summary using $\text{Bi}_2\text{O}_3$ as Catalyst (250 sccm Total Feed Flow Rate, 20 mol% Propylene and 3 mol% Oxygen in Feed).....	302
Table C22 - Membrane and Tubular Reactor Results Summary using $\text{Bi}_2\text{O}_3$ as Catalyst (250 sccm Total Feed Flow Rate, 20 mol% Propylene and 4 mol% Oxygen in Feed).....	303
Table C23 - Membrane and Tubular Reactor Results Summary using $\text{Bi}_2\text{O}_3$ as Catalyst (250 sccm Total Feed Flow Rate, 20 mol% Propylene and 6 mol% Oxygen in Feed).....	304
Table C24 - Membrane and Tubular Reactor Results Summary using $\text{Bi}_2\text{O}_3$ as Catalyst (187.5 sccm Total Feed Flow Rate, 10 mol% Propylene and 3 mol% Oxygen in Feed).....	305

## List of Tables in Appendix C (cont'd)

Table C25 - Membrane and Tubular Reactor Results Summary using $\text{Bi}_2\text{O}_3$ as Catalyst (187.5 sccm Total Feed Flow Rate, 15 mol% Propylene and 3 mol% Oxygen in Feed).....	306
Table C26 - Membrane and Tubular Reactor Results Summary using $\text{Bi}_2\text{O}_3$ as Catalyst (187.5 sccm Total Feed Flow Rate, 15 mol% Propylene and 4 mol% Oxygen in Feed).....	307
Table C27 - Membrane and Tubular Reactor Results Summary using $\text{Bi}_2\text{O}_3$ as Catalyst (187.5 sccm Total Feed Flow Rate, 20 mol% Propylene and 3 mol% Oxygen in Feed).....	308
Table C28 - Membrane and Tubular Reactor Results Summary using $\text{Bi}_2\text{O}_3$ as Catalyst (187.5 sccm Total Feed Flow Rate, 20 mol% Propylene and 4 mol% Oxygen in Feed).....	309
Table C29 - Membrane and Tubular Reactor Results Summary using $\text{Bi}_2\text{O}_3$ as Catalyst (187.5 sccm Total Feed Flow Rate, 20 mol% Propylene and 6 mol% Oxygen in Feed).....	310
Table C30 - Membrane and Tubular Reactor Results Summary using $\text{Bi}_2\text{O}_3$ as Catalyst (125 sccm Total Feed Flow Rate, 10 mol% Propylene and 3 mol% Oxygen in Feed).....	311
Table C31 - Membrane and Tubular Reactor Results Summary using $\text{Bi}_2\text{O}_3$ as Catalyst (125 sccm Total Feed Flow Rate, 10 mol% Propylene and 4 mol% Oxygen in Feed).....	312
Table C32 - Membrane and Tubular Reactor Results Summary using $\text{Bi}_2\text{O}_3$ as Catalyst (125 sccm Total Feed Flow Rate, 15 mol% Propylene and 3 mol% Oxygen in Feed).....	313
Table C33 - Membrane and Tubular Reactor Results Summary using $\text{Bi}_2\text{O}_3$ as Catalyst (125 sccm Total Feed Flow Rate, 15 mol% Propylene and 4 mol% Oxygen in Feed).....	314
Table C34 - Membrane and Tubular Reactor Results Summary using $\text{Bi}_2\text{O}_3$ as Catalyst (125 sccm Total Feed Flow Rate, 15 mol% Propylene and 6 mol% Oxygen in Feed).....	315



## List of Tables in Appendix C (cont'd)

Table C35 - Membrane and Tubular Reactor Results Summary using $\text{Bi}_2\text{O}_3$ as Catalyst (125 sccm Total Feed Flow Rate, 20 mol% Propylene and 4 mol% Oxygen in Feed).....	316
Table C36 - Membrane and Tubular Reactor Results Summary using $\text{Bi}_2\text{O}_3$ as Catalyst (125 sccm Total Feed Flow Rate, 20 mol% Propylene and 6 mol% Oxygen in Feed).....	317

Table C1 - Data for Evaluation Kinetics of ODHD of Propylene on Bi<sub>2</sub>O<sub>3</sub>  
(15 mol% propylene, 6 mol% oxygen)

Catalyst is		6.4 g of 16 x 20 mesh bismuth oxide		
Total Feed Rate		625 sccm		
Propylene Feed (mol%)		15		
Oxygen Feed (mol%)		6		
Temperature (°C)	Propylene Conversion (%)	Oxygen Conversion (%)	Propylene Converted to 1,5-Hexadiene (sccm)	Propylene Converted to Carbon Dioxide (sccm)
499.8	0.90	4.46	0.4665	0.3150
499.8	0.90	4.53	0.4737	0.3146
499.8	0.91	4.56	0.4756	0.3137
499.8	0.90	4.54	0.4770	0.3133
519.8	1.33	5.75	0.7645	0.3929
519.8	1.31	5.86	0.7636	0.4028
519.8	1.33	5.87	0.7669	0.3973
519.8	1.32	5.85	0.7693	0.4023
540.0	1.85	7.57	1.1815	0.5270
540.0	1.92	7.84	1.1818	0.5326
540.0	1.93	7.82	1.1854	0.5338
540.0	1.96	7.93	1.1907	0.5355
560.3	2.81	10.71	1.7495	0.7411
560.3	2.82	10.90	1.7528	0.7467
560.3	2.80	10.86	1.7551	0.7513
560.3	2.73	10.89	1.7609	0.7532

Table C2 - Data for Evaluation Kinetics of ODHD of Propylene on  $\text{Bi}_2\text{O}_3$   
(12.5 mol% propylene, 6 mol% oxygen)

Catalyst is		6.4 g of 16 x 20 mesh bismuth oxide		
Total Feed Rate		625 sccm		
Propylene Feed (mol%)		12.5		
Oxygen Feed (mol%)		6		
Temperature (°C)	Propylene Conversion (%)	Oxygen Conversion (%)	Propylene Converted to 1,5-Hexadiene (sccm)	Propylene Converted to Carbon Dioxide (sccm)
499.6	0.89	3.80	0.3763	0.2628
499.6	0.90	3.90	0.3773	0.2678
499.6	0.67	3.86	0.2430	0.2711
499.6	0.82	3.88	0.3683	0.2652
519.6	1.30	4.90	0.6163	0.3323
519.6	1.29	5.02	0.6139	0.3403
519.6	1.31	5.05	0.6193	0.3428
519.6	1.31	5.16	0.6201	0.3445
539.8	1.91	6.71	0.9597	0.4562
539.8	1.91	6.80	0.9622	0.4578
539.8	1.93	6.91	0.9694	0.4657
539.8	1.96	6.86	0.9753	0.4700
560.1	2.83	9.40	1.4413	0.6486
560.1	2.83	9.53	1.4414	0.6484
560.1	2.85	9.57	1.4451	0.6504
560.1	2.86	9.35	1.4464	0.6540

Note: Shaded data are outliers and are not used in development of kinetic models

Table C3 - Data for Evaluation Kinetics of ODHD of Propylene on  $\text{Bi}_2\text{O}_3$   
(10 mol% propylene, 6 mol% oxygen)

Catalyst is		6.4 g of 16 x 20 mesh bismuth oxide		
Total Feed Rate		625 sccm		
Propylene Feed (mol%)		10		
Oxygen Feed (mol%)		6		
Temperature (°C)	Propylene Conversion (%)	Oxygen Conversion (%)	Propylene Converted to 1,5-Hexadiene (sccm)	Propylene Converted to Carbon Dioxide (sccm)
500.5	0.97	3.79	0.3043	0.2987
500.5	0.87	3.40	0.3093	0.2303
500.5	0.87	3.44	0.3095	0.2292
500.5	0.88	3.49	0.3096	0.2358
520.5	1.28	4.23	0.5072	0.2889
520.5	1.29	4.43	0.5062	0.2967
520.5	1.30	4.45	0.5099	0.2958
520.5	1.30	4.37	0.5114	0.2955
540.6	2.00	5.80	0.7898	0.3906
540.6	2.02	5.93	0.7891	0.3913
540.6	2.02	5.94	0.7918	0.3933
540.6	2.02	6.02	0.7931	0.3956
560.9	2.92	8.02	1.1694	0.5398
560.9	2.88	7.97	1.1686	0.5414
560.9	2.91	8.12	1.1707	0.5491
560.9	2.91	8.39	1.1738	0.5535

Note: Shaded data are outliers and are not used in development of kinetic models

Table C4 - Data for Evaluation Kinetics of ODHD of Propylene on  $\text{Bi}_2\text{O}_3$   
(7.5 mol% propylene, 6 mol% oxygen)

Catalyst is		6.4 g of 16 x 20 mesh bismuth oxide		
Total Feed Rate		625 sccm		
Propylene Feed (mol%)		7.5		
Oxygen Feed (mol%)		6		
Temperature (°C)	Propylene Conversion (%)	Oxygen Conversion (%)	Propylene Converted to 1,5-Hexadiene (sccm)	Propylene Converted to Carbon Dioxide (sccm)
500.0	0.85	2.60	0.2202	0.1760
500.0	0.97	4.42	0.1965	0.2587
500.0	0.86	2.87	0.2223	0.1807
500.0	0.87	2.88	0.2216	0.1881
519.8	1.37	3.50	0.3595	0.2348
519.8	1.33	3.67	0.3577	0.2323
519.8	1.34	3.70	0.3587	0.2376
519.8	1.37	3.71	0.3608	0.2366
539.9	1.96	4.65	0.5594	0.3074
539.9	1.89	4.89	0.5322	0.3174
539.9	1.99	4.87	0.5635	0.3148
539.9	1.95	4.96	0.5683	0.3203
559.9	2.87	6.61	0.8338	0.4407
559.9	2.87	6.68	0.8333	0.4390
559.9	2.91	6.48	0.8494	0.4399
559.9	2.87	6.76	0.8364	0.4425

Note: Shaded data are outliers and are not used in development of kinetic models

Table C5 - Data for Evaluation Kinetics of ODHD of Propylene on  $\text{Bi}_2\text{O}_3$   
(10 mol% propylene, 5 mol% oxygen)

Catalyst is		6.4 g of 16 x 20 mesh bismuth oxide		
Total Feed Rate		625 sccm		
Propylene Feed (mol%)		10		
Oxygen Feed (mol%)		5		
Temperature (°C)	Propylene Conversion (%)	Oxygen Conversion (%)	Propylene Converted to 1,5-Hexadiene (sccm)	Propylene Converted to Carbon Dioxide (sccm)
500.5	0.91	3.90	0.3252	0.2410
500.5	0.87	3.90	0.3279	0.2156
500.5	0.87	3.85	0.3291	0.2126
500.5	0.90	4.02	0.3295	0.2342
520.2	1.23	4.69	0.4972	0.2680
520.2	1.27	4.81	0.5262	0.2655
520.2	1.28	4.88	0.5279	0.2689
520.2	1.28	4.88	0.5291	0.2661
540.7	1.96	6.32	0.8028	0.3526
540.7	1.94	6.22	0.8083	0.3540
540.7	1.96	6.45	0.8130	0.3548
540.7	1.98	6.62	0.8184	0.3591
561.0	2.86	8.81	1.1972	0.4952
561.0	2.88	9.26	1.2010	0.5015
561.0	2.85	8.99	1.2040	0.5009
561.0	2.87	9.04	1.2049	0.5021

Note: Shaded data are outliers and are not used in development of kinetic models

Table C6 - Data for Evaluation Kinetics of ODHD of Propylene on  $\text{Bi}_2\text{O}_3$   
(10 mol% propylene, 4 mol% oxygen)

Catalyst is		6.4 g of 16 x 20 mesh bismuth oxide		
Total Feed Rate		625 sccm		
Propylene Feed (mol%)		10		
Oxygen Feed (mol%)		4		
Temperature (°C)	Propylene Conversion (%)	Oxygen Conversion (%)	Propylene Converted to 1,5-Hexadiene (sccm)	Propylene Converted to Carbon Dioxide (sccm)
500.7	0.90	4.45	0.3482	0.2091
500.7	0.91	4.62	0.3565	0.2084
500.7	0.88	2.51	0.3563	0.1938
500.7	0.89	5.46	0.3537	0.1991
520.7	1.31	5.66	0.5616	0.2514
520.7	1.29	5.78	0.5605	0.2433
520.7	1.43	7.92	0.5638	0.3270
520.7	1.29	5.71	0.5539	0.2480
540.8	1.96	7.39	0.8479	0.3235
540.8	1.97	7.70	0.8478	0.3262
540.8	1.98	7.68	0.8506	0.3285
540.8	1.99	7.87	0.8529	0.3450
561.0	2.86	10.24	1.2396	0.4560
561.0	2.86	10.71	1.2367	0.4537
561.0	2.85	10.45	1.2408	0.4575
561.0	2.81	10.44	1.2441	0.4595

Note: Shaded data are outliers and are not used in development of kinetic models

Table C7 - Data for Evaluation Kinetics of ODHD of Propylene on  $\text{Bi}_2\text{O}_3$   
(10 mol% propylene, 3 mol% oxygen)

Catalyst is		6.4 g of 16 x 20 mesh bismuth oxide		
Total Feed Rate		625 sccm		
Propylene Feed (mol%)		10		
Oxygen Feed (mol%)		3		
Temperature (°C)	Propylene Conversion (%)	Oxygen Conversion (%)	Propylene Converted to 1,5-Hexadiene (sccm)	Propylene Converted to Carbon Dioxide (sccm)
501.1	0.92	5.31	0.3994	0.1773
501.1	0.93	5.61	0.4001	0.1817
501.1	0.93	5.53	0.4014	0.1772
501.1	0.92	5.45	0.3997	0.1761
521.0	1.34	6.74	0.6102	0.2240
521.0	1.33	6.92	0.6073	0.2222
521.0	1.34	7.05	0.6085	0.2268
521.0	1.34	6.96	0.6093	0.2228
541.2	1.97	9.00	0.8955	0.2921
541.2	2.00	9.43	0.8989	0.2973
541.2	2.01	9.36	0.9051	0.2970
541.2	2.02	9.67	0.9082	0.3088
561.4	2.89	12.72	1.3032	0.4112
561.4	2.88	12.99	1.3068	0.4187
561.4	2.88	12.96	1.3052	0.4188
561.4	2.86	12.99	1.2983	0.4173

Note: Shaded data are outliers and are not used in development of kinetic models



Table C8 - Data for Reaction of 1,5-Hexadiene and Oxygen on  $\text{Bi}_2\text{O}_3$   
(0.188 mol% 1,5-hexadiene, 6 mol% oxygen)

Catalyst is		2.56 g of 16 x 20 mesh bismuth oxide				
Feed Flow Rate =		250 sccm				
Feed 1,5-Hexadiene (mol%)		0.188 %				
Feed Oxygen (mol%)		6.0 %				
Temperature (°C)	1,5-Hexadiene Conversion %	Oxygen Conversion %	Conversion of 1,5-Hexadiene (sccm x 1000)			
			to CO <sub>2</sub>	to Benzene	to Ethylene	to Propylene
499.5	9.46	3.42	32.42	7.01	2.19	2.82
499.5	9.65	2.53	33.10	7.52	2.10	2.65
499.5	9.27	2.37	32.03	6.97	2.06	2.50
499.5	9.46	2.40	32.11	7.55	2.08	2.70
519.4	15.55	3.49	50.29	10.26	6.42	6.13
519.4	16.36	3.50	51.03	13.38	6.27	6.22
519.4	15.74	3.57	50.74	11.00	6.27	5.99
519.4	15.94	3.54	50.40	12.31	6.36	5.83
539.2	28.60	6.63	85.82	16.68	17.20	14.71
539.2	28.63	6.91	86.73	15.86	17.26	14.72
539.2	28.04	6.98	87.15	12.59	17.33	14.71
539.2	29.40	6.95	87.56	18.58	17.41	14.62
559.0	50.64	10.35	144.03	25.66	39.79	28.56
559.0	50.32	9.14	142.12	26.45	39.53	28.39
559.0	50.18	9.07	141.85	26.49	39.31	28.20
559.0	50.38	10.48	143.19	26.05	39.34	28.21

Note: Shaded data are outliers and are not used in development of kinetic models

Table C9 - Data for Reaction of 1,5-Hexadiene and Oxygen on  $\text{Bi}_2\text{O}_3$   
(0.192 mol% 1,5-hexadiene, 4 mol% oxygen)

Catalyst is		2.56 g of 16 x 20 mesh bismuth oxide				
Feed Flow Rate =		250 sccm				
Feed 1,5-Hexadiene (mol%)		0.192 %				
Feed Oxygen (mol%)		4.0 %				
Temperature (°C)	1,5-Hexadiene Conversion %	Oxygen Conversion %	Conversion of 1,5-Hexadiene (sccm x 1000)			
			to $\text{CO}_2$	to Benzene	to Ethylene	to Propylene
499.7	7.61	3.32	26.97	5.70	1.46	2.40
499.7	7.97	4.67	28.06	5.84	1.47	2.88
499.7	8.05	3.79	29.07	6.27	1.40	1.90
499.7	7.80	4.06	28.14	5.92	1.42	1.94
519.3	15.49	5.81	54.82	10.32	4.31	4.89
519.3	12.14	4.77	39.43	9.86	4.24	4.73
519.3	12.09	5.07	40.24	9.22	4.41	4.15
519.3	11.73	4.50	39.03	8.54	4.32	4.39
539.2	23.93	7.15	76.78	16.38	11.27	10.43
539.2	20.47	7.75	62.79	13.64	11.30	10.53
539.2	20.84	6.85	63.66	14.52	11.30	10.56
539.2	20.96	6.78	63.22	16.21	11.28	9.91
559.0	35.57	11.28	97.79	25.88	25.51	21.54
559.0	34.75	11.48	98.58	21.63	25.29	21.32
559.0	35.66	11.03	97.60	27.52	25.08	20.97
559.0	34.61	11.57	99.12	20.37	25.16	21.48

Note: Shaded data are outliers and are not used in development of kinetic models

Table C10 - Data for Reaction of 1,5-Hexadiene and Oxygen on  $\text{Bi}_2\text{O}_3$   
(0.194 mol% 1,5-hexadiene, 3 mol% oxygen)

Catalyst is		2.56 g of 16 x 20 mesh bismuth oxide				
Feed Flow Rate =		250 sccm				
Feed 1,5-Hexadiene (mol%)		0.194 %				
Feed Oxygen (mol%)		3.0 %				
Temperature (°C)	1,5-Hexadiene Conversion %	Oxygen Conversion %	Conversion of 1,5-Hexadiene (sccm x 1000)			
			to $\text{CO}_2$	to Benzene	to Ethylene	to Propylene
500.0	10.50	6.09	40.19	7.54	1.50	1.68
500.0	10.62	6.18	40.75	8.63	0.87	1.27
500.0	8.03	8.96	26.40	9.85	1.08	1.58
500.0	7.60	5.10	25.44	8.36	1.21	1.84
520.0	11.17	6.08	35.88	10.76	3.59	3.95
520.0	11.53	6.25	36.55	11.74	3.57	4.05
520.0	11.00	6.36	36.22	9.47	3.55	4.08
520.0	14.49	10.94	51.19	12.73	3.56	2.76
540.0	17.88	8.36	53.57	14.94	9.10	9.11
540.0	18.72	9.56	54.81	18.26	9.09	8.63
540.0	18.77	8.49	53.76	19.44	9.08	8.75
540.0	17.80	8.48	55.19	13.51	8.97	8.65
559.6	28.93	12.68	79.89	22.82	19.51	18.09
559.6	20.34	18.51	99.26	0.00	0.00	0.00
559.6	28.51	13.11	80.43	20.71	19.30	17.86
559.6	28.14	13.06	80.36	19.21	19.23	17.67

Note: Shaded data are outliers and are not used in development of kinetic models  
Horizontal-lined data are erroneous due to GC signal or GC integration problems

Table C11 - Data for Reaction of 1,5-Hexadiene and Oxygen on Bi<sub>2</sub>O<sub>3</sub>  
(0.196 mol% 1,5-hexadiene, 2 mol% oxygen)

Catalyst is		2.56 g of 16 x 20 mesh bismuth oxide				
Feed Flow Rate =		250 sccm				
Feed 1,5-Hexadiene (mol%)		0.196 %				
Feed Oxygen (mol%)		2.0 %				
Temperature (°C)	1,5-Hexadiene Conversion %	Oxygen Conversion %	Conversion of 1,5-Hexadiene (sccm x 1000)			
			To CO <sub>2</sub>	to Benzene	to Ethylene	to Propylene
500.0	5.81	2.84	20.58	6.06	0.91	0.93
500.0	5.70	2.90	21.02	6.08	0.84	
500.0	6.24	2.99	21.81	6.39	0.88	1.50
500.0	5.96	2.96	21.55	6.31	0.84	
520.0	12.41	9.73	43.95	10.38	2.84	3.64
520.0	9.37	8.79	30.39	9.27	2.83	3.43
520.0	12.66	10.46	45.03	11.09	2.89	3.06
520.0	9.73	9.65	30.86	10.87	2.87	3.05
540.0	15.62	10.77	44.66	16.85	7.37	7.66
540.0	16.14	11.09	45.11	19.14	7.18	7.64
540.0	16.21	11.41	44.33	20.57	7.17	7.39
540.0	16.39	11.92	45.66	20.01	7.13	7.53
559.6	23.88	17.77	64.39	24.61	13.73	14.29
559.6	23.71	16.46	64.97	23.25	13.72	14.25
559.6	25.08	16.68	65.44	29.67	13.67	14.13
559.6	24.58	16.44	64.35	28.38	13.71	13.98

Note: Shaded data are outliers and are not used in development of kinetic models  
Horizontal-lined data are erroneous due to GC signal or GC integration problems

Table C12 - Data for Reaction of 1,5-Hexadiene and Oxygen on Bi<sub>2</sub>O<sub>3</sub>  
(0.167 mol% 1,5-hexadiene, 2 mol% oxygen)

Catalyst is		2.56 g of 16 x 20 mesh bismuth oxide				
Feed Flow Rate =		250 sccm				
Feed 1,5-Hexadiene (mol%)		0.167 %				
Feed Oxygen (mol%)		2.0 %				
Temperature (°C)	1,5-Hexadiene Conversion %	Oxygen Conversion %	Conversion of 1,5-Hexadiene (sccm x 1000)			
			to CO <sub>2</sub>	to Benzene	to Ethylene	to Propylene
499.5	8.47	2.88	20.82	6.69		
499.5	10.43	4.42	<del>33.65</del>	7.37	0.76	1.66
499.5	6.86	2.82	20.35	6.29	0.69	1.27
499.5	6.74	2.73	19.53	6.64	0.68	1.24
519.3	10.41	7.00	27.58	<del>10.03</del>	2.74	3.02
519.3	9.93	7.25	27.77	<del>8.81</del>	2.38	2.41
519.3	11.13	7.62	28.07	13.28	2.39	2.63
519.3	10.86	7.22	27.29	12.62	2.51	2.82
539.3	16.24	10.77	39.77	15.13	6.37	6.40
539.3	21.72	10.51	<del>44.67</del>	<del>33.21</del>	6.03	6.61
539.3	16.93	10.84	40.44	18.42	6.03	5.64
539.3	14.62	10.45	39.69	<del>9.05</del>	6.00	6.19
558.7	29.72	14.13	<del>70.48</del>	28.95	12.09	12.31
558.7	25.35	13.29	56.32	25.14	12.04	12.11
558.7	25.56	14.30	55.49	26.54	12.18	12.27
558.7	25.51	13.02	56.50	25.62	12.05	12.11

Note: Shaded data are outliers and are not used in development of kinetic models  
Horizontal-lined data are erroneous due to GC signal or GC integration problems

Table C13 - Data for Reaction of 1,5-Hexadiene and Oxygen on Bi<sub>2</sub>O<sub>3</sub>  
(0.133 mol% 1,5-hexadiene, 2 mol% oxygen)

Catalyst is		2.56 g of 16 x 20 mesh bismuth oxide				
Feed Flow Rate =		250 sccm				
Feed 1,5-Hexadiene (mol%)		0.133 %				
Feed Oxygen (mol%)		2.0 %				
Temperature (°C)	1,5-Hexadiene Conversion %	Oxygen Conversion %	Conversion of 1,5-Hexadiene (sccm x 1000)			
			to CO <sub>2</sub>	to Benzene	to Ethylene	to Propylene
499.6	6.83	2.37	16.54	5.63	0.62	
499.6	11.22	3.94	29.65	6.03	0.40	1.31
499.6	6.60	2.30	15.97	5.64	0.39	
499.6	6.76	2.28	15.85	6.25	0.43	
519.3	10.14	3.70	21.24	8.82	1.73	2.02
519.3	14.21	5.23	20.99	22.10	1.67	2.60
519.3	11.38	7.05	22.32	11.79	1.70	2.11
519.3	9.99	6.72	21.61	7.66	1.67	2.34
539.0	15.64	7.44	29.90	12.93	4.57	4.72
539.0	16.38	9.48	31.26	13.69	4.62	5.05
539.0	16.30	7.40	30.81	13.98	4.58	4.97
539.0	16.53	7.25	30.80	15.18	4.59	4.53
558.6	24.73	9.90	43.55	19.40	9.70	9.78
558.6	24.99	10.20	43.71	20.48	9.58	9.54
558.6	25.34	10.15	43.49	21.79	9.51	9.67
558.6	25.14	10.89	43.73	20.89	9.52	9.68

Note: Shaded data are outliers and are not used in development of kinetic models  
Horizontal-lined data are erroneous due to GC signal or GC integration problems

Table C14 - Data for Reaction of 1,5-Hexadiene and Oxygen on Bi<sub>2</sub>O<sub>3</sub>  
(0.100 mol% 1,5-hexadiene, 2 mol% oxygen)

Catalyst is		2.56 g of 16 x 20 mesh bismuth oxide				
Feed Flow Rate =		250 sccm				
Feed 1,5-Hexadiene (mol%)		0.100 %				
Feed Oxygen (mol%)		2.0 %				
Temperature (°C)	1,5-Hexadiene Conversion %	Oxygen Conversion %	Conversion of 1,5-Hexadiene (sccm x 1000)			
			to CO <sub>2</sub>	to Benzene	to Ethylene	to Propylene
499.5	8.96	2.66	18.98	3.28	0.14	
499.5	6.00	1.81	11.89	3.02	0.10	
499.5	10.94	3.18	23.29	3.98	0.10	
499.5	6.34	1.86	12.35	3.40	0.09	
519.2	9.73	6.68	15.82	5.96	0.98	1.58
519.2	11.75	5.70	19.95	6.46	1.24	1.71
519.2	12.73	5.36	22.85	6.23	1.00	1.74
519.2	10.11	5.58	16.54	6.20	1.01	1.54
539.0	16.19	6.66	23.09	10.62	3.11	3.66
539.0	16.88	7.06	23.06	12.32	3.10	3.72
539.0	16.01	7.41	25.21	9.05	3.09	2.68
539.0	15.05	8.16	23.19	7.80	3.08	3.56
558.6	24.87	8.87	33.26	15.42	6.84	6.67
558.6	31.44	11.16	47.87	16.87	6.78	7.07
558.6	25.53	8.87	33.60	16.94	6.64	6.62
558.6	23.46	11.22	34.19	10.85	6.62	6.99

Note: Shaded data are outliers and are not used in development of kinetic models  
Horizontal-lined data are erroneous due to GC signal or GC integration problems

Table C15 - Summary of Propylene and Oxygen Conversion for Mass Transfer Tests on  $\text{Bi}_2\text{O}_3$  (W/F = 0.01024 g cat/sccm, 10 mol% Propylene and 3 mol% Oxygen in Feed)

Propylene Conversion (%)				
Temperature (°C)	Feed Flow Rate (sccm)			
	125	250	400	625
501	0.92	0.92	0.95	0.93
521	1.30	1.10	1.37	1.34
541	1.93	2.05	2.01	2.00
561	2.89	2.95	2.96	2.88
Oxygen Conversion (%)				
Temperature (°C)	Feed Flow Rate (sccm)			
	125	250	400	625
501	6.27	6.41	5.48	5.53
521	7.38	7.03	7.17	6.98
541	10.08	9.83	9.44	9.49
561	13.92	13.68	13.67	12.98

Table C16 - Summary of Propylene and Oxygen Conversion for Mass Transfer Tests on  $\text{Bi}_2\text{O}_3$  (W/F = 0.01024 g cat/sccm, 10 mol% Propylene and 6 mol% Oxygen in Feed)

Propylene Conversion (%)				
Temperature (°C)	Feed Flow Rate (sccm)			
	125	250	400	625
501	1.01	1.02	0.95	0.89
521	1.59	1.56	1.44	1.29
541	2.37	2.28	2.17	2.02
561	3.58	3.36	3.12	2.91
Oxygen Conversion (%)				
Temperature (°C)	Feed Flow Rate (sccm)			
	125	250	400	625
501	4.06	4.08	3.51	3.44
521	5.36	5.17	4.62	4.42
541	7.51	6.95	6.14	5.97
561	10.41	9.35	8.29	8.16



Table C17 - Membrane and Tubular Reactor Results Summary using  $\text{Bi}_2\text{O}_3$  as Catalyst (250 sccm Total Feed Flow Rate, 10 mol% Propylene and 3 mol% Oxygen in Feed)

Total Flow Rate	250 sccm			
Feed Propylene	10 mol %			
Feed Oxygen	3 mol %			
Nominal Furnace Temperature (°C)	490	510	530	550
<b>Membrane Reactor with <math>\text{Bi}_2\text{O}_3</math></b>				
Actual Temperature (°C)	495.8	516.7	537.4	558.7
Propylene Conversion (%)	3.23	4.30	5.67	7.28
Oxygen Conversion (%)	29.0	36.5	45.2	56.2
Propylene Selectivity to (%)				
CO	26.3	21.1	15.8	12.2
CO <sub>2</sub>	38.5	38.7	38.8	39.7
Ethylene	1.5	1.4	1.4	1.6
Acrolein	2.2	2.3	2.0	1.8
1,5-Hexadiene	31.5	36.5	40.4	41.9
Benzene	0.0	0.0	1.6	2.8
<b>Membrane Reactor Alone</b>				
Actual Temperature (°C)	494.1	514.6	534.8	555.1
Propylene Conversion (%)	2.05	2.38	2.76	3.20
Oxygen Conversion (%)	24.4	28.5	33.3	37.7
Propylene Selectivity to (%)				
CO	60.4	55.2	49.4	41.4
CO <sub>2</sub>	30.2	33.8	39.7	47.4
Ethylene	2.0	1.9	1.8	1.9
Acrolein	4.2	5.6	5.0	4.7
1,5-Hexadiene	3.2	3.5	4.1	4.6
<b>Tubular Reactor with <math>\text{Bi}_2\text{O}_3</math></b>				
Actual Temperature (°C)	504.5	524.8	545.8	566.8
Propylene Conversion (%)	2.44	3.73	5.45	7.76
Oxygen Conversion (%)	16.2	21.1	29.1	40.2
Propylene Selectivity to (%)				
CO <sub>2</sub>	34.2	28.2	26.9	27.0
Ethylene	0.7	0.9	1.3	1.8
1-Butene	0.0	0.0	0.1	0.9
Acrolein	0.0	4.3	4.9	4.9
1,5-Hexadiene	64.2	64.2	63.1	60.0
Benzene	0.9	2.4	3.7	5.4

Table C18 - Membrane and Tubular Reactor Results Summary using  $\text{Bi}_2\text{O}_3$  as Catalyst  
(250 sccm Total Feed Flow Rate, 15 mol% Propylene and 3 mol% Oxygen in Feed)

Total Flow Rate	250 sccm			
Feed Propylene	15 mol %			
Feed Oxygen	3 mol %			
Nominal Furnace Temperature (°C)	490	510	530	550
<b>Membrane Reactor with <math>\text{Bi}_2\text{O}_3</math></b>				
Actual Temperature (°C)	497.8	518.7	539.8	561.5
Propylene Conversion (%)	3.27	4.17	5.30	6.85
Oxygen Conversion (%)	43.7	52.1	63.3	79.2
Propylene Selectivity to (%)				
CO	27.5	21.2	16.2	12.0
CO <sub>2</sub>	38.0	37.7	38.2	38.2
Ethylene	1.7	1.5	1.5	1.7
Acrolein	1.8	2.1	1.6	1.4
1,5-Hexadiene	31.7	36.4	40.8	43.8
Benzene	0.0	1.1	1.7	2.9
<b>Membrane Reactor Alone</b>				
Actual Temperature (°C)	495.3	515.8	536.2	556.7
Propylene Conversion (%)	1.98	2.30	2.60	2.98
Oxygen Conversion (%)	32.7	38.4	44.5	51.7
Propylene Selectivity to (%)				
CO	58.3	52.7	46.9	41.5
CO <sub>2</sub>	31.8	36.6	42.0	47.5
Ethylene	2.1	1.8	1.8	1.8
Acrolein	5.5	6.5	6.5	6.0
1,5-Hexadiene	2.3	2.4	2.8	3.2
<b>Tubular Reactor with <math>\text{Bi}_2\text{O}_3</math></b>				
Actual Temperature (°C)	505.4	526.4	547.5	569.2
Propylene Conversion (%)	2.51	3.98	5.86	8.17
Oxygen Conversion (%)	22.9	30.6	43.6	61.9
Propylene Selectivity to (%)				
CO <sub>2</sub>	31.5	27.4	26.2	26.7
Ethylene	0.8	1.0	1.4	2.0
1-Butene	0.0	0.3	0.7	1.5
Acrolein	0.0	3.7	4.4	3.1
1,5-Hexadiene	67.1	65.2	63.6	61.0
Benzene	0.6	2.5	3.7	5.8

Table C19 - Membrane and Tubular Reactor Results Summary using  $\text{Bi}_2\text{O}_3$  as Catalyst  
(250 sccm Total Feed Flow Rate, 15 mol% Propylene and 4 mol% Oxygen in Feed)

Total Flow Rate	250 sccm			
Feed Propylene	15 mol %			
Feed Oxygen	4 mol %			
Nominal Furnace Temperature (°C)	490	510	530	550
<b>Membrane Reactor with <math>\text{Bi}_2\text{O}_3</math></b>				
Actual Temperature (°C)	499.2	520.2	541.5	563.4
Propylene Conversion (%)	3.55	4.47	5.72	7.30
Oxygen Conversion (%)	37.4	45.0	54.7	66.8
Propylene Selectivity to (%)				
CO	27.0	21.1	16.0	11.0
CO <sub>2</sub>	40.4	40.9	41.6	41.9
Ethylene	1.8	1.6	1.6	1.8
Acrolein	2.8	2.4	2.0	1.9
1,5-Hexadiene	28.0	33.0	37.5	40.9
Benzene	0.0	1.0	1.5	2.5
<b>Membrane Reactor Alone</b>				
Actual Temperature (°C)	495.7	516.3	536.7	557.2
Propylene Conversion (%)	2.15	2.47	2.82	3.16
Oxygen Conversion (%)	27.1	30.3	35.6	41.8
Propylene Selectivity to (%)				
CO	56.0	51.6	45.5	38.2
CO <sub>2</sub>	31.3	36.6	42.5	50.4
Ethylene	2.1	1.9	1.9	2.1
Acrolein	8.0	6.8	6.5	5.1
1,5-Hexadiene	2.6	3.1	3.6	4.2
<b>Tubular Reactor with <math>\text{Bi}_2\text{O}_3</math></b>				
Actual Temperature (°C)	506.1	527.1	548.6	570.3
Propylene Conversion (%)	2.57	4.20	6.09	8.53
Oxygen Conversion (%)	20.1	27.3	37.7	52.0
Propylene Selectivity to (%)				
CO <sub>2</sub>	37.4	31.8	30.1	29.2
Ethylene	0.9	1.0	1.4	2.0
1-Butene	0.0	0.2	0.8	1.4
Acrolein	0.0	5.0	4.3	4.3
1,5-Hexadiene	61.2	59.9	60.2	57.8
Benzene	0.5	2.1	3.3	5.1

Table C20 - Membrane and Tubular Reactor Results Summary using  $\text{Bi}_2\text{O}_3$  as Catalyst  
(250 sccm Total Feed Flow Rate, 20 mol% Propylene and 2 mol% Oxygen in Feed)

Total Flow Rate	250 sccm			
Feed Propylene	20 mol %			
Feed Oxygen	2 mol %			
Nominal Furnace Temperature (°C)	490	510	530	550
<b>Membrane Reactor with <math>\text{Bi}_2\text{O}_3</math></b>				
Actual Temperature (°C)	497.7	518.2		
Propylene Conversion (%)	2.74	3.30		
Oxygen Conversion (%)	7.2	80.4		
Propylene Selectivity to (%)				
CO	34.3	27.0		
CO <sub>2</sub>	34.5	34.6		
Ethylene	1.8	1.7		
Acrolein	2.4	2.0		
1,5-Hexadiene	27.0	34.0		
Benzene	0.0	0.7		
<b>Membrane Reactor Alone</b>				
Actual Temperature (°C)	495.6	516.0		
Propylene Conversion (%)	1.77	1.94		
Oxygen Conversion (%)	61.6	67.2		
Propylene Selectivity to (%)				
CO	60.1	56.1		
CO <sub>2</sub>	31.9	36.4		
Ethylene	2.3	2.3		
Acrolein	4.1	3.6		
1,5-Hexadiene	1.6	1.6		
<b>Tubular Reactor with <math>\text{Bi}_2\text{O}_3</math></b>				
Actual Temperature (°C)	505.4	526.4		
Propylene Conversion (%)	2.63	3.74		
Oxygen Conversion (%)	35.6	48.3		
Propylene Selectivity to (%)				
CO <sub>2</sub>	22.0	20.9		
Ethylene	0.8	1.0		
1-Butene	0.0	0.3		
Acrolein	5.9	4.3		
1,5-Hexadiene	69.4	70.7		
Benzene	2.0	2.7		

Table C21 - Membrane and Tubular Reactor Results Summary using  $\text{Bi}_2\text{O}_3$  as Catalyst  
(250 sccm Total Feed Flow Rate, 20 mol% Propylene and 3 mol% Oxygen in Feed)

Total Flow Rate	250 sccm			
Feed Propylene	20 mol %			
Feed Oxygen	3 mol %			
Nominal Furnace Temperature (°C)	490	510	530	550
<b>Membrane Reactor with <math>\text{Bi}_2\text{O}_3</math></b>				
Actual Temperature (°C)	499.4	520.4	541.8	
Propylene Conversion (%)	2.97	3.72	4.80	
Oxygen Conversion (%)	55.8	65.9	80.5	
Propylene Selectivity to (%)				
CO	33.7	26.6	19.7	
CO <sub>2</sub>	37.6	38.6	39.5	
Ethylene	1.8	1.6	1.5	
Acrolein	2.8	2.4	1.8	
1,5-Hexadiene	24.1	29.8	36.1	
Benzene	0.0	1.0	1.4	
<b>Membrane Reactor Alone</b>				
Actual Temperature (°C)	496.5	517.0	537.4	
Propylene Conversion (%)	1.95	2.21	2.48	
Oxygen Conversion (%)	45.8	50.4	58.7	
Propylene Selectivity to (%)				
CO	56.7	51.5	46.3	
CO <sub>2</sub>	34.2	39.2	45.5	
Ethylene	2.0	1.8	1.8	
Acrolein	5.3	5.5	4.2	
1,5-Hexadiene	1.8	2.0	2.2	
<b>Tubular Reactor with <math>\text{Bi}_2\text{O}_3</math></b>				
Actual Temperature (°C)	506.0	527.0	548.7	
Propylene Conversion (%)	2.66	3.96	5.72	
Oxygen Conversion (%)	28.3	37.2	52.8	
Propylene Selectivity to (%)				
CO <sub>2</sub>	27.2	24.7	24.2	
Ethylene	0.9	1.1	1.5	
1-Butene	0.0	0.4	0.9	
Acrolein	4.2	4.6	3.7	
1,5-Hexadiene	66.1	66.9	66.0	
Benzene	1.7	2.4	3.7	

Table C22 - Membrane and Tubular Reactor Results Summary using  $\text{Bi}_2\text{O}_3$  as Catalyst  
(250 sccm Total Feed Flow Rate, 20 mol% Propylene and 4 mol% Oxygen in Feed)

Total Flow Rate	250 sccm			
Feed Propylene	20 mol %			
Feed Oxygen	4 mol %			
Nominal Furnace Temperature (°C)	490	510	530	550
<b>Membrane Reactor with <math>\text{Bi}_2\text{O}_3</math></b>				
Actual Temperature (°C)	501.2	522.5	544.2	567.0
Propylene Conversion (%)	3.46	4.37	5.56	7.31
Oxygen Conversion (%)	48.7	58.1	70.4	89.0
Propylene Selectivity to (%)				
CO	27.2	21.2	15.6	11.0
CO <sub>2</sub>	40.4	40.7	41.2	40.9
Ethylene	1.8	1.6	1.6	1.8
Acrolein	2.2	2.0	1.3	1.2
1,5-Hexadiene	28.4	33.5	38.7	42.0
Benzene	0.0	1.0	1.6	3.1
<b>Membrane Reactor Alone</b>				
Actual Temperature (°C)	497.0	517.7	538.3	559.1
Propylene Conversion (%)	2.09	2.38	2.71	3.11
Oxygen Conversion (%)	34.7	40.5	47.1	55.4
Propylene Selectivity to (%)				
CO	55.1	49.4	44.1	38.3
CO <sub>2</sub>	34.7	40.2	45.5	50.9
Ethylene	2.0	1.9	1.9	2.0
Acrolein	6.0	6.0	5.6	5.6
1,5-Hexadiene	2.2	2.5	2.9	3.2
<b>Tubular Reactor with <math>\text{Bi}_2\text{O}_3</math></b>				
Actual Temperature (°C)	506.9	528.2	550.0	572.9
Propylene Conversion (%)	2.76	4.06	6.02	8.57
Oxygen Conversion (%)	24.4	32.5	46.6	66.7
Propylene Selectivity to (%)				
CO <sub>2</sub>	32.1	28.9	27.6	28.1
Ethylene	1.0	1.2	1.6	2.2
1-Butene	0.1	0.6	0.9	2.3
Acrolein	4.2	3.6	3.7	1.5
1,5-Hexadiene	61.0	63.6	62.7	60.0
Benzene	1.7	2.2	3.5	5.9

Table C23 - Membrane and Tubular Reactor Results Summary using  $\text{Bi}_2\text{O}_3$  as Catalyst (250 sccm Total Feed Flow Rate, 20 mol% Propylene and 6 mol% Oxygen in Feed)

Total Flow Rate	250 sccm			
Feed Propylene	20 mol %			
Feed Oxygen	6 mol %			
Nominal Furnace Temperature (°C)	490	510	530	550
<b>Membrane Reactor with <math>\text{Bi}_2\text{O}_3</math></b>				
Actual Temperature (°C)	503.5	525.5	547.7	570.4
Propylene Conversion (%)	3.77	4.79	6.12	7.96
Oxygen Conversion (%)	37.3	45.8	55.4	68.0
Propylene Selectivity to (%)				
CO	27.5	21.8	15.6	10.9
CO <sub>2</sub>	44.2	45.1	45.4	44.7
Ethylene	2.0	1.9	2.0	2.1
Acrolein	2.7	2.0	1.8	1.7
1,5-Hexadiene	23.6	28.5	34.0	38.1
Benzene	0.0	0.7	1.2	2.3
<b>Membrane Reactor Alone</b>				
Actual Temperature (°C)	498.2	519.2	540.1	561.1
Propylene Conversion (%)	2.42	2.86	3.28	3.76
Oxygen Conversion (%)	26.7	31.9	37.6	43.8
Propylene Selectivity to (%)				
CO	52.1	47.8	41.2	34.8
CO <sub>2</sub>	34.2	38.8	45.3	51.0
Ethylene	2.2	2.2	2.3	2.5
Acrolein	8.3	7.7	7.0	7.0
1,5-Hexadiene	3.2	3.5	4.2	4.7
<b>Tubular Reactor with <math>\text{Bi}_2\text{O}_3</math></b>				
Actual Temperature (°C)	507.8	529.2	551.2	575.2
Propylene Conversion (%)	2.90	4.12	6.20	9.24
Oxygen Conversion (%)	19.2	25.1	35.6	49.6
Propylene Selectivity to (%)				
CO <sub>2</sub>	37.6	34.2	31.7	31.2
Ethylene	1.1	1.3	1.6	2.2
1-Butene	0.2	0.7	1.0	2.2
Acrolein	7.3	4.0	4.6	4.5
1,5-Hexadiene	52.5	58.1	58.0	54.9
Benzene	1.4	1.8	3.0	4.9

Table C24 - Membrane and Tubular Reactor Results Summary using  $\text{Bi}_2\text{O}_3$  as Catalyst (187.5 sccm Total Feed Flow Rate, 10 mol% Propylene and 3 mol% Oxygen in Feed)

Total Flow Rate	187.5 sccm			
Feed Propylene	10 mol %			
Feed Oxygen	3 mol %			
Nominal Furnace Temperature (°C)	490	510	530	550
<b>Membrane Reactor with <math>\text{Bi}_2\text{O}_3</math></b>				
Actual Temperature (°C)	495.8	516.3	536.9	557.7
Propylene Conversion (%)	4.06	5.00	6.41	8.22
Oxygen Conversion (%)	37.2	44.2	53.6	66.0
Propylene Selectivity to (%)				
CO	30.9	24.6	18.3	13.9
CO <sub>2</sub>	38.3	38.8	40.0	40.6
Ethylene	1.8	1.6	1.5	1.7
Acrolein	3.0	2.8	2.2	1.9
1,5-Hexadiene	26.0	31.2	36.0	39.0
Benzene	0.0	1.0	2.0	2.9
<b>Membrane Reactor Alone</b>				
Actual Temperature (°C)	493.9	514.3	534.6	554.8
Propylene Conversion (%)	2.58	2.91	3.28	3.76
Oxygen Conversion (%)	29.1	31.8	36.5	42.4
Propylene Selectivity to (%)				
CO	59.6	56.5	51.1	45.7
CO <sub>2</sub>	28.5	32.7	36.8	41.5
Ethylene	2.2	2.1	2.0	2.0
Acrolein	6.1	5.2	6.5	6.8
1,5-Hexadiene	3.6	3.4	3.6	4.0
<b>Tubular Reactor with <math>\text{Bi}_2\text{O}_3</math></b>				
Actual Temperature (°C)	505.0	525.4	546.4	568.0
Propylene Conversion (%)	3.21	4.86	7.03	9.91
Oxygen Conversion (%)	20.3	27.3	37.3	53.6
Propylene Selectivity to (%)				
CO <sub>2</sub>	32.8	29.0	28.5	29.6
Ethylene	0.7	1.0	1.5	2.2
1-Butene	0.0	0.0	0.6	1.4
Acrolein	2.5	6.2	5.2	4.1
1,5-Hexadiene	61.9	61.3	59.9	56.1
Benzene	2.1	2.5	4.3	6.6



Table C25 - Membrane and Tubular Reactor Results Summary using  $\text{Bi}_2\text{O}_3$  as Catalyst (187.5 sccm Total Feed Flow Rate, 15 mol% Propylene and 3 mol% Oxygen in Feed)

Total Flow Rate	187.5 sccm			
Feed Propylene	15 mol %			
Feed Oxygen	3 mol %			
Nominal Furnace Temperature (°C)	490	510	530	550
<b>Membrane Reactor with <math>\text{Bi}_2\text{O}_3</math></b>				
Actual Temperature (°C)	497.5	518.1	538.9	560.0
Propylene Conversion (%)	3.92	4.88	6.16	7.83
Oxygen Conversion (%)	53.6	62.8	75.1	89.6
Propylene Selectivity to (%)				
CO	31.2	24.2	17.8	11.9
CO <sub>2</sub>	38.0	38.5	39.2	38.7
Ethylene	1.9	1.7	1.6	1.8
Acrolein	2.3	1.9	1.4	1.1
1,5-Hexadiene	26.6	32.5	38.2	42.8
Benzene	0.0	1.2	2.0	3.7
<b>Membrane Reactor Alone</b>				
Actual Temperature (°C)	495.3	515.6	535.9	556.2
Propylene Conversion (%)	2.45	2.78	3.14	3.59
Oxygen Conversion (%)	41.2	47.0	53.9	62.8
Propylene Selectivity to (%)				
CO	60.0	54.8	50.2	44.9
CO <sub>2</sub>	32.0	36.1	41.2	45.9
Ethylene	2.3	2.0	1.9	1.9
Acrolein	3.7	4.9	4.4	4.7
1,5-Hexadiene	2.0	2.2	2.3	2.6
<b>Tubular Reactor with <math>\text{Bi}_2\text{O}_3</math></b>				
Actual Temperature (°C)	505.9	526.9	548.3	570.2
Propylene Conversion (%)	3.33	4.83	6.98	9.76
Oxygen Conversion (%)	28.4	38.1	51.7	74.1
Propylene Selectivity to (%)				
CO <sub>2</sub>	29.6	27.2	26.4	27.1
Ethylene	0.9	1.1	1.6	2.2
1-Butene	0.0	0.3	0.9	1.9
Acrolein	3.5	3.9	4.3	2.7
1,5-Hexadiene	63.8	64.5	62.4	58.7
Benzene	2.2	2.9	4.4	7.3

Table C26 - Membrane and Tubular Reactor Results Summary using  $\text{Bi}_2\text{O}_3$  as Catalyst (187.5 sccm Total Feed Flow Rate, 15 mol% Propylene and 4 mol% Oxygen in Feed)

Total Flow Rate	187.5 sccm			
Feed Propylene	15 mol %			
Feed Oxygen	4 mol %			
Nominal Furnace Temperature (°C)	490	510	530	550
<b>Membrane Reactor with <math>\text{Bi}_2\text{O}_3</math></b>				
Actual Temperature (°C)	498.5	519.2	540.2	561.7
Propylene Conversion (%)	4.33	5.28	6.68	8.48
Oxygen Conversion (%)	45.5	53.1	64.0	78.0
Propylene Selectivity to (%)				
CO	29.2	23.2	17.3	12.3
CO <sub>2</sub>	41.0	41.7	42.2	42.7
Ethylene	1.8	1.6	1.6	1.8
Acrolein	2.3	2.0	1.8	1.4
1,5-Hexadiene	25.7	30.4	35.3	38.8
Benzene	0.0	1.1	1.8	3.0
<b>Membrane Reactor Alone</b>				
Actual Temperature (°C)	495.8	516.0	536.4	556.8
Propylene Conversion (%)	2.59	2.97	3.38	3.80
Oxygen Conversion (%)	32.0	37.2	43.0	50.2
Propylene Selectivity to (%)				
CO	58.9	53.2	47.7	41.6
CO <sub>2</sub>	32.1	36.2	41.2	47.2
Ethylene	2.3	2.0	1.9	2.0
Acrolein	4.0	5.7	5.8	5.4
1,5-Hexadiene	2.7	2.9	3.4	3.8
<b>Tubular Reactor with <math>\text{Bi}_2\text{O}_3</math></b>				
Actual Temperature (°C)	506.4	527.5	549	571.5
Propylene Conversion (%)	3.34	4.87	7.10	10.12
Oxygen Conversion (%)	23.6	31.1	42.7	62.1
Propylene Selectivity to (%)				
CO <sub>2</sub>	33.9	30.6	29.3	29.7
Ethylene	0.9	1.2	1.7	2.3
1-Butene	0.0	0.4	1.0	2.0
Acrolein	3.3	3.9	4.3	3.5
1,5-Hexadiene	59.9	61.4	59.9	56.1
Benzene	2.0	2.5	3.9	6.4

Table C27 - Membrane and Tubular Reactor Results Summary using  $\text{Bi}_2\text{O}_3$  as Catalyst (187.5 sccm Total Feed Flow Rate, 20 mol% Propylene and 3 mol% Oxygen in Feed)

Total Flow Rate	187.5 sccm			
Feed Propylene	20 mol %			
Feed Oxygen	3 mol %			
Nominal Furnace Temperature (°C)	490	510	530	550
<b>Membrane Reactor with <math>\text{Bi}_2\text{O}_3</math></b>				
Actual Temperature (°C)	498.7	519.4		
Propylene Conversion (%)	3.73	4.74		
Oxygen Conversion (%)	69.6	81.4		
Propylene Selectivity to (%)				
CO	32.7	24.9		
CO <sub>2</sub>	38.2	39.2		
Ethylene	1.9	1.7		
Acrolein	2.2	1.3		
1,5-Hexadiene	25.0	31.6		
Benzene	0.0	1.1		
<b>Membrane Reactor Alone</b>				
Actual Temperature (°C)	496.3	516.8		
Propylene Conversion (%)	2.54	2.77		
Oxygen Conversion (%)	55.7	62.9		
Propylene Selectivity to (%)				
CO	60.4	54.4		
CO <sub>2</sub>	32.0	38.0		
Ethylene	2.1	2.0		
Acrolein	4.0	4.0		
1,5-Hexadiene	1.5	1.6		
<b>Tubular Reactor with <math>\text{Bi}_2\text{O}_3</math></b>				
Actual Temperature (°C)	505.9	527.1		
Propylene Conversion (%)	3.20	4.69		
Oxygen Conversion (%)	33.0	44.9		
Propylene Selectivity to (%)				
CO <sub>2</sub>	26.9	24.9		
Ethylene	1.0	1.3		
1-Butene	0.4	0.8		
Acrolein	3.7	3.9		
1,5-Hexadiene	66.1	66.4		
Benzene	2.0	2.8		

Table C28 - Membrane and Tubular Reactor Results Summary using  $\text{Bi}_2\text{O}_3$  as Catalyst (187.5 sccm Total Feed Flow Rate, 20 mol% Propylene and 4 mol% Oxygen in Feed)

Total Flow Rate	187.5 sccm			
Feed Propylene	20 mol %			
Feed Oxygen	4 mol %			
Nominal Furnace Temperature ( $^{\circ}\text{C}$ )	490	510	530	550
<b>Membrane Reactor with <math>\text{Bi}_2\text{O}_3</math></b>				
Actual Temperature ( $^{\circ}\text{C}$ )	500.2	520.8	542.3	563.7
Propylene Conversion (%)	4.10	5.01	6.54	8.33
Oxygen Conversion (%)	57.6	67.3	82.3	97.4
Propylene Selectivity to (%)				
CO	29.6	23.0	16.2	10.0
$\text{CO}_2$	40.6	41.1	41.5	40.3
Ethylene	1.8	1.6	1.6	1.8
Acrolein	1.8	1.4	1.4	0.7
1,5-Hexadiene	26.2	31.9	37.2	42.8
Benzene	0.0	1.0	2.1	4.4
<b>Membrane Reactor Alone</b>				
Actual Temperature ( $^{\circ}\text{C}$ )	497.0	517.2	537.7	558.4
Propylene Conversion (%)	2.63	2.92	3.23	3.76
Oxygen Conversion (%)	44.3	49.9	57.8	68.1
Propylene Selectivity to (%)				
CO	56.6	51.9	46.5	41.2
$\text{CO}_2$	34.8	38.8	44.1	50.1
Ethylene	2.1	1.9	1.8	1.9
Acrolein	4.6	5.1	4.9	4.0
1,5-Hexadiene	1.9	2.3	2.7	2.8
<b>Tubular Reactor with <math>\text{Bi}_2\text{O}_3</math></b>				
Actual Temperature ( $^{\circ}\text{C}$ )	507.4	529.0	551.1	574.3
Propylene Conversion (%)	3.38	4.96	7.25	10.28
Oxygen Conversion (%)	29.9	39.0	55.8	76.1
Propylene Selectivity to (%)				
$\text{CO}_2$	31.8	28.9	27.8	28.1
Ethylene	1.0	1.3	1.7	2.3
1-Butene	0.0	0.7	1.2	2.4
Acrolein	3.7	3.6	4.3	2.9
1,5-Hexadiene	61.7	63.0	60.8	57.0
Benzene	1.8	2.5	4.1	7.2

Table C29 - Membrane and Tubular Reactor Results Summary using  $\text{Bi}_2\text{O}_3$  as Catalyst  
(250 sccm Total Feed Flow Rate, 20 mol% Propylene and 6 mol% Oxygen in Feed)

Total Flow Rate	187.5 sccm			
Feed Propylene	20 mol %			
Feed Oxygen	6 mol %			
Nominal Furnace Temperature ( $^{\circ}\text{C}$ )	490	510	530	550
<b>Membrane Reactor with <math>\text{Bi}_2\text{O}_3</math></b>				
Actual Temperature ( $^{\circ}\text{C}$ )	502.3	523.5	545.4	567.5
Propylene Conversion (%)	4.56	5.77	7.17	9.18
Oxygen Conversion (%)	44.7	54.0	64.5	78.8
Propylene Selectivity to (%)				
CO	28.5	23.6	16.7	11.6
$\text{CO}_2$	43.5	44.1	45.6	46.1
Ethylene	1.9	1.8	1.9	2.1
Acrolein	2.7	2.1	2.0	1.7
1,5-Hexadiene	23.4	27.6	32.3	35.7
Benzene	0.0	0.8	1.5	2.8
<b>Membrane Reactor Alone</b>				
Actual Temperature ( $^{\circ}\text{C}$ )	497.6	518.3	539.1	559.8
Propylene Conversion (%)	2.90	3.38	3.84	4.41
Oxygen Conversion (%)	32.1	37.7	44.5	52.4
Propylene Selectivity to (%)				
CO	53.8	48.9	43.5	37.2
$\text{CO}_2$	34.1	38.7	44.8	51.1
Ethylene	2.2	2.1	2.1	2.2
Acrolein	7.1	7.1	5.9	5.4
1,5-Hexadiene	2.8	3.2	3.7	4.1
<b>Tubular Reactor with <math>\text{Bi}_2\text{O}_3</math></b>				
Actual Temperature ( $^{\circ}\text{C}$ )	508.6	529.5	552.0	576.2
Propylene Conversion (%)	3.52	5.05	7.49	10.94
Oxygen Conversion (%)	23.7	30.5	43.3	62.0
Propylene Selectivity to (%)				
$\text{CO}_2$	37.7	34.2	32.3	31.8
Ethylene	1.1	1.4	1.9	2.7
1-Butene	0.5	0.9	1.7	2.7
Acrolein	5.6	4.0	4.4	4.7
1,5-Hexadiene	53.7	57.3	56.3	52.3
Benzene	1.5	2.1	3.5	5.8

Table C30 - Membrane and Tubular Reactor Results Summary using Bi<sub>2</sub>O<sub>3</sub> as Catalyst  
(125 sccm Total Feed Flow Rate, 10 mol% Propylene and 3 mol% Oxygen in Feed)

Total Flow Rate	125 sccm			
Feed Propylene	10 mol %			
Feed Oxygen	3 mol %			
Nominal Furnace Temperature (°C)	490	510	530	550
<b>Membrane Reactor with Bi<sub>2</sub>O<sub>3</sub></b>				
Actual Temperature (°C)	495.2	515.6	536.1	556.8
Propylene Conversion (%)	5.32	6.52	8.17	10.30
Oxygen Conversion (%)	50.6	59.2	71.3	86.9
Propylene Selectivity to (%)				
CO	29.5	23.6	17.6	12.6
CO <sub>2</sub>	41.0	41.5	42.7	43.0
Ethylene	2.1	1.9	1.9	2.1
Acrolein	2.4	2.0	1.1	0.7
1,5-Hexadiene	25.0	29.7	34.3	37.3
Benzene	0.0	1.3	2.4	4.3
<b>Membrane Reactor Alone</b>				
Actual Temperature (°C)	493.9	514.1	534.3	554.5
Propylene Conversion (%)	3.34	3.84	4.40	4.94
Oxygen Conversion (%)	35.6	41.6	47.9	56.3
Propylene Selectivity to (%)				
CO	61.1	57.6	53.9	49.0
CO <sub>2</sub>	27.3	30.7	34.9	39.7
Ethylene	2.7	2.6	2.5	2.5
Acrolein	6.0	6.0	5.5	5.1
1,5-Hexadiene	2.9	3.1	3.2	3.7
<b>Tubular Reactor with Bi<sub>2</sub>O<sub>3</sub></b>				
Actual Temperature (°C)	504.3	525.1	546.1	567.3
Propylene Conversion (%)	4.92	7.03	9.83	13.52
Oxygen Conversion (%)	30.9	41.6	55.8	79.2
Propylene Selectivity to (%)				
CO <sub>2</sub>	34.2	32.2	31.9	32.7
Ethylene	0.9	1.3	1.9	2.4
1-Butene	0.0	0.4	1.0	2.2
Acrolein	4.6	4.5	4.1	2.9
1,5-Hexadiene	57.4	57.8	55.2	49.8
Benzene	2.9	4.0	5.8	9.9

Table C31 - Membrane and Tubular Reactor Results Summary using  $\text{Bi}_2\text{O}_3$  as Catalyst  
(125 sccm Total Feed Flow Rate, 10 mol% Propylene and 4 mol% Oxygen in Feed)

Total Flow Rate	125 sccm			
Feed Propylene	10 mol %			
Feed Oxygen	4 mol %			
Nominal Furnace Temperature (°C)	490	510	530	550
<b>Membrane Reactor with <math>\text{Bi}_2\text{O}_3</math></b>				
Actual Temperature (°C)	495.6	516.0	536.7	556.8
Propylene Conversion (%)	5.65	6.97	8.64	10.87
Oxygen Conversion (%)	41.8	49.0	58.7	71.6
Propylene Selectivity to (%)				
CO	29.8	23.9	18.0	12.7
CO <sub>2</sub>	43.6	43.6	44.9	45.9
Ethylene	2.0	1.8	1.7	1.9
Acrolein	1.3	2.1	1.4	1.4
1,5-Hexadiene	23.3	27.4	31.9	34.7
Benzene	0.0	1.3	2.1	3.4
<b>Membrane Reactor Alone</b>				
Actual Temperature (°C)	494.3	514.6	534.8	554.8
Propylene Conversion (%)	3.85	4.26	4.77	5.36
Oxygen Conversion (%)	31.0	35.0	39.5	46.5
Propylene Selectivity to (%)				
CO	59.1	55.8	51.4	46.6
CO <sub>2</sub>	28.7	32.3	36.7	41.7
Ethylene	2.3	2.2	2.1	2.2
Acrolein	7.2	6.4	5.9	5.2
1,5-Hexadiene	2.7	3.3	3.9	4.3
<b>Tubular Reactor with <math>\text{Bi}_2\text{O}_3</math></b>				
Actual Temperature (°C)	504.7	525.4	542.3	562.5
Propylene Conversion (%)	4.77	7.07	10.19	14.37
Oxygen Conversion (%)	25.9	34.2	47.4	68.9
Propylene Selectivity to (%)				
CO <sub>2</sub>	40.8	36.9	35.6	36.4
Ethylene	1.0	1.3	1.9	2.7
1-Butene	0.0	0.5	1.0	2.2
Acrolein	0.0	2.6	3.9	3.2
1,5-Hexadiene	55.4	55.2	52.2	46.9
Benzene	2.8	3.5	5.4	8.7

Table C32 - Membrane and Tubular Reactor Results Summary using  $\text{Bi}_2\text{O}_3$  as Catalyst  
(125 sccm Total Feed Flow Rate, 15 mol% Propylene and 3 mol% Oxygen in Feed)

Total Flow Rate	125 sccm			
Feed Propylene	15 mol %			
Feed Oxygen	3 mol %			
Nominal Furnace Temperature ( $^{\circ}\text{C}$ )	490	510	530	550
<b>Membrane Reactor with <math>\text{Bi}_2\text{O}_3</math></b>				
Actual Temperature ( $^{\circ}\text{C}$ )	496.6	517.2		
Propylene Conversion (%)	5.22	6.43		
Oxygen Conversion (%)	74.3	85.9		
Propylene Selectivity to (%)				
CO	30.0	22.8		
$\text{CO}_2$	40.1	41.0		
Ethylene	2.2	2.1		
Acrolein	1.7	1.5		
1,5-Hexadiene	25.2	31.1		
Benzene	0.8	1.5		
<b>Membrane Reactor Alone</b>				
Actual Temperature ( $^{\circ}\text{C}$ )	494.9	515.3		
Propylene Conversion (%)	3.37	3.80		
Oxygen Conversion (%)	56.9	64.7		
Propylene Selectivity to (%)				
CO	60.7	56.8		
$\text{CO}_2$	29.8	35.1		
Ethylene	2.8	2.8		
Acrolein	5.0	3.6		
1,5-Hexadiene	1.7	1.7		
<b>Tubular Reactor with <math>\text{Bi}_2\text{O}_3</math></b>				
Actual Temperature ( $^{\circ}\text{C}$ )	505.3	526.4		
Propylene Conversion (%)	4.75	6.87		
Oxygen Conversion (%)	40.9	54.3		
Propylene Selectivity to (%)				
$\text{CO}_2$	30.8	29.0		
Ethylene	1.0	1.4		
1-Butene	0.4	0.8		
Acrolein	3.0	2.9		
1,5-Hexadiene	62.1	61.6		
Benzene	2.7	4.2		



Table C33 - Membrane and Tubular Reactor Results Summary using  $\text{Bi}_2\text{O}_3$  as Catalyst  
(125 sccm Total Feed Flow Rate, 15 mol% Propylene and 4 mol% Oxygen in Feed)

Total Flow Rate	125 sccm			
Feed Propylene	15 mol %			
Feed Oxygen	4 mol %			
Nominal Furnace Temperature (°C)	490	510	530	550
<b>Membrane Reactor with <math>\text{Bi}_2\text{O}_3</math></b>				
Actual Temperature (°C)	497.1	517.7	538.4	559.3
Propylene Conversion (%)	5.40	6.58	8.31	10.30
Oxygen Conversion (%)	59.0	68.5	83.0	95.6
Propylene Selectivity to (%)				
CO	30.5	23.7	16.7	10.6
CO <sub>2</sub>	41.6	42.9	44.2	43.0
Ethylene	2.0	1.8	1.8	2.0
Acrolein	2.0	1.5	1.0	0.7
1,5-Hexadiene	23.9	28.9	34.1	39.0
Benzene	0.0	1.2	2.2	4.7
<b>Membrane Reactor Alone</b>				
Actual Temperature (°C)	495.3	515.6	535.8	556.2
Propylene Conversion (%)	3.65	4.03	4.59	5.20
Oxygen Conversion (%)	44.9	50.9	58.7	68.7
Propylene Selectivity to (%)				
CO	59.1	56.1	51.2	46.5
CO <sub>2</sub>	31.3	35.5	39.7	45.2
Ethylene	2.4	2.2	2.2	2.2
Acrolein	5.1	3.7	4.2	3.3
1,5-Hexadiene	2.1	2.5	2.7	2.8
<b>Tubular Reactor with <math>\text{Bi}_2\text{O}_3</math></b>				
Actual Temperature (°C)	506.2	527.1	548.8	570.6
Propylene Conversion (%)	5.05	7.28	10.35	14.04
Oxygen Conversion (%)	35.5	48.3	68.2	92.9
Propylene Selectivity to (%)				
CO <sub>2</sub>	35.6	33.0	32.4	31.9
Ethylene	1.1	1.7	2.1	2.4
1-Butene	0.3	0.9	1.6	2.9
Acrolein	3.6	3.4	3.0	2.0
1,5-Hexadiene	57.0	57.3	54.7	49.9
Benzene	2.4	3.7	6.2	10.9

Table C34 - Membrane and Tubular Reactor Results Summary using  $\text{Bi}_2\text{O}_3$  as Catalyst  
(125 sccm Total Feed Flow Rate, 15 mol% Propylene and 6 mol% Oxygen in Feed)

Total Flow Rate	125 sccm			
Feed Propylene	15 mol %			
Feed Oxygen	6 mol %			
Nominal Furnace Temperature ( $^{\circ}\text{C}$ )	490	510	530	550
<b>Membrane Reactor with <math>\text{Bi}_2\text{O}_3</math></b>				
Actual Temperature ( $^{\circ}\text{C}$ )	498.5	519.2	540.1	561.7
Propylene Conversion (%)	6.20	7.44	9.33	11.80
Oxygen Conversion (%)	46.9	55.0	64.3	78.9
Propylene Selectivity to (%)				
CO	28.0	23.0	16.4	11.1
$\text{CO}_2$	46.7	47.3	48.6	49.5
Ethylene	2.0	1.8	1.8	2.0
Acrolein	1.8	1.5	1.7	1.5
1,5-Hexadiene	21.5	25.5	29.8	32.6
Benzene	0.0	0.9	1.7	3.3
<b>Membrane Reactor Alone</b>				
Actual Temperature ( $^{\circ}\text{C}$ )	495.8	516.2	536.6	557.0
Propylene Conversion (%)	4.00	4.53	5.17	5.90
Oxygen Conversion (%)	32.7	37.8	43.7	51.1
Propylene Selectivity to (%)				
CO	56.8	52.6	46.5	40.8
$\text{CO}_2$	31.3	35.7	40.9	46.6
Ethylene	2.3	2.1	2.1	2.1
Acrolein	6.8	6.1	6.3	5.8
1,5-Hexadiene	2.8	3.5	4.2	4.7
<b>Tubular Reactor with <math>\text{Bi}_2\text{O}_3</math></b>				
Actual Temperature ( $^{\circ}\text{C}$ )	506.9	528.1	549.7	572.8
Propylene Conversion (%)	5.18	7.37	10.53	14.94
Oxygen Conversion (%)	28.4	37.4	51.8	70.0
Propylene Selectivity to (%)				
$\text{CO}_2$	43.7	39.8	38.0	38.0
Ethylene	1.2	1.5	2.2	2.9
1-Butene	0.5	0.9	1.7	2.8
Acrolein	2.9	2.7	3.1	3.1
1,5-Hexadiene	49.7	52.0	50.2	45.0
Benzene	2.0	3.0	4.8	8.2

Table C35 - Membrane and Tubular Reactor Results Summary using  $\text{Bi}_2\text{O}_3$  as Catalyst  
(125 sccm Total Feed Flow Rate, 20 mol% Propylene and 4 mol% Oxygen in Feed)

Total Flow Rate	125 sccm			
Feed Propylene	20 mol %			
Feed Oxygen	4 mol %			
Nominal Furnace Temperature ( $^{\circ}\text{C}$ )	490	510	530	550
<b>Membrane Reactor with <math>\text{Bi}_2\text{O}_3</math></b>				
Actual Temperature ( $^{\circ}\text{C}$ )	498.9	519.2		
Propylene Conversion (%)	5.62	6.68		
Oxygen Conversion (%)	80.6	90.0		
Propylene Selectivity to (%)				
CO	27.2	20.7		
$\text{CO}_2$	42.6	42.2		
Ethylene	1.9	1.9		
Acrolein	1.3	1.1		
1,5-Hexadiene	26.3	32.5		
Benzene	0.9	1.6		
<b>Membrane Reactor Alone</b>				
Actual Temperature ( $^{\circ}\text{C}$ )	496.5	516.8		
Propylene Conversion (%)	3.54	3.90		
Oxygen Conversion (%)	60.4	68.5		
Propylene Selectivity to (%)				
CO	58.4	54.2		
$\text{CO}_2$	33.4	38.3		
Ethylene	2.4	2.3		
Acrolein	4.2	3.5		
1,5-Hexadiene	1.6	1.7		
<b>Tubular Reactor with <math>\text{Bi}_2\text{O}_3</math></b>				
Actual Temperature ( $^{\circ}\text{C}$ )	507.1	528.4		
Propylene Conversion (%)	4.98	7.16		
Oxygen Conversion (%)	44.8	60.7		
Propylene Selectivity to (%)				
$\text{CO}_2$	33.6	31.2		
Ethylene	1.2	1.5		
1-Butene	0.7	1.0		
Acrolein	2.4	2.7		
1,5-Hexadiene	59.6	59.7		
Benzene	2.5	3.8		

Table C36 - Membrane and Tubular Reactor Results Summary using  $\text{Bi}_2\text{O}_3$  as Catalyst  
(125 sccm Total Feed Flow Rate, 20 mol% Propylene and 6 mol% Oxygen in Feed)

Total Flow Rate	125 sccm			
Feed Propylene	20 mol %			
Feed Oxygen	6 mol %			
Nominal Furnace Temperature (°C)	490	510	530	550
<b>Membrane Reactor with <math>\text{Bi}_2\text{O}_3</math></b>				
Actual Temperature (°C)	500.0	520.8	542.5	563.3
Propylene Conversion (%)	5.82	7.13	9.10	11.39
Oxygen Conversion (%)	59.8	68.7	85.4	97.7
Propylene Selectivity to (%)				
CO	29.6	22.6	15.2	9.0
CO <sub>2</sub>	45.5	46.8	47.8	46.4
Ethylene	1.9	1.8	1.8	2.0
Acrolein	1.7	1.4	1.4	0.6
1,5-Hexadiene	21.3	26.5	31.7	36.8
Benzene	0.0	0.9	2.1	5.2
<b>Membrane Reactor Alone</b>				
Actual Temperature (°C)	497.0	517.5	537.9	558.6
Propylene Conversion (%)	3.90	4.43	5.02	5.79
Oxygen Conversion (%)	42.3	48.6	57.2	65.7
Propylene Selectivity to (%)				
CO	56.3	51.2	45.9	40.9
CO <sub>2</sub>	32.2	36.6	43.0	49.8
Ethylene	2.2	2.1	2.1	2.0
Acrolein	6.0	6.0	4.8	3.7
1,5-Hexadiene	3.3	4.1	4.2	3.6
<b>Tubular Reactor with <math>\text{Bi}_2\text{O}_3</math></b>				
Actual Temperature (°C)	508.1	529.8	552.4	575.7
Propylene Conversion (%)	5.12	7.46	10.90	15.15
Oxygen Conversion (%)	35.8	48.4	66.6	94.9
Propylene Selectivity to (%)				
CO <sub>2</sub>	40.3	36.6	35.1	34.6
Ethylene	1.3	1.6	2.2	2.6
1-Butene	0.7	1.3	2.1	3.1
Acrolein	2.7	3.2	3.1	2.4
1,5-Hexadiene	53.1	54.2	52.0	47.2
Benzene	2.0	3.1	5.5	10.1

## **Appendix D**

### **Reaction Data for Indium (III) Oxide Tests**

## List of Tables in Appendix D

Table D1 - Membrane Reactor Results Summary using 1 wt% In <sub>2</sub> O <sub>3</sub> supported on the Membrane as Catalyst (250 sccm Total Feed Flow Rate, 10 mol% Propylene and 3 mol% Oxygen in Feed).....	321
Table D2 - Membrane Reactor Results Summary using 1 wt% In <sub>2</sub> O <sub>3</sub> supported on the Membrane as Catalyst (250 sccm Total Feed Flow Rate, 10 mol% Propylene and 6 mol% Oxygen in Feed).....	321
Table D3 - Membrane Reactor Results Summary using 1 wt% In <sub>2</sub> O <sub>3</sub> supported on the Membrane as Catalyst (250 sccm Total Feed Flow Rate, 20 mol% Propylene and 3 mol% Oxygen in Feed).....	322
Table D4 - Membrane Reactor Results Summary using 1 wt% In <sub>2</sub> O <sub>3</sub> supported on the Membrane as Catalyst (250 sccm Total Feed Flow Rate, 20 mol% Propylene and 6 mol% Oxygen in Feed).....	322
Table D5 - Membrane Reactor Results Summary using 1 wt% In <sub>2</sub> O <sub>3</sub> supported on the Membrane as Catalyst (125 sccm Total Feed Flow Rate, 10 mol% Propylene and 3 mol% Oxygen in Feed).....	323
Table D6 - Membrane Reactor Results Summary using 1 wt% In <sub>2</sub> O <sub>3</sub> supported on the Membrane as Catalyst (125 sccm Total Feed Flow Rate, 10 mol% Propylene and 6 mol% Oxygen in Feed).....	323
Table D7 - Membrane Reactor Results Summary using 1 wt% In <sub>2</sub> O <sub>3</sub> supported on the Membrane as Catalyst (125 sccm Total Feed Flow Rate, 20 mol% Propylene and 3 mol% Oxygen in Feed).....	324
Table D8 - Membrane Reactor Results Summary using 1 wt% In <sub>2</sub> O <sub>3</sub> supported on the Membrane as Catalyst (125 sccm Total Feed Flow Rate, 20 mol% Propylene and 6 mol% Oxygen in Feed).....	324
Table D9 - Catalyst Activity Test Results Summary using 1 wt% In <sub>2</sub> O <sub>3</sub> Supported on 6.11 g Crushed VYCOR as Catalyst in Tubular Reactor - Tests at 250 sccm Total Feed Flow Rate, 20 mol% Propylene and 6 mol% Oxygen in Feed.....	325
Table D10 - Tubular Reactor Results Summary using 1 wt% In <sub>2</sub> O <sub>3</sub> supported on 6.11 g of Crushed VYCOR as Catalyst (250 sccm Total Feed Flow Rate, 10 mol% Propylene and 3 mol% Oxygen in Feed).....	326

## List of Tables in Appendix D (cont'd)

Table D11 - Tubular Reactor Results Summary using 1 wt% $\text{In}_2\text{O}_3$ supported on 6.11 g of Crushed VYCOR as Catalyst (250 sccm Total Feed Flow Rate, 10 mol% Propylene and 6 mol% Oxygen in Feed).....	326
Table D12 - Tubular Reactor Results Summary using 1 wt% $\text{In}_2\text{O}_3$ supported on 6.11 g of Crushed VYCOR as Catalyst (250 sccm Total Feed Flow Rate, 20 mol% Propylene and 3 mol% Oxygen in Feed).....	327
Table D13 - Tubular Reactor Results Summary using 1 wt% $\text{In}_2\text{O}_3$ supported on 6.11 g of Crushed VYCOR as Catalyst (250 sccm Total Feed Flow Rate, 20 mol% Propylene and 6 mol% Oxygen in Feed).....	327
Table D14 - Tubular Reactor Results Summary using 1 wt% $\text{In}_2\text{O}_3$ supported on 6.11 g of Crushed VYCOR as Catalyst (125 sccm Total Feed Flow Rate, 10 mol% Propylene and 3 mol% Oxygen in Feed).....	328
Table D15 - Tubular Reactor Results Summary using 1 wt% $\text{In}_2\text{O}_3$ supported on 6.11 g of Crushed VYCOR as Catalyst (125 sccm Total Feed Flow Rate, 10 mol% Propylene and 6 mol% Oxygen in Feed).....	328
Table D16 - Tubular Reactor Results Summary using 1 wt% $\text{In}_2\text{O}_3$ supported on 6.11 g of Crushed VYCOR as Catalyst (125 sccm Total Feed Flow Rate, 20 mol% Propylene and 3 mol% Oxygen in Feed).....	329
Table D17 - Tubular Reactor Results Summary using 1 wt% $\text{In}_2\text{O}_3$ supported on 6.11 g of Crushed VYCOR as Catalyst (125 sccm Total Feed Flow Rate, 20 mol% Propylene and 6 mol% Oxygen in Feed).....	329

Table D1 - Membrane Reactor Results Summary using 1 wt% In<sub>2</sub>O<sub>3</sub> supported on the Membrane as Catalyst (250 sccm Total Feed Flow Rate, 10 mol% Propylene and 3 mol% Oxygen in Feed)

Total Flow Rate	250 sccm			
Feed Propylene	10 mol %			
Feed Oxygen	3 mol %			
Nominal Furnace Temperature (°C)	430	450	470	490
Actual Temperature (°C)	433.0	453.7	474.7	496.1
Propylene Conversion (%)	1.60	2.09	2.78	3.74
Oxygen Conversion (%)	17.3	23.2	32.6	45.4
Propylene Selectivity to (%)				
CO	41.9	39.5	36.2	34.6
CO <sub>2</sub>	37.5	42.9	47.8	50.7
Ethylene	2.3	2.3	2.6	2.8
Acrolein	18.3	15.3	11.0	9.4
1,5-Hexadiene	0.0	0.0	2.4	2.5

Table D2 - Membrane Reactor Results Summary using 1 wt% In<sub>2</sub>O<sub>3</sub> supported on the Membrane as Catalyst (250 sccm Total Feed Flow Rate, 10 mol% Propylene and 6 mol% Oxygen in Feed)

Total Flow Rate	250 sccm			
Feed Propylene	10 mol %			
Feed Oxygen	6 mol %			
Nominal Furnace Temperature (°C)	430	450	470	490
Actual Temperature (°C)	433.5	454.7	476.4	499.7
Propylene Conversion (%)	2.01	2.78	3.83	5.89
Oxygen Conversion (%)	10.6	15.2	22.7	36.0
Propylene Selectivity to (%)				
CO	39.8	35.2	33.4	32.8
CO <sub>2</sub>	40.2	45.0	50.9	55.1
Ethylene	1.7	1.9	2.2	2.3
Acrolein	18.3	16.1	11.5	7.8
1,5-Hexadiene	0.0	1.8	2.0	2.0



Table D3 - Membrane Reactor Results Summary using 1 wt% In<sub>2</sub>O<sub>3</sub> supported on the Membrane as Catalyst (250 sccm Total Feed Flow Rate, 20 mol% Propylene and 3 mol% Oxygen in Feed)

Total Flow Rate	250 sccm			
Feed Propylene	20 mol %			
Feed Oxygen	3 mol %			
Nominal Furnace Temperature (°C)	430	450	470	490
Actual Temperature (°C)	434.7	455.4	476.2	497.2
Propylene Conversion (%)	1.50	1.73	2.00	2.55
Oxygen Conversion (%)	33.6	38.9	47.5	59.9
Propylene Selectivity to (%)				
CO	48.9	47.2	44.6	41.2
CO <sub>2</sub>	38.4	40.8	43.7	44.6
Ethylene	2.7	2.7	2.8	2.8
Acrolein	10.0	9.3	7.9	9.7
1,5-Hexadiene	0.0	0.0	1.0	1.7

Table D4 - Membrane Reactor Results Summary using 1 wt% In<sub>2</sub>O<sub>3</sub> supported on the Membrane as Catalyst (250 sccm Total Feed Flow Rate, 20 mol% Propylene and 6 mol% Oxygen in Feed)

Total Flow Rate	250 sccm			
Feed Propylene	20 mol %			
Feed Oxygen	6 mol %			
Nominal Furnace Temperature (°C)	430	450	470	490
Actual Temperature (°C)	435.2	456.4	477.9	500.9
Propylene Conversion (%)	1.66	2.03	2.66	3.74
Oxygen Conversion (%)	18.2	22.4	29.9	42.7
Propylene Selectivity to (%)				
CO	46.2	43.4	40.3	38.2
CO <sub>2</sub>	38.4	40.4	43.2	47.4
Ethylene	2.1	2.1	2.1	2.2
Acrolein	13.3	11.9	12.9	10.7
1,5-Hexadiene	0.0	1.2	1.5	1.5

Table D5 - Membrane Reactor Results Summary using 1 wt% In<sub>2</sub>O<sub>3</sub> supported on the Membrane as Catalyst (125 sccm Total Feed Flow Rate, 10 mol% Propylene and 3 mol% Oxygen in Feed)

Total Flow Rate	125 sccm			
Feed Propylene	10 mol %			
Feed Oxygen	3 mol %			
Nominal Furnace Temperature (°C)	430	450	470	490
Actual Temperature (°C)	432.8	453.2	473.9	494.4
Propylene Conversion (%)	2.56	3.36	4.35	5.33
Oxygen Conversion (%)	29.4	39.1	51.5	63.7
Propylene Selectivity to (%)				
CO	40.5	49.1	48.2	46.8
CO <sub>2</sub>	43.1	38.3	39.3	40.7
Ethylene	3.2	3.6	3.7	4.0
Acrolein	13.2	10.7	8.0	6.0
1,5-Hexadiene	0.0	1.7	2.1	2.4

Table D6 - Membrane Reactor Results Summary using 1 wt% In<sub>2</sub>O<sub>3</sub> supported on the Membrane as Catalyst (125 sccm Total Feed Flow Rate, 10 mol% Propylene and 6 mol% Oxygen in Feed)

Total Flow Rate	125 sccm			
Feed Propylene	10 mol %			
Feed Oxygen	6 mol %			
Nominal Furnace Temperature (°C)	430	450	470	490
Actual Temperature (°C)	433.3	454.2	475.6	497.3
Propylene Conversion (%)	3.41	4.67	6.37	8.74
Oxygen Conversion (%)	19.0	27.1	37.7	32.3
Propylene Selectivity to (%)				
CO	38.4	35.4	33.0	32.2
CO <sub>2</sub>	43.2	48.6	54.0	57.2
Ethylene	2.4	2.5	2.7	2.8
Acrolein	16.0	12.0	7.4	4.7
1,5-Hexadiene	0.0	1.5	1.9	2.1
Benzene	0.0	0.0	1.0	1.0

Table D7 - Membrane Reactor Results Summary using 1 wt% In<sub>2</sub>O<sub>3</sub> supported on the Membrane as Catalyst (125 sccm Total Feed Flow Rate, 20 mol% Propylene and 3 mol% Oxygen in Feed)

Total Flow Rate	125 sccm			
Feed Propylene	20 mol %			
Feed Oxygen	3 mol %			
Nominal Furnace Temperature (°C)	430	450	470	490
Actual Temperature (°C)	434.2	454.7	474.9	494.9
Propylene Conversion (%)	2.60	2.91	3.33	3.68
Oxygen Conversion (%)	57.9	65.4	75.3	82.3
Propylene Selectivity to (%)				
CO	50.1	49.1	48.2	46.8
CO <sub>2</sub>	37.8	38.3	39.3	40.7
Ethylene	3.4	3.6	3.7	4.0
Acrolein	8.7	8.0	7.6	7.3
1,5-Hexadiene	0.0	1.0	1.2	1.2

Table D8 - Membrane Reactor Results Summary using 1 wt% In<sub>2</sub>O<sub>3</sub> supported on the Membrane as Catalyst (125 sccm Total Feed Flow Rate, 20 mol% Propylene and 6 mol% Oxygen in Feed)

Total Flow Rate	125 sccm			
Feed Propylene	20 mol %			
Feed Oxygen	6 mol %			
Nominal Furnace Temperature (°C)	430	450	470	490
Actual Temperature (°C)	435.2	455.9	476.6	497.7
Propylene Conversion (%)	3.03	3.52	4.27	5.35
Oxygen Conversion (%)	34.0	39.8	47.9	61.4
Propylene Selectivity to (%)				
CO	47.8	46.2	44.1	42.2
CO <sub>2</sub>	38.8	40.3	42.3	44.6
Ethylene	2.7	2.7	2.6	2.7
Acrolein	9.9	9.7	9.7	9.1
1,5-Hexadiene	0.8	1.1	1.3	1.4

Table D9 - Catalyst Activity Test Results Summary for 1 wt% In<sub>2</sub>O<sub>3</sub> Supported on 6.11 g Crushed VYCOR as Catalyst in Tubular Reactor - Tests at 250 sccm Total Feed Flow Rate, 20 mol% Propylene and 6 mol% Oxygen in Feed

Nominal Furnace Temperature (°C)	430	450	470	490
Day 1				
Actual Temperature (°C)	456.4	481.6		
Propylene Conversion (%)	3.53	5.86		
Oxygen Conversion (%)	44.8	75.0		
Day 2				
Actual Temperature (°C)	449.1	475.6	500.9	515.8
Propylene Conversion (%)	2.00	3.75	6.25	7.97
Oxygen Conversion (%)	23.0	44.4	76.0	91.6
Day 3				
Actual Temperature (°C)	444.6	468.6	495.5	525.4
Propylene Conversion (%)	1.12	2.00	3.75	6.45
Oxygen Conversion (%)	10.6	21.0	42.1	72.2
Day 4				
Actual Temperature (°C)	444.1	466.5	491.0	519.4
Propylene Conversion (%)	0.85	1.62	2.96	5.40
Oxygen Conversion (%)	7.5	15.8	31.4	60.0
Day 5				
Actual Temperature (°C)	443.8	465.7	489.6	516.8
Propylene Conversion (%)	0.75	1.43	2.63	4.80
Oxygen Conversion (%)	6.6	1.4	26.9	52.6
Day 6				
Actual Temperature (°C)	444.3	466.3	490.3	520.3
Propylene Conversion (%)	0.68	1.21	2.40	4.48
Oxygen Conversion (%)	5.9	12.2	24.3	51.4
Day 7				
Actual Temperature (°C)	444.3	466.3	490.3	520.3
Propylene Conversion (%)	0.70	1.24	2.17	4.12
Oxygen Conversion (%)	6.0	11.3	22.2	46.5

Table D10 - Tubular Reactor Results Summary using 1 wt% In<sub>2</sub>O<sub>3</sub> supported on 6.11 g of Crushed VYCOR as Catalyst (250 sccm Total Feed Flow Rate, 10 mol% Propylene and 3 mol% Oxygen in Feed)

Total Flow Rate	250 sccm			
Feed Propylene	10 mol %			
Feed Oxygen	3 mol %			
Nominal Furnace Temperature (°C)	430	450	470	490
Actual Temperature (°C)	433.2	454.3	475.4	496.4
Propylene Conversion (%)	0.38-0.54	0.72-0.87	1.55	2.68
Oxygen Conversion (%)	4.1-7.1	8.2	16.4	28.8
Propylene Selectivity to (%)				
CO	9.0-13.0	12.0-14.2	24.4	25.3
CO <sub>2</sub>	31.0-49.0	42.2-47.6	45.8	48.8
Ethylene	1.0	2.2	2.7	3.3
Acrolein	38.0-54.3	35.9-43.8	27.1	20.1
1,5-Hexadiene	0.0	0.0	0.0	2.5

\*\* low rate of reaction at 430°C and 450°C lead to questionable results

Table D11 - Tubular Reactor Results Summary using 1 wt% In<sub>2</sub>O<sub>3</sub> supported on 6.11 g of Crushed VYCOR as Catalyst (250 sccm Total Feed Flow Rate, 10 mol% Propylene and 6 mol% Oxygen in Feed)

Total Flow Rate	250 sccm			
Feed Propylene	10 mol %			
Feed Oxygen	6 mol %			
Nominal Furnace Temperature (°C)	430	450	470	490
Actual Temperature (°C)	433.3	454.3	476.4	499.5
Propylene Conversion (%)	1.01	1.33	2.27	3.44
Oxygen Conversion (%)	3.9	5.9	10.5	18.1
Propylene Selectivity to (%)				
CO	37.9	25.4	25.0	24.3
CO <sub>2</sub>	20.3	33.6	38.4	45.8
Ethylene	1.0	1.9	2.7	3.7
Acrolein	40.8	39.1	31.3	23.6
1,5-Hexadiene	0.0	0.0	2.6	2.6

Table D12 - Tubular Reactor Results Summary using 1 wt%  $\text{In}_2\text{O}_3$  supported on 6.11 g of Crushed VYCOR as Catalyst (250 sccm Total Feed Flow Rate, 20 mol% Propylene and 3 mol% Oxygen in Feed)

Total Flow Rate	250 sccm			
Feed Propylene	20 mol %			
Feed Oxygen	3 mol %			
Nominal Furnace Temperature (°C)	430	450	470	490
Actual Temperature (°C)	435.3	455.3	476.4	497.4
Propylene Conversion (%)	0.41	0.65	1.21	2.10
Oxygen Conversion (%)	6.8	13.3	25.0	45.6
Propylene Selectivity to (%)				
CO	41.4	23.6	23.8	24.1
CO <sub>2</sub>	24.2	40.9	44.7	48.4
Ethylene	0.9	1.9	2.5	3.2
Acrolein	33.5	33.6	26.0	21.7
1,5-Hexadiene	0.0	0.0	3.0	2.6

Table D13 - Tubular Reactor Results Summary using 1 wt%  $\text{In}_2\text{O}_3$  supported on 6.11 g of Crushed VYCOR as Catalyst (250 sccm Total Feed Flow Rate, 20 mol% Propylene and 6 mol% Oxygen in Feed)

Total Flow Rate	250 sccm			
Feed Propylene	20 mol %			
Feed Oxygen	6 mol %			
Nominal Furnace Temperature (°C)	430	450	470	490
Actual Temperature (°C)	435.3	457.3	478.4	501.5
Propylene Conversion (%)	0.51	0.94	1.66	2.95
Oxygen Conversion (%)	4.3	8.3	15.8	30.8
Propylene Selectivity to (%)				
CO	29.1	27.3	22.2	23.6
CO <sub>2</sub>	25.4	34.6	40.6	45.8
Ethylene	1.0	1.9	2.6	3.3
Acrolein	44.5	36.2	31.9	24.8
1,5-Hexadiene	0.0	0.0	2.7	2.5

Table D14 - Tubular Reactor Results Summary using 1 wt% In<sub>2</sub>O<sub>3</sub> supported on 6.11 g of Crushed VYCOR as Catalyst (125 sccm Total Feed Flow Rate, 10 mol% Propylene and 3 mol% Oxygen in Feed)

Total Flow Rate	125 sccm			
Feed Propylene	10 mol %			
Feed Oxygen	3 mol %			
Nominal Furnace Temperature (°C)	430	450	470	490
Actual Temperature (°C)	432.2	453.3	473.3	494.4
Propylene Conversion (%)	0.70	1.40	2.42	3.84
Oxygen Conversion (%)	6.4	13.7	25.5	43.0
Propylene Selectivity to (%)				
CO	35.5	21.7	22.8	25.1
CO <sub>2</sub>	28.5	42.4	48.8	52.8
Ethylene	1.3	2.4	3.1	3.8
Acrolein	34.7	33.5	22.6	15.8
1,5-Hexadiene	0.0	0.0	2.7	2.5

\*\* low rate of reaction at 430°C leads to questionable results

Table D15 - Tubular Reactor Results Summary using 1 wt% In<sub>2</sub>O<sub>3</sub> supported on 6.11 g of Crushed VYCOR as Catalyst (125 sccm Total Feed Flow Rate, 10 mol% Propylene and 6 mol% Oxygen in Feed)

Total Flow Rate	125 sccm			
Feed Propylene	10 mol %			
Feed Oxygen	6 mol %			
Nominal Furnace Temperature (°C)	430	450	470	490
Actual Temperature (°C)	433.2	454.3	475.3	497.4
Propylene Conversion (%)	1.25	2.15	3.40	5.40
Oxygen Conversion (%)	5.5	10.2	17.7	29.7
Propylene Selectivity to (%)				
CO	25.8	25.0	22.7	24.0
CO <sub>2</sub>	30.2	37.8	45.0	49.7
Ethylene	1.5	2.4	3.3	4.2
Acrolein	42.5	34.8	26.7	19.9
1,5-Hexadiene	0.0	0.0	2.3	2.2

Table D16 - Tubular Reactor Results Summary using 1 wt% In<sub>2</sub>O<sub>3</sub> supported on 6.11 g of Crushed VYCOR as Catalyst (125 sccm Total Feed Flow Rate, 20 mol% Propylene and 3 mol% Oxygen in Feed)

Total Flow Rate	125 sccm			
Feed Propylene	20 mol %			
Feed Oxygen	3 mol %			
Nominal Furnace Temperature (°C)	430	450	470	490
Actual Temperature (°C)	434.3	455.4	475.4	495.4
Propylene Conversion (%)	0.78	1.06	1.86	2.95
Oxygen Conversion (%)	12.6	20.6	38.8	65.0
Propylene Selectivity to (%)				
CO	44.3	23.4	23.5	24.0
CO <sub>2</sub>	26.0	42.1	47.3	51.0
Ethylene	1.1	2.3	2.9	3.5
Acrolein	28.6	29.0	23.3	18.6
1,5-Hexadiene	0.0	3.2	3.0	2.9

\*\* low rate of reaction at 430°C leads to questionable results

Table D17 - Tubular Reactor Results Summary using 1 wt% In<sub>2</sub>O<sub>3</sub> supported on 6.11 g of Crushed VYCOR as Catalyst (125 sccm Total Feed Flow Rate, 20 mol% Propylene and 6 mol% Oxygen in Feed)

Total Flow Rate	125 sccm			
Feed Propylene	20 mol %			
Feed Oxygen	6 mol %			
Nominal Furnace Temperature (°C)	430	450	470	490
Actual Temperature (°C)	435.3	456.4	477.4	498.4
Propylene Conversion (%)	0.76	1.47	2.56	4.34
Oxygen Conversion (%)	6.7	13.6	26.0	47.5
Propylene Selectivity to (%)				
CO	28.3	22.6	22.1	24.0
CO <sub>2</sub>	30.1	38.4	44.4	49.0
Ethylene	1.6	2.2	3.0	3.6
Acrolein	40.0	34.2	27.9	21.2
1,5-Hexadiene	0.0	2.6	2.6	2.2



## Appendix E

### Fortran Code for Data Collection Program (OPTO 22)

The program makes reference to a number of FORTRAN subroutines necessary to interface with the OPTO 22 hardware. These subroutines are:

OP22IO  
HPTIME  
STRW  
DOWAIT  
RNDMAI  
CONK

and are available through R. Barton of the Department of Chemical and Materials Engineering (University of Alberta).

C DIMER0B.FOR  
C  
C This program has been designed to read information from the  
C Optomux 22 boards associated with the propylene dimerization  
C experimental equipment. At present the program is configured  
C only to read channels 0,1,2 as flowmeters (Matheson, Vacuum  
C General#1, Vacuum General#2) and channels 4,5 as thermocouples  
C (channel 4 as type K (new) and channel 5 as type K) on board 1.  
C  
C \*\*Program has been modified to accomodate 0-250 sccm Helium  
C flowmeter (Matheson - rec'd Dec 94) on Channel 0\*\*  
C  
C \*\*Program modified April 4/95 for type K T/C to replace previous  
C type J T/C on channel 4\*\*  
C  
C \*\*Program modified May 16/95 to change O2 flow calibration\*\*  
C  
C \*\*Program modified May 2/96 to change all 3 flow calibrations\*\*  
C  
C \*\*Program modified May 28/96 to change O2&C3 flow calibrations\*\*  
C  
C This program gives no output to the Optomux system. All the  
C flowrates and oven temperature are set manually at those  
C individual pieces of equipment. The program does, however,  
C require that the file EXINFO.DAT be supplied and that it  
C contain variables (in the following order):  
C       description of the catalyst (string)  
C       total flowrate in sccm  
C       helium flowrate in sccm  
C       oxygen flowrate in sccm  
C       propylene flowrate in sccm  
C       W/F ratio  
C       oven temperature  
C These values are for information only and are read into the  
C data output file.  
C  
C The program samples the Optomux once every 12 seconds and  
C combines 5 such readings to give minute averages which are  
C printed to the output file  
C

```

CHARACTER*1 StopCharacter
CHARACTER*2 BOARD1
CHARACTER*15 FNAME
CHARACTER*80 IN,OUT,CATALYST,MESSAGE
INTEGER*2 IERR(16),NCHAI,ICHAN1(5),ITIMES(5),IYEAR,IDATE(8)
INTEGER*2 K,I,J,IDATA(16)
INTEGER*4 HOLDT
REAL*8 TFLOW,HEFLOW,C3FLOW,O2FLOW,WOVERF,OVENT
REAL*8 START,EXPST,SAMPLET,DATAT
REAL*8 SUM1(5),SUM2(5),SUM3(5),SUM4(5),SUM5(5),TOTAL(5)
REAL*8 FLOW1,FLOW2,FLOW3,TC1,TC2
LOGICAL QuitEarly

```

```

C
C   Definition of the variables
C   StopCharacter - key used to halt the run
C   BOARD1 - Optomux address of Board 1
C   FNAME - output file name
C   IN - return message from Optomux upon receipt of an instr.
C   OUT - message sent to Optomux
C   CATALYST - string from input file describing catalyst
C   MESSAGE - a string for extra comments about the run
C   IERR - array of error codes from Optomux
C   NCHAI - number of analog input channels
C   ICHAN1 - array of slots on board 1 which are analog
C           inputs
C   ITIMES - array of time/date information
C   IYEAR - last 2 digits of year
C   IDATE - array of time/date info used to name outfile
C   I,J,K - loop variables
C   IDATA - decimal output from each channel read from Opto.
C   HOLDT - holding time between samples (100ths of seconds)
C   TFLOW - total flow (as info)
C   HEFLOW - helium flow (as info)
C   O2FLOW - oxygen flow (as info)
C   C3FLOW - propylene flow (as info)
C   WOVERF - W/F ratio (as info)
C   OVENT - oven temp set point (as info)
C   START - time for testing in dowait loop (100ths of sec.)
C   EXPST - experiment start time (100ths of seconds)
C   SAMPLET - time of a sample (100ths of seconds)
C   DATAT - time into experiment(minutes) when 1 minute
C           averages are printed
C   SUM1..SUM5 - array of holding variables for 1 minute
C           average calculations
C   TOTAL - holding values for totals of SUM1..SUM5
C   FLOW1..FLOW3, TC1,TC2 - 1 minute averages for the 5

```

```
C          sampled variables.
C      QuitEarly - flag used to stop program
C
C      STOPCHARACTER = 'S'
C
C      Set the holding time between samples to 12 seconds
C
C      HOLDT = 1200
C
C      Set the addresses of the Boards
C
C      BOARD1 = 'FF'
C      BOARD2 = 'FE'
C
C      Set up the serial port for the communication - port 0 - 9600,n,8,1
C
C      WRITE(*,*) 'NEXT STEP IS TO CALL TO PORTX'
C      CALL PORTX(227,0,IERR)
C      WRITE(*,*) 'NEXT STEP IS TO CALL TO OP22IO'

C      Do a power on Reset of the OPTO22
C
C      OUT = '>//BOARD1//A'
C      CALL OP22IO(OUT,IN)
C      OUT = '>//BOARD2//A'
C      CALL OP22IO(OUT,IN)
C
C      Set channels 0,1,2 (as flowmeters) and 4,5 (TC) as inputs (Board 1)
C      WRITE(*,*) 'NEXT STEP IS TO CALL TO OP22IO TO SET SLOTS'
C
C      OUT = '>//BOARD1//H0037'
C      CALL OP22IO(OUT,IN)
C
C      Correlate the ICHAN1 array with the input channels on board 1
C
C      NCHAI = 5
C      ICHAN1(1) = 0
C      ICHAN1(2) = 1
C      ICHAN1(3) = 2
C      ICHAN1(4) = 4
C      ICHAN1(5) = 5
```

C Open the file containing the run information

```
OPEN(5,FILE='EXINFO.DAT',ERR=990,STATUS='OLD')
```

C Read Data from file

```
WRITE(*,*) 'Reading data from EXINFO.DAT'
READ(5,*,ERR=995) CATALYST
READ(5,*,ERR=995) TFLOW
READ(5,*,ERR=995) HEFLOW
READ(5,*,ERR=995) O2FLOW
READ(5,*,ERR=995) C3FLOW
READ(5,*,ERR=995) WOVERF
READ(5,*,ERR=995) OVENT
READ(5,*,ERR=995) MESSAGE
CLOSE(5)
```

C

C Open OUTPUT file and give it a unique name (based on time & date)

C

```
CALL HPTIME(ITIMES,IYEAR)
IDATE(1)=ITIMES(5)/1000
ITIMES(5)=ITIMES(5)-IDATE(1)*1000
IDATE(2)=ITIMES(5)/100
ITIMES(5)=ITIMES(5)-IDATE(2)*100
IDATE(3)=ITIMES(5)/10
ITIMES(5)=ITIMES(5)-IDATE(3)*10
IDATE(4)=ITIMES(5)
IDATE(5)=ITIMES(4)/10
ITIMES(4)=ITIMES(4)-IDATE(5)*10
IDATE(6)=ITIMES(4)
IDATE(7)=ITIMES(3)/10
ITIMES(3)=ITIMES(3)-IDATE(7)*10
IDATE(8)=ITIMES(3)
FNAME=CHAR(IDATE(1)+48)//CHAR(IDATE(2)+48)//CHAR(IDATE(3)+48)//
&CHAR(IDATE(4)+48)//CHAR(IDATE(5)+48)//CHAR(IDATE(6)+48)//CHAR(
&IDATE(7)+48)//CHAR(IDATE(8)+48)/'.EXD'
WRITE(*,*) 'Data will be stored in ',FNAME
OPEN(7,FILE=FNAME,ERR=1017,STATUS='NEW')
GOTO 17
1017 WRITE(*,*) 'WARNING - file already exists and hence will be
& be overwritten'
OPEN(7,FILE=FNAME,STATUS='OLD')
17 CONTINUE
```

```

C Write out inputs to the OUTPUT file and to screen
  WRITE(7,*) 'PROPYLENE DIMERIZATION EXPERIMENT INFORMATION'
  WRITE(7,*) '-----'
  WRITE(7,*) ''
  WRITE(*,*) 'PROPYLENE DIMERIZATION EXPERIMENT INFORMATION'
  WRITE(*,*) '-----'
  WRITE(*,*) ''
  CALL HPTIME(ITIMES,IYEAR)
  WRITE(7,201) (ITIMES(5)/100),(ITIMES(5)-(ITIMES(5)/100)*100),IYEAR
  WRITE(*,201) (ITIMES(5)/100),(ITIMES(5)-(ITIMES(5)/100)*100),IYEAR
201  FORMAT(8X,'Date : ',I2,',',I2,',',I2)
     WRITE(7,202) (ITIMES(J),J=4,1,-1)
     WRITE(*,202) (ITIMES(J),J=4,1,-1)
202  FORMAT(8X,'Time : ',I2,',',I2,',',I2,',',I2)
     WRITE(7,*) ''
     WRITE(7,203) CATALYST
     WRITE(*,*) ''
     WRITE(*,203) CATALYST
203  FORMAT(2X,'The catalyst is ',A40)
     WRITE(7,204) TFLOW
     WRITE(*,204) TFLOW
204  FORMAT(2X,'The total gas flowrate is ',F7.1,' sccm')
     WRITE(7,205) WOVERF
     WRITE(*,205) WOVERF
205  FORMAT(2X,'The W/F ratio is ',F7.5,' g cat/sccm')
     WRITE(7,206) HEFLOW
     WRITE(*,206) HEFLOW
206  FORMAT(2X,'The helium flowrate is ',F7.1,' sccm')
     WRITE(7,207) O2FLOW
     WRITE(*,207) O2FLOW
207  FORMAT(2X,'The oxygen flowrate is ',F7.1,' sccm')
     WRITE(7,208) C3FLOW
     WRITE(*,208) C3FLOW
208  FORMAT(2X,'The propylene flowrate is ',F7.1,' sccm')
     WRITE(7,209) OVENT
     WRITE(*,209) OVENT
209  FORMAT(2X,'The oven temperature is ',F5.1,' C')
     WRITE(7,*) ''
     WRITE(7,210) MESSAGE
     WRITE(*,*) ''
     WRITE(*,210) MESSAGE
210  FORMAT(2X,'Note: ',A50)

```

```

  WRITE(7,*) ''
  WRITE(*,*) ''
C Write out the data header

```

```

C
WRITE(7,*) ' TIME HELIUM OXYGEN PROPYLENE TC1 TC2'
WRITE(7,*) ' (min) (sccm) (sccm) (sccm) (C) (C)'
WRITE(7,*) ' --- ---- - ---- - --- ---'
WRITE(*,*) ' TIME HELIUM OXYGEN PROPYLENE TC1 TC2'
WRITE(*,*) ' (min) (sccm) (sccm) (sccm) (C) (C)'
WRITE(*,*) ' --- ---- - ---- - --- ---'

C
C Set the start time for the entire experiment
CALL STRTW(EXPST)

C
C The main data gathering loop
C
400 DO 300 K=1,5
    SUM1(K) = 0.0
    SUM2(K) = 0.0
    SUM3(K) = 0.0
    SUM4(K) = 0.0
    SUM5(K) = 0.0
    TOTAL(K) = 0.0
300 CONTINUE
DO 310 I=1,5
    CALL STRTW(START)
    CALL DOWAIT(START,HOLDT,StopCharacter,QuitEarly)
    IF (QuitEarly) GOTO 450
    CALL RNDMAI(NCHAI,ICHAN1,IDATA,IERR,BOARD1)
C Convert the OPTOMUX data to flowrates for channels 0,1,2
    SUM1(I) = -(REAL(IDATA(1))/4095.*5)**2*0.40458+
+ REAL(IDATA(1))/4095.*5.*54.0535-2.601
    SUM2(I) = REAL(IDATA(2))/4095.*5.*1.5938-0.1309
    SUM3(I) = REAL(IDATA(3))/4095.*10.*8.16646-0.5705
C Convert the OPTOMUX data to temperatures for channels 4,5
    IF (IDATA(4).LT.-100.0) THEN
        SUM4(I) = 9999999.0
    ELSE
        SUM4(I) = CONK(IDATA(4))
    ENDIF
    IF (IDATA(5).LT.-100.0) THEN
        SUM5(I) = 9999999.0
    ELSE
        SUM5(I) = CONK(IDATA(5))
    ENDIF
310 CONTINUE

```

```
DO 320 J=1,5
  TOTAL(1) = TOTAL(1) + SUM1(J)
  TOTAL(2) = TOTAL(2) + SUM2(J)
  TOTAL(3) = TOTAL(3) + SUM3(J)
  TOTAL(4) = TOTAL(4) + SUM4(J)
  TOTAL(5) = TOTAL(5) + SUM5(J)
320  CONTINUE
  FLOW1 = TOTAL(1)/5.0
  FLOW2 = TOTAL(2)/5.0
  FLOW3 = TOTAL(3)/5.0
  TC1 = TOTAL(4)/5.0
  TC2 = TOTAL(5)/5.0
  CALL STRTW(SAMPLET)
  DATAT = (SAMPLET - EXPST)/60.0/100.0
  WRITE(7,330) DATAT,FLOW1,FLOW2,FLOW3,TC1,TC2
  WRITE(*,330) DATAT,FLOW1,FLOW2,FLOW3,TC1,TC2
330  FORMAT(1X,F6.1,T10,F6.2,T20,F6.2,T30,F6.2,T41,F5.1,T48,F5.1)
  GOTO 400
450  CONTINUE
  CLOSE(7)
  WRITE(*,*) 'The experiment has been terminated'
  WRITE(*,500) FNAME
500  FORMAT(1X,'The experimental data is contained in file ',A)
  GOTO 1000
990  WRITE(*,*) 'There is a problem opening EXINFO.DAT'
  WRITE(*,*) 'Please ensure that the file exists'
  GOTO 1000
995  WRITE(*,*) 'There is a problem reading the data in'
  WRITE(*,*) 'EXINFO.DAT - please check the file'
  GOTO 1000
1000 CONTINUE
  WRITE(*,*) 'The program has been terminated'
  STOP
  END
```